DYNAMICS OF MATTER WAVE PACKETS IN THE PRESENCE OF TIME-DEPENDENT ABSORPTION

M BARBIER

PhD

2017

DYNAMICS OF MATTER WAVE PACKETS IN THE PRESENCE OF TIME-DEPENDENT ABSORPTION

Maximilien BARBIER

A thesis submitted in partial fulfilment of the requirements of the University of Northumbria at Newcastle for the degree of Doctor of Philosophy

Research undertaken in the Department of Mathematics, Physics and Electrical Engineering

February 2017

Abstract

Atom-laser interaction is at the heart of the vibrant field of quantum optics. The dynamical properties of a moving atom submitted to a laser radiation are strongly influenced by the position- and time-dependence of the latter. The full physical state of the atom must include information about the centre-of-mass motion and the internal structure of the atom. It is challenging to obtain a complete description of the full state of the atom. However, there exists an alternative approach to the dynamics of an atom in the presence of a laser, which is based on the concept of matter-wave absorption.

In this thesis, we theoretically study the nonrelativistic one-dimensional motion of an electrically neutral quantum particle in the presence of a thin time-dependent absorber, representing the laser radiation. Our aim is to better understand the precise connection between time-dependent matter-wave absorption and the interaction between an atom and a localised time-dependent laser.

Our analysis is based on two different approaches to the problem. The first one describes the moving atom by a two-level system, and represents the laser radiation by an off-diagonal δ-potential. The second model treats the atom as a structureless particle, and describes the laser by a time-dependent absorbing barrier. While the former model can be derived from first principles, the treatment of the absorbing barrier in the latter model lacks a rigorous quantum mechanical justification. The main outcome of our work is to provide a solid physical ground for the absorber model, by explicitly connecting it to the δ-potential model. We have thus extended the range of theoretical tools useful for investigating the effects of time-dependent laser radiation on quantum matter.

Contents

Acknowledgements

My warmest thanks go to my parents, without whom I would certainly not be writing these words today. Their unfailing help and support allowed me to pursue studies in the field that has always been of the highest interest to me. This thesis is dedicated to them.

I am also deeply grateful to my supervisor Arseni Goussev for providing me with the great opportunity of pursuing PhD studies with him. His support proved fundamental from the early days of my application to the final days of writing the thesis. Our constant discussions made of the three years of my PhD an experience that I truly enjoyed.

Finally, I acknowledge financial support from Northumbria University.

Declaration

I declare that the work contained in this thesis has not been submitted for any other award and that it is all my own work. I also confirm that this work fully acknowledges opinions, ideas and contributions from the work of others. Any ethical clearance for the research presented in this thesis (Research project RE-EE-13-140402-533c0e0f7b8d5) has been approved. Approval has been sought and granted by the Faculty Ethics Committee on 30 April 2014.

Name: Maximilien Barbier

Signature:

Date:

Chapter 1

Introduction

Dynamics is one of the most obvious physical concepts, as motion occurs in everyday life. Building up on Galileo's pioneering work Newton stated his Second Law, then refined by Einstein two centuries later. However, difficulties arose when this classical approach to dynamics was applied to matter at its most fundamental level, for which a whole new framework was required. This resulted in Quantum Mechanics [1–5], the all-embracing theory of microscopic phenomena.

An important development allowed by the quantum-mechanical framework has been the conception of the laser. The physics of atom-laser interaction in particular is very rich and spans a wide range of phenomena. For instance, experimental breakthroughs made it possible to manipulate individual quantum systems via e.g. ion traps [6–9] or cavity quantum electrodynamics [10] and even made nondemolition measurements [11] possible. Furthermore, the coupling between a moving atom and a laser light can induce important modifications of the dynamical properties of the atom. This is adequately used in the field of ultracold atoms, where laser cooling can produce temperatures lower than the micro-Kelvin (see e.g. [12] for a general reference about modern atomic physics). It is also remarkable that some of the thought experiments devised in the early days of the quantum theory [13] can nowadays be realised in the laboratory [14, 15]. Atom-laser interaction then appears to be a valuable tool to study the foundations of Quantum Mechanics.

The question addressed in this thesis has one origin in atom-laser interaction. Consider an atom, whose internal structure can be described by the set $\{|j\rangle\}$ of its energy eigenstates. A laser radiation may then induce a transition from one internal state $|i\rangle$ to an other internal state $|f\rangle$. The dynamical properties of an atom submitted to a laser are greatly influenced by the position- and time-dependence of the laser light. For instance, in the case of a position-independent simple periodic laser the atom can undergo Rabi oscillations, or Rabi flopping [1, 16, 17]. A possible way of suppressing Rabi oscillations is by making the intensity of the laser depend on position [18]. The motion of an atom interacting with a position- and time-

dependent laser radiation is a fundamental problem in quantum optics. A complete description of a moving atom in interaction with a laser must take into account both the centre-of-mass motion and the evolution of the internal state of the atom. It is then instructive to note that little attention has been given to the theoretical study of the centre-of-mass motion of particles with an internal structure in the presence of a position-dependent laser light [18, 19].

An effective approach to the dynamics of an atom in the presence of a laser light is provided by the concept of *matter-wave absorption* (that will be discussed in more details later on). In its simplest setting, matter-wave absorption allows to map the problem of the interaction between an atom (having an internal structure) and a laser into the simpler problem of a *structureless* particle (representing the atom) submitted to an *absorbing barrier* (representing the laser). The state of the particle is now given by a usual one-component wave function. Possible laser-induced transitions in the original problem are here taken into account through a non-unitary dynamics of the system. Because of the non-unitarity of the dynamics, such problems are related to the general topic of non-Hermitian Quantum Mechanics (see e.g. [20] as a general reference). The laser can here be modelled by a complex absorbing potential [21]. However, the problem of a moving particle submitted to an absorbing barrier remains to date little studied (see e.g. [22] for a stationary non-Hermitian potential).

In this thesis, we theoretically study the nonrelativistic one-dimensional motion of an electrically neutral quantum particle submitted to a thin time-dependent absorber, modelling the interaction of a moving atom with a localised time-dependent laser radiation. The aim of this work is to better understand the precise connection between time-dependent matter-wave absorption and the interaction of an atom with a time-dependent laser. To the best of our knowledge, this subject spans a vastly uncharted territory.

The thesis is organised as follows. We present first in chapter 2 the analytical techniques we use to tackle an intrinsically time-dependent problem. We use the time-dependent approach of nonrelativistic quantum dynamics (see e.g. [23] as a general reference), based on the time-dependent Schrödinger equation (TDSE). Solving the TDSE yields the dynamical state of the system, that is a wave function, or wave packet, $\psi(x,t)$ for a structureless particle in the position representation (x and t denoting, respectively, the position and time variables). We recall the important notion of a propagator, which will prove useful to treat the TDSE. We then discuss the simple case of Gaussian wave packets, as it naturally leads to the frozen Gaussian regime used extensively in later calculations. As we will see, classical intuition can be adequately used in studying the dynamics of localised wave packets. We also recall the phase-space representation of a quantum state, focusing in particular on

the Husimi distribution. We conclude the chapter with a closer examination of the concept of matter-wave absorption.

The discussion of matter-wave absorption is then continued in greater details in chapter 3, where we introduce two models describing the interaction between a moving particle and a thin time-dependent laser beam. The first model is called the δ-potential model (DPM). This model is a time-dependent generalisation of the stationary atom-laser model introduced in [19]. It describes the motion of a two-level atom, with the two internal states $|1\rangle$ and $|2\rangle$, interacting with a localised time-dependent resonant laser light. The laser is represented by an off-diagonal δ-potential with a time-dependent amplitude $\Omega(t)$. The atom is initially prepared in the state $|1\rangle$. That is, the initial state is given by $\psi_0(x)|1\rangle$ in the position representation. The atom is assumed to be initially localised on the left of the laser, i.e. $\psi_0(x) = 0$ for $x \geqslant 0$ (the laser beam being localised at position $x = 0$). This model is thus relevant to describe the motion of a wave packet whose spatial extent σ is much larger than the spatial extent (in the direction of propagation of the packet) of the laser light. The effect of the potential is to mix the populations of the two levels as time evolves, so that the state of the atom at time t is given by $\psi_1(x,t)|1\rangle + \psi_2(x,t)|2\rangle$. We regard an atom in the state $|2\rangle$ as undetectable, i.e. *absorbed* by the laser, and are primarily interested in evaluating the component $\psi_1(x,t)$ of the detectable state $|1\rangle$. We then introduce an other model, aiming at constructing the component ψ_1 by means of time-dependent matter-wave absorption. This second approach is referred to as the aperture function model (AFM), and was initially devised in references [24] and [25]. It represents the laser radiation by an absorbing barrier, characterised by discontinuous time-dependent absorbing boundary conditions. The barrier is described by an aperture function $\chi(t)$. It is a dimensionless quantity that is related to the transparency of the barrier. The main advantage of the AFM over the DPM is that the former is exactly solvable for an *arbitrary* time-dependent aperture function, while the latter admits exact solutions only in very few cases. A serious drawback of the AFM however is that the particular absorbing boundary conditions describing the barrier lack a clear physical justification.

Therefore, the first objective of our work is to give a proper physical basis to the AFM. We do this by explicitly connecting it to the first-principles DPM. We conjecture at the end of chapter 3 a concrete relation between the time-dependent aperture function $\chi(t)$ and well-defined physical quantities characterising the atom-laser system in the DPM. The hypothesis connecting the AFM with the DPM, yet to be proven, is then justified in chapter 4 through a quantitative comparison between the two models. This comparison is performed using both analytical and numerical methods. Our analytical calculations make use of a particular semiclassical regime,

namely a frozen Gaussian regime. More precisely, this regime assumes the increase of the spatial spreading of a freely evolved Gaussian wave packet to be negligible as compared to the initial spreading of the packet. Such a regime can be adequately used to describe modern experiments based on ultracold atoms (see e.g. [26] regarding coherent backscattering of ^{87}Rb atoms, where the experimental parameters satisfy the semiclassical regime considered in this work). Assuming the connection between the AFM and the DPM, we demonstrate an excellent agreement between the physical predictions of the two models for both slowly varying barriers and the limit case of an instantaneously varying barrier. We then turn our attention to a numerical approach, where different atom-barrier systems are analysed. We observe again an excellent agreement between the two models in a semiclassical regime. As a result of this analysis, the AFM has been advanced and the link between the absorbing barrier and a physical laser is now unambiguous. Therefore, this model is relevant and valuable to study the motion of an atom in the presence of a time-dependent laser light. Indeed, the AFM allows one to analytically investigate the dynamical properties of the atom. In particular, contrary to the DPM, the AFM does not require to numerically solve a many-component TDSE. Note that these two chapters, chapters 3 and 4, resulted in our recently published work [27].

Having provided a sound physical basis to the AFM, we capitalise on the fact that it is exactly solvable to explore in chapter 5 various aspects of matter-wave absorption by time-dependent barriers. We identify some of the areas where we believe the AFM can prove valuable, and present some preliminary results. We first consider the example of a simple periodic time-dependent aperture function, and compute an exact expression of the Husimi representation of the transmitted state. We derive analytical results that prove valuable in understanding the phase-space structure of the Husimi distribution. We also treat the case of a Gaussian-like time-dependent aperture function, and again derive an analytical expression of the Husimi distribution. These two scenarios could provide valuable analytical insights for the study of time gratings and time slits. We then derive an expression for the Husimi distribution in the complex plane, and obtain an analytical result for a special example of aperture function. Finally, we formulate the important inverse problem, aiming at identifying the time-dependent barrier that could produce a desired target state.

The main outcome of our work is to give a strong physical ground to the AFM, originally a heuristic model, by explicitly connecting it to the DPM that can be derived from first principles. We clearly demonstrated how matter-wave absorption is able to adequately model atom-laser interaction. On a fundamental level, we have thus extended the range of theoretical tools appropriate for investigating the effects of time-dependent lasers on an atomic wave function. We also obtained valuable

physical insights regarding the dynamical properties of a moving quantum particle in the presence of time-dependent matter-wave absorption, a vastly unexplored area. Finally, the recently proposed reshaping of wave packets via time-dependent absorption [28], as well as the results obtained in this thesis, demonstrate a potential versatility of time-dependent matter-wave absorption for manipulating the quantum state of a particle. Therefore, we believe that the AFM will prove valuable in investigating the possibility of engineering any desired quantum state with a carefully tuned laser radiation.

Chapter 2

Fundamental concepts

In this thesis, we study the nonrelativistic *dynamical* properties of moving *localised* quantum wave packets submitted to a thin *time-dependent absorber*. Therefore, the purpose of this chapter is to introduce the various techniques we use to tackle this problem. It also provides a more detailed discussion of the fundamental concepts upon which our work is built, namely nonrelativistic quantum dynamics, localised wave packets and matter-wave absorption.

We consider the one-dimensional motion of a single nonrelativistic quantum particle of mass m. The direction of propagation of the particle is given by the usual Cartesian x-axis. The state of the system is described by a ket $|\psi\rangle$ vector of a Hilbert space $\mathscr{H}$. The state $|\psi\rangle$ contains all the information one can possibly know about the system. At the initial time t_0, the particle is taken to be in the state $|\psi_0\rangle$. For convenience, we set the initial time to be zero in the sequel, i.e. $t_0 = 0$[1]. The system then evolves in a time $t > 0$ towards the state $|\psi(t)\rangle$ under the influence of a Hamiltonian $H(\tau)$, with $0 < \tau < t$. The dynamics of the particle between the initial time and the final time t is hence governed by the *time-dependent Schrödinger equation* (TDSE), that is

$$i\hbar \frac{d}{d\tau} |\psi(\tau)\rangle = H(\tau)|\psi(\tau)\rangle \,, \tag{2.1}$$

for any $0 < \tau < t$. We emphasise that the Hamiltonian is taken to be *time-dependent*, which means that we consider *nonconservative* systems. We write H in the form

$$H(\tau) = H_0 + V(X, \tau) \,, \tag{2.2}$$

[1] At the cost of generality: as we will deal with nonconservative systems the propagator will not be invariant through a time translation. Hence the observation time t and the initial time t_0 *do not*, in general, appear only via the combination $t - t_0$.

where H_0 denotes the kinetic, free-particle Hamiltonian, i.e.

$$H_0 \equiv \frac{P^2}{2m}\,, \tag{2.3}$$

with P the momentum operator, and $V(X,\tau)$ denotes the potential to which the particle is submitted. The potential depends on time and on the position operator X, but not on the momentum operator P. The particle is said to be free if it is submitted to a constant potential. We emphasise two notations consistently used in the sequel, namely that the Latin character t will always represent the final time (sometimes also referred to as the observation time) and will be considered as a *fixed* parameter of the problem, while the Greek character τ will typically denote a *varying* time, $0 < \tau < t$.

The TDSE (2.1) is the dynamical equation of nonrelativistic Quantum Mechanics. A standard approach to solve the TDSE for time-independent Hamiltonians is to use separation of variables. The resulting equation for the position variable is the time-independent, or stationary, Schrödinger equation. Solving it yields the eigenvalues and eigenstates of the Hamiltonian. The solution of the TDSE is then given by a linear combination of these eigenstates with time-dependent coefficients. To add a time-dependent term to the Hamiltonian increases drastically the complexity of solving the TDSE. A typical approach would then be to use time-dependent perturbation theory [29, 30]. It proves useful in studying the effect of a weak time-dependent perturbation on the transition probabilities between the eigenstates of the unperturbed Hamiltonian. However, this approximation scheme is not suitable to describe the precise time evolution of the system for arbitrary time-dependent Hamiltonians.

We focus in the sequel on solving the TDSE directly, without any reference to the time-independent Schrödinger equation. To this respect, we introduce in section 2.1 the fundamental notion of a propagator. We then discuss in section 2.2 the motion of localised wave packets, using the important example of free Gaussian wave packets. This will naturally lead us to the frozen Gaussian regime. Section 2.3 is a reminder of Quantum Mechanics in phase space. We focus in particular on the Husimi distribution. Finally, we give in section 2.4 a more detailed presentation of the concept of matter-wave absorption, central topic of the present work.

2.1 Propagator for the time-dependent Schrödinger equation

In this section we recall some fundamental results about the TDSE (2.1).

First of all, note that the TDSE is a first order ordinary differential equation in time, which ensures that the state $|\psi(\tau)\rangle$ of the system at any time $\tau > 0$ is uniquely determined by the initial state $|\psi_0\rangle$. Therefore, there exists a certain operator $U(\tau)$ such that

$$|\psi(\tau)\rangle = U(\tau)|\psi_0\rangle \,, \tag{2.4}$$

for any $\tau > 0$. Because of its definition (2.4), the operator $U(\tau)$ is called the *(time-)evolution operator*. It embeds all the dynamical properties of the system and is independent of the initial state. Furthermore, the TDSE (2.1) is a linear and homogeneous differential equation, and thus admits a *superposition principle*, stating that *any* linear combination of solutions is itself a solution of the TDSE. This implies in particular that the evolution operator $U(\tau)$ is linear.

For simplicity, let us now assume the particle has no internal structure[2]. We use the position representation based on the position eigenvectors $\{|x\rangle\}$ [1, 2]. The dynamical state of the system at any time $\tau > 0$ is thus given by the wave function $\psi(x,\tau) \equiv \langle x|\psi(\tau)\rangle$. Therefore, projecting the equation (2.4) on the ket $|x\rangle$ and inserting the closure relation $\int_{-\infty}^{+\infty} dx\, |x\rangle\langle x| = \mathbb{1}$, with $\mathbb{1}$ being the identity operator, yields

$$\psi(x,\tau) = \int_{-\infty}^{+\infty} dx'\, K(x,x',\tau)\psi_0(x') \,, \tag{2.5}$$

where $K(x,x',\tau)$ denotes the matrix elements of the evolution operator $U(\tau)$ in the position representation, that is

$$K(x,x',\tau) \equiv \langle x|U(\tau)|x'\rangle \,. \tag{2.6}$$

The quantity $K(x,x',\tau)$ represents the probability amplitude for the system to evolve, in a time $\tau > 0$, from an initial position x' to a position x. For this reason, the quantity $K(x,x',\tau)$ is called the *propagator*. The propagator is a fundamental quantity of interest when dealing with the TDSE, because it embeds all the dynamics of the problem. Its main advantage is indeed transparent from the relation (2.5): once the propagator $K(x,x',\tau)$ is known, the dynamical state $\psi(x,\tau)$ of the system at any time τ can be constructed via a mere integral, and this for any initial state.

[2]This assumption will need to be relaxed when we later discuss the case of a two-level system. However, the conclusions to be drawn in the case of a structureless particle can be to a great extent generalised after merely replacing the wave function by a spinor.

Now, because the wave function $\psi(x,\tau)$ satisfies the TDSE[3]

$$i\hbar\frac{\partial}{\partial\tau}\,\psi(x,\tau)=\left[-\frac{\hbar^2}{2m}\frac{\partial^2}{\partial x^2}+V(x,\tau)\right]\psi(x,\tau)\,, \tag{2.7}$$

it can be readily seen from (2.5) that the propagator $K(x,x',\tau)$ itself satisfies the same differential equation, that is

$$\left[i\hbar\frac{\partial}{\partial\tau}+\frac{\hbar^2}{2m}\frac{\partial^2}{\partial x^2}-V(x,\tau)\right]K(x,x',\tau)=0\,. \tag{2.8a}$$

The initial condition (IC) is clearly fixed from the definition (2.6), and reads

$$K(x,x',0^+)=\delta(x-x')\,. \tag{2.8b}$$

The notation 0^+ used in (2.8b) merely stands for 0 approached from the positive semi axis. Finally, particular boundary conditions (BC's) at $x\to\pm\infty$ must be imposed on $K(x,x',\tau)$. Such BC's are inspired by the classical diffusion equation. It is well known [31] that the free-particle TDSE reduces to the diffusion equation under the substitution $\tau\to-i\,|\tau|$[4]. The propagator for the diffusion equation is required to vanish at $x\to\pm\infty$. This suggests to impose the same BC's on the propagator $K(x,x',\tau)$ of the TDSE under the substitution $\tau\to-i\,|\tau|$, that is

$$\lim_{x\to\pm\infty}K(x,x',\tau)=0\qquad\text{for}\qquad\tau=-i\,|\tau|\,. \tag{2.8c}$$

The set of equations (2.8) defines a well-posed problem because of the parabolic nature of the TDSE [31]. The validity of the BC's (2.8c) is determined from physical grounds.

For instance, the problem (2.8) must be able to describe the important case of a free particle, where $V(x,\tau)=0$. The unique solution to the corresponding problem, denoted by $K_0(x-x',\tau)$[5], is given by

$$K_0(x-x',\tau)=\sqrt{\frac{m}{2i\pi\hbar\tau}}\exp\left(i\,\frac{m(x-x')^2}{2\hbar\tau}\right)\,. \tag{2.9}$$

This expression indeed corresponds to the *free-particle propagator* (which can be

[3]Writing (2.1), (2.2) and (2.3) in the position representation, and using the correspondences $X\leftrightarrow x$ and $P\leftrightarrow-i\hbar\,\partial/\partial x$.

[4]The diffusion constant being $\hbar/2m$.

[5]This simpler notation is justified by the fact that the free-particle propagator is invariant under a space-translation, i.e. it depends on the positions x and x' only through $x-x'$. It is worth noting that in the case of a free particle the propagator is also invariant under a time-translation.

derived from different techniques, such as path integration [32]). The BC's (2.8c) are thus expected to be valid for potentials $V(x,\tau)$ that vanish at $x \to \pm\infty$.

The form (2.2) of the Hamiltonian can be conveniently combined with the fact that the free-particle propagator, which corresponds to the (free-particle) Hamiltonian H_0, is known. Indeed, this allows to write the (full) propagator $K(x,x',\tau)$ corresponding to the (full) Hamiltonian $H(\tau)$ in the form [33]

$$K(x,x',\tau) = K_0(x-x',\tau) - \frac{i}{\hbar}\int_0^\tau d\tau_1 \int_{-\infty}^{+\infty} dx_1\, K_0(x-x_1,\tau-\tau_1)V(x_1,\tau_1)K(x_1,x',\tau_1)\,. \quad (2.10)$$

This integral equation is known as the *time-dependent Lippmann-Schwinger equation*, and is equivalent to the TDSE (2.8a)[6]. Note that the (unknown) propagator appears in both sides of (2.10). Iteratively substituting the expression of $K(x,x',\tau)$ into the right hand side of (2.10) generates a Dyson series for the propagator K.

We now explore in more details the simple case of a free particle, and recall the important example of Gaussian wave packets. This provides an intuitive introduction to the frozen Gaussian regime that will be extensively used in the sequel.

2.2 Frozen Gaussian regime

In this section we specifically discuss the free motion of localised wave packets. To be more precise, we assume the initial state of the particle is the Gaussian wave packet $\psi_{\alpha_0,x_0,v_0}(x,0)$ given by

$$\psi_{\alpha_0,x_0,v_0}(x,0) = \left(\frac{2\,\alpha_0}{\pi}\right)^{\frac{1}{4}} \exp\left[-\alpha_0(x-x_0)^2 + i\frac{mv_0}{\hbar}(x-x_0)\right]\,, \quad (2.11)$$

where x_0 and v_0 correspond to the initial mean position and mean velocity of the particle, respectively, and α_0 is related to the spatial extent of the wave packet. Calling σ the width of the wave packet, related to the full width at half maximum through

$$FWHM = 2\sqrt{\ln 2}\sigma \approx 1.7\sigma\,, \quad (2.12)$$

the quantity α_0 is then given by

[6] Therefore, it does not embed any of the IC or BC's (2.8b)-(2.8c).

$$\alpha_0 = \frac{1}{2\sigma^2} > 0\,. \tag{2.13}$$

The reduced de Broglie wavelength $\lambda\!\!\!^{-}_0$ is then defined by

$$\lambda\!\!\!^{-}_0 \equiv \frac{\hbar}{m v_0}\,. \tag{2.14}$$

The particular choice (2.11) as the initial state of the system presents several advantages. First, it allows to build up a physical intuition of dynamics that will prove useful in more complicated physical setups. Furthermore, such an initial state is relevant on a more applied ground, as localised wave packets are routinely used in experiments with ultracold atoms (see e.g. [26,34,35]). For concreteness, we assume hereinafter that the parameters x_0 and v_0 in (2.11) satisfy

$$\begin{cases} x_0 < 0 \\ v_0 > 0 \end{cases}\,. \tag{2.15}$$

The particle is thus supposed to be initially localised on the left of the origin around the position x_0, and propagates to the right with a positive mean velocity v_0[7].

The state evolved freely from the initial state (2.11) in a time $\tau \geqslant 0$ is denoted by $\psi_{\alpha_0, x_0, v_0}(x, \tau)$, and reads, in view of (2.5),

$$\psi_{\alpha_0, x_0, v_0}(x, \tau) = \int_{-\infty}^{+\infty} dx'\, K_0(x - x', \tau) \psi_{\alpha_0, x_0, v_0}(x', 0)\,, \tag{2.16}$$

where the free-particle propagator K_0 is given by (2.9), and it is shown that $\psi_{\alpha_0, x_0, v_0}$ can be written in the form

$$\psi_{\alpha_0, x_0, v_0}(x, \tau) = \left(\frac{2\,\alpha_0}{\pi}\right)^{\frac{1}{4}} \sqrt{\frac{\alpha_\tau}{\alpha_0}} \exp\left[-\alpha_\tau\,(x - x_\tau)^2 + i\frac{m v_0}{\hbar}\,(x - x_\tau) + i\frac{m v_0^2}{2\hbar}\tau\right]\,, \tag{2.17}$$

where the two functions α_τ[8] and x_τ are defined by

[7] We will later consider a barrier located at the origin, i.e. at position $x = 0$. This will break the space symmetry of the free-particle situation considered here.

[8] Because the quantity α_τ is generally complex (see (2.18)), a particular branch of the complex square root is chosen in (2.17), namely the one where $\sqrt{i} = \exp(i\pi/4)$.

$$\alpha_\tau \equiv \frac{\alpha_0}{1 + i\frac{2\hbar\alpha_0}{m}\tau} \tag{2.18}$$

and

$$x_\tau \equiv x_0 + v_0\tau\,. \tag{2.19}$$

Therefore, it is readily seen from (2.17) that a freely evolved Gaussian wave packet remains Gaussian. This feature allows for exact evaluations of the expectation values of various observables.

Consider an observable $A(X, P)$, taken as an arbitrary function of the position and momentum operators X and P, respectively. The expectation value, denoted by $\langle A(X,P)\rangle_\tau$, of A when the system is in the dynamical state $\psi(x,\tau)$ at time $\tau \geqslant 0$ is defined by (in the position representation)

$$\langle A(X,P)\rangle_\tau \equiv \frac{\int_{-\infty}^{+\infty} dx\, \psi^*(x,\tau) A\left(x, -i\hbar\,\frac{\partial}{\partial x}\right)\, \psi(x,\tau)}{\int_{-\infty}^{+\infty} dx\, \psi^*(x,\tau)\psi(x,\tau)}\,, \tag{2.20}$$

where the asterisk denotes complex conjugation. It is thus straightforward to compute for instance the expectation values $\langle X\rangle_\tau$ and $\langle P\rangle_\tau$ of, respectively, the position and momentum operators when a free particle is in the Gaussian state (2.17), and it can be shown that

$$\langle X\rangle_\tau = x_\tau = x_0 + v_0\tau \tag{2.21}$$

and

$$\langle P\rangle_\tau = mv_0\,. \tag{2.22}$$

Differentiating (2.21) and (2.22) with respect to τ hence yields the following expressions for the time evolution of $\langle X\rangle_\tau$ and $\langle P\rangle_\tau$:

$$\frac{d}{d\tau}\langle X\rangle_\tau = \frac{\langle P\rangle_\tau}{m} \qquad \text{and} \qquad \frac{d}{d\tau}\langle P\rangle_\tau = 0\,. \tag{2.23}$$

Therefore, as can be readily seen on (2.23), the time evolution of the expectation values of the position and momentum operators is precisely governed by the *classical*

equations of motion when the dynamical state of a free particle is given by the Gaussian wave packet (2.17). This fact can actually be generalised to an arbitrary initial state as long as the Hamiltonian is a polynomial no higher than quadratic in both X and P, a special case of Ehrenfest's theorem [1, 2].

The Gaussian nature of the wave packet (2.17) allows for an exact evaluation of the standard deviations $(\Delta x)_\tau$ and $(\Delta p)_\tau$ of, respectively, the position and momentum operators at time $\tau \geqslant 0$, and it is shown that

$$(\Delta x)_\tau \equiv \sqrt{\langle X^2\rangle_\tau - \langle X\rangle_\tau^2} = \frac{\sigma}{\sqrt{2}}\sqrt{1+\frac{\hbar^2\tau^2}{m^2\sigma^4}} \tag{2.24}$$

and

$$(\Delta p)_\tau \equiv \sqrt{\langle P^2\rangle_\tau - \langle P\rangle_\tau^2} = \frac{\hbar}{\sqrt{2}\,\sigma}\,. \tag{2.25}$$

Note that the expressions (2.24) and (2.25) of the standard deviations allow to rewrite them in the form

$$(\Delta p)_\tau = (\Delta p)_0 = \frac{\hbar}{2\,(\Delta x)_0} \qquad \text{and} \qquad (\Delta x)_\tau = \sqrt{(\Delta x)_0^2 + \left[\frac{(\Delta p)_0\,\tau}{m}\right]^2}\,. \tag{2.26}$$

As it turns out, the freely evolved Gaussian wave packet (2.17) possesses an exact correspondence with a corresponding Gaussian distribution of *classical* free particles [36]. This correspondence hence offers a physical interpretation of the time-dependent width $(\Delta x)_\tau$ in terms of classical dynamics.

To see this, first note that the modulus squared of (2.17) can be written in the form

$$|\psi_{\alpha_0,x_0,v_0}(x,\tau)|^2 = \frac{1}{\sqrt{2\pi}\,(\Delta x)_\tau}\exp\left[-\frac{(x-x_\tau)^2}{2\,(\Delta x)_\tau^2}\right]\,. \tag{2.27}$$

Then consider a Gaussian distribution of classical free particles, initially given by

$$P_C(x,p,0) = \frac{1}{2\pi\Delta_x\Delta_p}\exp\left[-\frac{(x-x_0)^2}{2\Delta_x^2} - \frac{(p-p_0)^2}{2\Delta_p^2}\right]\,. \tag{2.28}$$

The particles are thus initially distributed around the mean position x_0 and mo-

mentum $p_0 \equiv mv_0$, with a spreading Δ_x in position and Δ_p in momentum. The distribution $P_C(x,p,\tau)$ at any time $\tau > 0$ obeys the free-particle Liouville equation, and it can be shown that

$$P_C(x,p,\tau) = \frac{1}{2\pi\Delta_x\Delta_p} \exp\left[-\frac{(x-x_\tau)^2}{2\Delta_x^2} - \frac{(p-p_0)^2}{2\Delta_p^2}\right] . \tag{2.29}$$

Integrating now (2.29) with respect to the momentum p yields

$$\int_{-\infty}^{+\infty} dp\, P_C(x,p,\tau) = \frac{1}{\sqrt{2\pi}\,(\Delta_x)_\tau} \exp\left[-\frac{(x-x_\tau)^2}{2\,(\Delta_x)_\tau^2}\right] , \tag{2.30}$$

where $(\Delta_x)_\tau$ is defined by

$$(\Delta_x)_\tau \equiv \sqrt{\Delta_x^2 + \left[\frac{\Delta_p \tau}{m}\right]^2} . \tag{2.31}$$

It is thus clear on (2.27) and (2.30) that the quantum and classical distributions of position x are exactly the same if we take the initial widths in both position and momentum to be equal, i.e. $\Delta_x = (\Delta x)_0$ and $\Delta_p = (\Delta p)_0$. Incidentally, this quantum-classical correspondence is exact upon assuming that the classical widths Δ_x and Δ_p satisfy the (minimum) uncertainty relation $\Delta_p = \hbar/2\Delta_x$.

The uncertainty relation can be readily obtained from (2.24) and (2.25), as it is seen that the uncertainties $(\Delta x)_\tau$ and $(\Delta p)_\tau$ satisfy

$$(\Delta x)_\tau\,(\Delta p)_\tau = \frac{\hbar}{2}\sqrt{1 + \frac{\hbar^2\tau^2}{m^2\sigma^4}} \geqslant \frac{\hbar}{2} , \tag{2.32}$$

for any $\tau \geqslant 0$. The (dimensionless) quantity $\hbar\tau/m\sigma^2$ can thus be readily seen on (2.24) as a measure of the increase of the spatial spreading of a freely propagated Gaussian wave packet as time evolves. Alternatively, it can be seen on (2.32) that $\hbar\tau/m\sigma^2$ quantifies the increase, as time evolves, of the global uncertainty of a freely propagated Gaussian wave packet. Now, if sufficiently short times τ are considered so that $\hbar\tau/m\sigma^2 \ll 1$ during the whole motion of the particle, then it is possible to neglect this term in (2.24) or (2.32). The moving wave packet thus spreads negligibly as time evolves.

It is useful to introduce the quantity ϵ, defined by

$$\epsilon \equiv \frac{\hbar t}{m\sigma^2} \,. \tag{2.33}$$

This parameter hence quantifies the increase of the spatial spreading of the freely-evolved Gaussian wave packet $\psi_{\alpha_0, x_0, v_0}$ after a time t. Therefore, the assumption

$$\epsilon \ll 1 \tag{2.34}$$

defines a particular regime that in the sequel will be referred to, in view of [37], as the *frozen Gaussian regime*. The name is rather self-explanatory, as the assumption (2.34) describes free Gaussian wave packets whose shape do not change in the course of their motion, i.e. as time evolves from 0 to the final value t, and hence appear "frozen". Since (2.32) can be written in the form

$$(\Delta x)_\tau \, (\Delta p)_\tau = \frac{\hbar}{2} + \mathcal{O}(\epsilon^2) \,, \tag{2.35}$$

for any $0 < \tau \leqslant t$, the regime defined by the condition (2.34) suggests the following physical picture. The system starts from the minimum uncertainty initial state (2.11) (as (2.32) implies that $(\Delta x)_0 \, (\Delta p)_0 = \hbar/2$), and is then described at any time $0 < \tau \leqslant t$ by the wave packet (2.17) that remains, to the first order in ϵ, a minimum uncertainty state. Therefore, during its motion the particle is as classical as it can be, for the fundamental quantum uncertainty stemming from Heisenberg's relation is kept at its minimum at any time $0 \leqslant \tau \leqslant t$.

This frozen Gaussian regime hence allows to simplify the expression (2.17) of the freely-evolved Gaussian wave packet $\psi_{\alpha_0, x_0, v_0}(x, \tau)$, for any $0 < \tau \leqslant t$. Indeed, in view of the definitions (2.18) and (2.33), the quantity α_τ can, in the frozen Gaussian regime, be written in the form

$$\alpha_\tau = \frac{\alpha_0}{1 + i\epsilon\frac{\tau}{t}} = \alpha_0 + \mathcal{O}\left(\epsilon\right) \,, \tag{2.36}$$

for any $0 < \tau \leqslant t$. Therefore, combining (2.17) with (2.36) yields in the frozen Gaussian regime

$$\psi_{\alpha_0, x_0, v_0}(x, \tau) = \left[1 + \mathcal{O}\left(\epsilon\right)\right] \psi_{\alpha_0, x_\tau, v_0}(x, 0) \mathrm{e}^{i\frac{mv_0^2}{2\hbar}\tau} \,, \tag{2.37}$$

for any $0 < \tau \leqslant t$.

Such a picture is only suitable for finite times, as it is clear from (2.32) that the uncertainty irremediably increases as time evolves (reaching a linear time dependence for large times). The value that the observation time t can achieve depends on the physical system under consideration. For instance, note on (2.33) that the parameter ϵ varies as the inverse of the mass. Therefore, any other parameter remaining constant, the heavier the particle the larger may t be for the condition (2.34) to be satisfied. As a matter of illustration we take two concrete examples. Consider for instance the two alkali-metal atoms[9] ^{7}Li and ^{87}Rb, with atomic masses $m_{\mathrm{Li}} = 7.016003$ u and $m_{\mathrm{Rb}} = 86.9091805$ u, respectively[10]. Suppose that the spatial dispersion and observation time are taken to be $\sigma = 30$ μm and $t = 100$ ms, respectively[11]. For such values we hence have $\epsilon_{\mathrm{Li}} \approx 1.006 \sim 1$ and $\epsilon_{\mathrm{Rb}} \approx 0.081 \ll 1$. While the ^{87}Rb atom evolves in the frozen Gaussian regime, the ^{7}Li atom does not.

Therefore, freely propagated Gaussian wave packets allowed us to introduce in a natural way the frozen Gaussian regime described by the assumption (2.34). If in general the dynamical state $\psi(x, \tau)$ of the system will obviously not be as simple as (2.17), the intuition provided by such simple localised wave packets will prove useful in the subsequent chapters. We now discuss how the dynamical properties of the system can be obtained from a phase-space representation of its dynamical state.

2.3 Quantum Mechanics in phase space

We start this section with a brief reminder from classical statistical mechanics. The dynamical state of an arbitrary classical system with N degrees of freedom is specified by the $2N$ numbers $(q, p) \equiv (q_1, \ldots, q_N, p_1, \ldots, p_N)$[12], where q and p are the generalised coordinates and momenta, respectively [38]. Therefore, the state of the system at a particular time τ is represented by a point with coordinates (q, p) in the $2N$-dimensional *phase space*. Any physical quantity $\mathscr{F}$ is then represented by a function $f(q, p, \tau)$. Now, for a macroscopic system a particular point (q, p) of the corresponding phase space is commonly referred to as a microstate of the system[13] [39]. The number N of degrees of freedom of a macroscopic system makes

[9] Alkali-metal atoms are often the systems of choice in modern ultracold atom-optics experiments because of their peculiar electronic structure, particularly suited to Bose-Einstein condensation (see e.g. [12]).

[10] The numerical values regarding the masses of the different atoms were taken from the NIST website in Spring 2015.

[11] Such values are for instance very similar to the experimental parameters in [26], where a cloud of ^{87}Rb atoms could propagate up to a time of 150 ms.

[12] For convenience, the time-dependence of the coordinates is not explicitly denoted in this discussion.

[13] If the microscopic constituents of the system are distinguishable. The situation is slightly more complicated in the case of indistinguishable particles, as a microstate would then be the set of all the phase-space points which are equivalent in exchanging particles.

it practically impossible (and effectively undesirable) to exactly specify its microstate at any time. Here enter statistical methods to characterise the state of the system. Indeed, a certain probability is assigned to each microstate, and the macrostate can then be viewed as a statistical mixture of microstates. More precisely, in view of the continuous nature of the phase space, the macrostate is constructed via a phase-space probability density $\rho^{(C)}(q,p,\tau)$, such that $\rho^{(C)}(q,p,\tau)dqdp$ gives the probability for the microstate of the system at time τ to lie in a $2N$-dimensional ball of volume $dqdp$ centred at the point (q,p). This probability density can then be used to compute the average value $f_{\rm av}(\tau)$ of any physical quantity $f(q,p,\tau)$ through the $2N$-dimensional integral over phase space

$$f_{\rm av}(\tau) = \int dqdp\, f(q,p,\tau)\rho^{(C)}(q,p,\tau)\,. \tag{2.38}$$

Consider now the quantum case. The basic idea underlying the phase space formulation of Quantum Mechanics is to build up a quantum equivalent, denoted by $\rho^{(Q)}(q,p,\tau)$, of the classical phase-space probability density $\rho^{(C)}(q,p,\tau)$. The most fundamental representation of the state of a quantum system is by means of the so-called density operator. It is really an other concept of a quantum state, which reduces to the usual concept of state as a vector of the Hilbert space $\mathscr{H}$ only in the particular case of pure states [40]. The general phase space formulation of Quantum Mechanics uses the formalism of density operators. However, the kind of system under study throughout this work is a single quantum particle evolving in one dimension, i.e. in a two-dimensional phase space. We do not use the formalism of density operators here[14], and we now specifically discuss the phase-space representation of the pure states of the system.

Therefore, suppose the particle is in the (pure) state $|\psi(\tau\rangle)$. Let $A(X,P)$ denote an observable, arbitrary function of the position and momentum operators X and P, respectively. Its true quantum expectation value, or in short its true quantum average, $\langle A(X,P)\rangle_\tau$ at time τ is thus given by

$$\langle A(X,P)\rangle_\tau \equiv \frac{\langle\psi(\tau)|A(X,P)|\psi(\tau)\rangle}{\langle\psi(\tau)|\psi(\tau)\rangle}\,, \tag{2.39}$$

and reduces to (2.20) in the position representation. Comparing now the quantum average (2.39) with the classical average (2.38), it would be desirable to construct the quantum phase-space distribution $\rho^{(Q)}(x,p,\tau)$ so that for any observable $A(X,P)$

[14] We assume for instance that the initial mean velocity v_0 of the particle is perfectly determined, which is strictly valid only for zero temperature. Any nonzero temperature would indeed induce variations around v_0 because of thermal agitation.

the phase-space quantum average of the observable A, defined by

$$\langle A(X,P)\rangle_{\tau}^{(Q)} \equiv \frac{\int dxdp\, A(x,p)\rho^{(Q)}(x,p,\tau)}{\int dxdp\, \rho^{(Q)}(x,p,\tau)}\,, \tag{2.40}$$

gives the true quantum average (2.39). One of the main difficulties in constructing such a phase-space function stems from the noncommutativity of the position and momentum operators [41]. Indeed, note that $A(x,p)$ in the numerator of (2.40) is a scalar function of the scalar variables x and p, which can thus be associated with different functions of the noncommutative operators X and P. Therefore, the quantum distribution $\rho^{(Q)}(x,p,\tau)$ can not be uniquely defined: there actually exists an infinite class of valid phase-space quantum distributions, depending solely on the association rule used to map the scalar quantity $A(x,p)$ to an operator function $A(X,P)$ [42,43]. All these distribution functions are equivalent on the mathematical level and contain the same physical information. However, depending on the problem under study one particular distribution function may be more convenient than an other. Examples of quantum phase-space distributions are the Wigner, the Glauber-Sudarshan or the Husimi distributions. We focus on the latter, which we now present in more details.

The phase-space representation of the pure state $|\psi(\tau)\rangle$ known as the *Husimi distribution*, denoted by $\mathcal{H}(\widetilde{x},\widetilde{v},\tau)$, is defined by

$$\mathcal{H}(\widetilde{x},\widetilde{v},\tau) \equiv |\langle \alpha_0,\widetilde{x},\widetilde{v}|\psi(\tau)\rangle|^2\,, \tag{2.41}$$

where $|\alpha_0,\widetilde{x},\widetilde{v}\rangle$ is by definition the minimum uncertainty state given in the position representation by the Gaussian wave packet

$$\psi_{\alpha_0,\widetilde{x},\widetilde{v}}(x,0) \equiv \langle x|\alpha_0,\widetilde{x},\widetilde{v}\rangle = \left(\frac{2\,\alpha_0}{\pi}\right)^{\frac{1}{4}} \exp\left[-\alpha_0(x-\widetilde{x})^2 + i\frac{m\widetilde{v}}{\hbar}(x-\widetilde{x})\right]\,, \tag{2.42}$$

with mean position $\widetilde{x}$ and mean velocity $\widetilde{v}$. The momentum $\widetilde{p}$ is defined through the simple relation

$$\widetilde{p} \equiv m\widetilde{v}\,. \tag{2.43}$$

The parameters $\widetilde{x}$ and $\widetilde{v}$ are taken to span the whole phase space, while the parameter α_0 (defined by (2.13)) is supposed to be fixed and does not explicitly appear as a parameter of $\mathcal{H}$. The *Husimi amplitude* $h(\widetilde{x},\widetilde{v},\tau)$, defined by

$$h(\widetilde{x},\widetilde{v},\tau) \equiv \langle \alpha_0,\widetilde{x},\widetilde{v}|\psi(\tau)\rangle\,, \tag{2.44}$$

is introduced so that the Husimi distribution $\mathcal{H}(\widetilde{x},\widetilde{v},\tau)$ can be written in the form

$$\mathcal{H}(\widetilde{x},\widetilde{v},\tau) = |h(\widetilde{x},\widetilde{v},\tau)|^2\ . \tag{2.45}$$

Writing (2.44) in the position representation then yields

$$h(\widetilde{x},\widetilde{v},\tau) = \int_{-\infty}^{+\infty} dx\, \psi^*_{\alpha_0,\widetilde{x},\widetilde{v}}(x,0)\psi(x,\tau)\,. \tag{2.46}$$

Using the identity (clear from the definitions (2.13) and (2.42))

$$\psi^*_{\alpha_0,\widetilde{x},\widetilde{v}}(x,0) = \psi_{\alpha_0,\widetilde{x},-\widetilde{v}}(x,0)\,, \tag{2.47}$$

the Husimi amplitude (2.46) is thus given by

$$h(\widetilde{x},\widetilde{v},\tau) = \int_{-\infty}^{+\infty} dx\, \psi_{\alpha_0,\widetilde{x},-\widetilde{v}}(x,0)\psi(x,\tau)\,. \tag{2.48}$$

It is readily seen from its definition (2.41) that the Husimi distribution quantifies the overlap between the minimum uncertainty state $|\alpha_0,\widetilde{x},\widetilde{v}\rangle$ and the state $|\psi(\tau)\rangle$ of the system at time τ. The integral (2.46) corresponds to the Hermitian inner product on the Hilbert space $\mathrm{L}^2(\mathbb{R})$ of the square-integrable functions. Therefore, the Cauchy-Schwarz inequality on $\mathrm{L}^2(\mathbb{R})$ [44] ensures that the Husimi distribution has the upper bound (note that by construction the Gaussian wave packet $\psi_{\alpha_0,\widetilde{x},\widetilde{v}}(x,0)$ is normalised)

$$\mathcal{H}(\widetilde{x},\widetilde{v},\tau) \leqslant \int_{-\infty}^{+\infty} dx\ |\psi(x,\tau)|^2\ , \tag{2.49}$$

with equality if and only if the state $\psi(x,\tau)$ is collinear to the Gaussian wave packet $\psi_{\alpha_0,\widetilde{x},\widetilde{v}}(x,0)$. On the other hand, the case $\mathcal{H}(\widetilde{x},\widetilde{v},\tau) = 0$ means that $\psi(x,\tau)$ is orthogonal to $\psi_{\alpha_0,\widetilde{x},\widetilde{v}}(x,0)$. Therefore, the Husimi distribution $\mathcal{H}(\widetilde{x},\widetilde{v},\tau)$ can be seen as a test of the $\widetilde{x}$- and $\widetilde{v}$-dependence of the dynamical state $\psi(x,\tau)$. By varying $\widetilde{x}$ and $\widetilde{v}$, the behaviour of $\psi(x,\tau)$ over the whole phase space can be probed, to see how close it is from a simple Gaussian wave packet centred at a particular phase-

space point. Some of the general properties of the Husimi distribution are now briefly discussed.

A first characteristic is that the marginal distributions of $\mathcal{H}(\widetilde{x},\widetilde{v},\tau)$ do not yield the position or momentum wave functions [40]. Indeed, its position marginal distribution, denoted by $\mathcal{X}(\widetilde{x},\tau)$, is given by

$$\mathcal{X}(\widetilde{x},\tau) \equiv \int_{-\infty}^{+\infty} d\widetilde{p}\, \mathcal{H}\left(\widetilde{x},\frac{\widetilde{p}}{m},\tau\right) = 2\pi\hbar \int_{-\infty}^{+\infty} dx\, \frac{1}{\sqrt{\pi}\sigma}\, \mathrm{e}^{-\frac{(x-\widetilde{x})^2}{\sigma^2}}\, |\langle x|\psi(\tau)\rangle|^2 \ , \quad (2.50)$$

while its momentum marginal distribution, denoted by $\mathcal{P}(\widetilde{p},\tau)$, is given by

$$\mathcal{P}(\widetilde{p},\tau) \equiv \int_{-\infty}^{+\infty} d\widetilde{x}\, \mathcal{H}\left(\widetilde{x},\frac{\widetilde{p}}{m},\tau\right) = 2\pi\hbar \int_{-\infty}^{+\infty} dp\, \frac{1}{\sqrt{\pi}}\frac{\sigma}{\hbar}\, \mathrm{e}^{-\frac{\sigma^2}{\hbar^2}(p-\widetilde{p})^2}\, |\langle p|\psi(\tau)\rangle|^2 \ . \quad (2.51)$$

Therefore, in view of the Gaussian representation of the δ-function

$$\delta(\xi) = \lim_{\eta\to 0} \frac{1}{\sqrt{\pi}\eta}\, \mathrm{e}^{-\frac{\xi^2}{\eta^2}} \ , \quad (2.52)$$

it is clear from (2.50) and (2.51) that

$$\lim_{\sigma\to 0} \mathcal{X}(\widetilde{x},\tau) = 2\pi\hbar\, |\langle\widetilde{x}|\psi(\tau)\rangle|^2 \quad (2.53)$$

and

$$\lim_{\sigma\to\infty} \mathcal{P}(\widetilde{p},\tau) = 2\pi\hbar\, |\langle\widetilde{p}|\psi(\tau)\rangle|^2 \ . \quad (2.54)$$

That is, the position (momentum) wave function can be asymptotically recovered at the cost of losing all the information about the momentum (position). It is worth recalling that there exist quantum phase-space distributions whose marginals are equal to the position and momentum wave functions [41], such as the Wigner distribution for instance.

In general, the true quantum expectation value of an observable A is not recovered simply from the phase-space relation (2.40) with the Husimi distribution. This stems from the specific rule required to associate the operator quantity $A(X,P)$ with the scalar quantity $A(x,p)$ in (2.40) when replacing $\rho^{(Q)}(x,p,\tau)$ by $\mathcal{H}(x,p/m,\tau)$ (see e.g. the review [41]). However, the expectation values $\langle X\rangle_\tau$ and $\langle P\rangle_\tau$ of, respectively,

the position and momentum operators are merely given by

$$\langle X\rangle_\tau = \frac{\int_{\mathbb{R}^2} d\widetilde{x}d\widetilde{p}\,\widetilde{x}\,\mathcal{H}\left(\widetilde{x},\frac{\widetilde{p}}{m},\tau\right)}{\int_{\mathbb{R}^2} d\widetilde{x}d\widetilde{p}\,\mathcal{H}\left(\widetilde{x},\frac{\widetilde{p}}{m},\tau\right)}\,, \tag{2.55}$$

and

$$\langle P\rangle_\tau = \frac{\int_{\mathbb{R}^2} d\widetilde{x}d\widetilde{p}\,\widetilde{p}\,\mathcal{H}\left(\widetilde{x},\frac{\widetilde{p}}{m},\tau\right)}{\int_{\mathbb{R}^2} d\widetilde{x}d\widetilde{p}\,\mathcal{H}\left(\widetilde{x},\frac{\widetilde{p}}{m},\tau\right)}\,. \tag{2.56}$$

Finally, we conclude this section with the simple example of the Husimi distribution associated with the Gaussian wave packet $\psi_{\alpha_0,\,x_\tau,\,v_0}(x,0)\exp(imv_0^2\tau/2\hbar)$[15]. In view of (2.48) the corresponding Husimi amplitude, denoted by $h^{(\mathrm{fr})}_{\mathrm{free}}(\widetilde{x},\widetilde{v},\tau)$[16], is defined by

$$h^{(\mathrm{fr})}_{\mathrm{free}}(\widetilde{x},\widetilde{v},\tau) \equiv \int_{-\infty}^{+\infty} dx\,\psi_{\alpha_0,\,\widetilde{x},\,-\widetilde{v}}(x,0)\psi_{\alpha_0,\,x_\tau,\,v_0}(x,0)\mathrm{e}^{i\frac{mv_0^2}{2\hbar}\tau}\,, \tag{2.57}$$

and thus, substituting the expression (2.42) into (2.57), it is shown (remember the definition (2.13) of α_0) that

$$h^{(\mathrm{fr})}_{\mathrm{free}}(\widetilde{x},\widetilde{v},\tau) = \exp\left\{-\frac{(\widetilde{x}-x_\tau)^2}{4\sigma^2} - \frac{m^2\sigma^2}{4\hbar^2}\,(\widetilde{v}-v_0)^2\right\}\mathrm{e}^{i\theta(\widetilde{x},\widetilde{v},\tau)}\,, \tag{2.58}$$

where the function θ is given by

$$\theta(\widetilde{x},\widetilde{v},\tau) = \frac{m}{2\hbar}\,(\widetilde{x}-x_\tau)\,(v_0+\widetilde{v}) + \frac{mv_0^2}{2\hbar}\tau\,. \tag{2.59}$$

The corresponding Husimi distribution $\mathcal{H}^{(\mathrm{fr})}_{\mathrm{free}}(\widetilde{x},\widetilde{v},\tau)$ is, in view of (2.45), defined by

$$\mathcal{H}^{(\mathrm{fr})}_{\mathrm{free}}(\widetilde{x},\widetilde{v},\tau) \equiv \left|h^{(\mathrm{fr})}_{\mathrm{free}}(\widetilde{x},\widetilde{v},\tau)\right|^2\,. \tag{2.60}$$

Substituting the expression (2.58) into (2.60) hence yields the *frozen Gaussian Husimi distribution*

[15] We recall that this particular wave packet is nothing but a freely evolved Gaussian wave packet in the frozen Gaussian regime.

[16] The superscript "(fr)" stands for "frozen".

$$\mathcal{H}^{(\mathrm{fr})}_{\mathrm{free}}(\widetilde{x},\widetilde{v},\tau) = \exp\left\{-\frac{(\widetilde{x}-x_\tau)^2}{2\sigma^2} - \frac{m^2\sigma^2}{2\hbar^2}\,(\widetilde{v}-v_0)^2\right\}. \tag{2.61}$$

This latter is Gaussian in both the position $\widetilde{x}$ and the velocity $\widetilde{v}$. It is clear that the Husimi distribution (2.61) is peaked in the phase space around the point (x_τ, v_0). The typical widths of this peak in the $\widetilde{x}$- and $\widetilde{v}$-directions, denoted by $(\Delta\widetilde{x})^{(\mathrm{fr})}_{\mathrm{free}}$ and $(\Delta\widetilde{v})^{(\mathrm{fr})}_{\mathrm{free}}$, respectively, are given by

$$(\Delta\widetilde{x})^{(\mathrm{fr})}_{\mathrm{free}} = \frac{\sigma}{\sqrt{2}} \tag{2.62}$$

and

$$(\Delta\widetilde{v})^{(\mathrm{fr})}_{\mathrm{free}} = \frac{\hbar}{\sqrt{2}m\sigma}\,. \tag{2.63}$$

The fact that $(\Delta\widetilde{x})^{(\mathrm{fr})}_{\mathrm{free}}$ is time-independent is a direct consequence of the frozen Gaussian regime, defined by the condition (2.34).

As can be readily seen from its definition (2.41), the Husimi distribution is always positive, unlike for instance the Wigner distribution. Being defined as an overlap with the probe Gaussian wave packet (2.42), the Husimi distribution will appear to be convenient in our subsequent calculations. We now conclude this chapter with a brief discussion of the notion of matter-wave absorption.

2.4 Matter-wave absorption

We introduce the concept of matter-wave absorption by means of a simple example, depicted on figure 1. Consider two identical atoms having two possible internal states, the ground state $|1\rangle$ of energy E_1 and the excited state $|2\rangle$ of energy E_2, with $E_1 < E_2$. An atom is assumed to be detectable only when it is in its ground state. Both atoms are initially prepared in the state $|1\rangle$, and they evolve in one dimension with some (mean) velocity v. They propagate freely until they encounter a laser beam. They cross the laser and then propagate again freely until the final time t. Now suppose that the frequency of the laser light has been precisely matched with the transition frequency between the two internal states $|1\rangle$ and $|2\rangle$ of the atoms. As it crosses the laser an atom may thus get excited by absorbing a photon: this is precisely what happens to one of the atoms. This means that if a measurement is performed at the final time t, the atom in its excited state can not be detected any

more. This atom is said to have been *absorbed* by the laser radiation. Conversely, the atom that remained in its ground state is said to have been *transmitted* through the laser (in other words, it survived the laser).

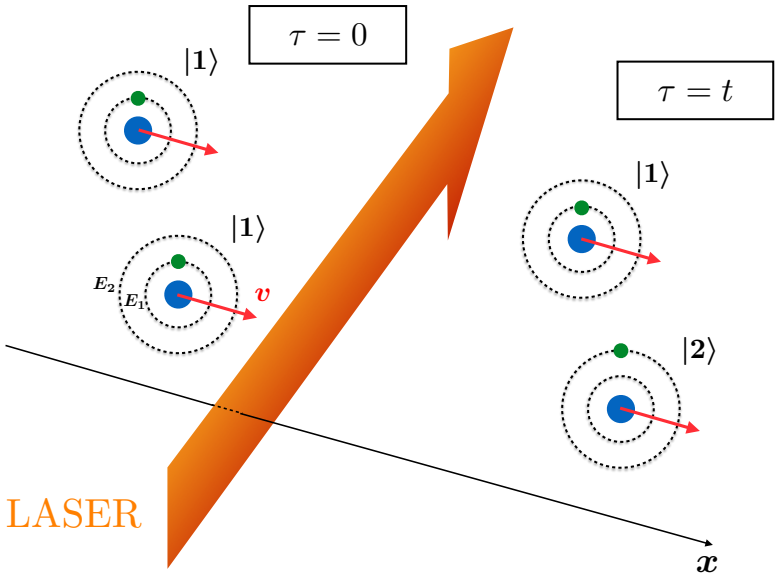

Figure 1: Illustration of the concept of matter-wave absorption.

Therefore, the atom has been absorbed if it became invisible during the process: from an initially detectable state, the system evolved into an undetectable state at the final time t. This behaviour can be seen in a vast range of physical setups, and is not restricted to atoms interacting with a laser beam. For instance, it might occur in an inelastic atomic collision where an atom may end up ionised, or else in chemistry where reacting molecules may get transformed into different chemical compounds. A key feature of matter-wave absorption can thus be readily identified: it implies in particular a non-conservation of the probability. Indeed, in the above example the initial probability $\mathscr{P}(0)$ to detect an atom is by construction 1. However, the corresponding probability at time t will in general be smaller than 1, $\mathscr{P}(t) \leqslant 1$.

On a more quantitative level, the dynamical state of an atom at time τ can be written as $\psi_1(x,\tau)|1\rangle + \psi_2(x,\tau)|2\rangle$, where the two components ψ_1 and ψ_2 satisfy the initial conditions $\int dx|\psi_1(x,0)|^2 = 1$ and $\psi_2(x,0) = 0$. In view of the above discussion, the component ψ_2 satisfies in general $\psi_2(x,\tau) \neq 0$ for $\tau > 0$. The non-conservation of the probability of detecting the atom stems from the non-conservation of the norm of the component ψ_1, that is

$$\frac{d}{d\tau}\left[\int_{-\infty}^{+\infty} dx\ |\psi_1(x,\tau)|^2\right] \neq 0\,. \tag{2.64}$$

It may be the case that only the time-evolution of the component $\psi_1(x,\tau)$ is of

practical interest. Treating the atom as a two-level system still requires to solve for both the components ψ_1 and ψ_2. That is, the component ψ_1 can not be derived independently of the other component ψ_2. Therefore, it may be convenient to approach the problem of determining only ψ_1 from a different point of view. Rather than a two-level system, consider a structureless quantum particle whose dynamical state is the wave function $\psi(x,\tau)$[17]. The question is: how can the wave function $\psi(x,\tau)$ follow the same dynamics as the component $\psi_1(x,\tau)$? A necessary condition is, as can be readily seen from (2.64), the non-conservation of the norm of the wave function ψ, that is

$$\frac{d}{d\tau}\left[\int_{-\infty}^{+\infty} dx\ |\psi(x,\tau)|^2\right] \neq 0\,. \tag{2.65}$$

A direct consequence is that the dynamics of such a quantum system *can not be unitary*.

A non-unitary dynamics of the wave function $\psi(x,\tau)$ may be obtained from a non-Hermitian Hamiltonian (see e.g. [20] for a general reference of non-Hermitian Quantum Mechanics). A typical approach is thus to include an absorbing complex potential into the Hamiltonian (see e.g. the review [21]). Such potentials describe generic absorbing *barriers* (such as for instance the laser beam in the above-discussed example). An other approach characterises the absorbing barrier by means of absorbing boundary conditions. In the next chapter, chapter 3, we present a specific example of how boundary conditions can adequately represent an absorbing barrier.

The latter model, termed in the sequel the aperture function model (AFM), was initially devised in Refs. [24] and [25]. It describes the one-dimensional motion of a structureless quantum particle submitted to a time-dependent pointlike absorbing barrier. Its main advantage is that it is exactly solvable for an arbitrary time-dependent barrier. However, while being mathematically consistent, it a priori lacks a clear physical basis. Indeed, the particular boundary conditions used to represent the absorbing barrier were not derived from first principles. It is the main purpose of the present work to give a strong physical ground to the AFM. This objective can hardly be achieved through comparing the AFM to a particular complex-potential-based model of time-dependent matter-wave absorption. Indeed, in such cases complex potentials are themselves approximations of the dynamics. Therefore, an unambiguous physical basis can be given to the AFM, which is already an approximation, only upon comparing it with a first-principles model. Such a model, referred to in the sequel as the δ-potential model (DPM), is discussed in section 3.1. It describes the interaction between a two-level atom and a thin time-

[17] In other words, the original two-channel problem is approached from a single-channel problem.

dependent laser beam. We emphasise that we focus in this thesis on a particular approach of matter-wave absorption (by means of absorbing boundary conditions), and do not treat the case of absorbing complex potentials. It is however worth recalling that complex potentials are powerful, and used in a wide range of physical applications, such as nuclear physics or scattering theory.

Equipped with the various techniques and concepts reviewed in this chapter, we are now in position to study the motion of localised wave packets in the presence of a time-dependent absorber. The next chapter, chapter 3, is thus devoted to presenting two different approaches of the problem.

Chapter 3

Models of a time-dependent absorbing barrier

In this chapter we introduce two different approaches of matter-wave absorption by a thin time-dependent barrier. The first one is called the δ-potential model (DPM), and is introduced in section 3.1. It provides a natural description of the problem discussed in section 2.4, where a two-level atom interacts with a localised time-dependent laser beam. The main advantage of the DPM is that it can be derived from first principles. We then present in section 3.2 a second model, termed here the aperture function model (AFM). It was initially devised in Refs. [24, 25], and represents a time-dependent absorbing barrier by means of particular boundary conditions. However, such absorbing boundary conditions lack an unambiguous physical justification. It is thus needed to advance the AFM to clarify its physical basis. To this end, we hypothesise in section 3.3 an explicit connection between the AFM and the DPM. It will then be the aim of the next chapter, chapter 4, to quantitatively justify this conjectured connection.

It is worth recalling here a remark from section 2.4. The main purpose of the present work is to provide a strong physical ground to the AFM. This could hardly be achieved by comparing the AFM to other models of absorbing barriers such as time-dependent absorbing complex potentials, as these latter are themselves approximations of the dynamics of a quantum system. Therefore, we do not consider absorbing complex potentials in the sequel.

3.1 δ-potential model

An atom can be viewed as a system of charged particles, while a laser radiation is described by an electromagnetic field. Therefore, atom-laser interaction is a special case of the more general problem of the interaction between a system of electric charges and an electromagnetic field. In this section we introduce a particular atom-

laser model: the δ-potential model (DPM). It describes the interaction between a moving two-level atom and a thin time-dependent laser beam. We first briefly discuss how it can be derived (details can be found in the appendix A).

Consider a system of charged particles, labelled with an index $n \in \mathbb{N}$. The $n^{-\text{th}}$ particle has a charge q_n and a mass m_n. The charges are submitted to an external electromagnetic field $\{\mathbf{E}_\text{e}(\mathbf{r},\tau), \mathbf{B}_\text{e}(\mathbf{r},\tau)\}$, treated classically. Now, suppose that the system of charges has a typical spatial extent a, for instance of the order of the Bohr radius $a_0 \approx 0.5$ Å. In the nonrelativistic limit, and assuming the *large wavelength approximation* in which the typical wavelength λ of the external field is much larger than a[1],

$$\frac{a}{\lambda} \ll 1\,, \tag{3.1}$$

it can be shown [45] that the dynamics of the system of charged particles submitted to the external field characterised by the potentials $\mathbf{A}_\text{e}$ and U_e is described by the minimal coupling Hamiltonian (Eq. (A.9))

$$H = \sum_n \frac{1}{2m_n}\left[\mathbf{p}_n - q_n\mathbf{A}_\text{e}(\mathbf{r}_n,\tau)\right]^2 + V_\text{Coul} + \sum_n q_n U_\text{e}(\mathbf{r}_n,\tau)\,, \tag{3.2}$$

where $\mathbf{r}_n$ and $\mathbf{p}_n$ denote, respectively, the position and momentum operators of the $n^{-\text{th}}$ particle, and

$$V_\text{Coul} = \frac{1}{4\pi\epsilon_0}\sum_{n>j}\frac{q_n q_j}{|\mathbf{r}_n - \mathbf{r}_j|} \tag{3.3}$$

represents the usual Coulomb interaction energy between different particles.

Note that no particular gauge needs to be specified regarding the external field in order to obtain the expression (3.2) of the Hamiltonian. It is however convenient to consider the gauge in which the vector potential vanishes. A gauge transformation is characterised in Quantum Mechanics by a unitary transformation [1]. It can then be shown [45] that for a *globally neutral* system of charges the *Göppert-Mayer transformation*, defined by the unitary operator

$$\mathcal{T} = \exp\left[-\frac{i}{\hbar}\,\mathbf{d}\cdot\mathbf{A}_\text{e}(\mathbf{C},\tau)\right]\,, \tag{3.4}$$

[1] If $a \sim a_0$, the large wavelength approximation is typically satisfied if $\lambda \gtrsim 10$ nm (extreme ultraviolet). In particular, this assumption is clearly satisfied for optical light ($\approx 400 - 700$ nm) and is even much better for microwaves (≈ 1 mm-1 m).

transforms the minimal coupling Hamiltonian (3.2) into the *electric dipole Hamiltonian* H_{ed} given by (Eq. (A.24))

$$H_{\text{ed}} = \sum_n \frac{\mathbf{p}_n^2}{2m_n} + V_{\text{Coul}} - \mathbf{d} \cdot \mathbf{E}_{\text{e}}(\mathbf{C}, \tau) \,, \tag{3.5}$$

where $\mathbf{C}$ is the centre of mass of the system of charges, i.e.

$$\mathbf{C} \equiv \frac{\sum\limits_n m_n \mathbf{r}_n}{\sum\limits_n m_n} \,, \tag{3.6}$$

and $\mathbf{d}$ is the electric dipole moment of the system with respect to its centre of mass, i.e.

$$\mathbf{d} \equiv \sum_n q_n \left(\mathbf{r}_n - \mathbf{C} \right) \,. \tag{3.7}$$

Suppose now that the system of charges is an atom of mass m, whose centre of mass evolves in one dimension, along the x-direction. Therefore, the state space $\mathscr{H}$ of the system is the tensor product of the state space $\mathscr{H}_x$ of the centre of mass with the state space $\mathscr{H}_{\text{int}}$ for the internal structure of the atom. The set $\{|x\rangle\}$, $x \in \mathbb{R}$, of position eigenstates is taken as a basis of $\mathscr{H}_x$ and the set $\{|j\rangle\}$, $j \in \mathbb{N}$, denotes a basis of $\mathscr{H}_{\text{int}}$. A basis of the full Hilbert space $\mathscr{H}$ is then given by $\{|x; j\rangle\}$, $x \in \mathbb{R}$ and $j \in \mathbb{N}$, where $|x; j\rangle = |x\rangle \otimes |j\rangle$. The centre-of-mass position and momentum operators are given by the operators X and P introduced in chapter 2. The atom is submitted to a laser radiation described by an electric field of the form

$$\mathbf{E}_{\text{e}}(X, \tau) = \mathcal{E}(\tau) \mathcal{F}(X) \mathbf{E}_0 \cos(\omega_l \tau) \,, \tag{3.8}$$

where $\mathcal{E}$ and $\mathcal{F}$ are two arbitrary scalar functions, and the constant vector $\mathbf{E}_0$ gives the polarisation direction of the electric field. The quantity ω_l is taken to be positive, $\omega_l > 0$. Consider now a particular atomic transition, corresponding to the internal states $|1\rangle$ and $|2\rangle$ of the atom. The energy E_2 of the state $|2\rangle$ is supposed to be larger than the energy E_1 of the state $|1\rangle$, $E_2 > E_1$. The frequency ω_l of the laser light is supposed to be *exactly resonant* with the transition $|1\rangle \to |2\rangle$, that is

$$\omega_l = \frac{E_2 - E_1}{\hbar} \,. \tag{3.9}$$

The condition (3.9) allows to restrict the Hilbert space $\mathscr{H}_{\text{int}}$ to a two-dimensional Hilbert space $\mathscr{H}_2$ (details can be found in section A.3). This is the *two-level approximation* [16, 17]).

A basis of $\mathscr{H}_2$ is readily given by $\{|1\rangle, |2\rangle\}$. The basis vectors $|1\rangle$ and $|2\rangle$ are then conveniently represented by the column vectors

$$|1\rangle = \begin{pmatrix} 1 \\ 0 \end{pmatrix} \qquad \text{and} \qquad |2\rangle = \begin{pmatrix} 0 \\ 1 \end{pmatrix} . \tag{3.10}$$

Therefore, in the interaction picture with respect to the internal degrees of freedom and using the rotating wave approximation, the Hamiltonian H_I describing the interaction of the moving two-level atom with the external field (3.8) is given by

$$H_I = \frac{P^2}{2m} \begin{pmatrix} 1 & 0 \\ 0 & 1 \end{pmatrix} + \hbar\Omega(\tau)\mathcal{F}(X) \begin{pmatrix} 0 & 1 \\ 1 & 0 \end{pmatrix} , \tag{3.11}$$

where the function $\Omega(\tau)$ is defined by

$$\Omega(\tau) \equiv -\frac{\mathcal{E}(\tau)}{2\hbar} \langle 2|\mathbf{d} \cdot \mathbf{E}_0|1\rangle . \tag{3.12}$$

.

The problem is now expressed in the position representation. Since the state space $\mathscr{H}$ of the moving two-level atom is the tensor product $\mathscr{H}_x \otimes \mathscr{H}_2$, the dynamical state $|\psi(\tau)\rangle$ of the system can be decomposed on the basis $\{|x; j\rangle\}$, $x \in \mathbb{R}$ and $j = 1, 2$, and reads

$$|\psi(\tau)\rangle = \int_{-\infty}^{+\infty} dx \sum_{j=1}^{2} \langle x; j|\psi(\tau)\rangle |x; j\rangle , \tag{3.13}$$

where the quantities $\langle x; j|\psi(\tau)\rangle$ are by construction complex numbers. It is readily seen on (3.13) that $|\psi(\tau)\rangle$ is fully specified by two wave functions $\psi_j(x, \tau) \equiv \langle x; j|\psi(\tau)\rangle$, $j = 1, 2$, which may conveniently be combined in the form of a column vector. Therefore, in the position representation, the dynamical state $|\psi(\tau)\rangle$ of the two-level atom is represented by

$$\widehat{\psi}(x, \tau) \equiv \begin{pmatrix} \psi_1(x, \tau) \\ \psi_2(x, \tau) \end{pmatrix} , \tag{3.14}$$

which is commonly referred to as a *spinor*[2]. Now, the position-dependent function $\mathcal{F}$ in (3.11) is taken to be a Dirac δ-function, that is

$$\mathcal{F}(\xi) = \delta(\xi)\,. \tag{3.15}$$

Because $\mathcal{F}$ embeds the spatial dependence of the electric field, we here consider with (3.15) the special case where the external electric field is homogeneous in the (y, z) plane (perpendicular to the x-direction), and only intercepts the direction of motion of the atom at the particular point $x = 0$. This particular dependence of the electric field on position must thus be viewed as describing the limit case of an infinitely thin (in the x-direction) laser sheet. This appears to be a natural description of the problem depicted on figure 1. Note that to model a physical laser beam by a pointlike δ-potential is an idealisation. This approximation is valid under the assumption that the spatial extent σ of the incident wave packet is much larger than the spatial extent (in the x-direction) of the laser light.

Substituting the expression (3.15) into (3.11) and using the position representation of the momentum operator P, we obtain the following Hamiltonian $\widehat{H}_{\mathrm{DPM}}$:

$$\widehat{H}_{\mathrm{DPM}} = \widehat{H}_0 + \widehat{V}(x, \tau)\,, \tag{3.16}$$

where

$$\widehat{H}_0 \equiv -\frac{\hbar^2}{2m}\frac{\partial^2}{\partial x^2}\begin{pmatrix} 1 & 0 \\ 0 & 1 \end{pmatrix} \tag{3.17}$$

is the matrix free-particle Hamiltonian, while

$$\widehat{V}(x, \tau) \equiv \hbar\Omega(\tau)\delta(x)\begin{pmatrix} 0 & 1 \\ 1 & 0 \end{pmatrix} \tag{3.18}$$

is the time-dependent δ-potential. For this reason, the model described by the Hamiltonian (3.16) is here termed the *δ-potential model* (DPM). The potential itself will often be referred to as the laser light, or the barrier, in the sequel. Note that the amplitude $\Omega(\tau)$ is, in view of its definition (3.12), directly related to the square root of the intensity of the laser[3]. It is taken to be a positive valued function of time

[2]More specifically, $\widehat{\psi}$ may also be called a *two-component* spinor.

[3]The intensity of an electromagnetic field is typically defined from the square of the electric field.

(which is possible by appropriately choosing the internal levels of the atom). It is also worth noting that this amplitude Ω has the physical dimension of a velocity[4].

Therefore, the dynamics of the system is governed by the TDSE

$$i\hbar\frac{\partial}{\partial\tau}\begin{pmatrix}\psi_1(x,\tau)\\ \psi_2(x,\tau)\end{pmatrix} = \widehat{H}_{\mathrm{DPM}}\begin{pmatrix}\psi_1(x,\tau)\\ \psi_2(x,\tau)\end{pmatrix}, \tag{3.19}$$

for any $0 < \tau < t$. In addition to the TDSE, usual Dirichlet boundary conditions are imposed on the components ψ_1 and ψ_2, that is

$$\lim_{x\to\pm\infty}\psi_1(x,\tau) = \lim_{x\to\pm\infty}\psi_2(x,\tau) = 0\,. \tag{3.20}$$

The notion of propagator, introduced in section 2.1 for a wave function, can be generalised here. The definition (2.5) is merely extended to the spinor $\widehat{\psi}$, and thus the dynamical state of the two-level atom at the final time t is given by

$$\widehat{\psi}(x,t) = \int_{-\infty}^{+\infty} dx'\,\widehat{K}(x,x',t)\widehat{\psi}(x',0)\,, \tag{3.21}$$

where $\widehat{K}$ is now a 2×2 matrix propagator,

$$\widehat{K}(x,x',t) = \begin{pmatrix}K_{11}(x,x',t) & K_{12}(x,x',t)\\ K_{21}(x,x',t) & K_{22}(x,x',t)\end{pmatrix}. \tag{3.22}$$

It is worth emphasising the strong physical basis of this model. As was briefly discussed in this section, it can indeed be derived from first principles using a reasonable set of assumptions, such as the large wavelength or rotating wave approximations. However, it admits exact, analytical solutions for the propagator only for very few specific time-dependent amplitudes Ω. A trivial example is the free two-level atom, for which $\Omega(\tau) = 0$ for any $\tau > 0$. In this case the propagator $\widehat{K}$ is merely given by the matrix free-particle propagator $\widehat{K}_0$, with

$$\widehat{K}_0(\xi,\tau) \equiv K_0(\xi,\tau)\begin{pmatrix}1 & 0\\ 0 & 1\end{pmatrix}. \tag{3.23}$$

A second example is the case of a time-independent amplitude, that is $\Omega(\tau) = \Omega_0$. An exact solution can indeed be obtained by means of the Lippmann-Schwinger

[4]Remember that $\int dx\delta(x) = 1$, and thus $\delta(x)$ has the dimension of the inverse of a length.

equation (2.10) and the method of Laplace transform [19]. The propagator, denoted by $\widehat{K}_{\Omega_0}$, is then given by

$$\widehat{K}_{\Omega_0}(\xi_1,\xi_2,\tau)=\widehat{K}_0(\xi_1-\xi_2,\tau)-\frac{m\Omega_0}{4\hbar}\sum_{j=\pm1}\mathrm{e}^{j\frac{m\Omega_0}{\hbar}(|\xi_1|+|\xi_2|)}\mathrm{e}^{i\frac{m\Omega_0^2}{2\hbar}\tau}\mathrm{erfc}(z_j)\begin{pmatrix}j & 1\\ 1 & j\end{pmatrix}, \tag{3.24}$$

where $\mathrm{erfc}(\cdot)=1-\mathrm{erf}(\cdot)$ is the complementary error function, and

$$z_j\equiv j\sqrt{i\frac{m\Omega_0^2}{2\hbar}\tau}+\sqrt{\frac{m}{2i\hbar\tau}}(|\xi_1|+|\xi_2|)\,, \tag{3.25}$$

with $j=\pm1$. Note that an alternative method to derive the propagator $\widehat{K}_{\Omega_0}$ is to introduce the linear combinations $\psi_\pm=\psi_1\pm\psi_2$ to obtain from the TDSE (3.19) two decoupled equations for ψ_+ and ψ_- separately. It is then possible to use the exact solution known for a single-channel time-independent δ-potential [46] (see also [33] for a Laplace-transform derivation) to obtain (3.24). This method can be advantageously applied to the example of a potential that is inversely proportional to time, i.e. $\Omega(\tau)=\Omega_1/\tau$, with Ω_1 a constant. Indeed, here again an exact propagator is known for the single-channel case [47]. Using this solution, we can then show that the matrix propagator, denoted by $\widehat{K}_{1/\tau}$, is given by

$$\widehat{K}_{1/\tau}(\xi_1,\xi_2,\tau)=\widehat{K}_0(\xi_1-\xi_2,\tau)-\frac{\Omega_1}{\Omega_1^2+\xi_2^2}K_0(|\xi_1|+|\xi_2|\,,\tau)\begin{pmatrix}\Omega_1 & i\,|\xi_2|\\ i\,|\xi_2| & \Omega_1\end{pmatrix}. \tag{3.26}$$

A generalisation of the latter exactly solvable case is studied in [48]. In the most general case however, i.e. for an arbitrary time-dependent amplitude $\Omega(\tau)$, the DPM is not exactly solvable. The TDSE (3.19) must then be solved by means of numerical methods.

Now, in view of the discussion relative to figure 1, we assume here that the atom is initially prepared in its lower energy state $|1\rangle$. Its initial state $\widehat{\psi}(x,0)$ is hence given by

$$\widehat{\psi}(x,0)=\begin{pmatrix}\psi_1(x,0)\\ 0\end{pmatrix}, \tag{3.27}$$

where the wave function $\psi_1(x,0)$ is supposed to be normalised,

$$\int_{-\infty}^{+\infty} dx\ |\psi_1(x,0)|^2 = 1\,. \tag{3.28}$$

Furthermore, to continue the analogy with figure 1, the atom is considered detectable when it is in the state $|1\rangle$, while it should be viewed as undetectable, or *absorbed*, when it is in the state $|2\rangle$. The initial condition (3.27) hence ensures that the atom is initially detectable. It is then clear that the effect of the δ-potential, being represented by an off-diagonal matrix, is to mix the populations of the two levels as time evolves, so that the probability of detecting the atom at any time $\tau > 0$ is in general different from 1. We are primarily interested in describing atoms which have survived the laser radiation. Therefore, the quantity of interest in this model is the component ψ_1 of the lower energy state of the atom. For clarity and convenience we relabel it as

$$\Psi_{\mathrm{DPM}}(\xi,\tau) \equiv \psi_1(\xi,\tau)\,. \tag{3.29}$$

Finally, we assume for concreteness that the atom is initially localised on the left of the laser. More precisely, we suppose that $\psi_1(x,0) \approx 0$ for any $x \geqslant 0$. Therefore, in view of (3.21), (3.22), (3.27) and (3.29), the wave function Ψ_{DPM} at the final time t is given by[5]

$$\Psi_{\mathrm{DPM}}(x,t) \approx \int_{-\infty}^{0} dx'\, K_{11}(x,x',t)\Psi_{\mathrm{DPM}}(x',0)\,. \tag{3.30}$$

We now introduce a second model, which approaches the problem of the interaction between a moving atom and a laser radiation from the point of view of matter-wave absorption.

3.2 Aperture function model

Here we present an alternative approach to the dynamics of the above two-level atom in its lower energy state. Consider the one-dimensional motion of a *structureless* particle of mass m, described by a wave function $\Psi_{\mathrm{AFM}}(x,\tau)$. As was already mentioned in section 2.4, in order for Ψ_{AFM} to have a similar time evolution as the wave function Ψ_{DPM}, the former must follow a non-unitary dynamics. The aim of this section is to introduce a possible description of non-unitary quantum dynamics

[5] To reduce the integration range from $]-\infty,+\infty[$ to $]-\infty,0[$ is justified in view of our later choice of a Gaussian wave packet as the initial state, hence making this approximation excellent.

by means of *absorbing boundary conditions*.

The model discussed here was originally devised in Refs. [24,25]. The particle is incident on an infinitely thin time-dependent absorbing barrier, located at position $x = 0$. The barrier is characterised by an arbitrary time-dependent function $\chi(\tau)$. This latter is called the aperture function, hence the name *aperture function model* (AFM) given here to this approach. The aperture function is a real-valued function of time, whose values range between 0 and 1. The case $\chi = 0$ corresponds to a barrier that completely absorbs matter waves, while the value $\chi = 1$ describes a perfectly transparent barrier. The presence of such an absorbing barrier is taken into account by imposing discontinuous time-dependent boundary conditions (BC's) on the wave function Ψ_{AFM} and its spatial derivative at $x = 0$. Such BC's appear as a time-dependent quantum mechanical generalisation of Kottler's treatment of diffraction of stationary fields at spatial apertures in black screens [49]. Kottler obtained similar predictions as with Kirchhoff's diffraction theory. The latter is found to be in good agreement with experimental data in the transmission region, that is in the region separated from the field source by the screen. It however lacks accuracy as compared to Sommerfeld's diffraction approach in the reflection region [50]. Therefore, the AFM is expected to yield relevant physical predictions at least on the side of the absorbing barrier opposite to the source. More precisely, and sticking to the choice already made at the end of the previous section for the DPM, we suppose that the particle is initially localised on the left of the barrier. That is, the initial state satisfies $\Psi_{\mathrm{AFM}}(x, 0) \approx 0$ for any $x > 0$. The transmission region is thus the region described by all the positive values of the position variable, that is $x > 0$. The region corresponding to $x < 0$ will be hereinafter referred to as the reflection region. Similarly to (3.30), the dynamical state $\Psi_{\mathrm{AFM}}(x, t)$ of the particle at the final time t is thus constructed from the initial state through

$$\Psi_{\mathrm{AFM}}(x, t) \approx \int_{-\infty}^{0} dx' \, K_{\mathrm{AFM}}(x, x', t) \Psi_{\mathrm{AFM}}(x', 0) \, . \tag{3.31}$$

The problem satisfied by the propagator K_{AFM} is now explicitly stated.

The propagator obeys the general problem (2.8), completed by two particular BC's at the point $x = 0$. These latter act as matching conditions between the two regions $x < 0$ and $x > 0$. More precisely, the propagator K_{AFM} obeys the free-particle TDSE on both sides of the barrier, that is

$$\left(i\hbar \frac{\partial}{\partial \tau} + \frac{\hbar^2}{2m} \frac{\partial^2}{\partial x^2} \right) K_{\mathrm{AFM}}(x, x', \tau) = 0 \, , \tag{3.32}$$

for any $0 < \tau < t$ and for $x, x' \neq 0$. It satisfies the initial condition

$$K_{\mathrm{AFM}}(x,x',0^+)=\delta(x-x') \tag{3.33}$$

and Dirichlet BC's at infinity,

$$\lim_{x\to\pm\infty} K(x,x',\tau)=0 \qquad \text{for} \qquad \tau=-i\,|\tau|\,. \tag{3.34}$$

Finally, the matching conditions, imposed on the propagator and its spatial derivative, at $x=0$ are given, for $x'<0$, by [25]

$$K_{\mathrm{AFM}}(x,x',\tau)\big|_{x=0^-}^{x=0^+} = -\left[1-\chi(\tau)\right] K_0(x,x',\tau)\big|_{x=0}\,, \tag{3.35}$$

$$\frac{\partial}{\partial x}K_{\mathrm{AFM}}(x,x',\tau)\bigg|_{x=0^-}^{x=0^+} = -\left[1-\chi(\tau)\right]\frac{\partial}{\partial x}K_0(x,x',\tau)\bigg|_{x=0}\,, \tag{3.36}$$

for $0<\tau<t$. The set of conditions formed by (3.32)-(3.36) forms a well-posed problem, whose main advantage is that it is *exactly solvable* for an *arbitrary* time-dependent aperture function χ. Indeed, it can be shown [25] that in the transmission region (i.e. for $x>0$)

$$K_{\mathrm{AFM}}(x,x',t)=\frac{1}{2}\int_0^t d\tau\,\chi(\tau)\left(\frac{x}{t-\tau}-\frac{x'}{\tau}\right)K_0(x,t-\tau)K_0(x',\tau)\,. \tag{3.37}$$

Combining (3.31) with (3.37) shows that the probability amplitude $\Psi_{\mathrm{AFM}}(x,t)$ of detecting the particle at position x (in the transmission region) at the final time t stems from summing the probability amplitudes associated with particular space-time paths. Any path, linking a point $x'<0$ to the point $x>0$, can be divided in two successive paths. First, a free motion from x' to the barrier in a time $\tau>0$, followed by a second free motion from the barrier to the point x in the remaining time $t-\tau$. Finally, each path is weighted by the value of the aperture function at the time τ at which the particle reaches the barrier, multiplied by the mean velocity at which the particle crosses the barrier[6]. The barrier itself can thus be viewed as a fictitious source, in accordance with the Huygens-Fresnel principle [24].

It is worth noting that the integral in (3.37) can be computed explicitly for

[6]Indeed, during the first (second) free motion the classical velocity is $v_1=-x'/\tau$ ($v_2=x/(t-\tau)$). Hence the particle reaches the barrier with the velocity v_1, and leaves it with the velocity v_2. The half sum of the two can thus be viewed as an average velocity for the particle crossing the barrier.

special examples of aperture functions χ. The simplest such example is the case of a completely transparent barrier, for which $\chi(\tau) = 1$ for any $\tau > 0$. In this case the particle propagates freely in unbounded space. The expression (3.37) of the propagator K_{AFM} corresponding to $\chi(\tau) = 1$ hence provides the following useful decomposition of the free-particle propagator K_0:

$$K_0(x - x', t) = \frac{1}{2}\int_0^t d\tau \left(\frac{x}{t-\tau} - \frac{x'}{\tau}\right) K_0(x, t-\tau) K_0(x', \tau)\,, \tag{3.38}$$

for any $x' < 0$ and $x > 0$. An other relevant example is the case of a sudden opening, at some time $0 < t_{\mathrm{o}} < t$, of a completely closed barrier. More precisely, the value of the aperture function is 0 for any $0 < \tau < t_{\mathrm{o}}$, and then 1 for any $t_{\mathrm{o}} < \tau < t$. The aperture function is thus given by $\chi(\tau) = \Theta(\tau - t_{\mathrm{o}})$, with Θ the Heaviside function. Such an instantaneously opening barrier is commonly referred to as the *Moshisnky shutter*, stemming from Moshinsky's paper [51] in which he introduced the concept of diffraction in time. Indeed, he showed that such a sharp removal of an absorbing barrier can induce oscillations in the particle's wave function whose mathematical structure is similar to the (spatial) Fresnel diffraction of light at a straight edge. Calling K_{M} the propagator obtained from (3.37) for such an aperture function (which we hence call the Moshinsky propagator), it is shown [24] that it can be written in the form

$$\begin{aligned} K_{\mathrm{M}}(x, x', t) &= \frac{1}{2}\int_{t_{\mathrm{o}}}^t d\tau \left(\frac{x}{t-\tau} - \frac{x'}{\tau}\right) K_0(x, t-\tau) K_0(x', \tau) \\ &= \int_{-\infty}^0 dx''\, K_0(x - x'', t - t_{\mathrm{o}}) K_0(x'' - x', t_{\mathrm{o}})\,. \end{aligned} \tag{3.39}$$

The very main advantage of the AFM is that it is exactly solvable, in the sense that the propagator is known for an arbitrary time-dependent aperture function. The expression (3.37) of the propagator can thus be used to obtain an essentially analytical form of the transmitted state $\Psi(x, t)$ at the final time t, evolved from an arbitrary initial state localised in the reflection region. This offers a versatile approach to investigate the effects of time-dependent absorbing barriers on the dynamics of localised wave packets. In particular, it was recently shown [28] that such barriers can be used to shift, split, squeeze and cool atomic wave packets. This demonstrates the practical interest of time-dependent matter-wave absorption, as it can be an efficient tool to manipulate the quantum state of an atom. However, we must at this stage point out a weakness of the AFM, rooted in the particular time-dependent BC's (3.35)-(3.36) used to describe the absorbing barrier. Indeed,

while being justified by Kirchhoff's diffraction theory for classical wave optics, such matching conditions lack a first-principles justification in the quantum mechanical context. In particular, remember that the main motivation in introducing the AFM is to provide a relevant theoretical tool to describe time-dependent atom-laser interactions. It must then be noted that the precise relation between the aperture function $\chi(\tau)$ (the fundamental free parameter of the AFM) and the physical quantities describing either the atom (e.g. its velocity) or the laser light (e.g. its intensity) is not at all clear.

Therefore, the main purpose of the present work is to provide a sound physical ground to the AFM. We now discuss how we can achieve this objective.

3.3 Conjectured connection between the two models

In view of how we introduced the concept of an absorbing barrier, it should be clear that the AFM is expected to have a link with the DPM. Therefore, the fundamental question at this point is the following: can we explicitly connect the AFM to the DPM? It is the aim of this section to outline the strategy we follow to obtain a clear positive answer to this question. The key element is to conjecture a concrete relation between the fundamental quantities of the models, namely the aperture function $\chi(\tau)$ for the AFM and the amplitude $\Omega(\tau)$ for the DPM. This connection will then be justified in the next chapter, chapter 4, through a quantitative comparison of the physical predictions of the two models.

We first briefly discuss how we can quantitatively compare the AFM and the DPM. This is done by investigating the two wave functions Ψ_{DPM} and Ψ_{AFM}, given by (3.30) and (3.31), respectively, in the transmission region. Such a comparison can only make sense if these two wave functions are both constructed from the *same* initial state, that is

$$\Psi_{\mathrm{DPM}}(x,0) = \Psi_{\mathrm{AFM}}(x,0) = \Psi_0(x)\,. \tag{3.40}$$

More concretely, we take the common initial wave function to be the Gaussian wave packet $\psi_{\alpha_0,x_0,v_0}(x,0)$ given by Eq. (2.11), namely

$$\Psi_0(x) = \psi_{\alpha_0,x_0,v_0}(x,0) = \left(\frac{1}{\pi\sigma^2}\right)^{\frac{1}{4}} \exp\left[-\frac{(x-x_0)^2}{2\sigma^2} + i\frac{mv_0}{\hbar}(x-x_0)\right]. \tag{3.41}$$

We recall that x_0 and v_0 correspond to the mean initial position and velocity, re-

spectively, of the particle, while σ quantifies the spatial extent of the wave packet (see (2.12)). The Gaussian wave packet (3.41) is clearly normalised. Now, remember that the relations (3.30) and (3.31) are only valid for initial states localised well inside the reflection region. Therefore, we must have that $\Psi_0(x)$ is negligible, $\Psi_0(x) \approx 0$, for any $x > 0$, which for the Gaussian wave packet (3.41) is satisfied if

$$0 < \sigma \ll |x_0| = -x_0 \,. \tag{3.42}$$

This indeed ensures that $\Psi_0(x) \approx 0$ for any value of x larger than $x_0 + N\sigma < 0$, where N is some number of the order of 1[7]. We then suppose that the particle, starting from the position $x_0 < 0$, propagates towards the barrier with a positive velocity, $v_0 > 0$. The time scale, denoted by t_c, characterising the free motion at velocity v_0[8] of the particle from its initial position x_0 to the barrier located at position $x = 0$ is given by

$$t_c \equiv \frac{|x_0|}{v_0} \,. \tag{3.43}$$

It precisely corresponds to the time needed for the equivalent classical particle to reach the barrier. Therefore, this particular time t_c is in the sequel referred to as the *classical time*. Finally, we recall that we are only interested in constructing the wave functions $\Psi_{\mathrm{DPM}}(x,t)$ and $\Psi_{\mathrm{AFM}}(x,t)$ in the transmission region. Therefore, the final time t must be large enough so as to allow the particle to have fully crossed the barrier. More precisely, we set t to fulfil the condition

$$|x_0| \lesssim v_0(t - t_c) \,, \tag{3.44}$$

which ensures that the freely evolved wave packet $\psi_{\alpha_0, x_0, v_0}(x,t)$ is centred around a position $v_0(t - t_c)$ which is well inside the transmission region[9].

Now, the key ingredient of the connection between the two models is to specify a concrete relation between the two fundamental parameters of the models, namely the aperture function $\chi(\tau)$ for the AFM and the amplitude $\Omega(\tau)$ for the DPM. On a

[7] We have typically $N = 5$ in view of the standard features of the normal distribution.

[8] Remember that in view of (2.22) the mean velocity of the freely evolved Gaussian wave packet $\psi_{\alpha_0, x_0, v_0}(x,\tau)$ is time-independent, and thus remains equal to v_0.

[9] More precisely, we want the observation time t to be such that $v_0(t - t_c) - N\sigma(t) > 0$, where $\sigma(t) \equiv \sigma\sqrt{1 + (\hbar t/m\sigma^2)^2}$ denotes the spatial extent of $\psi_{\alpha_0, x_0, v_0}(x,t)$, and N is some number of the order of 1. Indeed, $\psi_{\alpha_0, x_0, v_0}(x,t)$ is basically zero for any x such that $x < v_0(t - t_c) - 5\sigma(t)$. This will be ensured by the frozen Gaussian approximation, see below the complete definition (4.1) of the semiclassical regime.

more quantitative level, we must express χ as a function of Ω, that is $\chi(\tau) = T[\Omega(\tau)]$. We emphasise that at this point the function T can only be *conjectured*. Its validity will then be justified in chapter 4.

The particular form of this function T can be intuitively understood from the simple case of the time-independent δ-potential, for which $\Omega(\tau) = \Omega_0$. We start by looking for a scattering state solution to the corresponding TDSE (3.19) of the form

$$\begin{pmatrix} \psi_1(x,t) \\ \psi_2(x,t) \end{pmatrix} = e^{i(kx-\omega t)} \begin{cases} \begin{pmatrix} 1 \\ 0 \end{pmatrix} + \begin{pmatrix} R_{11} \\ R_{21} \end{pmatrix} e^{-2ikx} & \text{if } x < 0 \\ \begin{pmatrix} T_{11} \\ T_{21} \end{pmatrix} & \text{if } x > 0 \end{cases} , \tag{3.45}$$

where $k \equiv mv_0/\hbar$ and $\omega \equiv mv_0^2/2\hbar$. The quantities T_{11} and T_{21} are the transmission amplitudes associated with the states, or channels, $|1\rangle$ and $|2\rangle$, respectively, for an incident wave in the $|1\rangle$-channel. The quantities R_{11} and R_{21} are then the corresponding reflection amplitudes. These amplitudes are determined from the continuity of any solution of the TDSE, as well as the discontinuity of its spatial derivative, at $x = 0$. It can be in particular shown that the transmission amplitude to remain in the $|1\rangle$-channel is given by

$$T_{11} = \frac{1}{1 + (m\Omega_0/\hbar k)^2} = \frac{1}{1 + (\Omega_0/v_0)^2} . \tag{3.46}$$

We then take this transmission amplitude T_{11} as a definition of the function T relating the aperture function χ_0, describing a time-independent absorbing barrier, to the amplitude Ω_0 of a time-independent δ-potential, that is

$$\chi_0 = T(\Omega_0) \equiv \frac{1}{1 + (\Omega_0/v_0)^2} . \tag{3.47}$$

We then generalise this time-independent relation to arbitrary time-dependent barriers. Therefore, we conjecture that the AFM and the DPM are connected through the relation

$$\boxed{\chi(\tau) = \frac{1}{1 + [\Omega(\tau)/v_0]^2}} \tag{3.48}$$

for any $0 < \tau < t$. It is worth analysing some of the properties of the expression (3.48). It first clearly ensures that χ is a real dimensionless quantity whose values range between 0 and 1. Furthermore, note that for $\Omega/v_0 \ll 1$ we have $\chi \approx 1$.

This appears indeed reasonable, as we expect energetic particles to be relatively insensitive to the presence of a barrier. On the contrary, the case $\Omega/v_0 \gg 1$ yields $\chi \approx 0$. Here again this result makes sense, as an atom would be very unlikely to survive a laser light with a very high intensity.

We now provide analytical and numerical evidence of the conjectured connection (3.48).

Chapter 4

Quantitative comparison between two models of absorption

This chapter is devoted to an in-depth investigation of the connection between the DPM and the AFM discussed in chapter 3. It is shown that under the relation (3.48) the predictions of the two models in the transmission region are in excellent agreement in a semiclassical regime described by the conditions

$$\sigma \ll |x_0| \lesssim v_0(t - t_c) \ll \frac{m\sigma^2 v_0}{\hbar}\,, \tag{4.1}$$

where we recall that x_0 and v_0 denote the mean position and velocity, respectively, of the initial state Ψ_0, while σ quantifies its spatial dispersion. The leftmost condition in (4.1), $\sigma \ll |x_0|$, corresponds to the hypothesis (3.42) regarding the initial localisation of the particle in the reflection region. The second condition, $|x_0| \lesssim v_0(t-t_c)$, is nothing but the assumption (3.44). It ensures that the wave packet evolved freely from Ψ_0 is centred, at the final time t, around a point lying well inside the transmission region. Finally, the last condition, $v_0(t - t_c) \ll m\sigma^2 v_0/\hbar$, specifies in addition the localisation, at the final time t, of the freely evolved wave packet. Indeed, it implies[1] in particular that the final time t satisfies $\hbar t/m\sigma^2 \ll 1$. This is precisely the frozen Gaussian approximation (2.34) discussed in section 2.2. Therefore, the physical picture detailed by the assumptions (4.1) is clear: the initial state Ψ_0 is localised, and remains localised as it propagates freely in a time t. It is also worth noting that the left- and rightmost terms in (4.1) hence satisfy $\sigma \ll m\sigma^2 v_0/\hbar$, which is clearly equivalent to $\lambda\!\!\!^{-}_0 \ll \sigma$, with $\lambda\!\!\!^{-}_0$ the reduced de Broglie wavelength defined by (2.14).

We now divide our analysis in two main parts. We first use in section 4.1 the

[1] For completeness: first note that $|x_0| \ll m\sigma^2 v_0/\hbar$ implies that $\hbar t_c/m\sigma^2 \ll 1$. Then $v_0(t-t_c) \ll m\sigma^2 v_0/\hbar$ implies that $\hbar t/m\sigma^2 \ll 1 + \hbar t_c/m\sigma^2 \approx 1$.

conditions (4.1) to analytically demonstrate an excellent agreement between the DPM and the AFM in this particular semiclassical regime. As an analytical approach of the problem quickly gets highly non-trivial when we start to relax some of the assumptions (4.1), we then turn in section 4.2 to a numerical investigation. This allows to confront the two models beyond the semiclassical regime, as well as to treat different experimentally realistic scenarios.

4.1 Analytical approach

We start by analytically comparing the two wave functions Ψ_{DPM} and Ψ_{AFM} (Eqs. (3.30) and (3.31)) given by, in view of (3.40),

$$\Psi_{\mathrm{DPM}}(x,t) \approx \int_{-\infty}^{0} dx'\, K_{11}(x,x',t)\Psi_0(x') \tag{4.2}$$

and

$$\Psi_{\mathrm{AFM}}(x,t) \approx \int_{-\infty}^{0} dx'\, K_{\mathrm{AFM}}(x,x',t)\Psi_0(x')\,, \tag{4.3}$$

in two different scenarios. We first consider in subsection 4.1.1 the case of a slowly varying time-dependent barrier, and then treat in 4.1.2 the opposite example of an instantaneously varying barrier. In both cases the two wave functions are shown to be in strong agreement in a spatial region centred about the mean position x_t of the corresponding freely evolved wave packet, which in view of the definition (2.19) reads

$$x_t = x_0 + v_0 t\,. \tag{4.4}$$

4.1.1 Slowly varying barrier

The interest of considering the case of a slowly varying barrier is that it allows to derive, in the semiclassical regime described by (4.1), a well-posed problem for the component $K_{11}(x,x',t)$ of the full propagator $\widehat{K}(x,x',t)$ corresponding to the DPM. Indeed, let us first recall that, by definition of the propagator, $\widehat{K}$ must satisfy the same TDSE (3.19) than the spinor $\widehat{\psi}$. Therefore, in view of (3.16)-(3.18), the component $K_{11}(x,x',\tau)$ obeys the free-particle time-dependent Schrödinger equation on both sides of the barrier, i.e.

$$\left(\frac{\partial^2}{\partial x^2} + \frac{i}{\alpha}\frac{\partial}{\partial \tau}\right) K_{11}(x, x', \tau) = 0\,, \tag{4.5}$$

for any $0 < \tau < t$ and for $x, x' \neq 0$, and where we introduced the quantity α defined by

$$\alpha \equiv \frac{\hbar}{2m}\,. \tag{4.6}$$

By definition of a quantum propagator, $K_{11}(x, x', \tau)$ is subject to the initial condition

$$K_{11}(x, x', 0^+) = \delta(x - x')\,, \tag{4.7}$$

while the Dirichlet boundary conditions imposed on the wave function at infinity, namely (3.20), require

$$K_{11}(x \to \pm\infty, x', \tau) = 0 \quad \text{for} \quad \alpha = -i|\alpha|\,. \tag{4.8}$$

Note that we specified here the substitution $\alpha = -i|\alpha|$, which replaces the negative imaginary times requirement discussed in section 2.1 (see Eq. (2.8c))[2]. This is done in view of the later use of the method of Laplace transform, for which the time-related substitution $\tau = -i|\tau|$ as in (2.8c) is not convenient. Now, note that in addition to the IC (4.7) and the BC's at infinity (4.8), we also know one matching condition at $x = 0$. Indeed, because the position dependence of the potential rises from a δ-function, the two components ψ_1 and ψ_2 of the spinor $\widehat{\psi}$ must be continuous at $x = 0$ (as stems from the *hierarchy of singularities*, see [31]). Since $\psi_1 = \Psi_{\text{DPM}} = \int dx' K_{11}\Psi_0$, we see that $K_{11}(x, x', \tau)$ must itself be continuous at $x = 0$, i.e.

$$K_{11}(x, x', \tau)\big|_{x=0^-}^{x=0^+} = 0\,. \tag{4.9}$$

Therefore, finding one additional matching condition at $x = 0$ would yield a well-posed mathematical problem, uniquely determining the propagator $K_{11}(x, x', \tau)$. We could then try to solve it, and finally use the exact expression of K_{11} to construct the wave function Ψ_{DPM}.

It turns out that such a program can be completed, in the semiclassical regime,

[2]The validity of this procedure stems from the similarity of the TDSE satisfied by the component K_{11} under the two substitutions $\tau = -i|\tau|$ and $\alpha = -i|\alpha|$.

if the amplitude Ω varies slowly with time. We first find the matching condition satisfied by the spatial derivative of K_{11} at $x = 0$. We then find the exact solution of the resulting well-posed mathematical problem, and obtain the following expression for the propagator $K_{11}(x, x', t)$ (Eq. (4.55))[3]:

$$K_{11}(x, x', t) \approx \frac{1}{2} \int_0^t d\tau \left[\frac{x}{t-\tau} - \frac{x'}{\tau} \frac{x'^2 - \tau^2 \Omega(\tau)^2}{x'^2 + \tau^2 \Omega(\tau)^2} \right] K_0(x, t-\tau) K_0(x', \tau) \,. \quad (4.10)$$

As we can see from their respective expressions (3.37) and (4.10) the propagators K_{AFM} and K_{11} exhibit, in the semiclassical regime (4.1) and for a slowly varying barrier $\Omega(\tau)$, some similarities as well as important differences. First, note that they are given by similar integrals. Indeed, the probability amplitude $\Psi_{\mathrm{DPM}}(x, t)$ of detecting the atom in its ground state $|1\rangle$ at a position $x > 0$ at the final time t stems from summing the probability amplitudes associated with particular space-time paths. Any path, linking a point $x' < 0$ to the point $x > 0$, can be divided in two successive paths: i) a free motion from x' to the barrier in a time $\tau > 0$, followed by ii) an other free motion from the barrier to the point x in the remaining time $t - \tau$. This is the main similitude between the two propagators K_{AFM} and K_{11}. The first term involved in the factor between square brackets in (4.10) is also exactly the same than in the AFM propagator (3.37). It merely corresponds to the classical velocity $x/(t-\tau)$ at which the particle leaves the barrier. The way the barrier enters the propagator constitutes the important difference between the propagators K_{AFM} and K_{11}. Remember that in K_{AFM} the aperture function $\chi(\tau)$ is a mere modulation factor that multiplies the mean velocity at which the particle crosses the barrier. In K_{11} however the amplitude $\Omega(\tau)$ is not a global modulation factor any more. Indeed, it appears in a position- (via x') and time- (via τ) dependent fraction that multiplies only the classical velocity $-x'/\tau$ at which the particle reaches the barrier.

Finally, to conclude this subsection we use the explicit expressions (3.37) and (4.10) of the propagators $K_{\mathrm{AFM}}(x, x', t)$ and $K_{11}(x, x', t)$, respectively, to construct the two wave functions $\Psi_{\mathrm{AFM}}(x, t)$ and $\Psi_{\mathrm{DPM}}(x, t)$. Upon assuming the relation (3.48) between the aperture function $\chi(\tau)$ and the amplitude $\Omega(\tau)$, the two wave functions are shown to be in strong agreement in a neighbourhood of the point x_t.

Matching condition for $\partial_x K_{11}(x, x', \tau)$ at $x = 0$

The full propagator $\widehat{K}$ satisfies the TDSE

[3]The approximation stems from the use of the stationary phase approximation to obtain the missing BC for the spatial derivative of K_{11} at $x = 0$.

$$i\hbar\frac{\partial}{\partial\tau}\widehat{K}(x,x',\tau)=\left[\widehat{H}_0+\widehat{V}(x,\tau)\right]\widehat{K}(x,x',\tau)\,, \tag{4.11}$$

with $\widehat{H}_0$ and $\widehat{V}(x,\tau)$ given by (3.17) and (3.18), respectively. As we already mentioned, the propagator corresponding to $\widehat{H}_0$ is known, and is nothing but the matrix free-particle propagator $\widehat{K}_0$, given by (3.23). Therefore, we can extend the one-component time-dependent Lippmann-Schwinger equation (2.10) to the matrix propagator $\widehat{K}(x,x',\tau)$, and write the latter in the form

$$\begin{aligned}\widehat{K}(x,x',\tau)&=\widehat{K}_0(x-x',\tau)\\&\quad-\frac{i}{\hbar}\int_0^\tau d\tau_1\int_{-\infty}^{+\infty}dx''\widehat{K}_0(x-x'',\tau-\tau_1)\widehat{V}(x'',\tau_1)\widehat{K}(x'',x',\tau_1)\,,\end{aligned} \tag{4.12}$$

which in view of the simple form (3.18) of the potential $\widehat{V}$ reads, after performing the trivial integral over x'',

$$\widehat{K}(x,x',\tau)=\widehat{K}_0(x-x',\tau)-i\int_0^\tau d\tau_1\,\widehat{K}_0(x,\tau-\tau_1)\Omega(\tau_1)\begin{pmatrix}0&1\\1&0\end{pmatrix}\widehat{K}(0,x',\tau_1)\,. \tag{4.13}$$

We now write the successive iterations of the Lippmann-Schwinger equation (4.13), and thus write the propagator $\widehat{K}$ in the form of the Dyson series

$$\widehat{K}(x,x',\tau)=\widehat{K}_0(x-x',\tau)+\sum_{n=1}^{+\infty}\widehat{K}^{(n)}(x,x',\tau)\,, \tag{4.14}$$

where the general term $\widehat{K}^{(n)}(x,x',\tau)$ of the series is, in view of the expression (3.23) of $\widehat{K}_0$, given by

$$\begin{aligned}\widehat{K}^{(n)}(x,x',\tau)&=(-i)^n\int_0^\tau d\tau_n\int_0^{\tau_n}d\tau_{n-1}\cdots\int_0^{\tau_2}d\tau_1\,K_0(x,\tau-\tau_n)\\&\quad\times\Omega(\tau_n)K_0(0,\tau_n-\tau_{n-1})\cdots\Omega(\tau_2)K_0(0,\tau_2-\tau_1)\Omega(\tau_1)K_0(x',\tau_1)\begin{pmatrix}0&1\\1&0\end{pmatrix}^n\,.\end{aligned} \tag{4.15}$$

Since we straightforwardly show that

$$\begin{pmatrix} 0 & 1 \\ 1 & 0 \end{pmatrix}^{2k} = \begin{pmatrix} 1 & 0 \\ 0 & 1 \end{pmatrix} \quad \text{and} \quad \begin{pmatrix} 0 & 1 \\ 1 & 0 \end{pmatrix}^{2k+1} = \begin{pmatrix} 0 & 1 \\ 1 & 0 \end{pmatrix} \tag{4.16}$$

for any $k \in \mathbb{N}$, we readily see on (4.15) that the component

$$K_{11}^{(n)}(x, x', \tau) \equiv \left[\widehat{K}^{(n)}(x, x', \tau)\right]_{11} \tag{4.17}$$

of the matrix $\widehat{K}^{(n)}$ vanishes for odd n, i.e.

$$K_{11}^{(n)}(x, x', \tau) = 0 \tag{4.18}$$

for $n = 2k + 1$ with $k \geqslant 0$, and, for even n, is given by

$$\begin{aligned} K_{11}^{(n)}(x, x', \tau) = (-i)^n \int_0^{\tau} d\tau_n \int_0^{\tau_n} d\tau_{n-1} \cdots \int_0^{\tau_2} d\tau_1 \, K_0(x, \tau - \tau_n) \\ \times \Omega(\tau_n) K_0(0, \tau_n - \tau_{n-1}) \cdots \Omega(\tau_2) K_0(0, \tau_2 - \tau_1) \Omega(\tau_1) K_0(x', \tau_1) \end{aligned} \tag{4.19}$$

for $n = 2k$ with $k \geqslant 1$. Therefore, we now treat throughout this section the integer n as being *even*, that is

$$n = 2k \quad \text{with} \quad k \geqslant 1 \,. \tag{4.20}$$

In view of obtaining the derivative of K_{11} with respect to x, we first derive the derivative of the element $K_{11}^{(n)}$. To this end, we rewrite (4.19) in the slightly different form[4]

$$\begin{aligned} K_{11}^{(n)}(\xi_{n+1}, \xi_0, \tau_{n+1}) = (-i)^n \lim_{\xi_n \to 0} \cdots \lim_{\xi_1 \to 0} \int_0^{\tau_{n+1}} d\tau_n \cdots \int_0^{\tau_2} d\tau_1 \left(\prod_{j=1}^{n} \Omega(\tau_j) \right) \\ \times \left(\prod_{j=0}^{n} K_0(\xi_{j+1} - \xi_j, \tau_{j+1} - \tau_j) \right) , \end{aligned} \tag{4.21}$$

where we introduced the intermediate position ξ_j, and set for compactness $\xi_{n+1} \equiv x$

[4]The interchange between the limits and the integrals is justified in view of later on applying the propagator on a Gaussian wave packet, hence yielding absolutely convergent integrals.

and $\xi_0 \equiv x'$. We also introduced the notations $\tau_{n+1} \equiv \tau$ and $\tau_0 \equiv 0$ (this latter being merely the initial time). In view of the subsequent calculations we define the *dimensionless* quantities

$$\epsilon_j \equiv \frac{\xi_j}{|x_0|} \qquad \text{and} \qquad \eta_j \equiv \frac{\tau_j}{\tau} \equiv \frac{\tau_j}{\tau_{n+1}} \,. \tag{4.22}$$

We now differentiate (4.21) with respect to $x \equiv |x_0|\epsilon_{n+1}$ and, in view of the expression (2.9) of the free-particle propagator K_0, we get[5]

$$\begin{aligned} \frac{\partial}{\partial x} K_{11}^{(n)}(x, x', \tau) &= \frac{1}{|x_0|} \frac{\partial}{\partial \epsilon_{n+1}} K_{11}^{(n)}(|x_0|\epsilon_{n+1}, |x_0|\epsilon_0, \tau_{n+1}\eta_{n+1}) \\ &= \lim_{\epsilon_n \to 0} \cdots \lim_{\epsilon_1 \to 0} I^{(n)}(\epsilon_0, \ldots, \epsilon_{n+1}, \eta_{n+1}) \,, \end{aligned} \tag{4.23}$$

with

$$I^{(n)}(\epsilon_0, \ldots, \epsilon_{n+1}, \eta_{n+1}) \equiv \int_0^{\eta_{n+1}} d\eta_n \cdots \int_0^{\eta_2} d\eta_1 \, F(\eta_1, \ldots, \eta_n) e^{i\lambda\phi(\eta_1, \ldots, \eta_n)} \,, \tag{4.24}$$

where

$$\lambda \equiv \frac{m x_0^2}{2\hbar\tau} \tag{4.25}$$

is a dimensionless quantity, the amplitude F and the phase ϕ are defined by

$$F(\eta_1, \ldots, \eta_n) \equiv (-i)^n \left(\frac{m}{2i\pi\hbar}\right)^{\frac{n+1}{2}} \left(\prod_{j=1}^{n} \Omega(\tau\eta_j)\right) \frac{im|x_0|(\epsilon_{n+1} - \epsilon_n)}{\hbar(\eta_{n+1} - \eta_n)} \frac{\tau^{\frac{n-3}{2}}}{\sqrt{\prod_{j=0}^{n}(\eta_{j+1} - \eta_j)}} \tag{4.26}$$

and

$$\phi(\eta_1, \ldots, \eta_n) \equiv \sum_{j=0}^{n} \frac{(\epsilon_{j+1} - \epsilon_j)^2}{\eta_{j+1} - \eta_j} \,. \tag{4.27}$$

Now, remember that we consider here $0 < \tau < t$. Therefore, in the semiclassical

[5] Upon the n-dimensional change of variables in the integral defined by the map $(\eta_n, \ldots, \eta_1) = G(\tau_n, \ldots, \tau_1)$ as characterised by (4.22). It is straightforward to find the inverse G^{-1}, and hence the Jacobian, as well as the new domain of integration.

regime detailed by (4.1) we have in view of (4.25) that $\lambda \geqslant mx_0^2/2\hbar t \gg 1$. This suggests to use the *stationary phase approximation* to explicitly compute the integral (4.24). It is worth emphasising that the need for considering slowly varying barriers precisely stems from this use of the stationary phase approximation, as Ω is involved in the amplitude F of the integrand.

The very first thing is thus to find the stationary point $\boldsymbol{\eta}^{(s)} = \left(\eta_1^{(s)}, \ldots, \eta_n^{(s)}\right)$, defined by

$$\left.\frac{\partial \phi}{\partial \eta_j}\right|_{(\eta_1,\ldots,\eta_n)=\boldsymbol{\eta}^{(s)}} = 0\,, \tag{4.28}$$

for any $1 \leqslant j \leqslant n$. In addition to the defining equations (4.28), we also require the stationary point $\boldsymbol{\eta}^{(s)}$ to satisfy the constraint

$$0 < \eta_1^{(s)} < \cdots < \eta_n^{(s)} < 1\,. \tag{4.29}$$

This additional condition is imposed to ensure the existence of a neighbourhood of the stationary point $\boldsymbol{\eta}^{(s)}$ that is entirely contained into the original integration domain in (4.24)[6]. We can show that (4.28)-(4.29) admit the unique solution

$$\eta_j^{(s)} = \frac{\sum_{k=1}^{j} |\epsilon_k - \epsilon_{k-1}|}{\sum_{k=1}^{n+1} |\epsilon_k - \epsilon_{k-1}|}\,, \tag{4.30}$$

for any $1 \leqslant j \leqslant n$.

We now proceed to use the stationary phase approximation to evaluate $I^{(n)}$. The first step is to reduce the integration domain in (4.24) to a neighbourhood $\mathcal{N}^{(s)}$ of the stationary point $\boldsymbol{\eta}^{(s)}$. This new integration domain being by construction a region of stationary phase, we can Taylor expand the phase $\phi(\eta_1, \ldots, \eta_n)$ up to the second order in powers of $(\eta_j - \eta_j^{(s)})$. We then use the fact that for slowly varying barriers the amplitude F is basically an algebraic function of the integration variables. It can thus be taken as constant over $\mathcal{N}^{(s)}$, and equal to its value $F^{(s)} \equiv F\left(\eta_1^{(s)}, \ldots, \eta_n^{(s)}\right)$ at the stationary point. We can take it outside the integral, and we finally extend the integration region to $\mathbb{R}^n$. We are thus left with an n-dimensional Gaussian integral, which can be readily computed (see e.g. [52]) to yield

[6] If no stationary point satisfying (4.29) exists, then the dominant contribution to the integral (4.24) would not rise from a region of stationary phase.

$$I^{(n)}(\epsilon_0,\ldots,\epsilon_{n+1},\eta_{n+1}) \approx \left(\frac{2\pi}{\lambda}\right)^{\frac{n}{2}} \frac{F^{(s)}e^{i\lambda\phi^{(s)}+in\pi/4}}{\sqrt{\det\left(H^{(s)}\right)}}\,, \tag{4.31}$$

where $\phi^{(s)} \equiv \phi\left(\eta_1^{(s)},\ldots,\eta_n^{(s)}\right)$ is the value of the phase at the stationary point, while $H^{(s)}$ is the n-by-n Hessian matrix of ϕ at the stationary point. More precisely, the elements of $H^{(s)}$ are defined as

$$H_{jk}^{(s)} = \left.\frac{\partial^2\phi}{\partial\eta_j\,\partial\eta_k}\right|_{(\eta_1,\ldots,\eta_n)=\boldsymbol{\eta}^{(s)}}\,, \tag{4.32}$$

for any $1 \leqslant j \leqslant n$ and $1 \leqslant k \leqslant n$. Furthermore, the Hessian matrix $H^{(s)}$ is symmetric and tridiagonal, its elements being given by

$$H_{jj}^{(s)} = 2\left(\sum_{k=1}^{n+1}|\epsilon_k-\epsilon_{k-1}|\right)^3\left(\frac{1}{|\epsilon_j-\epsilon_{j-1}|}+\frac{1}{|\epsilon_{j+1}-\epsilon_j|}\right) \tag{4.33a}$$

for any $1 \leqslant j \leqslant n$, and

$$H_{j\,,j+1}^{(s)} = H_{j+1\,,j}^{(s)} = -2\frac{\left(\sum_{k=1}^{n+1}|\epsilon_k-\epsilon_{k-1}|\right)^3}{|\epsilon_{j+1}-\epsilon_j|} \tag{4.33b}$$

for any $1 \leqslant j \leqslant n-1$. Any other element $H_{jk}^{(s)}$ is zero, i.e. $H_{jk}^{(s)} = 0$ for all $|j-k| \geqslant 2$. We then show that the determinant of the Hessian matrix is given by (details can be found in the appendix B)

$$\det\left(H^{(s)}\right) = 2^n\frac{\left(\sum_{k=1}^{n+1}|\epsilon_k-\epsilon_{k-1}|\right)^{3n+1}}{\prod_{k=1}^{n+1}|\epsilon_k-\epsilon_{k-1}|}\,. \tag{4.34}$$

Combining (4.31) with (4.26), (4.27), (4.30) and (4.34), substituting the resulting expression of $I^{(n)}$ into (4.23) and taking the limits $\epsilon_1 \to 0$, ..., $\epsilon_n \to 0$, we obtain (remember that in view of (4.20) we have n even) the following expression for the spatial derivative of the term $K_{11}^{(2k)}(x,x',\tau)$:

$$\frac{\partial}{\partial x}K_{11}^{(2k)}(x,x',\tau) \approx \mathrm{sgn}(x)\,\frac{m\,(|x|-x')}{i\hbar\tau}\,(-1)^{k+1}K_0(|x|-x',\tau) \times \left[\frac{\tau^2}{(|x|-x')^2}\,\Omega\left(\frac{x'}{x'-|x|}\,\tau\right)^2\right]^k \quad (4.35)$$

for any $k \geqslant 1$, with

$$\mathrm{sgn}(\xi) \equiv \frac{\xi}{|\xi|} \quad (4.36)$$

the sign function.

Therefore, differentiating (4.14) with respect to x yields, in view of (4.18) and (4.35),

$$\frac{\partial}{\partial x}K_{11}(x,x',\tau) \approx \frac{\partial K_0}{\partial x} + \mathrm{sgn}(x)\,\frac{m(|x|-x')}{i\hbar\tau}\,K_0(|x|-x',\tau) \times \sum_{k=1}^{+\infty}(-1)^{k+1}\left[\frac{\tau^2}{(|x|-x')^2}\Omega\left(\frac{x'}{x'-|x|}\,\tau\right)^2\right]^k, \quad (4.37)$$

from which we easily obtain the jump of $\partial_x K_{11}(x,x',\tau)$ at $x=0$, namely

$$\frac{\partial}{\partial x}K_{11}(x,x',\tau)\Big|_{x=0^-}^{x=0^+} \approx -2\frac{mx'}{i\hbar\tau}K_0(x',\tau)\sum_{k=1}^{+\infty}(-1)^{k+1}\left[\frac{\tau^2}{x'^2}\,\Omega(\tau)^2\right]^k. \quad (4.38)$$

Note that we have the identities

$$K_0(x',\tau)\frac{mx'}{i\hbar\tau} = \frac{\partial}{\partial x}K_0(x-x',\tau)\Big|_{x=0} \quad (4.39)$$

and

$$\sum_{k=1}^{+\infty}(-1)^{k+1}z^k = \frac{z}{1+z} \quad (4.40)$$

for any z such that $|z|<1$[7]. Therefore, combining (4.38) with (4.39) and (4.40), we

[7]Since in view of (4.38) we have $z = \tau^2\Omega(\tau)^2/x'^2$, we must hence have $\Omega(\tau) < |x'|/\tau$. The conclusions drawn in this subsection are thus valid for slowly varying barriers that also satisfy this additional condition, which is not a severe restriction. Note in particular that the analysis

obtain the following matching condition for $\partial_x K_{11}(x, x', \tau)$ at $x = 0$:

$$\frac{\partial}{\partial x} K_{11}(x, x', \tau)\Big|_{x=0^-}^{x=0^+} \approx -\kappa(x', \tau)\, \frac{\partial}{\partial x} K_0(x - x', \tau)\Big|_{x=0}, \tag{4.41}$$

where we defined

$$\kappa(x', \tau) \equiv \frac{2}{1 + \left[\frac{x'}{\tau\Omega(\tau)}\right]^2}. \tag{4.42}$$

We can thus use this matching condition (4.41) to construct a well-posed problem for the propagator $K_{11}(x, x', \tau)$, which we now proceed to solve.

Derivation of $K_{11}(x, x', \tau)$

We now have a well-posed problem for the propagator $K_{11}(x, x', \tau)$, formed by i) the TDSE (4.5), ii) the IC (4.7), iii) the two BC's at infinity (4.8) and iv) the two matching conditions (4.9) and (4.41) for K_{11} and $\partial_x K_{11}$, respectively, at $x = 0$. We solve it using the method of Laplace transforms [44, 53]. In this chapter we denote with a bar the Laplace transform (with respect to τ) of an arbitrary function $f(\tau)$, that is

$$\bar{f}(s) = \mathscr{L}\left[f(\tau)\right] = \int_0^{+\infty} d\tau\, e^{-s\tau} f(\tau). \tag{4.43}$$

We now first take the Laplace transform of the TDSE (4.5), and get

$$\frac{\partial^2}{\partial x^2} \bar{K}_{11}(x, x', s) + \frac{is}{\alpha} \bar{K}_{11}(x, x', s) = \frac{i}{\alpha} \delta(x - x') \tag{4.44}$$

for $x, x' \neq 0$. From the same argument we already used regarding the continuity of $K_{11}(x, x', \tau)$ at $x = 0$ (namely the hierarchy of singularities, see [31]), we see on (4.44) that $\bar{K}_{11}$ and $\partial_x \bar{K}_{11}$ are continuous and discontinuous, respectively, at $x = x'$. We can thus rewrite the inhomogeneous equation (4.44) as the homogeneous equation

$$\frac{\partial^2}{\partial x^2} \bar{K}_{11}(x, x', s) + \frac{is}{\alpha} \bar{K}_{11}(x, x', s) = 0 \tag{4.45}$$

performed in subsection 4.1.2, as well as in section 4.2, is *completely independent* of this restriction. Indeed, in 4.1.2 we use an exact expression of the propagator K_{11}, while in 4.2 we either use known expressions of K_{11} or numerically solve the TDSE (3.19).

for $x, x' \neq 0$ and $x \neq x'$, whose solution is subject to the matching conditions

$$\bar{K}_{11}(x, x', s)\big|_{x=x'^-}^{x=x'^+} = 0 \tag{4.46a}$$

and

$$\frac{\partial}{\partial x}\bar{K}_{11}(x, x', s)\bigg|_{x=x'^-}^{x=x'^+} = \frac{i}{\alpha}\,. \tag{4.46b}$$

Finally, taking the Laplace transform of the four remaining BC's (4.8), (4.9) and (4.41), we obtain, respectively,

$$\bar{K}_{11}(x \to \pm\infty, x', s) = 0 \quad \text{for} \quad \alpha = -i|\alpha|\,, \tag{4.46c}$$

$$\bar{K}_{11}(x, x', s)\big|_{x=0^-}^{x=0^+} = 0\,, \tag{4.46d}$$

and[8]

$$\frac{\partial}{\partial x}\bar{K}_{11}(x, x', s)\bigg|_{x=0^-}^{x=0^+} = \bar{W}(s)\,, \tag{4.46e}$$

where the function $\bar{W}(s)$ is defined by

$$\bar{W}(s) = \mathscr{L}\left[-\kappa(x', \tau)\,\frac{\partial}{\partial x}K_0(x - x', \tau)\bigg|_{x=0}\right] = \frac{ix'}{2\alpha}\int_0^{+\infty} d\tau\, \mathrm{e}^{-s\tau}\kappa(x', \tau)\frac{K_0(x', \tau)}{\tau}\,. \tag{4.47}$$

We now proceed to derive the function $\bar{K}_{11}(x, x', s)$ uniquely defined by the problem formed by (4.45) and (4.46).

As we focus on wave packets initially localised in the reflection region, it is sufficient for our purpose to solve the above problem for negative values of x'. We can thus consider three well-defined regions of values of the variable x, with respect to an arbitrary fixed negative value of x': $\mathcal{R}_1$, corresponding to any $-\infty < x < x'$, then $\mathcal{R}_2$ for any $x' < x < 0$, and finally $\mathcal{R}_3$ defined by any $0 < x < +\infty$. The general solution of (4.45) is of similar form in each region and reads

$$\bar{K}_{11}^{(j)}(x, x', s) = A_j\,\mathrm{e}^{k_+ x} + B_j\,\mathrm{e}^{k_- x} \quad \text{for} \quad x \in \mathcal{R}_j\,, \tag{4.48}$$

where $A_j = A_j(x', s)$ and $B_j = B_j(x', s)$, with $j = 1, 2, 3$, are at this point arbitrary

[8]For clarity we temporarily replace the approximation sign in (4.41) by an equal sign throughout the subsequent Laplace transform derivation of K_{11}.

complex valued functions, while $k_+ = k_+(s)$ and $k_- = k_-(s)$ are given by[9]

$$k_\pm = \pm\, \mathrm{e}^{-i\frac{\pi}{4}} \sqrt{\frac{s}{\alpha}}\,, \tag{4.49}$$

We restrict the complex variable s to the complex plane branch $-\pi < \arg(s) < \pi$, so that we have $\mathrm{Re}(\sqrt{s}) > 0$. Therefore, we obtain from (4.46c) that

$$B_1 = A_3 = 0\,. \tag{4.50}$$

We then use the four matching conditions (4.46a), (4.46b), (4.46d), and (4.46e) to obtain the matrix equation

$$\begin{pmatrix} -\,\mathrm{e}^{k_+x'} & \mathrm{e}^{k_+x'} & \mathrm{e}^{k_-x'} & 0 \\ k_+\mathrm{e}^{k_+x'} & k_+\mathrm{e}^{k_+x'} & -k_-\mathrm{e}^{k_-x'} & 0 \\ 0 & -1 & -1 & 1 \\ 0 & -k_+ & -k_- & k_- \end{pmatrix} \begin{pmatrix} A_1 \\ A_2 \\ B_2 \\ B_3 \end{pmatrix} = \begin{pmatrix} 0 \\ \frac{i}{\alpha} \\ 0 \\ \bar{W} \end{pmatrix}. \tag{4.51}$$

Solving the equation (4.51), we get the remaining four coefficients A_1, A_2, B_2 and B_3:

$$A_1 = \frac{\mathrm{e}^{-i\frac{\pi}{4}}}{2}\,\frac{\mathrm{e}^{-k_+x'}}{\sqrt{\alpha s}} - \frac{\mathrm{e}^{i\frac{\pi}{4}}}{2}\sqrt{\frac{\alpha}{s}}\,\bar{W}(s)\,, \tag{4.52a}$$

$$A_2 = -\,\frac{\mathrm{e}^{i\frac{\pi}{4}}}{2}\sqrt{\frac{\alpha}{s}}\,\bar{W}(s)\,, \tag{4.52b}$$

$$B_2 = \frac{\mathrm{e}^{-i\frac{\pi}{4}}}{2}\,\frac{\mathrm{e}^{-k_-x'}}{\sqrt{\alpha s}}\,, \tag{4.52c}$$

$$B_3 = \frac{\mathrm{e}^{-i\frac{\pi}{4}}}{2}\,\frac{\mathrm{e}^{-k_-x'}}{\sqrt{\alpha s}} - \frac{\mathrm{e}^{i\frac{\pi}{4}}}{2}\sqrt{\frac{\alpha}{s}}\,\bar{W}(s)\,. \tag{4.52d}$$

Substituting the results (4.50) and (4.52) into the general expression (4.48) yields the solutions $\bar{K}_{11}^{(j)}(x, x', s)$, $j = 1, 2, 3$, in all three regions $\mathcal{R}_1$, $\mathcal{R}_2$ and $\mathcal{R}_3$. We then take the inverse Laplace transform of each of these solutions to obtain the corresponding solutions $K_{11}^{(j)}(x, x', \tau)$, $j = 1, 2, 3$, of the original time-dependent problem. The key results to use in taking the inverse Laplace transform are

[9] We choose a particular branch of the complex square root, namely the one where $\sqrt{i} = \exp(i\pi/4)$.

$$\mathscr{L}^{-1}\left[\frac{\mathrm{e}^{-a\sqrt{s}}}{\sqrt{s}}\right] = \frac{1}{\sqrt{\pi\tau}}\mathrm{e}^{-\frac{a^2}{4\tau}} \tag{4.53}$$

for $\mathrm{Re}(a) \geq 0$ [54], combined with the convolution theorem in computing the inverse Laplace transform of terms of the form $\left[\exp\left(-a\sqrt{s}\right)/\sqrt{s}\right]\bar{W}(s)$ with $\mathrm{Re}(a) \geq 0$. As a result, we get that any $K_{11}^{(j)}(x,x',\tau)$, $j=1,2,3$, has the exact same form in each of the regions $\mathcal{R}_1$, $\mathcal{R}_2$, and $\mathcal{R}_3$. Therefore, this readily gives the propagator $K_{11}(x,x',\tau)$ for any $x \in \mathbb{R}$, and we have[10]

$$K_{11}(x,x',\tau) \approx K_0(x-x',\tau) + \frac{1}{2}\int_0^\tau d\tau_1 \, \frac{x'\kappa(x',\tau_1)}{\tau_1} K_0(x,\tau-\tau_1)K_0(x',\tau_1)\,, \tag{4.54}$$

this result being valid for any $0<\tau<t$ and $x'<0$. Finally, using the decomposition (3.38) of the free-particle propagator $K_0(x-x',\tau)$ allows to rewrite (4.54) in the form

$$K_{11}(x,x',\tau) \approx \frac{1}{2}\int_0^\tau d\tau_1 \left[\frac{x}{\tau-\tau_1} - \frac{x'}{\tau_1}\frac{x'^2-\tau_1^2\Omega(\tau_1)^2}{x'^2+\tau_1^2\Omega(\tau_1)^2}\right] K_0(x,\tau-\tau_1)K_0(x',\tau_1)\,, \tag{4.55}$$

where we also used the definition (4.42) of the function $\kappa(x',\tau_1)$.

We can now substitute the expression (4.54) of the propagator K_{11} into (4.2) to obtain an essentially analytical expression of the wave function Ψ_{DPM}. This allows for an effective comparison between Ψ_{AFM} and Ψ_{DPM}, as we now discuss.

Comparison between the wave functions Ψ_{AFM} and Ψ_{DPM}

We first substitute the known expression (3.37) of the propagator $K_{\mathrm{AFM}}(x,x',t)$ into (4.3). We can thus write the wave function $\Psi_{\mathrm{AFM}}(x,t)$ in the form (remember the initial state (3.40))

$$\Psi_{\mathrm{AFM}}(x,t) \approx \int_0^t d\tau \int_{-\infty}^0 dx' \, F_{\mathrm{AFM}}(x,x',\tau,t)K_0(x,t-\tau)K_0(x',\tau)\Psi_0(x')\,, \tag{4.56}$$

where the function F_{AFM} is defined by

$$F_{\mathrm{AFM}}(x,x',\tau,t) \equiv \frac{1}{2}\,\chi(\tau)\left(\frac{x}{t-\tau} - \frac{x'}{\tau}\right)\,. \tag{4.57}$$

[10] The approximation sign stems from the BC (4.41), which was an approximation due to the use of the stationary phase approximation that was used to derive it.

We now substitute the expression (4.54) of the propagator $K_{11}(x, x', t)$ into (4.2), and use the decomposition (3.38) of the free-particle propagator K_0. We hence write the wave function $\Psi_{\mathrm{DPM}}(x, t)$ in the form

$$\Psi_{\mathrm{DPM}}(x,t) \approx \int_0^t d\tau \int_{-\infty}^0 dx'\, F_{\mathrm{DPM}}(x, x', \tau, t) K_0(x, t-\tau) K_0(x', \tau) \Psi_0(x')\,, \quad (4.58)$$

with F_{DPM} defined by

$$\begin{aligned} F_{\mathrm{DPM}}(x, x', \tau, t) &\equiv \frac{1}{2}\left\{\frac{x}{t-\tau} - \frac{x'}{\tau}\left[1 - \kappa(x', \tau)\right]\right\} \\ &= \frac{1}{2}\left(\frac{x}{t-\tau} - \frac{x'}{\tau}\left\{1 - \frac{2}{1 + \left[\frac{x'}{\tau\Omega(\tau)}\right]^2}\right\}\right)\,, \end{aligned} \quad (4.59)$$

where we used the definition (4.42) of the function $\kappa(x', \tau)$.

Now, suppose that we pick the values of the two wave functions Ψ_{AFM} and Ψ_{DPM} at the particular point $x = x_t$ (given by (4.4)). We can then show that the unique stationary point of the phase (coming from K_0 and Ψ_0) in the double integrals (4.56) and (4.58) that lies inside the domain of integration is the point $(\tau, x') = (t_c, x_0)$, with t_c the classical time defined by (3.43). Furthermore, note that the two functions F_{AFM} and F_{DPM} are, for the slowly varying barriers we consider in this section, mere algebraic functions of the integration variables, and thus change slowly as compared to the exponential terms due to K_0 and Ψ_0. Therefore, if we restrict our attention to values of the wave functions Ψ_{AFM} and Ψ_{DPM} in the close vicinity of the point $x = x_t$, then the dominant contributions to the integrals (4.56) and (4.58) raise from a neighbourhood of the point $(\tau, x') = (t_c, x_0)$, over which the algebraic functions F_{AFM} and F_{DPM} can be considered as constant and equal to their values for $x = x_t$, $x' = x_0$ and $\tau = t_c$. Note that in view of their definitions (4.57) and (4.59) we have

$$F_{\mathrm{AFM}}(x_t, x_0, t_c, t) = v_0 \chi(t_c) \quad (4.60)$$

and

$$F_{\mathrm{DPM}}(x_t, x_0, t_c, t) = \frac{v_0}{1 + \left[\Omega(t_c)/v_0\right]^2}\,, \quad (4.61)$$

respectively. Therefore, we can now readily see from (4.60) and (4.61) that if the aperture function $\chi(\tau)$ is related to the amplitude $\Omega(\tau)$ of the laser light through

(3.48), then we have

$$F_{\mathrm{AFM}}(x_t, x_0, t_c, t) = F_{\mathrm{DPM}}(x_t, x_0, t_c, t)\,, \tag{4.62}$$

and, consequently, $\Psi_{\mathrm{AFM}}(x,t) \simeq \Psi_{\mathrm{DPM}}(x,t)$ around the point $x = x_t$.

Therefore, we showed that in the semiclassical regime described by (4.1) the AFM and the DPM are in strong agreement in their predictions in a spatial vicinity of the point x_t in the case of slowly varying barriers. It is worth emphasising that this result is valid for *arbitrary* slowly varying barriers. We now turn our attention to the opposite case of an instantaneously varying barrier.

4.1.2 Moshinsky shutter

Here we consider the Moshinsky shutter, which we already introduced in the previous chapter in section 3.2 in connection with the propagator $K_{\mathrm{M}}(x, x', t)$ given by the integral (3.39). We recall that in the context of the AFM the Moshinsky shutter is characterised by a Heaviside-type aperture function. Here we assume that the shutter opens precisely at the classical time t_c[11], and thus we have

$$\chi(\tau) = \Theta(\tau - t_c)\,. \tag{4.63}$$

We now use the relation (3.48) to construct the time-dependent amplitude $\Omega(\tau)$ corresponding to the aperture function (4.63), and we have

$$\Omega(\tau) = \begin{cases} +\infty & , \quad 0 < \tau < t_c \\ 0 & , \quad t_c < \tau < t \end{cases}\,. \tag{4.64}$$

We now proceed to construct and compare the wave functions $\Psi_{\mathrm{AFM}}(x,t)$ and $\Psi_{\mathrm{DPM}}(x,t)$ corresponding to (4.63) and (4.64), respectively, in the transmission region.

We start with Ψ_{AFM}. We already know from section 3.2 that the propagator corresponding to the aperture function (4.63) is the propagator K_{M} given by (3.39). Therefore, substituting this propagator K_{M} with $t_{\mathrm{o}} = t_c$ into the expression (4.3) we get for the wave function $\Psi_{\mathrm{AFM}}(x,t)$

[11] This particular choice for the opening time of the barrier stems from the definition (3.43) of t_c. Indeed, it precisely corresponds to the arrival time of the centre of the incident wave packet at the barrier. In other words, $\tau = t_c$ is the moment where the incident wave packet is the most sensitive to any change of the transparency of the barrier.

$$\Psi_{\mathrm{AFM}}(x,t) \approx \int_{-\infty}^{0} dx''\, K_0(x-x'',t-t_c) \int_{-\infty}^{0} dx'\, K_0(x''-x',t_c)\Psi_0(x')\,. \tag{4.65}$$

In the semiclassical regime specified by (4.1) we can extend to $\mathbb{R}$ the integral with respect to x', hence yielding an exact Gaussian integral, while the remaining integral over x'' yields an error function. We hence obtain

$$\Psi_{\mathrm{AFM}}(x,t) \approx \left(\frac{1}{\pi\sigma^2}\right)^{1/4} \sqrt{\frac{\hbar(t-t_c)}{2m(x-x_t)^2}}\, \mathrm{e}^{i\beta} z_{\mathrm{M}} \mathrm{e}^{z_{\mathrm{M}}^2} \left[1-\mathrm{erf}\,(-z_{\mathrm{M}})\right]\,, \tag{4.66}$$

with $\mathrm{erf}(\cdot)$ the error function, and where we defined

$$\beta \equiv \frac{mx^2}{2\hbar(t-t_c)} + \frac{mv_0^2 t_c}{2\hbar} - \frac{3\pi}{4}\,, \tag{4.67}$$

and

$$z_{\mathrm{M}} \equiv \mathrm{e}^{i\frac{3\pi}{4}} \sqrt{\frac{m(x-x_t)^2}{2\hbar(t-t_c)}}\, \frac{1}{\sqrt{1+i\frac{\hbar(t-t_c)}{m\sigma^2}}}\,. \tag{4.68}$$

Note that

$$i\frac{mx^2}{2\hbar(t-t_c)} + z_{\mathrm{M}}^2 = -\frac{(x-x_t)^2}{2\sigma^2}\frac{1}{1+i\frac{\hbar(t-t_c)}{m\sigma^2}} + i\frac{mv_0 x}{\hbar} - i\frac{mv_0^2(t-t_c)}{2\hbar}\,. \tag{4.69}$$

Therefore, combining (4.66) with (4.67)-(4.69), we see, in the semiclassical regime (4.1) and using the fact that the error function is odd, i.e. $\mathrm{erf}\,(-z_{\mathrm{M}}) = -\mathrm{erf}\,(z_{\mathrm{M}})$, that the wave function $\Psi_{\mathrm{AFM}}(x,t)$ can be written in the form

$$\Psi_{\mathrm{AFM}}(x,t) \approx \frac{1}{2}\psi_{\alpha_0,x_t,v_0}(x,0)\mathrm{e}^{i\frac{mv_0^2}{2\hbar}t}\left[1+\mathrm{erf}\left(e^{i\frac{3\pi}{4}}\sqrt{\frac{m(x-x_t)^2}{2\hbar(t-t_c)}}\right)\right]\,. \tag{4.70}$$

The behaviour of the function (4.70) (more precisely, of its modulus squared) is illustrated on figure 2 in the particular case of the alkali-metal atom ^{87}Rb. The function $\Psi_{\mathrm{AFM}}(x,t)$ corresponding to the Moshinsky shutter (4.63) will also be analysed numerically for different alkali-metal atoms in section 4.2.4. It will be seen that the main effect of the Moshinsky shutter is to induce *oscillations* of the probability

density of the transmitted wave packet as compared to a freely evolved packet.

Now, before we construct the wave function $\Psi_{\mathrm{DPM}}(x,t)$ corresponding to the barrier described by (4.64), we first derive the corresponding propagator $K_{11}(x,x',t)$. It is worth noting that in view of (4.64) the Hamiltonian can be decomposed in a time-independent Hamiltonian for any $0<\tau<t_c$ (with an infinite potential barrier) followed by a different time-independent Hamiltonian for any $t_c<\tau<t$ (with an identically zero potential). Therefore, we can write the full propagator $\widehat{K}$ in the form

$$\widehat{K}(x,x',t)=\int_{-\infty}^{+\infty}dx''\,\widehat{K}_0(x-x'',t-t_c)\widehat{K}_\infty(x'',x',t_c)\,, \tag{4.71}$$

where $\widehat{K}_0$ is the matrix free-particle propagator (3.23), while $\widehat{K}_\infty$ is the limit of the propagator $\widehat{K}_{\Omega_0}$, given by (3.24) and corresponding to a time-independent amplitude $\Omega(\tau)=\Omega_0$ for the DPM, for an infinitely large amplitude Ω_0, i.e.

$$\widehat{K}_\infty(\xi_1,\xi_2,\tau)=\lim_{\Omega_0\to+\infty}\widehat{K}_{\Omega_0}(\xi_1,\xi_2,\tau)\,. \tag{4.72}$$

For clarity we recall here the results (3.24) and (3.25), namely

$$\widehat{K}_{\Omega_0}(\xi_1,\xi_2,\tau)=\widehat{K}_0(\xi_1-\xi_2,\tau)-\frac{m\Omega_0}{4\hbar}\sum_{j=\pm1}\mathrm{e}^{j\frac{m\Omega_0}{\hbar}(|\xi_1|+|\xi_2|)}\mathrm{e}^{i\frac{m\Omega_0^2}{2\hbar}\tau}\mathrm{erfc}(z_j)\begin{pmatrix}j & 1\\ 1 & j\end{pmatrix} \tag{4.73}$$

with

$$z_j=j\sqrt{i\frac{m\Omega_0^2}{2\hbar}\tau}+\sqrt{\frac{m}{2i\hbar\tau}}(|\xi_1|+|\xi_2|)\,, \tag{4.74}$$

where $j=\pm1$. Note that the argument of the first term of z_j is either $\pi/4$ (for $j=1$) or $-3\pi/4$ (for $j=-1$). Furthermore, as long as $\xi_1,\xi_2\neq0$[12] the argument of the second term of z_j is $-\pi/4$. Therefore, it is clear from (4.74) that $-3\pi/4<\arg(z_j)<\pi/4$. Furthermore, note that independently of the values of the variables ξ_1, ξ_2 or τ we have $\lim_{\Omega_0\to+\infty}|z_j|=+\infty$. Therefore, we substitute the asymptotic expansion of the complementary error function [55]

[12]This condition being automatically satisfied in our case since i) the initial state is localised in the reflection region, hence ξ_2 is in particular strictly smaller than 0, and ii) we are only interested in constructing the wave function in the transmission region, ξ_1 is in particular strictly larger than 0.

$$\mathrm{erfc}(z_j) \simeq \frac{\mathrm{e}^{-z_j^2}}{\sqrt{\pi} z_j} \tag{4.75}$$

into (4.73), and in view of (4.72) take the limit $\Omega_0 \to +\infty$ in the resulting expression of $\widehat{K}_{\Omega_0}$, to finally obtain for the propagator $\widehat{K}_\infty$

$$\widehat{K}_\infty(\xi_1, \xi_2, \tau) \approx \widehat{K}_0(\xi_1 - \xi_2, \tau) - \widehat{K}_0(|\xi_1| + |\xi_2|, \tau)\,. \tag{4.76}$$

Finally, we substitute this result (4.76) into the expression (4.71) of the DPM propagator to get the following expression for the component K_{11}:

$$\begin{aligned} K_{11}(x, x', t) \approx & \int_{-\infty}^{+\infty} dx''\, K_0(x - x'', t - t_c) K_0(x'' - x', t_c) \\ & - \int_{-\infty}^{+\infty} dx''\, K_0(x - x'', t - t_c) K_0(|x''| + |x'|, t_c)\,. \end{aligned} \tag{4.77}$$

Therefore, we can now construct the wave function $\Psi_{\mathrm{DPM}}(x, t)$ by substituting the propagator (4.77) into the expression (4.2). Dividing first the integrations with respect to the variable x'' into integrals over negative and positive values of x'' only, and using the fact that the initial state is localised in the reflection region (which allows to write $|x'| = -x'$), we get

$$\begin{aligned} \Psi_{\mathrm{DPM}}(x, t) \approx & \, \Psi_{\mathrm{AFM}}(x, t) \\ & - \int_{-\infty}^{0} dx''\, K_0(x - x'', t - t_c) \int_{-\infty}^{0} dx'\, K_0(-x'' - x', t_c) \Psi_0(x')\,. \end{aligned} \tag{4.78}$$

Computing now the integrals in (4.78), we show that within the semiclassical regime detailed by (4.1) the wave function $\Psi_{\mathrm{DPM}}(x, t)$ is given by

$$\Psi_{\mathrm{DPM}}(x, t) \approx \Psi_{\mathrm{AFM}}(x, t) + \Delta\Psi(x, t)\,, \tag{4.79}$$

where the "correction" $\Delta\Psi(x, t)$ is defined by

$$\Delta\Psi(x, t) \equiv \left(\frac{1}{\pi\sigma^2}\right)^{1/4} \sqrt{\frac{\hbar(t - t_c)}{2\pi m(x + x_t)^2}}\, e^{i\beta}\,, \tag{4.80}$$

with β given by (4.67).

Therefore, it follows from the expressions (4.70) and (4.79) of Ψ_{AFM} and Ψ_{DPM}, respectively, that the values of the two wave functions are very close to each other in the vicinity of the spatial point $x = x_t$. Indeed, considering values of the variable x sufficiently close to x_t, we have

$$|\Delta\Psi(x,t)| < \sqrt{\frac{\hbar t}{m x_t^2}}\,|\Psi_{\mathrm{AFM}}(x,t)| \ll \sqrt{\frac{\hbar t}{m\sigma^2}}\,|\Psi_{\mathrm{AFM}}(x,t)| \ll |\Psi_{\mathrm{AFM}}(x,t)|\,, \quad (4.81)$$

which is valid for any x in a close vicinity of x_t. This result for an instantaneously varying barrier hence complements the one obtained in section 4.1.1 for the opposite case of slowly varying barriers. Indeed, here again we see that in the semiclassical regime described by (4.1) the AFM and the DPM are in strong agreement in their predictions in a spatial vicinity of the point x_t. It is however important to note that this conclusion breaks down as we move away from the particular point $x = x_t$. To illustrate this important point we evaluate the probability densities, predicted from the two models, to detect the particle far in the transmission region, that is at values x such that

$$x \gg x_t\,. \quad (4.82)$$

First note on (4.68) that in this case we have $|z_{\mathrm{M}}| \gg 1$. Since it is clear that in the semiclassical regime we have $\arg(z_{\mathrm{M}}) \approx 3\pi/4 < \pi$, we can thus write an asymptotic expansion of the error function $\mathrm{erf}(-z_{\mathrm{M}})$, and we have

$$\mathrm{erf}(-z_{\mathrm{M}}) \simeq 1 + \frac{\mathrm{e}^{-z_{\mathrm{M}}^2}}{\sqrt{\pi}\,z_{\mathrm{M}}}\,. \quad (4.83)$$

Substituting the expansion (4.83) into the expression (4.66) hence yields for Ψ_{AFM}

$$\Psi_{\mathrm{AFM}}(x,t) \approx -\left(\frac{1}{\pi\sigma^2}\right)^{1/4}\sqrt{\frac{\hbar(t-t_c)}{2\pi m(x-x_t)^2}}\,\mathrm{e}^{i\beta}\,. \quad (4.84)$$

Therefore, we can write the probability density $|\Psi_{\mathrm{AFM}}|^2$ in the form

$$|\Psi_{\mathrm{AFM}}(x,t)|^2 \approx \xi_{\mathrm{M}}\,\frac{1}{(x-x_t)^2}\,, \quad (4.85)$$

where

$$\xi_{\mathrm{M}} \equiv \frac{\hbar(t-t_c)}{2\pi m\sigma\sqrt{\pi}} \tag{4.86}$$

is a constant having the dimension of a length. Combining the expression (4.79) of the DPM wave function with the expressions (4.80), (4.84) and (4.86) of $\Delta\Psi$, Ψ_{AFM} and ξ_{M}, respectively, we get that for large values of x the probability density $|\Psi_{\mathrm{DPM}}|^2$ is given by

$$|\Psi_{\mathrm{DPM}}(x,t)|^2 \approx \xi_{\mathrm{M}}\left[\frac{1}{(x-x_t)^2} - \frac{x+3x_t}{(x-x_t)(x+x_t)^2}\right]. \tag{4.87}$$

We now rewrite the expressions (4.85) and (4.87) in terms of the new variable $y = 1/x$, so that in the regime studied here where x is large we have basically $y \ll 1$ (regardless of the dimensions). We then Taylor expand the two probability densities about $y = 0$, up to the fourth order in y[13]. We finally change back the variable y to the original variable $x = 1/y$, and thus obtain the following expansions of the probability densities $|\Psi_{\mathrm{AFM}}|^2$ and $|\Psi_{\mathrm{DPM}}|^2$ for $x \gg x_t$:

$$|\Psi_{\mathrm{AFM}}(x,t)|^2 = \frac{\xi_{\mathrm{M}}}{x^2} + \mathcal{O}\left(\frac{1}{x^3}\right) \tag{4.88}$$

and

$$|\Psi_{\mathrm{DPM}}(x,t)|^2 = \frac{4x_t^2\xi_{\mathrm{M}}}{x^4} + \mathcal{O}\left(\frac{1}{x^5}\right). \tag{4.89}$$

Therefore, it is clear from (4.88) and (4.89) that the wave functions constructed from the two models exhibit a different behaviour far in the tails. Indeed, we have $|\Psi_{\mathrm{AFM}}|^2 \sim 1/x^2$ and $|\Psi_{\mathrm{DPM}}|^2 \sim 1/x^4$ for $x \gg x_t$.

An explicit example of how the probability densities predicted by the two models behave in the transmission region is illustrated on figure 2 for the particular case of the alkali-metal atom ^{87}Rb, of atomic mass $m_{\mathrm{Rb}} = 86.9091805$ u. The numerical values of the parameters characterising the initial state Ψ_0 are taken to be $x_0 = -0.15$ mm, $\sigma = 30$ μm and $v_0 = 3$ mm/s. The classical time is then $t_c = 50$ ms, while we choose a final time $t = 100$ ms $= 2t_c$, implying that $x_t = 0.15$ mm $= |x_0|$ (we also mention that in this case $\xi_{\mathrm{M}} \approx 0.11$ μm). Remember that we already briefly discussed this particular atom at the end of section 2.2, and saw that for such values

[13] This is needed for $|\Psi_{\mathrm{DPM}}|^2$.

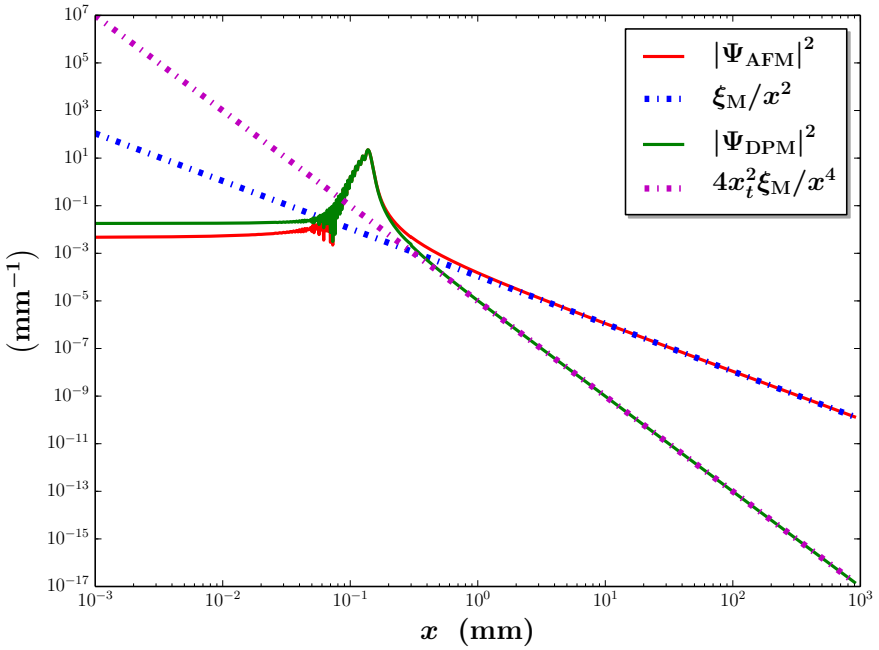

Figure 2: Probability densities $|\Psi_{\mathrm{AFM}}|^2$ and $|\Psi_{\mathrm{DPM}}|^2$, along with their asymptotic expansions as $x \to \infty$, for the alkali-metal atom ^{87}Rb.

of the parameters it behaves semiclassically to a very good approximation (as the increase of the spreading at the final time t, quantified by the parameter ϵ defined by (2.33), is in this case $\epsilon_{\mathrm{Rb}} \approx 0.081 \ll 1$). The expressions (4.70) and (4.79) hence accurately describe the state of the atom at the final time t as described by the AFM and the DPM, respectively. Therefore, figure 2 displays, on a log-log scale, the probability densities $|\Psi_{\mathrm{AFM}}|^2$ (solid red curve) and $|\Psi_{\mathrm{DPM}}|^2$ (solid green curve) obtained from (4.70) and (4.79), respectively, with respect to the position x. We consider a wide range of values of x so as to span a representative subset of the transmission region. In addition, we plot the corresponding asymptotic expressions of $|\Psi_{\mathrm{AFM}}|^2$ (dash-dotted blue curve) and $|\Psi_{\mathrm{DPM}}|^2$ (dash-dotted magenta curve) obtained from the expansions (4.88) and (4.89), respectively. It is thus clear that, as we saw in (4.81), the two models are in excellent agreement in the spatial region centred around the point $x_t = 0.15$ mm, as the red and green curves are indistinguishable in this case. However, the predictions of the two models become radically different as we move away from x_t, and we can see that the expansions (4.88) and (4.89) provide excellent approximations of the probability densities $|\Psi_{\mathrm{AFM}}|^2$ and $|\Psi_{\mathrm{DPM}}|^2$, respectively, already for $x \approx 0.9$ mm $= 6x_t$.

Therefore, we considered in this section the two opposite examples of an (arbitrary) slowly varying barrier (subsection 4.1.1) and of an instantaneously opening barrier (subsection 4.1.2). We obtained, in both cases, analytical results demonstrating an excellent agreement between the predictions of the two models, the AFM and the DPM, if their fundamental parameters, namely the aperture function $\chi(\tau)$ for

the AFM and the amplitude $\Omega(\tau)$ for the DPM, are precisely related through (3.48). However, such conclusions could only be obtained in the vicinity of the point $x = x_t$, which we recall represents the position of the corresponding freely-propagating classical particle at time t. We now proceed to numerically approach the problem, as this allows to analyse the predictions of the two models in a broader spatial region, as well as go beyond the semiclassical regime characterised by the assumptions (4.1).

4.2 Numerical results

We now numerically evaluate the two wave functions $\Psi_{\rm AFM}$ and $\Psi_{\rm DPM}$ in order to investigate the validity of the relation between χ and Ω in both the semiclassical and the deep quantum regimes. We first discuss the strategy we use for making such an analysis.

A quantitative comparison between $\Psi_{\rm AFM}(x,t)$ and $\Psi_{\rm DPM}(x,t)$ can be obtained from two complementary quantities. The first one is the *fidelity*, denoted by $M\,(t)$, and is defined by

$$M\,(t) \equiv \frac{\left|\int_{x_A}^{x_B} dx\; \Psi^{\star}_{\rm AFM}\,(x,t)\;\Psi_{\rm DPM}\,(x,t)\right|^2}{\mathscr{P}_{\rm AFM}\,(t)\;\mathscr{P}_{\rm DPM}\,(t)}\,, \tag{4.90}$$

where x_A and x_B, $0 < x_A < x_B$, are two numerical parameters to be chosen so as to enclose a representative part of the transmitted wave function, and

$$\mathscr{P}_{\rm AFM\,,\,DPM}\,(t) \equiv \int_{x_A}^{x_B} dx\;\left|\Psi_{\rm AFM\,,\,DPM}\,(x,t)\right|^2 \tag{4.91}$$

represents the probability of detecting the particle in the spatial region $x_A < x < x_B$ at time t, as predicted by the AFM or the DPM. By construction, the fidelity $M\,(t)$ quantifies the overlap, within the region $x_A < x < x_B$ and at the time t, between the wave functions $\Psi_{\rm AFM}$ and $\Psi_{\rm DPM}$, and takes values between 0 and 1[14]. If $M = 0$ the two wave functions are orthogonal and hence do not overlap at all, while $M = 1$ corresponds to collinear wave functions. We can thus see the fidelity M as a test of the x-dependence of the two wave functions $\Psi_{\rm AFM}$ and $\Psi_{\rm DPM}$ within the region $x_A < x < x_B$. However, note that M is insensitive to the overall amplitude of $\Psi_{\rm AFM}$ and $\Psi_{\rm DPM}$, and hence must be completed with an other measure of similarity between the two wave functions. A simple choice is to consider the *probability ratio*, denoted by $R\,(t)$, defined by

[14]The fact that M admits 1 as an upper bound is a direct consequence of the Cauchy-Schwarz inequality on $L^2\,([x_A, x_B])$ (see e.g. [44]).

$$R(t) \equiv \frac{\mathscr{P}_{\mathrm{DPM}}(t)}{\mathscr{P}_{\mathrm{AFM}}(t)}. \tag{4.92}$$

This latter merely compares the probabilities of finding the particle in the region $x_A < x < x_B$ at time t, as predicted by the AFM and the DPM, and is by construction a positive quantity.

The combination of the fidelity M and of the probability ratio R allows us to make a complete comparison between the wave functions Ψ_{AFM} and Ψ_{DPM}. To see this, consider the particular case where $M(t) = R(t) = 1$. First, note that $M(t) = 1$ implies that $\Psi_{\mathrm{DPM}}(x,t) = \lambda \Psi_{\mathrm{AFM}}(x,t)$, with λ a so far arbitrary complex number[15]. Now, the additional condition $R(t) = 1$ implies that $|\lambda| = 1$. Therefore, we see that $M(t) = R(t) = 1$ implies that $\Psi_{\mathrm{AFM}}(x,t) = \Psi_{\mathrm{DPM}}(x,t)$ in the region $x_A < x < x_B$, up to a global phase factor which has no physical relevance. This means that both the AFM and the DPM predict the same physical state for the particle at time t. On the other hand, if for instance $M(t) = 0$, the states predicted by the AFM or the DPM are orthogonal and thus completely different. Therefore, the closer are both the fidelity M and the probability ratio R to 1, the better is the agreement between the predictions of the AFM and the DPM.

We numerically analyse the dynamics of four different physical systems, namely the alkali-metal atoms ^{7}Li, ^{23}Na, ^{41}K and ^{87}Rb. Such atoms are widely used in modern ultracold atom-optics experiments. Their respective masses are, in atomic units, $m_{\mathrm{Li}} = 7.016003$ u, $m_{\mathrm{Na}} = 22.989767$ u, $m_{\mathrm{K}} = 40.961825$ u and $m_{\mathrm{Rb}} = 86.9091805$ u, respectively[16]. We make only the mass vary, and take all four atoms to share the following values of parameters. The initial Gaussian wave packet, as given by (3.41), is characterised by the mean position $x_0 = -0.15$ mm (remember that $x = 0$ is the position of the barrier), mean velocity $v_0 = 3$ mm/s and width $\sigma = 30$ μm. This yields a classical time $t_c = 50$ ms. We then take the final time to be $t = 100$ ms $= 2t_c$, hence implying the value $x_t = 0.15$ mm $= |x_0|$ for the position of the corresponding freely propagated classical particle. It is worth noting that such values are, for instance, very similar to the experimental parameters used in [26], where a cloud of ^{87}Rb atoms could propagate up to a time of 150 ms.

It is easily seen that increasing the mass of the system makes the atom behave more and more semiclassically. Indeed, let us compare the values of the rightmost term from the semiclassical conditions (4.1)[17] for the lightest and the heaviest atoms considered here, namely ^{7}Li and ^{87}Rb, respectively. In the case of ^{7}Li, we have

[15] This stems from the equality case of the Cauchy-Schwarz inequality on $L^2([x_A, x_B])$ (see e.g. [44]).

[16] We recall that these numerical values were taken from the NIST website in Spring 2015.

[17] All the other terms in (4.1) are independent of the mass m, and are thus the same for all four atoms.

$m_{\mathrm{Li}}\sigma^2 v_0/\hbar \simeq 0.3$ mm, which is comparable to $v_0(t-t_c) = 0.15$ mm. However, in the case of ^{87}Rb, we have $m_{\mathrm{Rb}}\sigma^2 v_0/\hbar \simeq 3.7$ mm, which is more than 20 times larger than $v_0(t-t_c) = 0.15$ mm. Therefore, whereas the last condition in (4.1) is not satisfied for ^{7}Li, it is clearly satisfied for ^{87}Rb. Therefore, considering moving particles of different masses[18] allows us to investigate the validity of the connection between the AFM and the DPM both in the deep quantum regime (for ^{7}Li) and in the semiclassical regime (for ^{87}Rb).

Now that we outlined our general strategy, we analyse four complementary scenarios. We first present in section 4.2.1 the simplest case of a time-independent barrier before we address in section 4.2.2 the slightly more complicated (though exactly solvable) case of an algebraically (slowly) varying barrier characterised, in the context of the DPM, by $\Omega(\tau) = \Omega_1/\tau$ (with Ω_1 a constant). We then discuss in section 4.2.3 the case of exponentially (rapidly) varying barriers (whose practical interest has been first shown in [28]). Finally, we consider in section 4.2.4 an instantaneously varying barrier in the form of the Moshinsky shutter that we treated analytically in section 4.1.2. In each of these scenarios, and for any atom, we evaluate and compare the wave functions $\Psi_{\mathrm{AFM}}(x,t)$ and $\Psi_{\mathrm{DPM}}(x,t)$ in view of the relation (3.48) between the aperture function $\chi(\tau)$ and the amplitude $\Omega(\tau)$.

4.2.1 Time-independent barrier

We begin with a time-independent barrier for which $\chi(\tau) = \chi_0$ and $\Omega(\tau) = \Omega_0$, where in view of (3.48) χ_0 and Ω_0 are related through

$$\chi_0 = \frac{1}{1+(\Omega_0/v_0)^2}\,. \tag{4.93}$$

In this case, the AFM propagator (3.37) reduces to $K_{\mathrm{AFM}} = \chi_0 K_0$, and thus substituting this propagator into (4.3) readily yields the attenuated freely evolved Gaussian wave packet $\Psi_{\mathrm{AFM}} = \chi_0 \Psi_{\mathrm{free}}$, where we introduce for convenience the notation Ψ_{free} for the freely evolved Gaussian wave packet ψ_{α_0,x_0,v_0} given by (2.17), i.e.

$$\Psi_{\mathrm{free}}(x,\tau) \equiv \psi_{\alpha_0,x_0,v_0}(x,\tau)\,. \tag{4.94}$$

Furthermore, the propagator $\widehat{K}$ for a time-independent δ-potential is already known to be the propagator $\widehat{K}_{\Omega_0}$ given by (3.24). The wave function Ψ_{DPM} can thus be constructed by substituting $K_{11} = \left(\widehat{K}_{\Omega_0}\right)_{11}$ into (4.2).

We now compute the fidelity M and the probability ratio R, as defined by (4.90)

[18] Or equivalently, since the velocity is the same for any atom, of different momenta.

and (4.92), respectively, for the different atoms. Therefore, we must first of all fix the boundaries of the integration region $x_A < x < x_B$. Here we choose $x_A = x_t - 4(\Delta x)_t$ and $x_B = x_t + 4(\Delta x)_t$, where $(\Delta x)_t$ is the position uncertainty, given by (2.24), of the free-particle wave packet $\Psi_{\text{free}}(x,t)$. This choice is made in view of the expression $\Psi_{\text{AFM}} = \chi_0 \Psi_{\text{free}}$ of the AFM wave function, for which we already know that such a region $x_A < x < x_B$ contains the dominant part of the transmitted wave packet. The factor 4 is arbitrary, and ensures a comparison between Ψ_{AFM} and Ψ_{DPM} on a broad spatial interval. For the sake of concreteness we here give the values of $(\Delta x)_t$ for the different atoms: we have $(\Delta x)_t \simeq 30.1$ μm for ^{7}Li, 22.2 μm for ^{23}Na, 21.5 μm for ^{41}K, and 21.3 μm for ^{87}Rb.

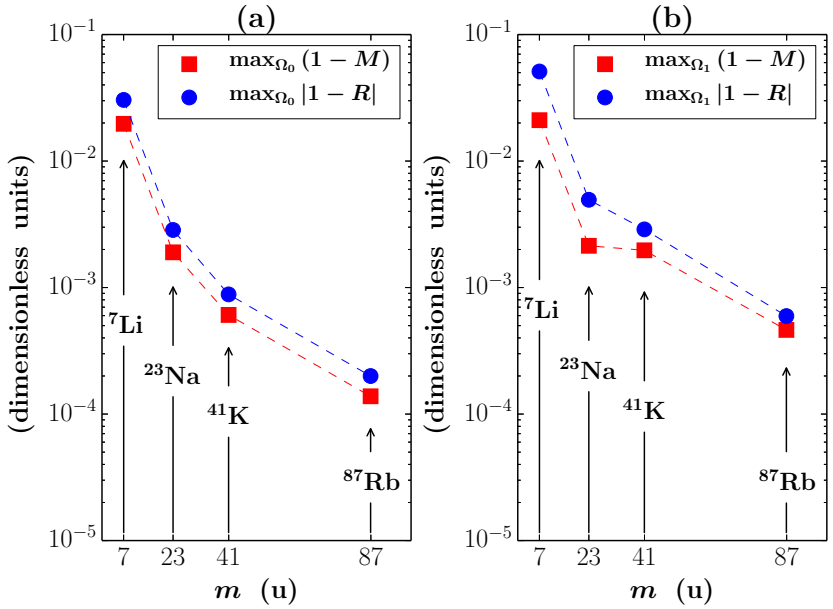

Figure 3: Maximal deviations of the fidelity M (red squares) and probability ratio R (blue circles) from 1 for four different alkali atoms in the case of (a) a time-independent barrier (the deviations are maximised with respect to Ω_0), and (b) an algebraic barrier for which $\Omega(\tau) = \Omega_1/\tau$ (the deviations are maximised with respect to Ω_1).

As discussed in the opening of the section 4.2, the closer are both the fidelity M and the probability ratio R to 1 the better is the agreement between the predictions of the two models. Therefore, we display on figure 3(a) the values of the deviations of M and R from 1, i.e. $(1-M)$ and $|1-R|$[19], respectively, for the different atoms. More precisely, we evaluate, in view of the relation (4.93), the wave functions Ψ_{AFM} and Ψ_{DPM} for each atom at the same values of Ω_0 over the range $0 \leqslant \Omega_0 \leqslant 100 v_0$. We

[19]We take the absolute value of $(1-R)$ since the probability ratio, as defined by (4.92), can take any positive value. The fidelity M however is by construction a quantity whose values range between 0 and 1. Note that to take the absolute value of $(1-R)$ is sufficient here since our sole purpose is to investigate whether the probability ratio R gets closer to 1 (either from values larger or smaller than 1) as we increase the mass of the system.

then determine, over this range, the maximum values $\max_{\Omega_0}(1-M)$ and $\max_{\Omega_0}|1-R|$ of the deviations from 1 of M and R, respectively[20]. We clearly see on figure 3(a) that both $\max_{\Omega_0}(1-M)$ (red squares) and $\max_{\Omega_0}|1-R|$ (blue circles) decrease by over two orders of magnitude as the atomic mass increases from m_{Li} to m_{Rb}. Note that this behaviour is solely due to the change of mass (or, equivalently, momentum) of the atom, as any atom is otherwise characterised by the exact same parameters and submitted to the exact same barrier strengths. Therefore, we can conclude from 3(a) that the agreement between the wave functions Ψ_{AFM} and Ψ_{DPM} quickly improves as the atom becomes more semiclassical. Note in particular that the wave functions predicted by the two models appear to be almost indistinguishable for both ^{41}K and ^{87}Rb, as M and R deviate from 1 by less than 0.1% already for potassium.

4.2.2 Algebraic barrier

We now consider a time-dependent barrier corresponding, in the context of the DPM, to a potential that is inversely proportional to time, i.e. $\Omega(\tau) = \Omega_1/\tau$ with Ω_1 a constant. We already saw in the previous chapter (section 3.1) that the DPM is exactly solvable in this case and admits the propagator $\widehat{K}_{1/\tau}$ given by (3.26). We can thus construct Ψ_{DPM} by substituting the element

$$K_{11}(x,x',t) = K_0(x-x',t) - \frac{\Omega_1^2}{\Omega_1^2+x'^2}K_0(|x|+|x'|,t) \tag{4.95}$$

of the full propagator $\widehat{K}_{1/\tau}$ into the integral (4.2) which is then computed numerically. The AFM wave function is obtained from (4.3) and the propagator (3.37) upon substituting the aperture function obtained from (3.48), namely here

$$\chi(\tau) = \frac{1}{1+(\Omega_1/v_0\tau)^2}\,, \tag{4.96}$$

and again evaluating the resulting integral numerically. We then compute the fidelity M and the probability ratio R, taking here again $x_A = x_t - 4(\Delta x)_t$ and $x_B = x_t + 4(\Delta x)_t$ (as we did for the time-independent barrier treated in subsection 4.2.1). Indeed, we expect the freely evolved wave packet Ψ_{free} to still be representative of the transmitted wave packet for the slowly varying barrier studied here.

We then make a similar analysis than in the time-independent case of subsection 4.2.1. Namely, we maximise, for the different atoms, the deviations of the

[20]Different numerical errors may build up in constructing the wave functions Ψ_{AFM} and Ψ_{DPM} for each atom at a same value of Ω_0. To compare the maximum deviations $(1-M)$ and $|1-R|$ over the whole range of values of Ω_0 between each atom allows us to focus on the global behaviour of the fidelity M and the probability ratio R as we increase the mass of the system.

fidelity and of the probability ratio from 1 over the range of barrier strengths $0 \leqslant \Omega(t_c) \leqslant 100v_0$ at the classical time t_c[21]. The results are presented on figure 3(b), and the observations are again very similar to the time-independent case. We clearly see that both $\max_{\Omega_1}(1-M)$ (red squares) and $\max_{\Omega_1}|1-R|$ (blue circles) decrease as the atomic mass increases from m_{Li} to m_{Rb}. Therefore, we conclude from 3(b) that the wave functions Ψ_{AFM} and Ψ_{DPM} are in better agreement when the atom becomes more semiclassical. Note in particular that the wave functions predicted by the two models appear to be almost indistinguishable for ^{87}Rb, as M and R deviate from 1 by less than 0.1% in this case.

4.2.3 Exponential barriers

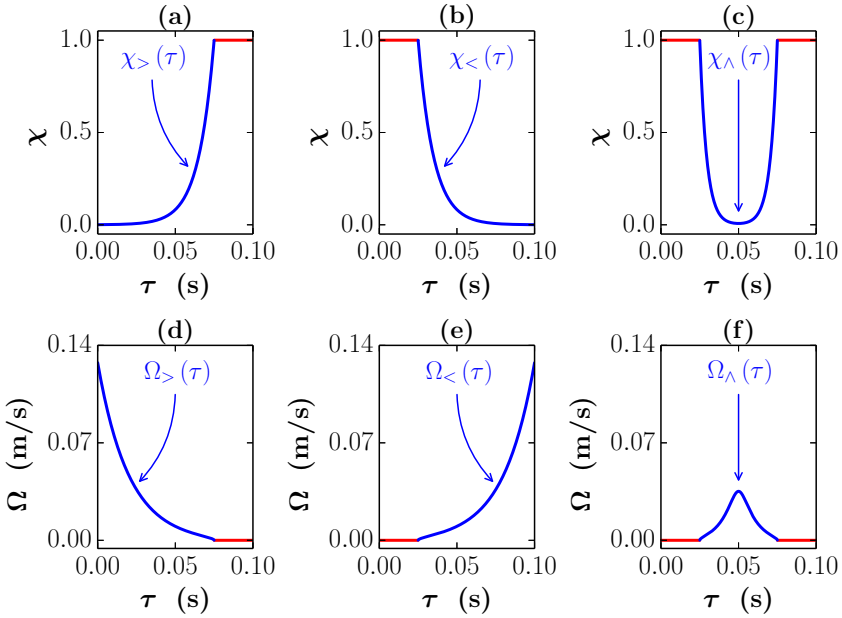

Figure 4: Aperture function $\chi(\tau)$ and the corresponding atom-laser interaction strength $\Omega(\tau)$, obtained in view of the relation (3.48), in three different scenarios. (a) $\chi(\tau) = \min\{\chi_>(\tau), 1\}$, with $\chi_>(\tau) \equiv \exp[\gamma(\tau - 3t_c/2)]$ and $\gamma = 100$ s^{-1}, (b) $\chi(\tau) = \min\{\chi_<(\tau), 1\}$, with $\chi_<(\tau) \equiv \exp[\gamma(\tau - t_c/2)]$ and $\gamma = -100$ s^{-1}, (c) $\chi(\tau) = \min\{\chi_\wedge(\tau), 1\}$, with $\chi_\wedge(\tau) \equiv \cosh[\gamma(\tau - t_c)]/\cosh(\gamma t_c/2)$ and $\gamma = 225$ s^{-1}, (d) $\Omega(\tau) = \Omega_>(\tau) \equiv v_0\sqrt{1/\chi_>(\tau) - 1}$ for $\tau < 3t_c/2$, and $\Omega(\tau) = 0$ for $\tau \geq 3t_c/2$, (e) $\Omega(\tau) = 0$ for $\tau \leq t_c/2$, and $\Omega(\tau) = \Omega_<(\tau) \equiv v_0\sqrt{1/\chi_<(\tau) - 1}$ for $\tau > t_c/2$, and (f) $\Omega(\tau) = \Omega_\wedge(\tau) \equiv v_0\sqrt{1/\chi_\wedge(\tau) - 1}$ for $|\tau - t_c| < t_c/2$, and $\Omega(\tau) = 0$ for $|\tau - t_c| \geq t_c/2$.

We now turn our attention to rapidly varying barriers. We consider time-dependent barriers corresponding, in the context of the AFM, to aperture functions $\chi(\tau)$ having an exponential dependence on time. As was recently proposed in [28],

[21] We chose to vary $\Omega(t_c)$ as the classical time t_c precisely corresponds to the arrival time of the centre of the incident wave packet, that is the time at which the particle is the most sensitive to the variations of the time-dependent barrier.

such barriers can be used to manipulate the quantum state of a moving particle. They can indeed induce shifting, splitting or else squeezing of the transmitted wave function. Here we focus on the shifting and the splitting, and thus consider the three different time-dependent scenarios illustrated on figure 4.

Figures 4(a), 4(b) and 4(c) display the three different aperture functions $\chi_>(\tau)$, $\chi_<(\tau)$ and $\chi_\wedge(\tau)$, respectively, while figures 4(d), 4(e) and 4(f) display the three different corresponding amplitudes, obtained from χ through the relation (3.48), $\Omega_>(\tau)$, $\Omega_<(\tau)$ and $\Omega_\wedge(\tau)$, respectively. It is worth emphasising that all these barriers depend exponentially on time in the vicinity of the classical time t_c. This exponential dependence is illustrated by the blue curves on figure 4. Now, as is discussed in [28], the form of $\chi(\tau)$ for values of τ sufficiently far from t_c only yields minor contributions to the transmitted wave packet. Therefore, we can safely consider χ (and by extension also Ω) to be constant for such values of τ. This corresponds to the red parts of the curves on figure 4. The AFM wave function is as usual constructed from (4.3) and the propagator (3.37) for the relevant aperture function χ. We then numerically evaluate the resulting integral. However, here the DPM wave function can only be obtained by numerically solving the TDSE (3.19) for the spinor. This is done by means of a Crank-Nicolson algorithm [56] (details may be found in appendix C).

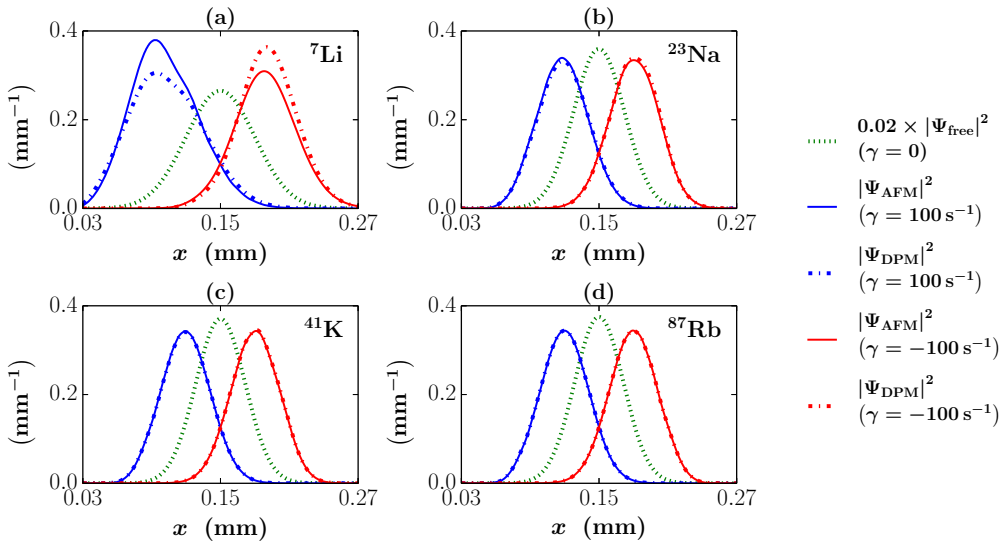

Figure 5: Probability densities $|\Psi_{\text{AFM}}|^2$ (solid curves) and $|\Psi_{\text{DPM}}|^2$ (dash-dotted curves) for (a) ^{7}Li, (b) ^{23}Na, (c) ^{41}K and (d) ^{87}Rb as functions of the position x. Blue curves correspond to the barrier specified in Figs. 4(a) and 4(d). Red curves correspond to the barrier specified in Figs. 4(b) and 4(e). The dotted green curve represents the scaled probability density of the corresponding free-particle wave packet.

We first focus on the barriers described by 4(a)-4(b) (for the AFM) and 4(d)-4(e) (for the DPM), and compute the corresponding wave functions for the four atoms

^{7}Li, ^{23}Na, ^{41}K and ^{87}Rb. Figure 5 shows the corresponding probability densities predicted by the AFM (solid curves) and the DPM (dash-dotted curves) as functions of the position x. The blue curves correspond to the barriers illustrated on figures 4(a) and 4(d). They were thus obtained from an aperture function defined by $\chi(\tau) = \min\{\chi_>(\tau), 1\}$, with $\chi_>(\tau) = \exp[\gamma(\tau - 3t_c/2)]$ and $\gamma = 100$ s^{-1}. The red curves correspond to the barriers illustrated on figures 4(b) and 4(e), and thus were obtained from an aperture function defined by $\chi(\tau) = \min\{\chi_<(\tau), 1\}$, with $\chi_<(\tau) = \exp[\gamma(\tau - t_c/2)]$ and $\gamma = -100$ s^{-1}. To emphasise the effect of such time-dependent barriers, we also plot the scaled probability density of the free-particle Gaussian wave packet $0.02\,|\Psi_{\text{free}}(x,t)|^2$ (dotted green curve)[22]. This latter represents the profile that would be obtained for a fully transparent barrier, i.e. for $\gamma = 0$. Therefore, it is clear on figure 5 that the barriers 4(a) and 4(d) or 4(b) and 4(e) have *shifted* the transmitted wave packets as compared to the freely evolved wave packet. A quantitative estimate of such a shift was obtained in [28], and is characterised by a distance $\Delta \simeq -\gamma\sigma^2/v_0$ with respect to the centre x_t of Ψ_{free}. It was however also shown in [28] that such barriers do not change the average velocity of the particle. Indeed, the mean velocity of the shifted wave packets remains equal to v_0.

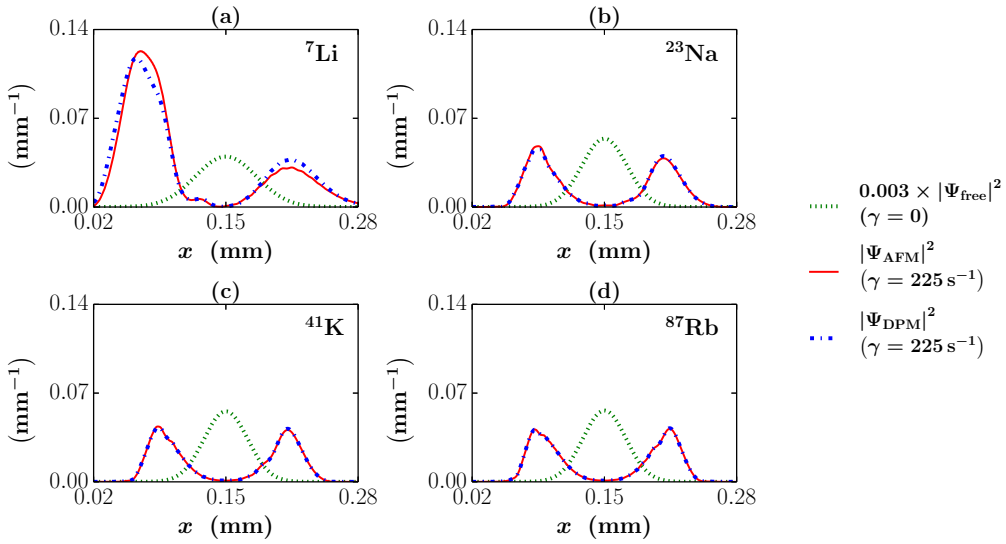

Figure 6: Probability densities $|\Psi_{\text{AFM}}|^2$ (solid red curve) and $|\Psi_{\text{DPM}}|^2$ (dash-dotted blue curve) for (a) ^{7}Li, (b) ^{23}Na, (c) ^{41}K and (d) ^{87}Rb as functions of the position x. The curves correspond to the barrier specified in Figs. 4(c) and 4(f). The dotted green curve represents the scaled probability density of the corresponding free-particle wave packet.

We now analyse the barriers represented on figures 4(c) (for the AFM) and 4(f) (for the DPM). Here again we compute the corresponding wave functions for the four atoms ^{7}Li, ^{23}Na, ^{41}K and ^{87}Rb. These are constructed in this case from an

[22]The presence of an absorbing barrier lowers the overall amplitude of the transmitted wave packet, hence the need for a scaling factor here for Ψ_{free}.

aperture function of the form $\chi(\tau) = \min\{\chi_\wedge(\tau), 1\}$, with $\chi_\wedge(\tau) \equiv \cosh[\gamma(\tau - t_c)]/\cosh(\gamma t_c/2)$ and $\gamma = 225\ \mathrm{s}^{-1}$. We can see on figure 6 the corresponding probability densities $|\Psi_{\mathrm{AFM}}(x,t)|^2$ (solid red curve) and $|\Psi_{\mathrm{DPM}}(x,t)|^2$ (dash-dotted blue curve), plotted with respect to the position x. Here again, we plot (dotted green curve) the scaled probability density of the free-particle Gaussian wave packet $0.003\,|\Psi_{\mathrm{free}}(x,t)|^2$. As is clearly displayed on figure 6, barriers akin to 4(c) and 4(f) produce a spatial *splitting* of the transmitted wave packet as compared to the freely evolved Gaussian wave packet.

We can readily see on figures 5 and 6 that the agreement between the two models improves as we increase the mass of the system. Indeed, whereas there are clear (though not stringent)[23] discrepancies between the probability densities $|\Psi_{\mathrm{AFM}}|^2$ and $|\Psi_{\mathrm{DPM}}|^2$ in the case of ^{7}Li, they can barely be distinguished already for ^{23}Na, and look exactly the same for both ^{41}K and ^{87}Rb. We can make a more quantitative statement by computing, here again, the deviations of the fidelity and of the probability ratio from 1 for the different barriers. In all three cases (i.e. for shifting and splitting), we observe that the values of $(1 - M)$ and $|1 - R|$ decrease by approximately two orders of magnitude as we increase the mass from ^{7}Li to ^{87}Rb.

4.2.4 Moshinsky shutter

We conclude our numerical analysis by taking a closer look at the Moshinsky shutter, already treated analytically in subsection 4.1.2. We recall that it corresponds to an instantaneously opening barrier, characterised by the aperture function (4.63) (for the AFM) and thus, using the relation (3.48), by the amplitude (4.64) (for the DPM). Furthermore, the propagators K_{AFM} and K_{11} for both the AFM and the DPM are known exactly in this particular case, and are given by (3.39) and (4.77), respectively. Therefore, the AFM wave function is obtained from combining (4.3) with the propagator (3.39). Similarly, Ψ_{DPM} results from substituting the propagator (4.77) into (4.2).

We show on figure 7 the probability densities $|\Psi_{\mathrm{AFM}}(x,t)|^2$ (solid red curve) and $|\Psi_{\mathrm{DPM}}(x,t)|^2$ (dash-dotted blue curve) as functions of the position x. Here again, we represent for reference the probability density of the free-particle Gaussian wave packet $|\Psi_{\mathrm{free}}(x,t)|^2$ (dotted green curve). The effect of the Moshinsky shutter is thus to create *oscillations* of the transmitted wave packet, these latter being more and more pronounced as we increase the mass of the system.

We clearly see on figure 7 that the agreement between the two models again improves as the atom becomes more semiclassical. Indeed, computing the deviations

[23] Indeed, in the case of lithium the maximum deviation of the fidelity from 1 occurs for the splitting, and we have $(1 - M) \approx 0.018$, that is less than 2%, which is still a relatively high value for the fidelity. The most important difference then comes mostly from the overall amplitude, what is reflected in the deviations of the probability ratio from 1.

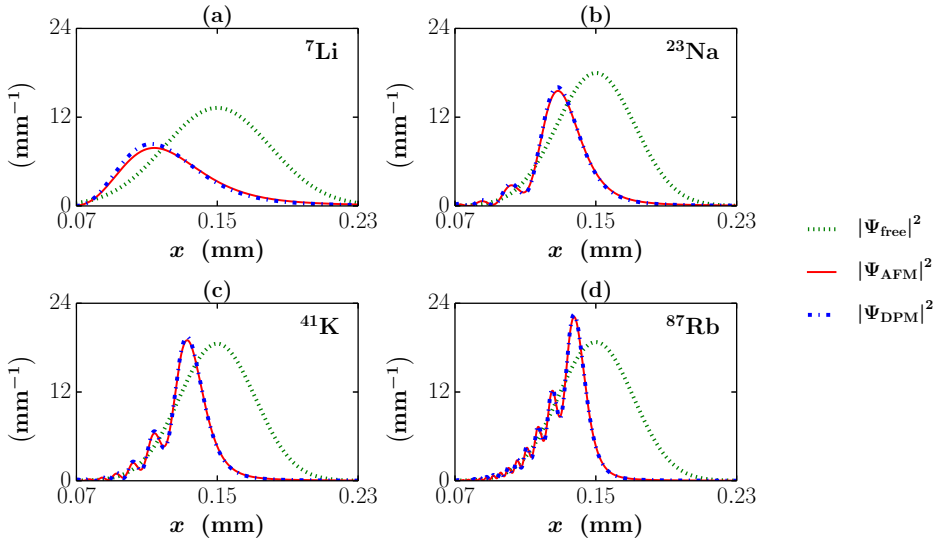

Figure 7: Probability densities $|\Psi_{\rm AFM}(x,t)|^2$ (solid red curve) and $|\Psi_{\rm DPM}(x,t)|^2$ (dash-dotted blue curve) for (a) ^{7}Li, (b) ^{23}Na, (c) ^{41}K and (d) ^{87}Rb evaluated for the case of the Moshinsky shutter, i.e. for an aperture function of the form (4.63). The dotted green curve represents the probability density of the corresponding free-particle wave packet.

of the fidelity and of the probability ratio from 1 shows that $(1-M)$ decreases by approximately 14 times as we go from lithium to rubidium (from roughly 0.0071 for ^{7}Li to 0.0005 for ^{87}Rb), while $|1-R|$ decreases by approximately 17 times (from roughly 0.0223 for ^{7}Li to 0.0013 for ^{87}Rb). This numerical treatment hence perfectly confirms the analytical conclusions obtained in subsection 4.1.2, and clarifies the extent of the spatial region, centred around the point $x_t = 0.15$ mm, over which the predictions of the model are in good agreement.

Chapter 5

Prospects for the aperture function model

In the previous chapter we justified the connection between the AFM and the DPM that was conjectured in chapter 3 (namely the relation (3.48)). As a result, the aperture function model (AFM) now possesses a strong physical ground. Indeed, it is now clear how the aperture function $\chi(\tau)$ is related to well-defined physical quantities characterising the atom-laser system. Therefore, we can now capitalise on the essentially analytical nature of the AFM to explore various aspects of matter-wave absorption by time-dependent barriers. The purpose of this final chapter is then to formulate various physical questions where we believe the AFM can prove valuable. We present some preliminary results and identify possible directions for future research.

The structure of the propagator K_{AFM}, as given by (3.37), combined with the choice of the Gaussian wave packet (3.41) as the initial state, strongly suggests to focus on the Husimi representation of the transmitted wave packet. The Husimi distribution was introduced in section 2.3, and we first present in section 5.1 the mathematical basis necessary to our subsequent analysis. We then turn our attention in sections 5.2 and 5.3 to two specific examples of time-dependent barriers, namely of simple periodic and Gaussian type, respectively, before we reformulate the problem from a complex analysis perspective in section 5.4. Finally, we formulate in section 5.5 the inverse problem, aiming at determining the time-dependent barrier that would produce a desired target (transmitted) state.

5.1 Husimi representation of the transmitted state

In this section we discuss the general features of the Husimi distribution associated with the AFM wave function. First of all, we recall that the fundamental expression (3.37) of the propagator $K_{\mathrm{AFM}}(x, x', t)$ is only valid for negative values of the

source variable x' (initial state localised in the reflection region), and for positive values of the position x (final state localised in the transmission region). Such conditions are satisfied within the semiclassical regime described by (4.1), which we here reproduce for completeness:

$$\sigma \ll |x_0| \lesssim v_0(t-t_c) \ll \frac{m\sigma^2 v_0}{\hbar}\,. \tag{5.1}$$

Most of the analytical results presented in this chapter are precisely derived from these assumptions (5.1), and thus concern semiclassical systems. It is hence worth emphasising at this stage that the conclusions drawn in chapter 4 provide us with concrete physical examples of such systems. Indeed, the analysis presented in the sequel can in particular be applied to the alkali-metal atom ^{87}Rb, and is still reliable for ^{41}K, for the numerical parameters detailed in section 4.2 (which we recall are experimentally relevant).

We will eventually show that in the semiclassical regime (5.1) the AFM Husimi amplitude, which we denote by $h^{(\mathrm{fr})}_{\mathrm{AFM}}(\widetilde{x},\widetilde{v},t)$, can be written in the form (Eqs. (5.25) and (5.24))

$$h^{(\mathrm{fr})}_{\mathrm{AFM}}(\widetilde{x},\widetilde{v},t) = \frac{v_0+\widetilde{v}}{2\sigma\sqrt{\pi}}\int_{-\infty}^{+\infty} d\tau\, \chi(\tau) \mathrm{e}^{\phi^{(\mathrm{fr})}(\tau)}\,, \tag{5.2}$$

with

$$\begin{aligned}\phi^{(\mathrm{fr})}(\tau) \equiv -\alpha_0\left[\widetilde{x}-\widetilde{v}(t-\tau)\right]^2 - \alpha_0\left(x_0+v_0\tau\right)^2 + i\frac{m\widetilde{v}}{\hbar}\left[\widetilde{x}-\widetilde{v}(t-\tau)\right] \\ - i\frac{mv_0}{\hbar}\left(x_0+v_0\tau\right) + i\frac{m\widetilde{v}^2}{2\hbar}(t-\tau) + i\frac{mv_0^2}{2\hbar}\tau\,.\end{aligned} \tag{5.3}$$

The advantage of the expression (5.2) is that the argument $\phi^{(\mathrm{fr})}(\tau)$ of the exponent is a quadratic function of the integration variable τ. This is reminiscent of the use of the frozen Gaussian regime to neglect the time-dependent increase of the spreading of a freely evolved Gaussian wave packet. We can then conveniently choose the aperture function $\chi(\tau)$ in order to make the integral in (5.2) Gaussian in nature, and thus obtain an analytical expression of the AFM Husimi amplitude. This will be done in sections 5.2 and 5.3 in the case of a simple periodic and a Gaussian aperture function, respectively. We now proceed to derive the results (5.2)-(5.3).

Substituting the propagator (3.37) into the expression (4.3) of the AFM wave function, we show, in view of the initial state (3.41), that Ψ_{AFM} is given by

$$\Psi_{\mathrm{AFM}}(x,t) = \int_0^t d\tau\, \frac{\chi(\tau)}{2} \left[\frac{x}{t-\tau} + \frac{v_0\, \alpha_\tau}{\alpha_{t_c}} \right] K_0(x, t-\tau) \psi_{\alpha_0, x_0, v_0}(0,\tau)\,, \tag{5.4}$$

where $\psi_{\alpha_0, x_0, v_0}(x,\tau)$ and α_τ are given by (2.17) and (2.18), respectively. We now construct the Husimi distribution associated with the state (5.4). Denoting it $\mathcal{H}_{\mathrm{AFM}}(\widetilde{x}, \widetilde{v}, t)$, we have in view of (2.45)

$$\mathcal{H}_{\mathrm{AFM}}(\widetilde{x}, \widetilde{v}, t) \equiv \left| h_{\mathrm{AFM}}(\widetilde{x}, \widetilde{v}, t) \right|^2\,, \tag{5.5}$$

where in view of (2.48), and because the semiclassical regime (5.1) ensures that $\Psi_{\mathrm{AFM}}\ (x,t) \simeq 0$ for any $x < 0$, the Husimi amplitude $h_{\mathrm{AFM}}(\widetilde{x}, \widetilde{v}, t)$ is defined by

$$h_{\mathrm{AFM}}(\widetilde{x}, \widetilde{v}, t) \equiv \int_0^{+\infty} dx\, \psi_{\alpha_0, \widetilde{x}, -\widetilde{v}}(x,0) \Psi_{\mathrm{AFM}}(x,t)\,. \tag{5.6}$$

In view of (2.42) and (5.4)[1], we show that the Husimi amplitude (5.6) is given by

$$h_{\mathrm{AFM}}(\widetilde{x}, \widetilde{v}, t) = \int_0^t d\tau\, \frac{\chi(\tau)}{2} \left[\frac{\widetilde{v}\, \alpha_{t-\tau}}{\alpha_{\widetilde{t}}} + \frac{v_0\, \alpha_\tau}{\alpha_{t_c}} \right] \psi_{\alpha_0, \widetilde{x}, -\widetilde{v}}(0, t-\tau) \psi_{\alpha_0, x_0, v_0}(0,\tau)\,, \tag{5.7}$$

where the quantity $\widetilde{t}$, inspired by the definition (3.43) of the classical time t_c, is given by

$$\widetilde{t} \equiv \frac{\widetilde{x}}{\widetilde{v}}\,. \tag{5.8}$$

It is also useful to introduce, in view of the definition (2.14) of $\lambda\!\!\!^{-}_0$, the corresponding reduced de Broglie wavelength $\widetilde{\lambda\!\!\!^{-}}$ of the Gaussian wave packet $\psi_{\alpha_0, \widetilde{x}, -\widetilde{v}}$, and we have

$$\widetilde{\lambda\!\!\!^{-}} \equiv \frac{\hbar}{m\widetilde{v}}\,. \tag{5.9}$$

Furthermore, $\psi_{\alpha_0, \widetilde{x}, -\widetilde{v}}(x,\tau)$ merely corresponds to the state evolved freely from the minimum uncertainty Gaussian wave packet $\psi_{\alpha_0, \widetilde{x}, -\widetilde{v}}(x,0)$ in a time τ, and is thus given (similarly to (2.17)) by

[1] And re-extending the integration region to $\mathbb{R}$ in view of $\Psi_{\mathrm{AFM}}(x,t) \simeq 0$ for any $x < 0$.

$$\psi_{\alpha_0,\widetilde{x},-\widetilde{v}}(x,\tau) \equiv \int_{-\infty}^{+\infty} dx'\, K_0(x-x',\tau)\psi_{\alpha_0,\widetilde{x},-\widetilde{v}}(x',0)$$
$$= \left(\frac{2\,\alpha_0}{\pi}\right)^{\frac{1}{4}} \sqrt{\frac{\alpha_\tau}{\alpha_0}} \exp\left\{-\alpha_\tau\,(x-\widetilde{x}_\tau)^2 - i\frac{m\widetilde{v}}{\hbar}\,(x-\widetilde{x}_\tau) + i\frac{m\widetilde{v}^2}{2\hbar}\tau\right\}, \quad (5.10)$$

where $\widetilde{x}_\tau$ is defined (similarly to (2.19)) by

$$\widetilde{x}_\tau \equiv \widetilde{x} - \widetilde{v}\tau\,. \quad (5.11)$$

Therefore, in view of the expressions (2.17) and (5.10), we can write the Husimi amplitude (5.7) in the more explicit form

$$h_{\mathrm{AFM}}(\widetilde{x},\widetilde{v},t) = \int_0^t d\tau\,\frac{\chi(\tau)}{2}\left[\frac{\widetilde{v}\,\alpha_{t-\tau}}{\alpha_{\widetilde{t}}} + \frac{v_0\,\alpha_\tau}{\alpha_{t_c}}\right]\sqrt{\frac{2}{\pi\alpha_0}}\sqrt{\alpha_{t-\tau}\,\alpha_\tau}\,\mathrm{e}^{\phi(\tau)}\,, \quad (5.12)$$

where the function $\phi(\tau)$ is defined by

$$\phi(\tau) \equiv -\alpha_{t-\tau}\,[\widetilde{x}-\widetilde{v}(t-\tau)]^2 - \alpha_\tau\,(x_0+v_0\tau)^2 + i\frac{m\widetilde{v}}{\hbar}\,[\widetilde{x}-\widetilde{v}(t-\tau)]$$
$$- i\frac{mv_0}{\hbar}\,(x_0+v_0\tau) + i\frac{m\widetilde{v}^2}{2\hbar}(t-\tau) + i\frac{mv_0^2}{2\hbar}\tau\,. \quad (5.13)$$

The semiclassical structure of the phase (5.13) is an interesting question and should require some further investigation.

It is worth discussing at this point the simple example of a time-independent barrier, for which the aperture function is merely $\chi(\tau)=\chi_0$. As was already mentioned in subsection 4.2.1, in such a case the AFM wave function, denoted by $\Psi_{\chi_0}(x,t)$ is simply given by

$$\Psi_{\chi_0}(x,t) = \chi_0\psi_{\alpha_0,x_0,v_0}(x,t)\,. \quad (5.14)$$

Now, remember that the semiclassical assumptions (5.1) imply in particular the frozen Gaussian condition[2] $\epsilon \equiv \hbar t/m\sigma^2 \ll 1$. Therefore, combining (5.14) with (2.37) yields in the frozen Gaussian regime

[2]Remember the definition (2.33) of the corresponding small parameter ϵ.

$$\Psi_{\chi_0}(x,t) = [1+\mathcal{O}(\epsilon)]\,\chi_0\psi_{\alpha_0,\,x_t,\,v_0}(x,0)\mathrm{e}^{i\frac{mv_0^2}{2\hbar}t}\,. \tag{5.15}$$

We now construct the Husimi amplitude corresponding to the state (5.15). Denoting it $h_{\chi_0}(\widetilde{x},\widetilde{v},t)$, we have in view of (5.6) and (5.15)

$$h_{\chi_0}(\widetilde{x},\widetilde{v},t) = \int_0^{+\infty} dx\,\psi_{\alpha_0,\,\widetilde{x},\,-\widetilde{v}}(x,0)\Psi_{\chi_0}(x,t) = [1+\mathcal{O}(\epsilon)]\,\chi_0 h_{\text{free}}^{(\text{fr})}(\widetilde{x},\widetilde{v},t)\,, \tag{5.16}$$

where the function $h_{\text{free}}^{(\text{fr})}$ is the frozen Gaussian Husimi amplitude given by (2.58). Finally, the corresponding Husimi distribution $\mathcal{H}_{\chi_0}(\widetilde{x},\widetilde{v},t)$ is, in view of (5.5) and (2.60), given by

$$\mathcal{H}_{\chi_0}(\widetilde{x},\widetilde{v},t) \equiv |h_{\chi_0}(\widetilde{x},\widetilde{v},t)|^2 = [1+\mathcal{O}(\epsilon)]\,\chi_0^2\mathcal{H}_{\text{free}}^{(\text{fr})}(\widetilde{x},\widetilde{v},t)\,, \tag{5.17}$$

where we recall that the frozen Gaussian Husimi distribution $\mathcal{H}_{\text{free}}^{(\text{fr})}$ is given by (2.61), i.e.

$$\mathcal{H}_{\text{free}}^{(\text{fr})}(\widetilde{x},\widetilde{v},t) = \exp\left\{-\frac{(\widetilde{x}-x_t)^2}{2\sigma^2} - \frac{m^2\sigma^2}{2\hbar^2}\,(\widetilde{v}-v_0)^2\right\}. \tag{5.18}$$

The phase-space structure of the Husimi distribution $\mathcal{H}_{\chi_0}$, as given by (5.17), hence stems directly from the behaviour of the frozen Gaussian Husimi distribution $\mathcal{H}_{\text{free}}^{(\text{fr})}$, which we already discussed at the end of section 2.3. It is hence peaked around the phase-space point (x_t, v_0), and the typical widths of the peak in the $\widetilde{x}$- and $\widetilde{v}$-directions are given by $(\Delta\widetilde{x})_{\text{free}}^{(\text{fr})}$ (Eq. (2.62)) and $(\Delta\widetilde{v})_{\text{free}}^{(\text{fr})}$ (Eq. (2.63)), respectively.

Now, the analysis performed in the previous chapter, and in particular the numerical results presented in section 4.2, suggest that the most important values of the transmitted wave function $\Psi_{\text{AFM}}(x,t)$ occur in a spatial region $0 < x_A \leqslant x \leqslant x_B$ centred around the position $x_t = x_0 + v_0 t$ of the corresponding classical free particle. In the case of ^{87}Rb, we saw for all the different time-dependent scenarios considered in section 4.2 (i.e., from time-independent to instantaneously varying barriers) that it is typically sufficient to take $x_A = x_t - 5\sigma = 0$ and $x_B = x_t + 5\sigma = 0.30\ \text{mm} = 2x_t$.

The study of the wave function $\Psi_{\text{AFM}}(x,t)$ in the semiclassical regime can thus be adequately restricted to a neighbourhood of the classical position x_t. We now extend this notion to the phase space. That is, it seems reasonable to suppose that the most important values of the Husimi distribution $\mathcal{H}_{\text{AFM}}(\widetilde{x},\widetilde{v},t)$ occur in a

neighbourhood of the classical phase-space point (x_t, v_0)[3]. To be more precise, we now restrict the analysis of the Husimi distribution $\mathcal{H}_{\mathrm{AFM}}(\widetilde{x}, \widetilde{v}, t)$ to the region of the phase space where the quantity $\widetilde{t}$ (defined by (5.8)) satisfies

$$\widetilde{t} \ll \frac{m\sigma^2}{\hbar} \,. \tag{5.19}$$

In the case of ^{87}Rb and for the numerical parameters used in section 4.2, we have $x_t/v_0 = 50$ ms and $m\sigma^2/\hbar \approx 1232$ ms, that is $x_t/v_0 \approx m\sigma^2/25\hbar$. Therefore, we can for instance see that the condition (5.19) is satisfied for the phase-space points $(\widetilde{x}, \widetilde{v})$ for which $\widetilde{v} \simeq v_0$ and $\widetilde{x}$ takes values as large as $\widetilde{x} = 3x_t = x_t + 10\sigma$. Similarly, phase-space points $(\widetilde{x}, \widetilde{v})$ such that $\widetilde{x} \simeq x_t$ and $\widetilde{v}$ takes values as small as $\widetilde{v} = v_0/3 = v_0 - 116\,(\Delta\widetilde{v})^{(\mathrm{fr})}_{\mathrm{free}}$ also satisfy the condition (5.19). This latter hence appears as a suitable condition to characterise a phase-space neighbourhood of the classical point (x_t, v_0). Note also that the condition (5.19) can be viewed as a frozen Gaussian condition for the probe Gaussian wave packet $\psi_{\alpha_0, \widetilde{x}, -\widetilde{v}}$ involved in the definition (5.6) of $h_{\mathrm{AFM}}(\widetilde{x}, \widetilde{v}, t)$. It is worth emphasising that we only qualitatively motivated the assumption (5.19), and did not provide a general, unambiguous mathematical proof. We must thus keep this condition in mind, and consistently check that our subsequent conclusions indeed concern only the phase-space region characterised by (5.19).

Building up on the above discussion, we now simplify the expression (5.12) of the Husimi amplitude $h_{\mathrm{AFM}}(\widetilde{x}, \widetilde{v}, t)$. Indeed, note that in our regime described by the conditions (5.1) and (5.19) we can, in view of the definition (2.18) of α_τ, write

$$\alpha_\tau = \alpha_{t-\tau} = \alpha_0 + \mathcal{O}(\epsilon) \,, \tag{5.20}$$

for any $0 < \tau < t$, and

$$\frac{1}{\alpha_{t_c}} = \frac{1}{\alpha_{\widetilde{t}}} = \frac{1}{\alpha_0} + \mathcal{O}(\epsilon) \,. \tag{5.21}$$

Therefore, combining (5.12)-(5.13) with (5.20) and (5.21) yields the following expression for the AFM Husimi amplitude in the semiclassical regime and in a neighbourhood of the classical point (x_t, v_0):

$$h_{\mathrm{AFM}}(\widetilde{x}, \widetilde{v}, t) = [1 + \mathcal{O}(\epsilon)]\, h^{(\mathrm{fr})}_{\mathrm{AFM}}(\widetilde{x}, \widetilde{v}, t) \,, \tag{5.22}$$

[3]That is, the phase-space point at which the frozen Gaussian Husimi distribution $\mathcal{H}^{(\mathrm{fr})}_{\mathrm{free}}$ is peaked.

where the frozen AFM Husimi amplitude $h^{(\mathrm{fr})}_{\mathrm{AFM}}$ is defined by

$$h^{(\mathrm{fr})}_{\mathrm{AFM}}(\widetilde{x},\widetilde{v},t) \equiv \frac{v_0+\widetilde{v}}{2\sigma\sqrt{\pi}} \int_0^t d\tau\, \chi(\tau) \mathrm{e}^{\phi^{(\mathrm{fr})}(\tau)}\,, \tag{5.23}$$

with

$$\begin{aligned}\phi^{(\mathrm{fr})}(\tau) \equiv -\alpha_0 \left[\widetilde{x}-\widetilde{v}(t-\tau)\right]^2 - \alpha_0 \left(x_0+v_0\tau\right)^2 + i\frac{m\widetilde{v}}{\hbar}\left[\widetilde{x}-\widetilde{v}(t-\tau)\right] \\ - i\frac{mv_0}{\hbar}\left(x_0+v_0\tau\right) + i\frac{m\widetilde{v}^2}{2\hbar}(t-\tau) + i\frac{mv_0^2}{2\hbar}\tau\,.\end{aligned} \tag{5.24}$$

Finally, we assume[4] that the integration domain in (5.23) can be extended from $0<\tau<t$ to $\mathbb{R}$, so that $h^{(\mathrm{fr})}_{\mathrm{AFM}}$ reads

$$h^{(\mathrm{fr})}_{\mathrm{AFM}}(\widetilde{x},\widetilde{v},t) = \frac{v_0+\widetilde{v}}{2\sigma\sqrt{\pi}} \int_{-\infty}^{+\infty} d\tau\, \chi(\tau) \mathrm{e}^{\phi^{(\mathrm{fr})}(\tau)}\,. \tag{5.25}$$

Now, we can readily see on (5.24) that the function $\phi^{(\mathrm{fr})}$ is quadratic in the integration variable τ. Therefore, the expression (5.25) of the frozen AFM Husimi amplitude strongly suggests to consider particular time-dependent barriers for which an analytical expression of $h^{(\mathrm{fr})}_{\mathrm{AFM}}$ can be obtained. This is precisely the spirit of the next two sections. In section 5.2 we consider a simple periodic aperture function, while section 5.3 is devoted to the study of a Gaussian-like $\chi(\tau)$. The interest of such barriers is manifest, as the resulting integral in (5.25) is Gaussian in nature.

5.2 Simple periodic aperture function

In this section we consider a simple periodic aperture function of the form

$$\chi(\tau) = \gamma_0 + \gamma_1 \cos(\omega_1\tau) = \gamma_0 + \frac{\gamma_1}{2}\left(\mathrm{e}^{i\omega_1\tau} + \mathrm{e}^{-i\omega_1\tau}\right)\,, \tag{5.26}$$

where ω_1, γ_0 and γ_1 are positive constants. The coefficients γ_0 and γ_1 can not be chosen arbitrarily, as the values of $\chi(\tau)$ must range between 0 and 1 for any $\tau\in\mathbb{R}$. We substitute (5.26) into (5.25) and perform the resulting Gaussian integral to obtain the following expression of the frozen AFM Husimi amplitude $h^{(\mathrm{fr})}_{\mathrm{AFM}}$:

[4] This is qualitatively justified in the neighbourhood of the classical point (x_t, v_0).

$$h_{\mathrm{AFM}}^{(\mathrm{fr})}(\widetilde{x},\widetilde{v},t)=\frac{1}{\sqrt{2}}\frac{v_0+\widetilde{v}}{\sqrt{v_0^2+\widetilde{v}^2}}\left[\gamma_0\,h_0(\widetilde{x},\widetilde{v})+\frac{\gamma_1}{2}\,h_+(\widetilde{x},\widetilde{v})+\frac{\gamma_1}{2}\,h_-(\widetilde{x},\widetilde{v})\right], \quad (5.27)$$

where the functions $h_0(\widetilde{x},\widetilde{v})$ and $h_\pm(\widetilde{x},\widetilde{v})$ are defined by

$$h_0(\widetilde{x},\widetilde{v})\equiv\exp\left\{\frac{1}{2\sigma^2\left(v_0^2+\widetilde{v}^2\right)}\left[\widetilde{v}\widetilde{x}_t+v_0x_0+i\frac{m\sigma^2}{2\hbar}\left(v_0^2-\widetilde{v}^2\right)\right]^2\right.$$
$$\left.-\frac{\widetilde{x}_t^2+x_0^2}{2\sigma^2}+i\frac{m}{\hbar}\left(\widetilde{v}\widetilde{x}-v_0x_0-\frac{\widetilde{v}^2t}{2}\right)\right\} \quad (5.28)$$

and

$$h_\pm(\widetilde{x},\widetilde{v})\equiv\exp\left\{\frac{1}{2\sigma^2\left(v_0^2+\widetilde{v}^2\right)}\left[\widetilde{v}\widetilde{x}_t+v_0x_0+i\frac{m\sigma^2}{2\hbar}\left(v_0^2-\widetilde{v}^2\right)\pm i\omega_1\sigma^2\right]^2\right.$$
$$\left.-\frac{\widetilde{x}_t^2+x_0^2}{2\sigma^2}+i\frac{m}{\hbar}\left(\widetilde{v}\widetilde{x}-v_0x_0-\frac{\widetilde{v}^2t}{2}\right)\right\}, \quad (5.29)$$

where we recall that $\widetilde{x}_t$ is defined by (5.11). The Husimi distribution $\mathcal{H}_{\mathrm{AFM}}^{(\mathrm{fr})}$ is, in view of (5.5), given by the square modulus of the Husimi amplitude (5.27). It will hence involve the square modulus of h_0, h_+ and h_-, but also the cross products of these latter. The complete structure of $\mathcal{H}_{\mathrm{AFM}}^{(\mathrm{fr})}$ in the phase-space is thus a priori complicated, and the most general way to analyse its behaviour is by means of a numerical implementation of the expressions (5.27)-(5.29). We can nevertheless obtain valuable analytical results that accurately describe, under certain conditions, the structure of $\mathcal{H}_{\mathrm{AFM}}^{(\mathrm{fr})}$ in the region of the phase space characterised by the condition (5.19). Indeed, it turns out that for some values of ω_1 the cross products between h_0, h_+ and h_- are negligible. Furthermore, the structure of the Husimi distribution then merely stems from the individual structures of $|h_0|^2$, $|h_+|^2$ and $|h_-|^2$, regardless of the global prefactor $(v_0+\widetilde{v})^2/(v_0^2+\widetilde{v}^2)$. We will thus see that in the corresponding regime of values of the frequency ω_1, the phase-space structure of $\mathcal{H}_{\mathrm{AFM}}^{(\mathrm{fr})}$ consists in three independent peaks. Analytical results regarding the positions and typical widths of these three peaks can be derived (Eqs. (5.32), (5.35)-(5.36), (5.37)-(5.39),(5.40)-(5.42)).

Therefore, we now study the phase-space structure of the modulus of the functions h_0 and $h_\pm$. Note that for symmetry reasons it is sufficient to focus on either h_+ or h_-, as one is obtained from the other under substituting ω_1 by $-\omega_1$. Furthermore, $h_\pm$ reduces to h_0 by taking $\omega_1=0$. Here we choose to analyse $|h_+|$ (details of

calculation can be found in the appendix D).

From the definition (5.29) of h_+, we see that $|h_+|$ can be written in the form

$$|h_+(\widetilde{x},\widetilde{v})| = \mathrm{e}^{\phi_+(\widetilde{x},\widetilde{v})}\,, \tag{5.30}$$

where the function ϕ_+ is defined by

$$\phi_+(\widetilde{x},\widetilde{v}) \equiv -\frac{(v_0\widetilde{x}-\widetilde{v}x_t)^2}{2\sigma^2\,(v_0^2+\widetilde{v}^2)} + \frac{m^2\sigma^2v_0^2}{2\hbar^2}\frac{\widetilde{v}^2}{v_0^2+\widetilde{v}^2} - \left(\frac{\sigma^2\omega_1^2}{2}+\frac{m\sigma^2v_0^2\omega_1}{\hbar}\right)\frac{1}{v_0^2+\widetilde{v}^2} - \frac{m^2\sigma^2}{8\hbar^2}\widetilde{v}^2 + \frac{m\sigma^2\omega_1}{2\hbar} - \frac{m^2\sigma^2v_0^2}{8\hbar^2}\,. \tag{5.31}$$

We show that the only critical point $(\widetilde{x}_+,\widetilde{v}_+)$ of ϕ_+ that lies inside the phase-space region described by (5.19) is given by

$$(\widetilde{x}_+,\widetilde{v}_+) = \left(x_t\sqrt{1+2\mu_+}\;,\; v_0\sqrt{1+2\mu_+}\right)\,, \tag{5.32}$$

where the dimensionless quantity μ_+ is defined by

$$\mu_+ \equiv \frac{\hbar\omega_1}{mv_0^2} > 0\,, \tag{5.33}$$

where we used the fact that $\omega_1 > 0$ by assumption. We show that (5.32) corresponds to a point where ϕ_+ admits a *strict local maximum*. Finally, we write the second order Taylor expansion of ϕ_+ about the critical point $(\widetilde{x}_+,\widetilde{v}_+)$, and we get

$$\phi_+(\widetilde{x},\widetilde{v}) = -\frac{(\widetilde{x}-\widetilde{x}_+)^2}{4\left(\sigma_{\widetilde{x}}^{(+)}\right)^2} - \frac{(\widetilde{v}-\widetilde{v}_+)^2}{4\left(\sigma_{\widetilde{v}}^{(+)}\right)^2} + \frac{t-t_c}{4\sigma^2}\frac{(\widetilde{x}-\widetilde{x}_+)\,(\widetilde{v}-\widetilde{v}_+)}{1+\mu_+}\,, \tag{5.34}$$

where the quantities $\sigma_{\widetilde{x}}^{(+)}$ and $\sigma_{\widetilde{v}}^{(+)}$ are given by

$$\sigma_{\widetilde{x}}^{(+)} = \sigma\sqrt{1+\mu_+}\,, \tag{5.35}$$

$$\sigma_{\widetilde{v}}^{(+)} = v_0\frac{\lambda\!\!\!^{-}_0}{\sigma}\sqrt{\frac{1+\mu_+}{1+2\mu_+}}\,. \tag{5.36}$$

Therefore, we see that the function $|h_+(\widetilde{x},\widetilde{v})|$ is peaked around the point $(\widetilde{x}_+,\widetilde{v}_+)$, the typical widths of the peak in the $\widetilde{x}$- and $\widetilde{v}$-directions being characterised by $\sigma_{\widetilde{x}}^{(+)}$ and $\sigma_{\widetilde{v}}^{(+)}$, respectively.

Now, remember that in view of (5.28) and (5.29) the function h_+ reduces to h_0 in the case where $\omega_1 = 0$. Furthermore, h_- is obtained from h_+ under substituting ω_1 by $-\omega_1$. We can thus use the above results regarding $|h_+|$ to deduce the behaviour of both $|h_0|$ and $|h_-|$. We then see that the function $|h_0(\widetilde{x},\widetilde{v})|$ is peaked around the point

$$(\widetilde{x}_0,\widetilde{v}_0) = (x_t, v_0)\,, \tag{5.37}$$

the typical widths of the peak in the $\widetilde{x}$- and $\widetilde{v}$-directions being characterised by

$$\sigma_{\widetilde{x}}^{(0)} = \sigma \tag{5.38}$$

and

$$\sigma_{\widetilde{v}}^{(0)} = v_0 \frac{\lambda\!\!\!^{-}_0}{\sigma}\,, \tag{5.39}$$

respectively. Furthermore, the function $|h_-(\widetilde{x},\widetilde{v})|$ is peaked around the point

$$(\widetilde{x}_-,\widetilde{v}_-) = \left(x_t\sqrt{1-2\mu_+}\ ,\ v_0\sqrt{1-2\mu_+}\right)\,, \tag{5.40}$$

the typical widths of the peak in the $\widetilde{x}$- and $\widetilde{v}$-directions being characterised by

$$\sigma_{\widetilde{x}}^{(-)} = \sigma\sqrt{1-\mu_+} \tag{5.41}$$

and

$$\sigma_{\widetilde{v}}^{(-)} = v_0\frac{\lambda\!\!\!^{-}_0}{\sigma}\sqrt{\frac{1-\mu_+}{1-2\mu_+}}\,, \tag{5.42}$$

respectively. It is hence worth emphasising that the above analysis is valid only for values of ω_1 such that

$$\mu_+ < \frac{1}{2}\,. \tag{5.43}$$

Indeed, if the condition (5.43) is not satisfied the critical point $(\widetilde{x}_-, \widetilde{v}_-)$ given in (5.40) is complex.

We can now discuss the phase-space structure of the AFM Husimi distribution $\mathcal{H}^{(\mathrm{fr})}_{\mathrm{AFM}}$ given, in view of (5.5), by the square modulus of the Husimi amplitude (5.27), that is

$$\mathcal{H}^{(\mathrm{fr})}_{\mathrm{AFM}}(\widetilde{x},\widetilde{v},t) = \frac{1}{2}\frac{(v_0+\widetilde{v})^2}{v_0^2+\widetilde{v}^2}\left\{\gamma_0^2\,|h_0(\widetilde{x},\widetilde{v})|^2 + \frac{\gamma_1^2}{4}\,|h_+(\widetilde{x},\widetilde{v})|^2 + \frac{\gamma_1^2}{4}\,|h_-(\widetilde{x},\widetilde{v})|^2 + \gamma_0\gamma_1 \right.$$
$$\left. \times\ \mathrm{Re}\left[h_0^*(\widetilde{x},\widetilde{v})h_+(\widetilde{x},\widetilde{v})\right] + \gamma_0\gamma_1\mathrm{Re}\left[h_0^*(\widetilde{x},\widetilde{v})h_-(\widetilde{x},\widetilde{v})\right] + \frac{\gamma_1^2}{2}\mathrm{Re}\left[h_+^*(\widetilde{x},\widetilde{v})h_-(\widetilde{x},\widetilde{v})\right]\right\}. \tag{5.44}$$

The behaviour of the three first terms in the curly bracket in the right hand side of (5.44), namely $|h_0|^2$, $|h_+|^2$ and $|h_-|^2$, is perfectly clear, as has been discussed above. Furthermore, remember that we have $|\mathrm{Re}(z)| \leqslant |z|$ for any $z \in \mathbb{C}$. The magnitude of the cross terms in (5.44) is hence always bounded by the product of the corresponding modulus of the individual functions. Now, we know the positions and typical widths of the individual peaks for $|h_0|$, $|h_+|$ and $|h_-|$. Therefore, we clearly see from the analytical results obtained above that these cross terms can be neglected if the frequency ω_1 is sufficiently large so as to make each of these peaks sufficiently separated in the phase space. For clarity, we illustrate this on the term $|h_0|\,|h_+|$ regarding the $\widetilde{v}$-direction. We know that $|h_0|$ and $|h_+|$ are peaked at $\widetilde{v}_0$ (Eq. (5.37)) and $\widetilde{v}_+$ (Eq. (5.32)), the typical widths of the peaks being $\sigma^{(0)}_{\widetilde{v}}$ (Eq. (5.39)) and $\sigma^{(+)}_{\widetilde{v}}$ (Eq. (5.36)). Therefore, a reasonable assumption for these two peaks to be sufficiently separated in the $\widetilde{v}$-direction is to require

$$\widetilde{v}_0 + N\sigma^{(0)}_{\widetilde{v}} < \widetilde{v}_+ - N\sigma^{(+)}_{\widetilde{v}}\,, \tag{5.45}$$

where N is some number of the order of 1. A similar reasoning can be done regarding the two other cross terms $|h_0|\,|h_-|$ and $|h_+|\,|h_-|$. If the frequency ω_1 is chosen sufficiently large so as to satisfy conditions of the form (5.45), and at the same time remains sufficiently small so as to satisfy (5.43), then we expect the cross terms in (5.44) to be negligible. Furthermore, in the region of interest of the phase space, the values of the prefactor $(v_0+\widetilde{v})^2/(v_0^2+\widetilde{v}^2)$ in (5.44) are expected to vary slowly as compared to the values of the exponential terms inside the bracket. Therefore, this

analysis suggests that for a certain regime of values of ω_1 the Husimi distribution $\mathcal{H}^{(\mathrm{fr})}_{\mathrm{AFM}}$ presents a simple phase-space structure, formed by three separated peaks centred around the phase-space points $(\widetilde{x}_-, \widetilde{v}_-)$, $(\widetilde{x}_0, \widetilde{v}_0)$ and $(\widetilde{x}_+, \widetilde{v}_+)$.

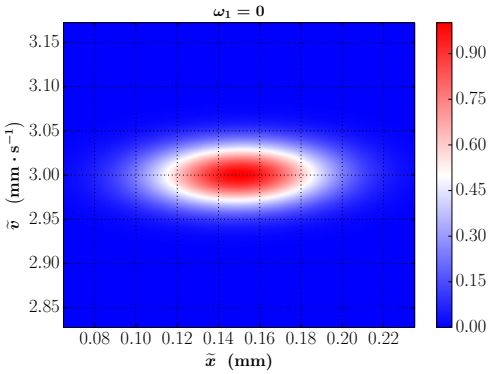

(a) Husimi distribution for $\omega_1 = 0$

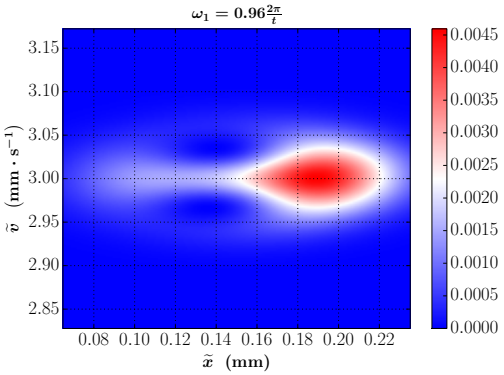

(b) Husimi distribution for $\omega_1 = 0.96 \times 2\pi/t$

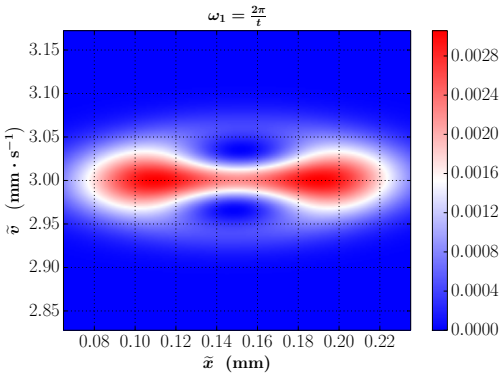

(c) Husimi distribution for $\omega_1 = 2\pi/t$

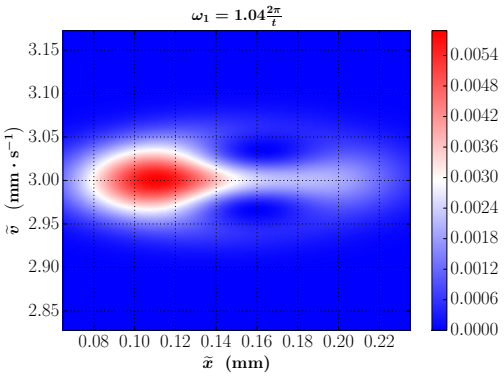

(d) Husimi distribution for $\omega_1 = 1.04 \times 2\pi/t$

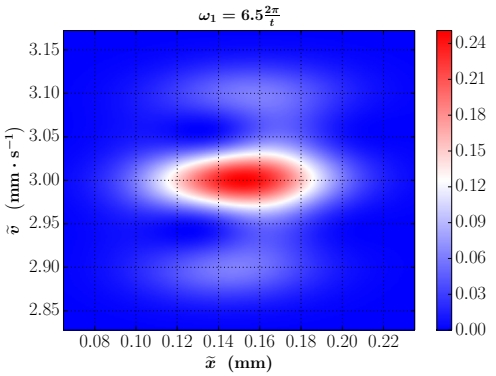

(e) Husimi distribution for $\omega_1 = 6.5 \times 2\pi/t$

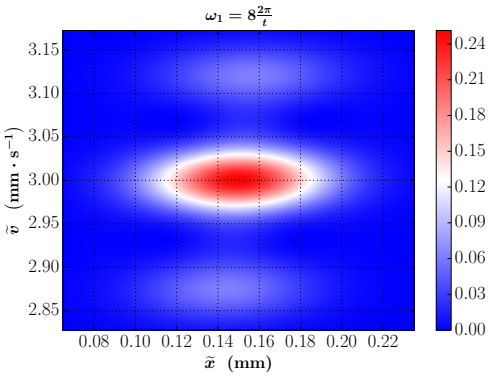

(f) Husimi distribution for $\omega_1 = 8 \times 2\pi/t$

Figure 8: Husimi distribution $\mathcal{H}^{(\mathrm{fr})}_{\mathrm{AFM}}(\widetilde{x}, \widetilde{v}, t)$, as given by (5.44), for different values of the frequency ω_1 and in the case of the alkali-metal atom ^{87}Rb. The numerical parameters are those used in section 4.2 (in addition, we take here $\gamma_0 = \gamma_1 = 1/2$).

The above discussion is illustrated on figure 8. Here we plot the AFM Husimi distribution $\mathcal{H}^{(\mathrm{fr})}_{\mathrm{AFM}}(\widetilde{x}, \widetilde{v}, t)$, as given by (5.44), in the case of the alkali-metal atom

^{87}Rb for the numerical parameters detailed in section 4.2. We take the coefficients γ_0 and γ_1 to be equal to 1/2, $\gamma_0 = \gamma_1 = 1/2$[5]. We consider six different values of the frequency ω_1. On figure 8a is shown the Husimi distribution obtained for $\omega_1 = 0$. This corresponds to the case of a free particle, and thus the AFM Husimi distribution is merely the free Husimi $\mathcal{H}^{(\mathrm{fr})}_{\mathrm{free}}$, peaked around the point (x_t, v_0) as expected. Increasing the value of ω_1 then shifts the Husimi distribution in the positive $\widetilde{x}$-direction (as compared to the free position x_t), and lowers the overall amplitude. This shift stops at some point, and the Husimi distribution starts to split, as can be seen on figure 8b (for which $\omega_1 = 0.96 \times 2\pi/t$). This splitting is then symmetric for $\omega_1 = 2\pi/t$, as is clear from figure 8c. Note that this case corresponds to a minimum value of the overall amplitude, the maximum value of the Husimi distribution being approximatively 0.003. This reflects important destructive interferences due to the cross terms in (5.44). Increasing ω_1 eventually leads to a Husimi distribution that is shifted in the negative $\widetilde{x}$-direction (as compared to the free position x_t), as displayed on figure 8d where $\omega_1 = 1.04 \times 2\pi/t$.

The values of ω_1 corresponding to figures 8b-8d are too small to satisfy (5.45). Indeed, for $\omega_1 = 2\pi/t$ we have for instance $\widetilde{v}_0 = 3.0$ mm/s and $\widetilde{v}_+ \approx 3.015$ mm/s, while $\sigma^{(0)}_{\widetilde{v}} \approx \sigma^{(+)}_{\widetilde{v}} \approx 0.024$ mm/s. Therefore, the cross products in (5.44) can not be neglected, and hence the nontrivial structure of $\mathcal{H}^{(\mathrm{fr})}_{\mathrm{AFM}}(\widetilde{x}, \widetilde{v}, t)$. If we keep increasing ω_1, we again observe this splitting phenomenon, which however becomes less important. For a sufficiently high frequency ω_1, the magnitude of the cross terms in (5.44) is not large enough to induce the splitting, and the Husimi distribution starts to be mostly determined by the individual terms $|h_0|^2$, $|h_+|^2$ and $|h_-|^2$. This leads to the behaviour observed on figure 8e, where $\omega_1 = 6.5 \times 2\pi/t$. Here we start to identify three, almost independent, peaks, and this value of ω_1 is hence almost large enough so as to satisfy (5.45). Indeed, we have for instance $\widetilde{v}_0 = 3.0$ mm/s and $\widetilde{v}_+ \approx 3.098$ mm/s (in good agreement with the data), while $\sigma^{(0)}_{\widetilde{v}} \approx \sigma^{(+)}_{\widetilde{v}} \approx 0.024$ mm/s. Finally, we consider on figure 8f the value $\omega_1 = 8 \times 2\pi/t$. Here we clearly distinguish three independent peaks, and the analytical results obtained above yield for instance $\widetilde{v}_0 = 3.0$ mm/s and $\widetilde{v}_+ \approx 3.120$ mm/s, in excellent agreement with the numerical results. Furthermore, we have in this case for instance $\sigma^{(0)}_{\widetilde{v}} \approx \sigma^{(+)}_{\widetilde{v}} \approx 0.024$ mm/s, which makes the condition (5.45) satisfied for $N = 2$.

Therefore, we obtained in this section analytical results that provide a valuable physical intuition about the phase-space structure of the AFM Husimi distribution $\mathcal{H}^{(\mathrm{fr})}_{\mathrm{AFM}}$ in the case of the simplest periodic aperture function of the form (5.26). It is now required to proceed to a deeper investigation of the regime where the simple three-peaks structure of the Husimi distribution is not yet valid. In this regime (small values of ω_1), destructive interferences due to the cross terms in (5.44) are

[5]This choice ensures that the aperture function (5.26) takes values ranging between 0 and 1.

important, and can for instance lead to the non-trivial structure of figure 8c. It would then be instructive to compare the effects observed for the periodic aperture function (5.26) with classical counterparts obtained in stationary wave optics. Finally, an other possible research direction would be to investigate the possibility of designing a quantum interferometer by means of time-dependent absorbing barriers. Indeed, a simple periodic aperture function of the form (5.26) can divide a Gaussian Husimi distribution in three independent peaks that propagate with different (mean) velocities. They hence may accumulate different phases during their subsequent motion (e.g. evolving in a time-dependent potential), and could later be recombined to analyse their interferences.

After the simple periodic aperture function considered in this section, we now turn our attention to a different time-dependent barrier that still allows to compute the integral (5.25) exactly.

5.3 Gaussian aperture function

Here we discuss a second example of time-dependent barrier for which the integral in (5.25) can be performed exactly. After the sinusoidal time-dependence analysed in section 5.2, we consider in this section the case of a Gaussian-like aperture function, namely

$$\chi(\tau) = \exp\left\{-\frac{\Gamma^2 v_0^2}{\sigma^2}\,(\tau - T_0)^2\right\}, \tag{5.46}$$

where $T_0 \in \mathbb{R}_+$ denotes the time at which the barrier is fully transparent (i.e. $\chi(T_0) = 1$), and $\Gamma \in \mathbb{R}_+$ is a dimensionless parameter related to the inverse of the typical opening time of the barrier. That is, $\Gamma = 0$ corresponds to a fully transparent barrier (and must correspond to the free particle case), and $\Gamma \gg 1$ describes a barrier transparent only for a very short time. Substituting the expression (5.46) into (5.25) and computing the resulting Gaussian integral, we show that the Husimi amplitude $h^{(\mathrm{fr})}_{\mathrm{AFM}}(\widetilde{x}, \widetilde{v}, t)$ can be written in the form

$$h^{(\mathrm{fr})}_{\mathrm{AFM}}(\widetilde{x}, \widetilde{v}, t) = \frac{1}{\sqrt{2}}\,\frac{v_0 + \widetilde{v}}{\sqrt{(1+2\Gamma^2)v_0^2 + \widetilde{v}^2}}\,\mathrm{e}^{\frac{1}{2}\phi_{\mathrm{g}}(\widetilde{x},\widetilde{v})}\,\mathrm{e}^{i\theta_{\mathrm{g}}(\widetilde{x},\widetilde{v})}, \tag{5.47}$$

where the two real functions ϕ_{g} and θ_{g} are defined by

$$\phi_{\rm g}(\widetilde{x},\widetilde{v}) \equiv \frac{1}{\sigma^2}\frac{1}{(1+2\Gamma^2)v_0^2+\widetilde{v}^2}\left\{\left[\widetilde{v}\,(\widetilde{x}-\widetilde{v}t)+v_0x_0-2T_0\Gamma^2v_0^2\right]^2 - \frac{m^2\sigma^4}{4\hbar^2}\left(v_0^2-\widetilde{v}^2\right)^2\right\} - \frac{(\widetilde{x}-\widetilde{v}t)^2}{\sigma^2} - \frac{x_0^2}{\sigma^2} - \frac{2T_0^2\Gamma^2v_0^2}{\sigma^2} \quad (5.48)$$

and

$$\theta_{\rm g}(\widetilde{x},\widetilde{v}) \equiv \frac{m}{2\hbar}\frac{v_0^2-\widetilde{v}^2}{(1+2\Gamma^2)v_0^2+\widetilde{v}^2}\left[\widetilde{v}\,(\widetilde{x}-\widetilde{v}t)+v_0x_0-2T_0\Gamma^2v_0^2\right] + \frac{m}{\hbar}\left(\widetilde{v}\widetilde{x}-v_0x_0-\frac{\widetilde{v}^2t}{2}\right). \quad (5.49)$$

Therefore, the Husimi distribution $\mathcal{H}^{(\rm fr)}_{\rm AFM}$ is, in view of (5.5), given by the square modulus of the Husimi amplitude (5.47), and we have

$$\mathcal{H}^{(\rm fr)}_{\rm AFM}(\widetilde{x},\widetilde{v},t) \equiv \left|h^{(\rm fr)}_{\rm AFM}(\widetilde{x},\widetilde{v},t)\right|^2 = \frac{1}{2}\frac{(v_0+\widetilde{v})^2}{(1+2\Gamma^2)v_0^2+\widetilde{v}^2}\,{\rm e}^{\phi_{\rm g}(\widetilde{x},\widetilde{v})}\,. \quad (5.50)$$

We now investigate the behaviour of the Husimi distribution (5.50) in the phase space, and determine its critical points (details can be found in the appendix E).

We first show that the function $\phi_{\rm g}(\widetilde{x},\widetilde{v})$ admits three real critical points, given by

$$\left(\widetilde{x}_0^{(\rm g)}\,,\,\widetilde{v}_0^{(\rm g)}\right) = (0,0)\,, \quad (5.51a)$$

$$\left(\widetilde{x}_\pm^{(\rm g)}\,,\,\widetilde{v}_\pm^{(\rm g)}\right) = \left(\pm\frac{1}{1+2\Gamma^2}\left[x_t+2\Gamma^2v_0\,(t-T_0)\right]\,,\,\pm v_0\right), \quad (5.51b)$$

these expressions being valid for an *arbitrary* Γ. Now, we show that the critical points $(\overline{x},\overline{v})$ of the Husimi distribution $\mathcal{H}^{(\rm fr)}_{\rm AFM}$ must satisfy (if $\overline{v}\neq -v_0$)

$$\overline{x} = \frac{t-t_c}{1+2\Gamma^2}\left[1+2\Gamma^2\frac{v_0\,(t-T_0)}{x_t}\right]\overline{v}\,, \quad (5.52)$$

and

$$\frac{m^2\sigma^2}{4\hbar^2 v_0}\,(\overline{v}-v_0)\,\overline{v}\,(\overline{v}+v_0)^2\left(\overline{v}-iv_0\sqrt{3+4\Gamma^2}\right)\left(\overline{v}+iv_0\sqrt{3+4\Gamma^2}\right)$$
$$+\left[\overline{v}-v_0\left(1+2\Gamma^2\right)\right]\left[\overline{v}^2+v_0^2\left(1+2\Gamma^2\right)\right]=0\,. \quad (5.53)$$

Therefore, the critical velocity $\overline{v}$ is determined by the $6^{-\text{th}}$ order polynomial equation (5.53). We solve it in the extreme case of a very wide Gaussian aperture function, i.e. for $\Gamma=\delta\Gamma\ll 1$, and we get

$$\overline{v}=v_0+\delta\widetilde{v}=v_0+2v_0\frac{\hbar t_c}{m\sigma^2}\,\frac{\hbar t_c}{mx_0^2}\,\delta\Gamma^2\,. \quad (5.54)$$

Therefore, the result (5.54) suggests that Gaussian-like barriers described by aperture functions of the form (5.46) can induce a change of the expectation value of the velocity of the particle. It is however worth emphasising that the velocity shift $\delta\widetilde{v}$ predicted by (5.54) is very small in the semiclassical regime described by (5.1). Indeed, we have in this case $\hbar t_c/mx_0^2\ll\hbar t_c/m\sigma^2\ll 1$. We now need to relax the approximation $\Gamma\ll 1$ to investigate whether we can observe a significant velocity shift.

To this end, we numerically evaluate the AFM Husimi distribution $\mathcal{H}^{(\text{fr})}_{\text{AFM}}(\widetilde{x},\widetilde{v},t)$, as given by (5.50), in the case of the alkali-metal atom ^{87}Rb for the numerical parameters detailed in section 4.2. We consider two different opening times T_0 and two different widths Γ of the Gaussian aperture function (5.46). Results are shown on figure 9 for $\Gamma=25,50$ and $T_0=t_c,1.2t_c$. We clearly see in all cases that such a Gaussian aperture function induces a shift, in the positive $\widetilde{v}$-direction, of the expectation value of the velocity of the particle, as compared to the velocity $v_0=3$ mm/s expected in the free-particle case. Comparing figures 9b and 9d to figures 9a and 9c, respectively, shows that increasing Γ (i.e. decreasing the width of the Gaussian (5.46)) increases the magnitude of this velocity shift. The counterpart however is a significant spreading over a wide region of the phase space. Furthermore, keeping the width Γ constant and changing the opening time T_0 seems to leave the average velocity unaffected, while changing the average position $\widetilde{x}$. This can be seen upon comparing figures 9c and 9d to figures 9a and 9b, respectively. These observations are fully consistent with the expression (5.52) of the critical position $\overline{x}$ and the equation (5.53) characterising the critical velocity $\overline{v}$. Indeed, we can readily see on (5.53) that the critical velocity $\overline{v}$ is independent of the opening time T_0. Furthermore, as is clear from (5.52) the critical position $\overline{x}$ depends on the opening time through $t-T_0$, multiplied by a positive quantity. Therefore, increasing the value of the opening time T_0 decreases the magnitude of $\overline{x}$.

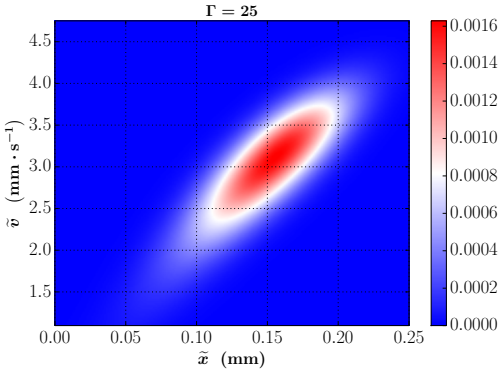

(a) Husimi distribution for $\Gamma = 25$ and $T_0 = t_c$

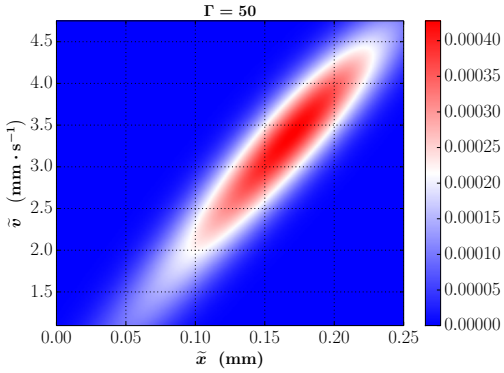

(b) Husimi distribution for $\Gamma = 50$ and $T_0 = t_c$

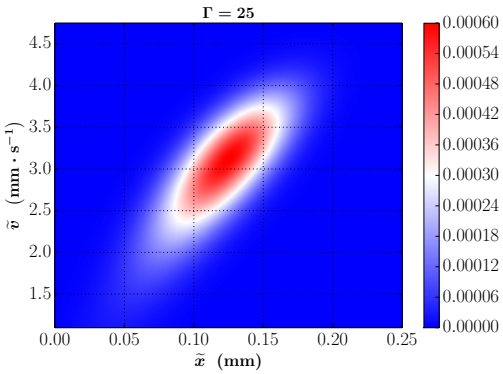

(c) Husimi distribution for $\Gamma = 25$ and $T_0 = 1.2t_c$

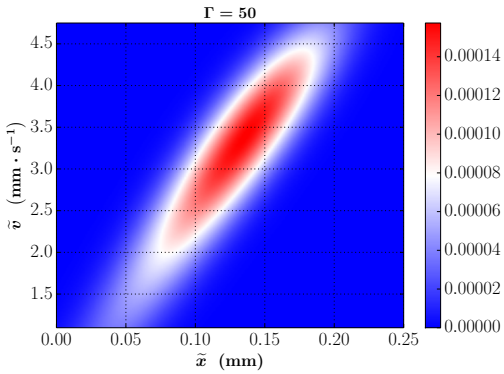

(d) Husimi distribution for $\Gamma = 50$ and $T_0 = 1.2t_c$

Figure 9: Husimi distribution $\mathcal{H}^{(\mathrm{fr})}_{\mathrm{AFM}}(\widetilde{x}, \widetilde{v}, t)$, as given by (5.50), for different values of Γ and T_0 and in the case of the alkali-metal atom ^{87}Rb. The numerical parameters are those used in section 4.2.

The prediction of a velocity shift obtained in the limit case $\Gamma \ll 1$ (Eq. (5.54)) has thus been (qualitatively) confirmed by numerically evaluating the AFM Husimi distribution (5.50). Therefore, we obtained in this section a proof-of-principle demonstration of the ability of a time-dependent absorbing barrier to modify the mean velocity of an incident quantum particle. Combining this effect with e.g. the spatial shifting or splitting, first evidenced in [28] and treated in the previous chapter (section 4.2.3), hence demonstrates a potential versatility of time-dependent matter-wave absorption for wave-packet manipulation.

It would now be interesting to investigate whether analytical results could be obtained in the opposite limit case $\Gamma \to \infty$. Indeed, this case describes a barrier that is transparent only for a very short time. It can thus be viewed as the limit of a narrow time slit. A time slit is described by an aperture function of the form $\chi(\tau) = \Theta(\tau - t_1)\Theta(t_2 - \tau)$, with Θ the Heaviside function and $0 < t_1 < t_2$. The limit $\Gamma \to \infty$ can then be compared to the limit $t_1 \to t_2$. A time slit is a generalisation of the Moshinsky shutter studied in chapter 4 and can thus give rise to diffraction in

time effects, as was studied by Moshinsky in [57]. The next step could then be to consider two successive Gaussian aperture functions, which could describe a double (time) slit setup. It could then be generalised to several successive slits, describing a time grating. It would then be instructive to make a comparison with classical stationary wave optics.

The analysis of the two sections 5.2 and 5.3 was based on two particular time-dependent barriers (Eqs. (5.26) and (5.46)) designed to produce a Gaussian integral in the expression (5.25) of $h^{(\mathrm{fr})}_{\mathrm{AFM}}$. In the next section we approach the problem of computing the AFM Husimi amplitude from a totally different point of view.

5.4 Husimi amplitude in the complex plane

In the last two sections we considered particular aperture functions $\chi(\tau)$ designed to make the integral in the expression (5.25) of $h^{(\mathrm{fr})}_{\mathrm{AFM}}(\widetilde{x},\widetilde{v},t)$ Gaussian in nature. Remember that this expression of the AFM Husimi amplitude was obtained upon neglecting the time-dependent spreading terms in (5.12). More precisely, we approximated, both in the prefactor and the exponent of the integrand in (5.12), the time-dependent terms α_τ and $\alpha_{t-\tau}$ by their initial value α_0. The purpose of this section is to relax part of these approximations by keeping the time-dependent quantities α_τ and $\alpha_{t-\tau}$ in the exponent[6]. This breaks down the quadratic nature of the argument of the exponential term, and by extension the possible Gaussian nature of the integral. Therefore, a different strategy must now be followed in order to compute this integral.

Here we propose to tackle this problem by means of the *residue theorem* (see e.g. [58] as a general reference regarding complex analysis), as is formulated in subsection 5.4.1. The main difficulty of this approach is the necessity of computing a residue at an *essential singularity*. We will consider in subsection 5.4.3 a particular example of aperture function χ (Eq. (5.89)) for which the latter residue can be expressed as a single series (involving Bessel functions of the first kind). The aperture function (5.89) presents the advantage of modelling an algebraic, smoothly opening barrier. The results presented in this section could thus pave the way towards an analytical investigation of the effects of such a barrier on the transmitted wave packet.

We now discuss how the problem of computing the AFM Husimi amplitude can be formulated by means of residue theory. We consider again the expression (5.12) of $h_{\mathrm{AFM}}(\widetilde{x},\widetilde{v},t)$, and in particular focus on the phase $\phi(\tau)$ given by (5.13). We note that the latter can be written in the form

[6] As we did in the previous sections we still approximate α_τ and $\alpha_{t-\tau}$ by α_0 in the prefactor. Indeed, the main contribution of the time-dependent terms α_τ and $\alpha_{t-\tau}$ to the integral is a priori expected to rise from the exponential term rather than from the algebraic term.

$$\phi(\tau) = \frac{Z_0}{\tau - z_0} + \frac{Z_1}{\tau - z_1} - \frac{1}{2}\left(\frac{\sigma}{\widetilde{\lambda}}\right)^2 - \frac{1}{2}\left(\frac{\sigma}{\lambda\!\!\!^{-}_0}\right)^2 , \tag{5.55}$$

where the complex numbers z_0, Z_0, z_1 and Z_1 (independent of the variable τ) are defined by

$$z_0 \equiv i\frac{m\sigma^2}{\hbar} , \tag{5.56a}$$

$$Z_0 \equiv -\frac{i}{2}\left(\frac{\sigma}{\lambda\!\!\!^{-}_0}\right)^2 \left(1 + i\frac{\lambda\!\!\!^{-}_0 \, |x_0|}{\sigma^2}\right)^2 \frac{m\sigma^2}{\hbar} , \tag{5.56b}$$

$$z_1 \equiv t - i\frac{m\sigma^2}{\hbar} , \tag{5.56c}$$

$$Z_1 \equiv \frac{i}{2}\left(\frac{\sigma}{\widetilde{\lambda}}\right)^2 \left(1 + i\frac{\widetilde{\lambda}\widetilde{x}}{\sigma^2}\right)^2 \frac{m\sigma^2}{\hbar} . \tag{5.56d}$$

Note that the quantities (5.56) all have the physical dimensions of a time. Therefore, in view of (5.12), (5.20) and (5.21), we write the Husimi amplitude h_{AFM} in the form

$$h_{\mathrm{AFM}}(\widetilde{x}, \widetilde{v}, t) = [1 + \mathcal{O}(\epsilon)] \int_0^t d\tau \, h(\tau) , \tag{5.57}$$

where the function $h(\tau)$ (for simplicity we drop here the explicit dependence on the phase-space variables $\widetilde{x}$ and $\widetilde{v}$) is given by, in view of the expression (5.55) of ϕ,

$$h(\tau) = \mathfrak{h}\chi(\tau) \mathrm{e}^{\frac{Z_0}{\tau - z_0} + \frac{Z_1}{\tau - z_1}} , \tag{5.58}$$

with

$$\mathfrak{h} \equiv \frac{v_0 + \widetilde{v}}{2\sigma\sqrt{\pi}} \mathrm{e}^{-\frac{1}{2}\left(\frac{\sigma}{\widetilde{\lambda}}\right)^2 - \frac{1}{2}\left(\frac{\sigma}{\lambda\!\!\!^{-}_0}\right)^2} . \tag{5.59}$$

Defining for convenience

$$I_{\mathrm{AFM}} \equiv \int_0^t d\tau \, h(\tau) , \tag{5.60}$$

which in view of (5.57) is nothing but the AFM Husimi amplitude in the frozen

Gaussian regime, we now discuss how we can use residue theory to evaluate this integral I_{AFM}.

5.4.1 Formulation of the integral

We first introduce the complex integral I_R, defined by

$$I_R \equiv \oint_{\mathcal{C}_R} dz\, h(z)\,, \tag{5.61}$$

where the integration contour $\mathcal{C}_R$ is run in the positive direction, and consists in a simple closed contour (i.e. a Jordan contour) in the complex plane, given by

$$\mathcal{C}_R = \mathcal{C}_R^{(1)} \cup \mathcal{C}_R^{(2)}\,, \tag{5.62}$$

where the two simple smooth contours $\mathcal{C}_R^{(1)}$ and $\mathcal{C}_R^{(2)}$ are defined by

$$\mathcal{C}_R^{(1)} = \{z \in \mathbb{R} \mid z \in [-R, R]\} \tag{5.63}$$

and

$$\mathcal{C}_R^{(2)} = \left\{z \in \mathbb{C} \mid z = R\,\mathrm{e}^{i\theta}\,,\, \theta \in [0, \pi]\right\}\,, \tag{5.64}$$

with $R > 0$. The two contours $\mathcal{C}_R^{(1)}$ and $\mathcal{C}_R^{(2)}$, along with their orientation, are depicted on figure 10. Therefore, combining (5.61) with (5.62)-(5.64), taking the limit $R \to +\infty$ in the resulting expression of I_R and calling I the value (assuming it exists) of the corresponding limit, we get

$$I \equiv \lim_{R\to+\infty} I_R = \int_{-\infty}^{+\infty} d\tau\, h(\tau) + \lim_{R\to+\infty}\left[iR\int_0^{\pi} d\theta\, \mathrm{e}^{i\theta} h\left(R\,\mathrm{e}^{i\theta}\right)\right]\,. \tag{5.65}$$

Therefore, we readily see from (5.65) that we can actually write the integral (5.60) in the form

$$I_{\mathrm{AFM}} = I - \left(I^{(-)} + I^{(+)}\right) - I_{\mathcal{C}}\,, \tag{5.66}$$

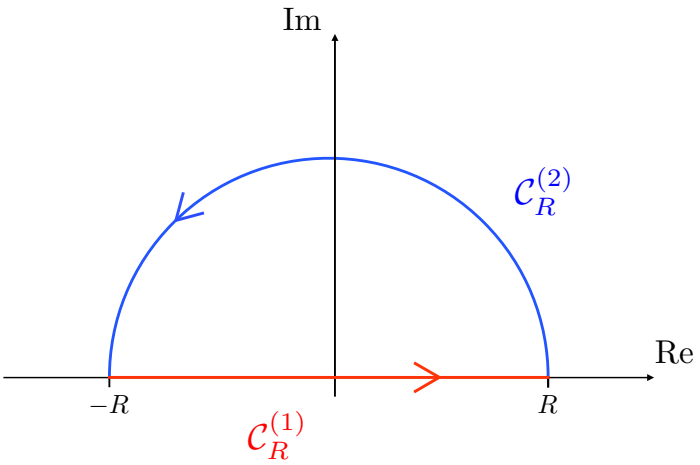

Figure 10: Contours $\mathcal{C}_R^{(1)}$, corresponding to the segment line $[-R, R]$ of the real axis, and $\mathcal{C}_R^{(2)}$, corresponding to the upper half-circle with centre the origin and radius R, defining the closed contour $\mathcal{C}_R$.

where the integrals $I^{(-)}$, $I^{(+)}$ and $I_{\mathcal{C}}$ are defined by

$$I^{(-)} \equiv \int_{-\infty}^{0} d\tau\, h(\tau)\,, \tag{5.67a}$$

$$I^{(+)} \equiv \int_{t}^{+\infty} d\tau\, h(\tau)\,, \tag{5.67b}$$

$$I_{\mathcal{C}} \equiv \lim_{R\to+\infty} \left[iR \int_0^{\pi} d\theta\, \mathrm{e}^{i\theta} h\left(R\,\mathrm{e}^{i\theta}\right) \right]. \tag{5.67c}$$

We show (details can be found in the appendix F) that a sufficient condition for the integral $I_{\mathcal{C}}$ to vanish is given by

$$\lim_{R\to+\infty} \left[R\,\mathrm{e}^{i\theta} \chi\left(R\,\mathrm{e}^{i\theta}\right) \right] = 0\,. \tag{5.68}$$

Furthermore, if we assume that $t > \widetilde{t}$ we can derive (as is shown in appendix G) the following global upper bound for $\left|I^{(-)} + I^{(+)}\right|$:

$$\begin{aligned} \left|I^{(-)} + I^{(+)}\right| \leqslant{}& \frac{v_0 + \widetilde{v}}{2\sigma\sqrt{\pi}} \exp\left[-\frac{1}{2} \left(\frac{\widetilde{x}_t}{\sigma} \right)^2 \right] \max\left[\mathrm{e}^{-\frac{1}{2}\left(\frac{\sigma}{\lambda_0}\right)^2}, \mathrm{e}^{-\frac{1}{2}\left(\frac{x_0}{\sigma}\right)^2} \right] \int_{-\infty}^{0} d\tau\, |\chi(\tau)| \\ &+ \frac{v_0 + \widetilde{v}}{2\sigma\sqrt{\pi}} \exp\left[-\frac{1}{2} \left(\frac{x_t}{\sigma} \right)^2 \right] \max\left[\mathrm{e}^{-\frac{1}{2}\left(\frac{\widetilde{x}}{\sigma}\right)^2}, \mathrm{e}^{-\frac{1}{2}\left(\frac{\sigma}{\lambda}\right)^2} \right] \int_{t}^{+\infty} d\tau\, |\chi(\tau)|\,. \end{aligned} \tag{5.69}$$

The actual values of the integrals appearing in the right hand side of (5.69) must be computed, or estimated, for any particular example of aperture function $\chi(\tau)$. It is worth noting that in view of the condition (5.68), we know in particular that $\chi(\tau)$ must go to zero faster than $1/\tau$ as $\tau \to \pm\infty$. This ensures that the integrals involved in the right hand side of the inequality (5.69) certainly exist for any physically realistic aperture function $\chi(\tau)$. Therefore, we see from the expression (5.66) of the integral I_{AFM} that $I_{\mathcal{C}}$ plays no role as long as the aperture function χ satisfies the condition (5.68). Furthermore, we can view the terms $I^{(-)}$ and $I^{(+)}$ as mere corrections to the integral I_{AFM}, the order of this correction being provided by the upper bound (5.69). Therefore, the only important term in the decomposition (5.66) is I. This latter is by construction an integral over a closed contour in the complex plane. Therefore, we now discuss how we can approach the problem of computing I, and thus by extension the AFM Husimi amplitude I_{AFM}, by means of the residue theorem.

We first recall the expression of I which in view of (5.65) and (5.61) can be written as

$$I = \oint_{\mathcal{C}_\infty} dz\, h(z)\,, \tag{5.70}$$

where $\mathcal{C}_\infty$ is the positively oriented simple closed contour consisting in the real axis and the upper half circle of centre the origin and infinite radius. For convenience, we introduce the notations $\mathcal{R}_{\mathcal{C}}$ and $\mathcal{C}(Z\,,\rho)$, with

$$\mathcal{R}_{\mathcal{C}} \equiv \{z \in \mathbb{C} \mid z \text{ enclosed by } \mathcal{C}\}\,, \tag{5.71}$$

which hence denotes the interior of the closed contour $\mathcal{C}$, and

$$\mathcal{C}(Z\,,\rho) \equiv \{z \in \mathbb{C} \mid |z - Z| = \rho\}\,, \tag{5.72}$$

which hence denotes the circle of centre Z and radius ρ.

Now, it is clear on the expression (5.58) that the two points z_0 and z_1 are *essential singularities* of the function $h(z)$. Furthermore, we readily see on (5.56a) and (5.56c) that $\mathrm{Im}(z_0) = m\sigma^2/\hbar > 0$ and $\mathrm{Im}(z_1) = -m\sigma^2/\hbar < 0$. Therefore, the integration contour $\mathcal{C}_\infty$ in (5.70) only encloses the essential singularity z_0, the other essential singularity z_1 lying in the lower half plane, and hence in the exterior of $\mathcal{C}_\infty$. We now assume that the function $\chi(z)$ only possesses *isolated singularities* $Z^{(j)}$, $j \in \mathbb{N}$, within the region $\mathcal{R}_{\mathcal{C}_\infty}$. It is hence analytic on $\mathcal{R}_{\mathcal{C}_\infty} \setminus \left\{Z^{(j)}\right\}_{j\in\mathbb{N}}$, and thus the

function $h(z)$ itself is analytic on $\mathcal{R}_{\mathcal{C}_\infty} \setminus \left\{ \{z_0\} \, , \left\{ Z^{(j)} \right\}_{j \in \mathbb{N}} \right\}$. Therefore, according to the Cauchy Residue Theorem we have

$$I = \oint_{\mathcal{C}_\infty} dz \, h(z) = 2\pi i \left[\mathrm{Res} \left(h(z) \, , z_0 \right) + \sum_{j \in \mathbb{N}} \mathrm{Res} \left(h(z) \, , Z^{(j)} \right) \right] , \tag{5.73}$$

where $\mathrm{Res} \left(h(z) \, , Z \right)$ denotes the *residue* of the function $h(z)$ at the complex point Z. If we assume that all the singularities $Z^{(j)}$, $j \in \mathbb{N}$, of the aperture function $\chi(z)$ are poles[7], then the residues $\mathrm{Res} \left(h(z) \, , Z^{(j)} \right)$ are straightforward to compute. The main obstacle in computing the integral I from the residue theorem is then to derive the residue $\mathrm{Res} \left(h(z) \, , z_0 \right)$ at the essential singularity z_0. Indeed, residues at essential singularities are notoriously hard to deal with, as they do not admit any general formula and must be tackled individually. Here we briefly present one particular example of aperture function for which the residue $\mathrm{Res} \left(h(z) \, , z_0 \right)$ can be computed. We first rewrite this residue in a convenient form.

5.4.2 The residue $\mathrm{Res} \left(h(z) \, , z_0 \right)$

By definition of the residue, we have

$$\mathrm{Res} \left(h(z) \, , z_0 \right) = \frac{1}{2\pi i} \oint_{\mathscr{C}_{z_0}} dz \, h(z) \, , \tag{5.74}$$

where $\mathscr{C}_{z_0}$ is a simple closed contour enclosing z_0 such that $h(z)$ is analytic on and inside $\mathscr{C}_{z_0}$ except at the point z_0. For convenience, we take the contour $\mathscr{C}_{z_0}$ to be the circle $\mathcal{C}(z_0 \, , r)$ of centre z_0 and radius r. Note that the radius r can not assume arbitrary values, because z_0 must be the *only* singularity of $h(z)$ inside the circle $\mathcal{C}(z_0 \, , r)$. For definiteness, we introduce the quantity r_{z_0}, defined by

$$r_{z_0} \equiv \min \left[\left| z_0 - z_1 \right| \, , \left(\left| z_0 - Z^{(j)} \right| \right)_{j \in \mathbb{N}} \right] . \tag{5.75}$$

It thus merely corresponds to the distance between z_0 and the nearest singularity of $h(z)$. Therefore, assuming that the radius r satisfies the condition $r < r_{z_0}$, then $\mathcal{C}(z_0 \, , r)$ is a valid integration contour for (5.74), and we get in view of (5.58)

[7] It may have essential singularities in the lower half plane though, as they would not be located inside the integration contour of the integral I, and hence would not contribute.

$$\mathrm{Res}\left(h(z)\,,z_0\right)=\frac{\mathfrak{h}}{2\pi i}\oint_{\mathcal{C}(z_0\,,r)}dz\,\chi(z)\,\mathrm{e}^{\frac{Z_0}{z-z_0}+\frac{Z_1}{z-z_1}}\,. \tag{5.76}$$

We now make the change of variable $z\to w$ in (5.76), where w and z are related through the *Möbius transformation*

$$w=\frac{-z+z_1}{z-z_0}\,, \tag{5.77}$$

for which the inverse transformation reads

$$z=\frac{z_0w+z_1}{w+1}\,. \tag{5.78}$$

First note that under the change of variable (5.77) the orientation of the integration contour is reversed, and thus we formally write

$$\oint\to\oint\,. \tag{5.79}$$

Now, remember that $\mathcal{C}(z_0\,,r)$ is described by the set of all $z\in\mathbb{C}$ satisfying the equation

$$zz^*-z_0^*z-z_0z^*+z_0z_0^*-r^2=0\,. \tag{5.80}$$

Therefore, substituting (5.78) into (5.80) yields the following equation for w:

$$ww^*-(-1)^*w-(-1)w^*+(-1)(-1)^*-\left(\frac{|z_0-z_1|}{r}\right)^2=0\,, \tag{5.81}$$

where we recognize the equation defining the circle $\mathcal{C}\left(-1\,,|z_0-z_1|/r\right)$ of centre -1 and radius $|z_0-z_1|/r$, for which we have the condition $|z_0-z_1|/r>|z_0-z_1|/r_{z_0}$ (with r_{z_0} defined by (5.75)). Therefore, the integration contour $\mathcal{C}(z_0\,,r)$ is mapped on to the contour $\mathcal{C}\left(-1\,,|z_0-z_1|/r\right)$ under the Möbius transformation (5.77). The Jacobian of this latter reads

$$dz=dw\frac{z_0-z_1}{(w+1)^2}\,, \tag{5.82}$$

and in view of (5.78) we have

$$\frac{Z_0}{z-z_0}+\frac{Z_1}{z-z_1}=\frac{1}{z_1-z_0}\left(Z_0w-\frac{Z_1}{w}\right)+\frac{Z_0-Z_1}{z_1-z_0}\,. \tag{5.83}$$

Therefore, combining (5.78), (5.79), (5.81), (5.82) and (5.83), we see that under the Möbius transformation (5.77) the residue (5.76) can be written in the form

$$\begin{aligned}\mathrm{Res}\left(h(z)\,,z_0\right)=\frac{\mathfrak{h}\left(z_1-z_0\right)}{2\pi i}\mathrm{e}^{\frac{Z_0-Z_1}{z_1-z_0}}\\ \times\oint_{\mathcal{C}\left(-1,\frac{|z_0-z_1|}{r}\right)}\frac{dw}{\left(w+1\right)^2}\,\chi\left(\frac{z_0w+z_1}{w+1}\right)\,\mathrm{e}^{\frac{1}{z_1-z_0}\left(Z_0w-\frac{Z_1}{w}\right)}\,.\end{aligned} \tag{5.84}$$

Now, noting that

$$Z_0w-\frac{Z_1}{w}=\sqrt{Z_0Z_1}\left(\sqrt{\frac{Z_0}{Z_1}}w-\sqrt{\frac{Z_1}{Z_0}}\frac{1}{w}\right)\,, \tag{5.85}$$

we make the change of variable $w\to z$ in (5.84), with

$$z=\sqrt{\frac{Z_0}{Z_1}}w\,. \tag{5.86}$$

It is then straightforward to see that under the transformation (5.86) the residue (5.84) can be written in the form

$$\mathrm{Res}\left(h(z)\,,z_0\right)=\frac{\mathfrak{h}\left(z_1-z_0\right)}{2\pi i}\mathrm{e}^{\frac{Z_0-Z_1}{z_1-z_0}}\sqrt{\frac{Z_1}{Z_0}}\oint_{\mathcal{C}\left(-\sqrt{\frac{Z_0}{Z_1}},\left|\sqrt{\frac{Z_0}{Z_1}}\right|\frac{|z_0-z_1|}{r}\right)}dz\,h_{\mathcal{M}}(z)\,, \tag{5.87}$$

where the function $h_{\mathcal{M}}$[8] is given by

$$h_{\mathcal{M}}(z)=\frac{1}{\left(\sqrt{\frac{Z_1}{Z_0}}z+1\right)^2}\,\chi\left(\frac{z_0\sqrt{\frac{Z_1}{Z_0}}z+z_1}{\sqrt{\frac{Z_1}{Z_0}}z+1}\right)\,\mathrm{e}^{\frac{\sqrt{Z_0Z_1}}{z_1-z_0}\left(z-\frac{1}{z}\right)}\,. \tag{5.88}$$

Now, remember that r must satisfy $r<r_{z_0}$. Since in view of its definition (5.75) we have in particular $r_{z_0}\leqslant|z_0-z_1|$, we see that $|z_0-z_1|/r>1$. Therefore,

[8]The subscript $\mathcal{M}$ stands for "Möbius".

the integration contour in (5.87) contains the point $z = 0$, which is precisely an essential singularity of the integrand $h_{\mathcal{M}}$ (namely of $\exp(1/z)$). If we assume that the aperture function χ only possesses at most poles inside the integration contour, the main difficulty of computing the residue $\mathrm{Res}\,(h(z)\,, z_0)$ given by (5.87) is thus to compute the residue $\mathrm{Res}\,(h_{\mathcal{M}}(z)\,, 0)$ of $h_{\mathcal{M}}$ at 0. We here give an explicit example of aperture function χ for which this last step can actually be performed.

5.4.3 A particular example

We consider in this subsection the particular case where the aperture function χ is given by

$$\chi(z) = \frac{1}{1 + \nu_0^2 z^2}\,, \tag{5.89}$$

where ν_0 is a constant having the dimension of the inverse of a time. Clearly such an aperture function satisfies $0 \leqslant \chi(\tau) \leqslant 1$ for any $\tau \in \mathbb{R}$, and is analytic in $\mathbb{C}$ except at the two simple poles $z = \pm i/\nu_0$. Furthermore, it clearly satisfies the condition (5.68). Therefore, this aperture function (5.89) fits perfectly the complex formulation introduced above. It presents the main advantage of allowing for an explicit evaluation of the residue $\mathrm{Res}\,(h_{\mathcal{M}}(z)\,, 0)$ of $h_{\mathcal{M}}$ at its essential singularity $z = 0$. Indeed, we can in this case identify the residue from the Laurent series of the function $h_{\mathcal{M}}$ about 0, as we now discuss.

By definition of the residue, we have

$$\mathrm{Res}\,(h_{\mathcal{M}}(z)\,, 0) = \frac{1}{2\pi i} \oint_{\mathscr{C}_0} dz\, f_{\mathcal{M}}(z) g_{\mathcal{M}}(z)\,, \tag{5.90}$$

with $\mathscr{C}_0$ a simple closed contour enclosing 0 such that $h_{\mathcal{M}}(z)$ is analytic on and inside $\mathscr{C}_0$ except at the point $z = 0$, and where the two functions $f_{\mathcal{M}}$ and $g_{\mathcal{M}}$ are, in view of (5.88), given by

$$f_{\mathcal{M}}(z) = \frac{1}{\left(\sqrt{\frac{Z_1}{Z_0}} z + 1\right)^2} \chi\left(\frac{z_0 \sqrt{\frac{Z_1}{Z_0}} z + z_1}{\sqrt{\frac{Z_1}{Z_0}} z + 1}\right)\,. \tag{5.91}$$

and

$$g_{\mathcal{M}}(z) = \mathrm{e}^{\frac{\sqrt{Z_0 Z_1}}{z_1 - z_0}\left(z - \frac{1}{z}\right)}\,. \tag{5.92}$$

Note that we know the Laurent series of the function $g_{\mathcal{M}}$ about 0. Indeed, this latter precisely corresponds to the generating function of the Bessel functions of the first kind, denoted by $J_n(z)$, and we have [59]

$$g_{\mathcal{M}}(z) = \sum_{n=-\infty}^{+\infty} J_n\left(\frac{2\sqrt{Z_0 Z_1}}{z_1 - z_0}\right) z^n \,. \tag{5.93}$$

Now, combining (5.91) with the aperture function (5.89), and using partial fractions, we get for $f_{\mathcal{M}}$

$$f_{\mathcal{M}}(z) = \frac{\sqrt{Z_0}}{2i\sqrt{Z_1}\nu_0\,(z_0 - z_1)}\left(\frac{1}{z - z_+} - \frac{1}{z - z_-}\right) , \tag{5.94}$$

where the complex numbers $z_\pm$ are defined by

$$z_\pm \equiv -\frac{\sqrt{Z_0}}{\sqrt{Z_1}(1 + \nu_0^2 z_0^2)}\left[1 + \nu_0^2 z_0 z_1 \mp i\nu_0(z_0 - z_1)\right] . \tag{5.95}$$

Note that

$$\frac{1}{z - Z} = -\frac{1}{Z}\sum_{n=0}^{+\infty}\left(\frac{z}{Z}\right)^n , \tag{5.96}$$

for any $Z \neq 0$. Combining (5.94) with (5.96) hence yields the following Taylor series of the function $f_{\mathcal{M}}$ about 0:

$$f_{\mathcal{M}}(z) = \frac{\sqrt{Z_0}}{2i\sqrt{Z_1}\nu_0\,(z_0 - z_1)}\left[\frac{1}{z_-}\sum_{n=0}^{+\infty}\left(\frac{z}{z_-}\right)^n - \frac{1}{z_+}\sum_{n=0}^{+\infty}\left(\frac{z}{z_+}\right)^n\right] . \tag{5.97}$$

We now combine this Taylor series of $f_{\mathcal{M}}$ about 0 with the Laurent series (5.93) of $g_{\mathcal{M}}$ about 0 to write the Laurent series of the function $h_{\mathcal{M}} \equiv f_{\mathcal{M}} g_{\mathcal{M}}$ about 0. We are only interested in getting the residue of $h_{\mathcal{M}}$ at 0, i.e. the term proportional to $1/z$ in the full Laurent series. Therefore, only the principal part[9] of the Laurent series of $g_{\mathcal{M}}$ is important to this respect. We define for convenience the function $\mathcal{L}$ as

[9] That is, the part of the series corresponding to (strictly) negative powers of z.

$$\mathcal{L}(Z) \equiv \left[\sum_{n=0}^{+\infty}\left(\frac{z}{Z}\right)^n\right]\left[\sum_{n=1}^{+\infty} J_{-n}\left(\frac{2\sqrt{Z_0 Z_1}}{z_1 - z_0}\right)\frac{1}{z^n}\right] . \tag{5.98}$$

Combining (5.98) with the Cauchy product of two infinite series, namely

$$\left(\sum_{n=0}^{+\infty} a_n\right)\left(\sum_{n=0}^{+\infty} b_n\right) = \sum_{n=0}^{+\infty}\left(\sum_{k=0}^{n} a_k b_{n-k}\right) , \tag{5.99}$$

and splitting the resulting sum over n into one sum over even integers only and one over odd integers only, we write $\mathcal{L}$ in the form

$$\mathcal{L}(Z) = \sum_{n=1}^{+\infty}\left[\sum_{k=0}^{2n-1}\frac{1}{Z^k} J_{k-2n}\left(\frac{2\sqrt{Z_0 Z_1}}{z_1 - z_0}\right)\frac{1}{z^{2(n-k)}}\right] + \sum_{n=0}^{+\infty}\left[\sum_{k=0}^{2n}\frac{1}{Z^k} J_{k-(2n+1)}\left(\frac{2\sqrt{Z_0 Z_1}}{z_1 - z_0}\right)\frac{1}{z^{2(n-k)+1}}\right] . \tag{5.100}$$

The first term in the right hand side of (5.100) contains only even inverse powers of z, and hence does not contribute to the residue

$$\mathcal{L}_{-1}(Z) \equiv \mathrm{Res}\left\{\left[\sum_{n=0}^{+\infty}\left(\frac{z}{Z}\right)^n\right] g_{\mathcal{M}}(z) , 0\right\} , \tag{5.101}$$

which corresponds to the coefficient of the term of $\mathcal{L}(Z)$ proportional to $1/z$. Therefore, this residue (5.101) is obtained from the second term in the right hand side of (5.100) by keeping only the terms of the double sum for which $n = k$, and we get, using the identity $J_{-n}(z) = (-1)^n J_n(z)$ [55],

$$\mathcal{L}_{-1}(Z) = Z\sum_{n=1}^{+\infty}\frac{(-1)^n}{Z^n} J_n\left(\frac{2\sqrt{Z_0 Z_1}}{z_1 - z_0}\right) . \tag{5.102}$$

Now, combining (5.90) with the Taylor series (5.97) and the definition (5.101) yields

$$\mathrm{Res}\left(h_{\mathcal{M}}(z) , 0\right) = \frac{\sqrt{Z_0}}{2i\sqrt{Z_1}\nu_0\left(z_0 - z_1\right)}\left[\frac{1}{z_-}\mathcal{L}_{-1}(z_-) - \frac{1}{z_+}\mathcal{L}_{-1}(z_+)\right] . \tag{5.103}$$

Finally, substituting the expression (5.102) into (5.103) yields the following expression for the residue $\mathrm{Res}\left(h_{\mathcal{M}}(z)\,,0\right)$ of $h_{\mathcal{M}}$ at its essential singularity $z=0$:

$$\mathrm{Res}\left(h_{\mathcal{M}}(z)\,,0\right)=\frac{\sqrt{Z_0}}{2i\sqrt{Z_1}\nu_0\left(z_0-z_1\right)}\sum_{n=1}^{+\infty}(-1)^n\left(\frac{1}{z_-^n}-\frac{1}{z_+^n}\right)J_n\left(\frac{2\sqrt{Z_0Z_1}}{z_1-z_0}\right)\,. \tag{5.104}$$

Combining (5.57), (5.60), (5.66), (5.73), (5.87) and (5.104), we hence get the following expression for the AFM Husimi amplitude $h_{\mathrm{AFM}}(\widetilde{x},\widetilde{v},t)$ for the aperture function (5.89):

$$h_{\mathrm{AFM}}(\widetilde{x},\widetilde{v},t)\approx-\frac{\pi\hbar}{\nu_0}\mathrm{e}^{\frac{Z_0-Z_1}{z_1-z_0}}\sum_{n=1}^{+\infty}(-1)^n\left(\frac{1}{z_-^n}-\frac{1}{z_+^n}\right)J_n\left(\frac{2\sqrt{Z_0Z_1}}{z_1-z_0}\right)+\mathrm{Res(poles)}\,, \tag{5.105}$$

where the first term in the right hand side precisely comes from the residue at the essential singularity, which was the non-trivial step. The second term denotes residues that must be computed for poles, which can be easily done.

It would now be instructive to investigate the expression (5.105) in more details, and in particular analyse the behaviour of the series. The next step would then be to identify other types of aperture functions that make the computation of the residue at the essential singularity tractable.

After the particular aperture functions considered in the previous sections, we now conclude this chapter by setting up the important inverse problem.

5.5 Open problem: engineering of quantum states

The physical scenarios discussed so far, both in chapter 4 and 5, share a common feature. Indeed, we set up a particular time-dependent barrier, and then study the effects, in the transmission region, of such a barrier on the physical state $\Psi(x,t)$ at the final time t. Such an approach proved useful, as it provided valuable predictions such as e.g. a shift, both in position and velocity, of the final state of the system. A natural question rises at this point: can we find the solution to the *inverse problem*? That is, can we determine the particular time-dependent barrier that would produce a given target state? To give an answer to this question is of fundamental and practical interest, as it would allow to efficiently engineer any desired physical state. In view of the definitions (3.31) and (3.37) of the wave function Ψ_{AFM} and the propagator K_{AFM}, respectively, the basic problem to solve is to determine the aperture function $\chi(\tau)$ from the expression

$$g(t) = \int_0^t d\tau\, \chi(\tau) f(\tau)\,, \tag{5.106}$$

where the two functions f and g are known. In (5.106) the function f is determined by the fixed initial state, while the function g is the desired (final) target state.

A possible approach of this inverse problem is suggested by the study of a sinusoidal barrier performed in section 5.2. We saw that a closed form expression of the AFM Husimi amplitude $h^{(\mathrm{fr})}_{\mathrm{AFM}}$ can be obtained (Eq. (5.27)) for a simple periodic aperture function (Eq. (5.26)). We can then by extension obtain a closed form expression of the AFM Husimi distribution for any aperture function written as a Fourier series, with undetermined coefficients a_n and b_n. The resulting Husimi amplitude $h^{(\mathrm{fr})}_{\mathrm{AFM}}$ is thus a *functional* of the Fourier coefficients a_n and b_n. We then choose a specific target state in the form of a target Husimi amplitude h_{tar}, and construct the fidelity $\mathscr{F}_{\mathrm{AFM}\,,\mathrm{tar}}$ between the AFM and the target Husimi amplitudes $h^{(\mathrm{fr})}_{\mathrm{AFM}}$ and h_{tar}, respectively. This fidelity, defined as the overlap, over the phase-space, between $h^{(\mathrm{fr})}_{\mathrm{AFM}}$ and h_{tar}, is thus by construction a functional of the Fourier coefficients a_n and b_n. The higher the value of $\mathscr{F}_{\mathrm{AFM}\,,\mathrm{tar}}$, the better is the agreement between the two Husimi amplitudes $h^{(\mathrm{fr})}_{\mathrm{AFM}}$ and h_{tar}. Therefore, we want to *maximise* this fidelity $\mathscr{F}_{\mathrm{AFM}\,,\mathrm{tar}}$. This approach however appears to be numerically challenging. Indeed, the fidelity presents a large number of local maxima in its parameter space spanned by the Fourier coefficients a_n and b_n. The *global* maximum is thus hard to reach. This work is currently in progress.

This is only one possibility, and other approaches may be adequate to tackle this fundamental problem.

Chapter 6

Conclusion

In this thesis we studied the one-dimensional motion, along the x-direction, of a nonrelativistic, electrically neutral quantum particle through a thin time-dependent laser beam. We discussed in particular two possible theoretical descriptions of such a problem in the ideal case of a pointlike time-dependent barrier, representing the limit case of an infinitely thin laser sheet with a time-dependent intensity.

The first approach is what we called the δ-potential model (DPM), and was discussed in section 3.1. Here the laser radiation, having a time-dependent amplitude $\Omega(\tau)$, is supposed to be resonant with a given transition of a moving atom. This latter is then treated as a two-level system, whose dynamical state at a time $\tau > 0$ is represented by the spinor $\widehat{\psi}(x,\tau)$ (Eq. (3.14)), of components $\psi_1(x,\tau)$ and $\psi_2(x,\tau)$. We focus on the component $\psi_1(x,\tau) = \Psi_{\mathrm{DPM}}(x,\tau)$ (Eq. (3.29)). We then introduced in section 3.2 the aperture function model (AFM), describing the motion of a structureless particle, of wave function $\Psi_{\mathrm{AFM}}(x,t)$, in the presence of a time-dependent absorbing barrier. The barrier is characterised by discontinuous time-dependent absorbing boundary conditions of Kottler type (Eqs. (3.35)-(3.36)). The only free parameter of the model is the aperture function $\chi(\tau)$, which is involved in the boundary conditions. Its values range between 0 (fully closed) and 1 (fully transparent), and it is related to the transparency of the barrier.

The drawback of the latter model is that the aperture function, and subsequently the time-dependent absorbing boundary conditions (3.35)-(3.36) as well, a priori lack a clear, first-principles, quantum mechanical justification. The main outcome of this work is the advancement of the AFM, as we explicitly connected it to the DPM (which has a strong physical basis). We did this by conjecturing a concrete relation (Eq. (3.48)) between the aperture function χ and well-defined physical parameters characterising the atom-laser system, namely the amplitude Ω of the laser light and the mean velocity v_0 of the incident particle. This conjectured relation was justified through a quantitative comparison between the wave functions $\Psi_{\mathrm{AFM}}(x,t)$ and $\Psi_{\mathrm{DPM}}(x,t)$, evolved from the same initial Gaussian wave packet $\Psi_0(x)$ (Eqs. (3.40)-

(3.41)) and evaluated in the transmission region at the final time t. We performed this analysis using both analytical and numerical methods, as discussed at length in chapter 4. In all the different, complementary, time-dependent scenarios considered, the conjectured relation (3.48) led to an excellent agreement, within a semiclassical regime described by the conditions (4.1), between the predictions of the AFM and the DPM.

The main outcome of this analysis is the advancement of the AFM. Originally a purely mathematical model, it now possesses a solid physical basis. Furthermore, the ability of this model to describe a laser radiation by an absorbing barrier is now transparent from the relation (3.48), which precisely relates the aperture function $\chi(\tau)$ of the barrier to the amplitude $\Omega(\tau)$ of the laser. Therefore, we have extended the range of theoretical tools relevant to investigate the motion of atoms submitted to localised time-dependent lasers. Thus, we believe our work contributed to better understanding the precise connection between time-dependent matter-wave absorption and the interaction of an atom with a time-dependent laser radiation.

The AFM can be adequately used to investigate various aspects of matter-wave absorption by time-dependent barriers. Indeed, we can now capitalise on its essentially analytical nature to explore various physical scenarios. We obtained for instance a closed form expression of the AFM Husimi amplitude $h^{(\mathrm{fr})}_{\mathrm{AFM}}$ (Eq. (5.27)) for a simple periodic aperture function (Eq. (5.26)). While valuable analytical results were obtained, a deeper investigation of the phase-space structure of the Husimi distribution is necessary. In particular, certain values of the frequency of the periodic barrier imply destructive interferences that result in non trivial effects such as an apparent splitting of the Husimi distribution (see figure 8). It would also be instructive to compare the effects observed for this simple periodic aperture function with classical counterparts obtained in stationary wave optics.

We were also able to obtain a closed form expression of $\mathcal{H}_{\mathrm{AFM}}$ (Eq. (5.50)) for a Gaussian-like aperture function (Eq. (5.46)). We observed, both analytically and numerically, an effective shift of the mean velocity of the particle in this case. Combining this new effect with the recently evidenced [28] spatial shifting and splitting demonstrates a potential versatility of time-dependent matter-wave absorption for wave-packet manipulation. A deeper analytical study of Gaussian-like aperture functions is needed, as only the case of a very wide Gaussian, i.e. $\Gamma \ll 1$, could have been treated so far. Investigating the opposite limit case $\Gamma \to \infty$ would for instance be of interest, as it would then describe a narrow time slit, i.e. a barrier that is transparent only for a very short time. Such time slits are known to give rise to diffraction in time effects. Generalisations to a time grating, by means of several successive narrow Gaussians, could then be possible directions of future research.

We also derived an expression for the AFM Husimi distribution in the com-

plex plane by means of the residue theorem. The main difficulty of this approach stemmed from the necessity of computing the residue at an essential singularity. We provided a particular example of aperture function (Eq. (5.89)) for which the residue at the essential singularity can be expressed as a series (Eq. (5.104)). This particular solution now requires a closer attention. Residues at essential singularities are notorious to be challenging to compute. It would then be interesting to design additional examples for which an exact expression of the Husimi distribution can be derived.

Finally, we formulated in section 5.5 the important inverse problem, aiming at constructing the time-dependent barrier required to engineer a desired target state. We briefly presented a possible approach that we are currently considering. This problem is of fundamental interest, as an answer could provide an efficient tool to engineer any physically relevant quantum state.

The AFM is an exact model. Such models are of fundamental importance, as they provide analytical insights that prove useful in exploring more complicated systems. Only few exactly solvable quantum mechanical time-dependent models are known, see e.g. [60] [48] [33] [61]. For the DPM, only a very few specific examples of time-dependent barriers exist for which the propagator can be found. It is thus remarkable that the AFM is exactly solvable for an *arbitrary* time-dependent barrier. Therefore, the AFM appears as a valuable tool to explore the vastly uncharted territory of the dynamics of a quantum particle in the presence of a time-dependent absorber. It already proved useful in advancing the proof-of-principle demonstration of the ability of time-dependent matter-wave absorption to efficiently manipulate the quantum state of a particle. We believe our work might set the ground for a deeper study of the AFM in particular, and of time-dependent matter-wave absorption in general.

Appendix A

Light-matter interaction

In this appendix we recall some standard results regarding light-matter interaction. We begin in section A.1 with a brief reminder of the minimal coupling Hamiltonian, widely used in atomic physics. The electric dipole Hamiltonian is then derived from the minimal coupling Hamiltonian in section A.2. Finally, the two-level approximation is justified in section A.3 by considering the simple example of the hydrogen atom.

A.1 Minimal coupling Hamiltonian

From the classical point of view, matter is on its most fundamental level described by Newtonian mechanics, while light is an electromagnetic wave whose behaviour is governed by Maxwell's theory. Light-matter interaction hence involves a combination of these two pillars of classical physics.

Consider a system of charged particles, labelled with an index $n \in \mathbb{N}$. The $n^{-\text{th}}$ particle has a charge q_n, a mass m_n and a position $\mathbf{r}_n$. The electric and magnetic fields at point $\mathbf{r}$ and time τ created by the whole set of particles are denoted by $\mathbf{E}(\mathbf{r},\tau)$ and $\mathbf{B}(\mathbf{r},\tau)$, respectively. The corresponding vector and scalar potentials are $\mathbf{A}(\mathbf{r},\tau)$ and $U(\mathbf{r},\tau)$, respectively. The set {particles + field} forms the dynamical system whose evolution must be characterised. The system can in addition be submitted to an external field described by the potentials $\{\mathbf{A}_{\text{e}}(\mathbf{r},\tau), U_{\text{e}}(\mathbf{r},\tau)\}$. By external is meant that the (external) particles generating this field are not considered as components of the dynamical system.

The quantum formalism is constructed from the Hamiltonian formulation of classical mechanics. As was first proposed by Schwarzchild, it is possible to express classical electrodynamics from a Hamilton (least action) principle (see e.g. [45]). It can be shown that the independent variables of the electromagnetic field are its transverse components $\{\mathbf{A}_\perp(\mathbf{r}), \dot{\mathbf{A}}_\perp(\mathbf{r})\}$. The canonical conjugate momenta associated with the dynamical variables $\mathbf{r}_n$ and $\mathbf{A}_\perp(\mathbf{r})$ of the system are denoted by $\mathbf{p}_n$

and $\mathbf{\Pi}_\perp(\mathbf{r})$, respectively. The classical Hamiltonian is then conveniently written not in the real $\mathbf{r}$-space, but rather in the related $\mathbf{k}$-space obtained from a spatial Fourier transform. Finally, the canonical quantisation proceeds by extending the classical dynamical variables into operators, set to satisfy particular commutation relations. Replacing a dynamical variable by its corresponding operator into the classical Hamiltonian hence produces the quantum Hamiltonian for a system of electric charges in the presence of an external electromagnetic field.

The state space $\mathscr{H}$ of the system {particles + field}, submitted to an external electromagnetic field[1], is the tensor product of the state space $\mathscr{H}_P$ of the particles with the state space $\mathscr{H}_{\text{field}}$ of the transverse field. The nonrelativistic evolution of the system is governed by the Hamiltonian H [45]

$$H = H_P + H_{\text{field}} + H_I \,, \tag{A.1}$$

with, in the Coulomb gauge for the electromagnetic field generated by the particles,

$$H_P \equiv \sum_n \frac{1}{2m_n} \left[\mathbf{p}_n - q_n \mathbf{A}_{\text{e}}(\mathbf{r}_n, \tau)\right]^2 + V_{\text{Coul}} + \sum_n q_n U_{\text{e}}(\mathbf{r}_n, \tau) \,, \tag{A.2a}$$

$$H_{\text{field}} \equiv \epsilon_0 \int_{\mathbb{R}^3/2} d\mathbf{k} \left[\frac{\bar{\mathbf{\Pi}}^*_\perp(\mathbf{k}) \cdot \bar{\mathbf{\Pi}}_\perp(\mathbf{k})}{\epsilon_0^2} + c^2 k^2 \bar{\mathbf{A}}^*_\perp(\mathbf{k}) \cdot \bar{\mathbf{A}}_\perp(\mathbf{k}) \right] \,, \tag{A.2b}$$

$$H_I \equiv -\sum_n \frac{q_n}{m_n} \left[\mathbf{p}_n - q_n \mathbf{A}_{\text{e}}(\mathbf{r}_n, \tau)\right] \cdot \mathbf{A}_\perp(\mathbf{r}_n) + \sum_n \frac{q_n^2}{2m_n} \mathbf{A}^2_\perp(\mathbf{r}_n) \,, \tag{A.2c}$$

where

$$V_{\text{Coul}} \equiv \frac{1}{8\pi\epsilon_0} \sum_{n \neq j} \frac{q_n q_j}{|\mathbf{r}_n - \mathbf{r}_j|} \tag{A.3}$$

represents the Coulomb interaction energy between the different particles, while ϵ_0 and c are the vacuum permittivity and speed of light in the vacuum, respectively. The function $\bar{f}(\mathbf{k})$ is the Fourier transform of the function $f(\mathbf{r})$. The norm of the vector $\mathbf{k}$ is given by $k \equiv \sqrt{\mathbf{k} \cdot \mathbf{k}}$, while $\mathbb{R}^3/2$ formally denotes a half space obtained from $\mathbb{R}^3$. By construction, the term H_P represents the energy of the particles. The second term, H_{field}, represents the energy of the field generated by the dynamics of the particles. Finally, H_I describes the interaction between the charged particles

[1]The external field is treated classically, in the sense that it is not described by operators with specific commutation relations.

and their own field. It is worth emphasising that the Coulomb gauge was used with respect to the field created by the particles, and that to this point no specific gauge has been chosen regarding the external field. The minimal coupling Hamiltonian can now be justified from the Hamiltonian (A.1).

The term H_P only contains the dynamical variables associated with the particles (namely $\mathbf{r}_n$ and $\mathbf{p}_n$), and thus acts in $\mathscr{H}_P$. Conversely, H_{field} refers only to the dynamical variables of the field (namely $\mathbf{A}_\perp$ and $\mathbf{\Pi}_\perp$), and thus acts in $\mathscr{H}_{\text{field}}$. It may be the case that only the behaviour of the particles is under study[2]. Concrete information about the particles is obtained through measurements of physical quantities specific to the particles, such as e.g. their position or energy. An arbitrary such quantity $\mathscr{G}$ is thus represented in Quantum Mechanics by an observable G acting in $\mathscr{H}_P$. By construction, it must in particular commute with H_{field}. Consider now the Heisenberg picture, in which the dynamics of the system is encompassed in the dynamics of the observables themselves. The evolution of an arbitrary particle observable G is thus governed by the Heisenberg equation

$$\frac{dG}{d\tau} = \frac{1}{i\hbar}\left[G, H_P + H_I\right] , \tag{A.4}$$

which is independent of the field term H_{field}. Therefore, the dynamics of the particles is completely described by the "restricted" Hamiltonian $H_P + H_I$.

For convenience, the interaction Hamiltonian is now rewritten in the form $H_I = H_I^{(1)} + H_I^{(2)}$, with

$$H_I^{(1)} \equiv -\frac{q_n}{m_n}\left[\mathbf{p}_n - q_n \mathbf{A}_{\text{e}}(\mathbf{r}_n, \tau)\right] \cdot \mathbf{A}_\perp(\mathbf{r}_n) , \tag{A.5a}$$

$$H_I^{(2)} \equiv \frac{q_n^2}{2m_n}\mathbf{A}_\perp^2(\mathbf{r}_n) . \tag{A.5b}$$

It can be shown (see e.g [62]), at least in the nonrelativistic limit considered here, that the interaction between the particles and the transverse field is in general negligible as compared to their Coulomb interactions (these latter are involved in the term V_{Coul} of the particle Hamiltonian H_P). For instance (see in particular paper 5.3 in [62])[3], in the case of a single electron bound to an infinitely heavy nucleus the term $H_I^{(2)}$ can be interpreted as a correction to the rest mass energy of the electron. The term $H_I^{(1)}$ is then seen as being responsible for corrections that may be interpreted as variations of the Coulomb potential felt by the electron and of the mass of the electron due to vacuum fluctuations and self-reaction, respectively.

[2]Which is exactly the case in the present thesis.

[3]In this paper no external fields are present.

Such effects, and subsequently the interaction Hamiltonian H_I itself, are neglected in the sequel.

Note that the expression (A.1) is by construction unable to take into account the spin degree of freedom of the charged particles. Indeed, the spin is a purely quantum quantity. Since (A.1) is obtained from the classical Hamiltonian, it cannot contain any reference to a quantity which does not exist classically. It is nevertheless possible to add spin-related contributions to the Hamiltonian in a heuristic way[4]. The spin of the $n^{-\text{th}}$ particle is represented by a spin operator $\mathbf{S}_n$ (which must thus be considered as an additional dynamical variable of the particle). The spin Hamiltonian $H_n^{(S)}$ describing the interaction energy between the spin and the external magnetic field is given by

$$H_n^{(S)} \equiv -\sum_n g_n \frac{q_n}{2m_n} \mathbf{S}_n \cdot \mathbf{B}_\text{e}(\mathbf{r}_n, \tau)\,, \tag{A.6}$$

where g_n denotes the so-called Landé factor of the $n^{-\text{th}}$ particle, and is a dimensionless quantity whose typical magnitude is of the order of 1. The order of magnitude of this spin interaction can be compared with the magnitude of the term $H_P^{(1)} = q_n \mathbf{p}_n \cdot \mathbf{A}_\text{e}/2m_n$ rising from the particle Hamiltonian H_P. The typical orders of the operators are $|\mathbf{S}_n| \sim S$, $|\mathbf{B}_\text{e}| \sim B$, $|\mathbf{p}_n| \sim p$ and $|\mathbf{A}_\text{e}| \sim A$. First note that the eigenvalues of the spin operator are of the order of $\hbar$[5], and thus $S \sim \hbar$. Furthermore, by definition of the vector potential $\mathbf{B}_\text{e} = \nabla \times \mathbf{A}_\text{e}$, that is $\bar{\mathbf{B}}_\text{e} = i\mathbf{k} \times \bar{\mathbf{A}}_\text{e}$ in the Fourier space. Therefore, for a typical mode $\mathbf{k}$ of the magnetic field $B \sim kA$, and thus, in view of (A.6) and $g_n \sim 1$, $H_n^{(S)} \sim q_n \hbar k A/m_n$. It is also clear that $H_P^{(1)} \sim q_n p A/m_n$. Therefore, the ratio between $H_n^{(S)}$ and $H_P^{(1)}$ is of the order

$$\frac{H_n^{(S)}}{H_P^{(1)}} \sim \frac{\hbar k}{p}\,. \tag{A.7}$$

If the system of charges is an atom, the ratio $\hbar/p$ can not, in view of the uncertainty relation, exceed the characteristic length scale of the system. The typical length scale of an atom is the Bohr radius $a_0 \equiv 4\pi\epsilon_0\hbar^2/m_e e^2 \approx 0.5$ Å, with m_e and e the mass and the charge, respectively, of the electron. Since $k = 2\pi/\lambda$, λ being the wavelength of the typical mode of the external electromagnetic field, the ratio (A.7) can thus be rewritten as

[4]This approach is more rigorously justified from the nonrelativistic limit of the Dirac equation.
[5]For an electron the eigenvalues of the z-component of $\mathbf{S}$ are $\pm\hbar/2$.

$$\frac{H_n^{(S)}}{H_P^{(1)}} \sim \frac{a_0}{\lambda} \,. \tag{A.8}$$

Therefore, the spin interaction is negligible as long as the typical wavelength λ of the external field is much larger than the size of the atom, that is typically $\lambda \gtrsim 10$ nm (extreme ultraviolet). In particular, this assumption is clearly satisfied for optical light ($\approx 400 - 700$ nm) and is even much better for microwaves (≈ 1 mm-1 m).

Finally, it is worth recalling that the expression (A.1) is nonrelativistic. To relax this hypothesis requires to give a covariant formulation of electrodynamics. A possible such formulation can be obtained from the Lorentz gauge. However, the task is much more difficult than in the nonrelativistic case using the Coulomb gauge. It is here only said, as an example, that the nonrelativistic limit of the Dirac equation for the hydrogen atom yields correction terms to the Hamiltonian H, such as the spin-orbit coupling or the Darwin term, which allow to analyse the fine structure of the hydrogen atom [29]. The relative contributions of these relativistic corrections with respect to the usual Coulomb Hamiltonian are typically of the order of α^2, $\alpha \approx 1/137$ being the fine structure constant.

Therefore, the different approximations discussed above lead to the following Hamiltonian describing the dynamics of a system of charged particles submitted to an external electromagnetic field characterised by the potentials $\mathbf{A}_\mathrm{e}$ and U_e:

$$H = \sum_n \frac{1}{2m_n} \left[\mathbf{p}_n - q_n \mathbf{A}_\mathrm{e}(\mathbf{r}_n, \tau)\right]^2 + V_\mathrm{Coul} + \sum_n q_n U_\mathrm{e}(\mathbf{r}_n, \tau) \,, \tag{A.9}$$

commonly known as the minimal coupling Hamiltonian. We now discuss an alternative form of the Hamiltonian known as the *electric dipole Hamiltonian*.

A.2 Electric dipole Hamiltonian

The electric dipole Hamiltonian can be derived from the minimal coupling Hamiltonian (A.9) through a specific electromagnetic gauge transformation. As is well-known [1], an electromagnetic gauge transformation is described in Quantum Mechanics by a unitary transformation. A quantum electromagnetic gauge transformation between a gauge $\mathscr{J}$ and a gauge $\mathscr{J}'$ is thus characterised by a unitary operator $\mathcal{T}$ acting on both the states and the operators. It can then be shown that the TDSE is covariant under a gauge transformation. More precisely, the TDSE reads $i\hbar\partial_\tau|\psi(\tau)\rangle = H|\psi(\tau)\rangle$ in the gauge $\mathscr{J}$, and $i\hbar\partial_\tau|\psi'(\tau)\rangle = H'|\psi'(\tau)\rangle$ in the gauge $\mathscr{J}'$. It is important to keep in mind that the Hamiltonian of the problem

studied here is not in general a true physical quantity, as it involves the electromagnetic potentials. The Hamiltonian H' in the gauge $\mathscr{J}'$ is then related to the Hamiltonian H in the gauge $\mathscr{J}$ through

$$H' = \mathcal{T} H \mathcal{T}^\dagger + i\hbar \left(\frac{d\mathcal{T}}{d\tau} \right) \mathcal{T}^\dagger \,. \tag{A.10}$$

Remember that no specific gauge has been chosen regarding the external field in order to obtain the minimal coupling Hamiltonian (A.9). It proves useful to apply a transformation switching from a gauge $\mathscr{J}$ described by the potentials $\mathbf{A}_\mathrm{e}$ and U_e to a gauge $\mathscr{J}'$ in which $\mathbf{A}'_\mathrm{e} = \mathbf{0}$. This particular transformation is known as the *Göppert-Mayer transformation* (see e.g. [45]), and is characterised by the unitary operator

$$\mathcal{T} = \exp\left[-\frac{i}{\hbar}\, \mathbf{d} \cdot \mathbf{A}_\mathrm{e}(\mathbf{C}, \tau) \right] , \tag{A.11}$$

where the operator $\mathbf{C}$ represents the centre of mass of the system, that is

$$\mathbf{C} \equiv \frac{1}{M} \sum_n m_n \mathbf{r}_n \,, \tag{A.12}$$

with

$$M \equiv \sum_n m_n \tag{A.13}$$

the total mass of the system, while $\mathbf{d}$ is the *electric dipole moment* (here with respect to the centre of mass $\mathbf{C}$), defined by

$$\mathbf{d} \equiv \sum_n q_n \left(\mathbf{r}_n - \mathbf{C} \right) . \tag{A.14}$$

For convenience, we also introduce the total charge Q of the system, defined by

$$Q \equiv \sum_n q_n \,. \tag{A.15}$$

Now, suppose that the system has a typical spatial extent a, for instance of the

order of the Bohr radius a_0, and that the typical wavelength λ[6] of the external field is much larger than a,

$$\frac{a}{\lambda} \ll 1\,, \tag{A.16}$$

commonly referred to as the *large wavelength approximation*. It is worth noting that this approximation was already required to neglect the spin interaction (see section A.1), and thus does not introduce any additional hypothesis. This allows to Taylor expand the potentials $\mathbf{A}_\mathrm{e}$ and U_e about the centre of mass $\mathbf{C}$[7], that is, for any particle,

$$\mathbf{A}_\mathrm{e}(\mathbf{r}_n, \tau) \approx \mathbf{A}_\mathrm{e}(\mathbf{C}, \tau)\,, \tag{A.17}$$

$$U_\mathrm{e}(\mathbf{r}_n, \tau) \approx U_\mathrm{e}(\mathbf{C}, \tau) + [\nabla U_\mathrm{e}(\mathbf{r}, \tau)]|_\mathbf{C} \cdot (\mathbf{r}_n - \mathbf{C})\ , \tag{A.18}$$

where the first order term must be kept in the scalar potential in view of the possible case of a neutral system, for which $Q = 0$[8]. Substituting the expansions (A.17) and (A.18) into (A.9) hence yields the following "large wavelength Hamiltonian":

$$H = \sum_n \frac{1}{2m_n} \left[\mathbf{p}_n - q_n \mathbf{A}_\mathrm{e}(\mathbf{C}, \tau)\right]^2 + V_\mathrm{Coul} + Q U_\mathrm{e}(\mathbf{C}, \tau) + \mathbf{d} \cdot [\nabla U_\mathrm{e}(\mathbf{r}, \tau)]|_\mathbf{C}\ . \tag{A.19}$$

The expression (A.19) of the minimal coupling Hamiltonian H in the gauge $\mathscr{J}$ is the starting point to obtain the Hamiltonian H', related to H through (A.10), in the Göppert-Mayer gauge $\mathscr{J}'$.

Note on (A.11) that the operator $\mathcal{T}$ (and thus its adjoint as well) is a function of the position operators $\mathbf{r}_n$ only. Therefore, the only non-trivial part in computing $\mathcal{T} H \mathcal{T}^\dagger$ rises from the terms of the Hamiltonian H involving the momentum operators $\mathbf{p}_n$. Within the large wavelength approximation, it can be shown [45] that

[6] The field does by no means need to be monochromatic.

[7] Indeed, the first term of the Taylor series involves the first derivatives ∇f, f one of the potentials. In Fourier space it is thus of the form $\mathbf{k}\bar{f}$. Therefore, the ratio between the first and zero order terms of the Taylor expansion about $\mathbf{C}$ is of the order of $|\mathbf{r} - \mathbf{C}|k|f(\mathbf{C})|/|f(\mathbf{C})|$, that is, since $|\mathbf{r} - \mathbf{C}| \sim a$ and $\lambda = 2\pi/k$, of the order of a/λ.

[8] Otherwise, the term involving U_e in the Hamiltonian would vanish for $Q = 0$, thus killing completely the contribution of the scalar potential. It would then not be possible to find back the electric field later on to write (A.22).

$$\mathcal{T}H\mathcal{T}^\dagger = \sum_n \frac{\mathbf{p}_n^2}{2m_n} + V_{\text{Coul}} + \mathbf{d}\cdot[\nabla U_{\text{e}}(\mathbf{r},\tau)]|_{\mathbf{C}} - \frac{Q}{M}\left(\sum_n \mathbf{p}_n\right)\cdot\mathbf{A}_{\text{e}}(\mathbf{C},\tau) + QU_{\text{e}}(\mathbf{C},\tau) + \frac{Q^2}{2M}\mathbf{A}_{\text{e}}^2(\mathbf{C},\tau)\,. \quad \text{(A.20)}$$

Furthermore, differentiating (A.11) with respect to τ readily yields

$$i\hbar\left(\frac{d\mathcal{T}}{d\tau}\right)\mathcal{T}^\dagger = \mathbf{d}\cdot\dot{\mathbf{A}}_{\text{e}}(\mathbf{C},\tau)\,. \quad \text{(A.21)}$$

Finally, note that the relation between an electric field and the corresponding potentials yields

$$\mathbf{d}\cdot[\nabla U_{\text{e}}(\mathbf{r},\tau)]|_{\mathbf{C}} + \mathbf{d}\cdot\dot{\mathbf{A}}_{\text{e}}(\mathbf{C},\tau) = -\mathbf{d}\cdot\mathbf{E}_{\text{e}}(\mathbf{C},\tau)\,. \quad \text{(A.22)}$$

Therefore, substituting the results (A.20), (A.21) and (A.22) into (A.10) yields the so-called *electric dipole Hamiltonian*

$$H' = \sum_n \frac{\mathbf{p}_n^2}{2m_n} + V_{\text{Coul}} - \mathbf{d}\cdot\mathbf{E}_{\text{e}}(\mathbf{C},\tau) - \frac{Q}{M}\left(\sum_n \mathbf{p}_n\right)\cdot\mathbf{A}_{\text{e}}(\mathbf{C},\tau) + QU_{\text{e}}(\mathbf{C},\tau) + \frac{Q^2}{2M}\mathbf{A}_{\text{e}}^2(\mathbf{C},\tau)\,. \quad \text{(A.23)}$$

The name electric dipole Hamiltonian stems from the term $-\mathbf{d}\cdot\mathbf{E}_{\text{e}}(\mathbf{C},\tau)$, acting as the interaction Hamiltonian in the simple case of a system of charges which is globally neutral, i.e. for which $Q = 0$, where the Hamiltonian (A.23) has the simple expression

$$H' = \sum_n \frac{\mathbf{p}_n^2}{2m_n} + V_{\text{Coul}} - \mathbf{d}\cdot\mathbf{E}_{\text{e}}(\mathbf{C},\tau)\,. \quad \text{(A.24)}$$

It is worth noting that this electric dipole interaction has been already obtained restricting to the lowest order for the Taylor expansion (A.17) of the vector potential $\mathbf{A}_{\text{e}}$. Considering also the first order terms could thus be viewed as a higher order dipole approximation, as these are also linear in $\mathbf{r} - \mathbf{C}$. Keeping such terms makes the Hamiltonian less simple than (A.23), as additional terms such as for instance the Röntgen Hamiltonian appear [63]. More generally, considering higher order terms

in the Taylor expansions of the potentials would involve the higher order multipole moments.

We now illustrate some general features of the electric dipole Hamiltonian (A.24) on the simple example of the hydrogen atom. This will naturally lead to the two-level approximation.

A.3 Hydrogen atom and two-level approximation

The hydrogen atom is a system of two charged particles: the proton, with charge e, mass $m_{\rm pr}$, position $\mathbf{r}_{\rm pr}$ and momentum $\mathbf{p}_{\rm pr}$, and the electron, with charge $-e$, mass $m_{\rm el}$, position $\mathbf{r}_{\rm el}$ and momentum $\mathbf{p}_{\rm el}$. The total mass of the system is $M \equiv m_{\rm el}+m_{\rm pr}$, while its so-called reduced mass is $\mu \equiv m_{\rm el}m_{\rm pr}/(m_{\rm el}+m_{\rm pr})$. Furthermore, in addition to the centre of mass $\mathbf{C} \equiv (m_{\rm el}\mathbf{r}_{\rm el}+m_{\rm pr}\mathbf{r}_{\rm pr})/M$ and the total momentum $\mathbf{P} \equiv \mathbf{p}_{\rm el}+\mathbf{p}_{\rm pr}$, we also define the relative position $\mathbf{r}_\mu \equiv \mathbf{r}_{\rm el}-\mathbf{r}_{\rm pr}$ and the relative momentum $\mathbf{p}_\mu \equiv \mu(\mathbf{p}_{\rm el}/m_{\rm el}-\mathbf{p}_{\rm pr}/m_{\rm pr})$. The electric dipole Hamiltonian $H_{\rm ed}$ for the hydrogen atom is given, in view of (A.3), (A.14) and (A.24), by

$$H_{\rm ed} \equiv \frac{\mathbf{P}^2}{2M}+\frac{\mathbf{p}_\mu^2}{2\mu}-\frac{e^2}{4\pi\epsilon_0}\frac{1}{|\mathbf{r}_\mu|}+e\mathbf{r}_\mu\cdot\mathbf{E}_{\rm e}(\mathbf{C},\tau)\,. \tag{A.25}$$

Note that the only nonzero commutators of the operators $\mathbf{C}$, $\mathbf{P}$, $\mathbf{r}_\mu$ and $\mathbf{p}_\mu$ are [1]

$$\left[C^{(j)}\,,\,P^{(k)}\right]=i\hbar\delta_{jk}\,, \tag{A.26}$$

$$\left[r_\mu^{(j)}\,,\,p_\mu^{(k)}\right]=i\hbar\delta_{jk}\,, \tag{A.27}$$

with $j,k=x,y,z$.

First consider the case where no external field is present. The Hamiltonian hence reduces to the free hydrogen atom Hamiltonian

$$H_{\rm ed}^{\rm free}=\frac{\mathbf{P}^2}{2M}+H_\mu\,, \tag{A.28}$$

where

$$H_\mu \equiv \frac{\mathbf{p}_\mu^2}{2\mu}-\frac{e^2}{4\pi\epsilon_0}\frac{1}{|\mathbf{r}_\mu|}\,. \tag{A.29}$$

Therefore, the commutation relations (A.26) and (A.27) allow to treat the hydrogen atom as a set of two independent fictitious particles. There is indeed the *centre of mass*, of mass M, described by the position and momentum operators $\mathbf{C}$ and $\mathbf{P}$, respectively, evolving under the Hamiltonian $\mathbf{P}^2/2M$. Then there is the *relative particle*, of mass μ, and whose position and momentum are represented by the operators $\mathbf{r}_\mu$ and $\mathbf{p}_\mu$, respectively. The dynamics of this relative particle is governed by the Hamiltonian H_μ. The state space $\mathscr{H}$ of the system is thus the tensor product of the state space $\mathscr{H}_C$ of the centre of mass with the state space $\mathscr{H}_\mu$ of the relative particle[9]. The set $\{|\mathbf{r}\rangle\}$ of position eigenstates is taken as a basis of the Hilbert space $\mathscr{H}_C$. Now, as is well known [1] it is possible to determine the eigenstates $|n,l,m\rangle$ of the Hamiltonian H_μ, and hence the (discrete) set $\{|n,l,m\rangle\}$, with $n \geqslant 1, 0 \leqslant l \leqslant n-1$ and $-l \leqslant m \leqslant l$, is taken as a basis of the Hilbert space $\mathscr{H}_\mu$. Remember that in the position representation $\langle \mathbf{r}|n,l,m\rangle = \psi_{nlm}(r,\theta,\phi) = R_{nl}(r)Y_{lm}(\theta,\phi)$, with R_{nl} the solutions to the radial Schrödinger equation and Y_{lm} the spherical harmonics. Therefore, a basis $\{|\mathbf{r};n,l,m\rangle\}$ of the full Hilbert space $\mathscr{H}$, with $|\mathbf{r};n,l,m\rangle = |\mathbf{r}\rangle \otimes |n,l,m\rangle$, can easily be constructed.

Suppose now that the hydrogen atom is submitted to a simple periodic external field, that is

$$\mathbf{E}_\mathrm{e}(\mathbf{r},\tau) = \mathbf{E}_0 \cos(\omega_l \tau)\,, \tag{A.30}$$

with $\mathbf{E}_0$ being position- and time-independent, and where the frequency ω_l is taken to be positive. Note in particular that the interaction term in the Hamiltonian (A.25) hence only involves the position operator $\mathbf{r}_\mu$ associated with the relative particle. Therefore, the external field (A.30) has no impact on the dynamics of the centre of mass, and only influences the evolution of the dynamical state $|\psi(\tau)\rangle_\mu \in \mathscr{H}_\mu$ of the relative particle. To simplify, the degeneracy of the energy eigenstates $|n,l,m\rangle$ is ignored, and thus the basis of $\mathscr{H}_\mu$ is merely rewritten $\{|E_k\rangle\}$, with $H_\mu|E_k\rangle = E_k|E_k\rangle$. Expanding $|\psi(\tau)\rangle_\mu$ on this basis yields

$$|\psi(\tau)\rangle_\mu = \sum_k c_k(\tau) \mathrm{e}^{-i\frac{E_k}{\hbar}\tau} |E_k\rangle\,, \tag{A.31}$$

where the coefficient $c_k(\tau)$ hence represents, by construction, the probability amplitude of finding the relative particle in the state $|E_k\rangle$ at time τ.

It is now assumed that the relative particle is initially in the state $|\psi(0)\rangle_\mu = |E_i\rangle$ of energy E_i, and that the strength of the external field (A.30) is weak enough so

[9] That is, $\mathscr{H}_C$ and $\mathscr{H}_\mu$ are just two different subsets of $L^2(\mathbb{R}^3)$.

as to make the use of time-dependent perturbation theory possible. It can then be shown [16,17] that, to the first order in the perturbation, the probability amplitude $c_f(\tau)$ to find the relative particle in the state $|E_f\rangle$ of energy $E_f \neq E_i$ at time τ is given by

$$c_f(\tau) = -\frac{e}{2\hbar}\langle E_f|\mathbf{r}_\mu \cdot \mathbf{E}_0|E_i\rangle \left[\frac{\mathrm{e}^{i(\omega_{fi}+\omega_l)\tau}-1}{\omega_{fi}+\omega_l} + \frac{\mathrm{e}^{i(\omega_{fi}-\omega_l)\tau}-1}{\omega_{fi}-\omega_l}\right], \tag{A.32}$$

where

$$\omega_{fi} \equiv \frac{E_f - E_i}{\hbar} \tag{A.33}$$

denotes the transition frequency between the two levels $|E_i\rangle$ and $|E_f\rangle$. For concreteness, the case $\omega_{fi} > 0$ is considered here.

Note that the closer is ω_l to the transition frequency ω_{fi}, the smaller (in absolute value) is the difference $\omega_{fi} - \omega_l$. Therefore, assume that

$$|\omega_{fi} - \omega_l| \ll \omega_l\,, \tag{A.34}$$

commonly referred to as the *(quasi-)resonance condition*. Under this resonance condition the antiresonant terms, involving the sum $\omega_{fi} + \omega_l$, in (A.32) can thus be neglected with respect to the resonant terms, involving the difference $\omega_{fi} - \omega_l$[10]: this corresponds to the so-called *rotating wave approximation*. Furthermore, note that any probability amplitude $c_{f'}(\tau)$ to find the relative particle in any other state $|E_{f'}\rangle$, $E_{f'} \neq E_f$, at time τ is also of the form (A.32). The resonance condition (A.34) in turn implies that any nonresonant transition $|E_i\rangle \to |E_{f'}\rangle$ is very unlikely as compared to the resonant transition $|E_i\rangle \to |E_f\rangle$. This allows to neglect all the nonresonant transitions, and hence focus, when the frequency ω_l of the external field is fixed and satisfies (A.34), on the specific transition $|E_i\rangle \to |E_f\rangle$[11]. Therefore, in the presence of the simple periodic external field (A.30) the state $|\psi(\tau)\rangle_\mu$ of the relative particle, rather than an element of $\mathscr{H}_\mu$, can be restricted to a two-dimensional subset $\mathscr{H}_2 \subset \mathscr{H}_\mu$. This is the so-called *two-level approximation*.

The subset $\mathscr{H}_2$ is a two-dimensional Hilbert space. A basis of $\mathscr{H}_2$ is readily provided by the two states $|E_i\rangle$ and $|E_f\rangle$, that can be represented as column vectors,

[10] This can be done by comparison of i) the time-dependent terms, as the modulus of the ratio antiresonant/resonant gives $|\omega_{fi} - \omega_l|/|\omega_{fi} + \omega_l| \ll \omega_l$, and then of ii) the time-independent terms, as the modulus of the ratio antiresonant/resonant again gives $|\omega_{fi} - \omega_l|/|\omega_{fi} + \omega_l| \ll \omega_l$.

[11] As it turns out the antiresonant term in (A.32) can be even smaller than some nonresonant probabilities: dropping the antiresonant terms hence makes it almost mandatory to neglect the nonresonant contributions as well [17].

$$|E_i\rangle = \begin{pmatrix} 1 \\ 0 \end{pmatrix} \qquad \text{and} \qquad |E_f\rangle = \begin{pmatrix} 0 \\ 1 \end{pmatrix} . \tag{A.35}$$

The operators acting in $\mathscr{H}_2$ are then represented as 2×2 matrices. The states $|E_i\rangle$ and $|E_f\rangle$ are by construction eigenstates of the Hamiltonian H_μ associated with the eigenvalues $\hbar\omega_i$ and $\hbar\omega_f$, respectively. Hence H_μ can be written in the form

$$H_\mu = \frac{\hbar}{2}(\omega_i + \omega_f) \begin{pmatrix} 1 & 0 \\ 0 & 1 \end{pmatrix} + \frac{\hbar}{2}\,\omega_{fi} \begin{pmatrix} -1 & 0 \\ 0 & 1 \end{pmatrix} ,$$

where the first term is nothing but a matrix commuting with any operator. It has no impact on the dynamics and can thus be dropped[12]. The Hamiltonian H_μ is thus merely given by

$$H_\mu = \frac{\hbar}{2}\,\omega_{fi} \begin{pmatrix} -1 & 0 \\ 0 & 1 \end{pmatrix} . \tag{A.36}$$

Now, suppose that the external field is of the more general form

$$\mathbf{E}_\mathrm{e}(\mathbf{r}, \tau) = \mathbf{E}(\mathbf{r}, \tau) \cos(\omega_l \tau) , \tag{A.37}$$

with $\mathbf{E}$ an arbitrary function of $\mathbf{r}$ and τ. Because $\mathbf{E}_\mathrm{e}(\mathbf{C}, \tau)$ involves only the centre of mass operator $\mathbf{C}$, it acts (by construction of the tensor product) as the identity operator in the space $\mathscr{H}_2$. The interaction term in the electric dipole Hamiltonian (A.25) hence reads

$$e\mathbf{r}_\mu \cdot \mathbf{E}_\mathrm{e}(\mathbf{C}, \tau) = \sum_{j,k=i}^{f} e\langle E_j|\mathbf{r}_\mu|E_k\rangle \cdot \mathbf{E}(\mathbf{C}, \tau) \cos(\omega_l \tau) |E_j\rangle\langle E_k| . \tag{A.38}$$

Now, remember that the eigenstates $|E_j\rangle$ of the hydrogen atom have a definite parity, that is $\langle -\mathbf{r}|E_j\rangle = \psi_{n_j l_j m_j}(-\mathbf{r}) = (-1)^{l_j} \psi_{n_j l_j m_j}(\mathbf{r})$. This implies that the diagonal elements of $\mathbf{r}_\mu$ are identically zero,

$$\langle E_i|\mathbf{r}_\mu|E_i\rangle = \langle E_f|\mathbf{r}_\mu|E_f\rangle = 0 , \tag{A.39}$$

[12] A unitary transformation can be performed through the action of the operator $\exp[i\hbar(\omega_i + \omega_f)\mathbb{1}]$, which does nothing except adding a global phase to the states, which has no physical impact.

and that its non-diagonal elements can only be different from zero if the two states $|E_i\rangle$ and $|E_f\rangle$ have opposite parities. Therefore, from now on it is assumed that the frequency ω_l of the external field matches a transition between two states of *opposite parities*. Furthermore, suppose that the relative phase between the two states $|E_i\rangle$ and $|E_f\rangle$ has been so chosen to ensure that[13]

$$\langle E_i|\mathbf{r}_\mu|E_f\rangle = \langle E_f|\mathbf{r}_\mu|E_i\rangle\,. \tag{A.40}$$

Combining (A.38) with (A.39) and (A.40) hence yields the matrix form of the operator $e\mathbf{r}_\mu \cdot \mathbf{E}_\mathrm{e}(\mathbf{C},\tau)$

$$e\mathbf{r}_\mu \cdot \mathbf{E}_\mathrm{e}(\mathbf{C},\tau) = \hbar\,\mathcal{V}(\mathbf{C},\tau)\cos(\omega_l\tau)\begin{pmatrix}0 & 1\\ 1 & 0\end{pmatrix}\,, \tag{A.41}$$

where the function $\mathcal{V}$ is defined by

$$\mathcal{V}(\mathbf{C},\tau) \equiv \frac{e}{\hbar}\langle E_f|\mathbf{r}_\mu|E_i\rangle \cdot \mathbf{E}(\mathbf{C},\tau)\,. \tag{A.42}$$

The rotating wave approximation can now be invoked to rewrite (A.41), and

$$e\mathbf{r}_\mu \cdot \mathbf{E}_\mathrm{e}(\mathbf{C},\tau) = \frac{\hbar}{2}\,\mathcal{V}(\mathbf{C},\tau)\begin{pmatrix}0 & \mathrm{e}^{i\omega_l\tau}\\ \mathrm{e}^{-i\omega_l\tau} & 0\end{pmatrix}\,, \tag{A.43}$$

where $\mathrm{e}^{-i\omega_l\tau}$ rather than $\mathrm{e}^{i\omega_l\tau}$ appears in the second row so as to preserve the Hermitian nature of the operator.

In the particular example where $\mathbf{E}(\mathbf{C},\tau) = \mathbf{E}_0$, the function $\mathcal{V}$ is the usual Rabi frequency. In such a case the state $|\psi(\tau)\rangle_\mu \in \mathscr{H}_2$ of the relative particle oscillates between the two eigenstates $|E_i\rangle$ and $|E_f\rangle$, a well-known example of so-called *Rabi oscillations*, also called *Rabi flopping* [1,16,17]. Suppression of such Rabi oscillations might occur in various physical setups, for instance through submitting the two-level system to an additional time-dependent perturbation [64]. An other way of suppressing Rabi oscillations, related to the physical problem studied in the present thesis, is to submit a *moving* two-level system to a *position-dependent* external field [18]. Indeed, when $\mathbf{E}(\mathbf{C},\tau) = \mathbf{E}_0$ the interaction term $e\mathbf{r}_\mu \cdot \mathbf{E}_\mathrm{e}(\mathbf{C},\tau)$ in the Hamiltonian (A.25) only couples the external field to the relative particle. The

[13] In the case of the hydrogen atom this can be done by appropriately choosing the magnetic quantum numbers m_i and m_f. Indeed, the only complex contribution of the wave function $\psi_{nlm}(r,\theta,\phi)$ is via $\mathrm{e}^{im\phi}$. The condition (A.40) is then for instance satisfied for $m_f = m_i$.

free evolution of the centre of mass and the dynamics of the relative particle, that is of the two-level system, under the influence of the simple periodic field can thus be treated separately. This separation is then impossible when the external field is position-dependent, as the external field is now coupled to both the relative particle (through $\mathbf{r}_\mu$) and the centre of mass (through $\mathbf{E}(\mathbf{C},\tau)$). In this case it is important to treat the global system {centre of mass + relative particle}, described by the dynamical state $|\psi(\tau)\rangle \in \mathscr{H}$.

Finally, the operator $\mathbf{P}^2/2M$, representing the kinetic energy of the centre of mass, is easily written in the basis $\{|E_i\rangle, |E_f\rangle\}$. Since this operator is defined on the centre-of-mass state space $\mathscr{H}_C$, it acts as the identity operator on any element of $\mathscr{H}_2$ and thus reads

$$\frac{\mathbf{P}^2}{2M} = \frac{\mathbf{P}^2}{2M}\begin{pmatrix} 1 & 0 \\ 0 & 1 \end{pmatrix} . \tag{A.44}$$

Therefore, combining the expression (A.25) of H_{ed} with (A.36). (A.43) and (A.44) yields the following Hamiltonian governing the two-level system:

$$H_{\text{ed}} = \frac{\mathbf{P}^2}{2M}\begin{pmatrix} 1 & 0 \\ 0 & 1 \end{pmatrix} + \frac{\hbar}{2}\omega_{fi}\begin{pmatrix} -1 & 0 \\ 0 & 1 \end{pmatrix} + \frac{\hbar}{2}\mathcal{V}(\mathbf{C},\tau)\begin{pmatrix} 0 & \mathrm{e}^{i\omega_l\tau} \\ \mathrm{e}^{-i\omega_l\tau} & 0 \end{pmatrix} . \tag{A.45}$$

The form of the Hamiltonian (A.45) suggests to work in an interaction picture [1,65] with respect to the Hamiltonian H_μ of the relative particle in the absence on an external field. To this end, introduce the unitary operator $\mathcal{T}_I$ given by (using (A.36))

$$\mathcal{T}_\mathcal{I} \equiv \mathrm{e}^{\frac{i}{\hbar}H_\mu\tau} = \begin{pmatrix} \mathrm{e}^{-i\omega_{fi}\tau/2} & 0 \\ 0 & \mathrm{e}^{i\omega_{fi}\tau/2} \end{pmatrix} , \tag{A.46}$$

The state $|\psi(\tau)\rangle_I$ in the interaction picture is constructed from the state $|\psi(\tau)\rangle$ through $|\psi(\tau)\rangle_I = \mathcal{T}_\mathcal{I}|\psi(\tau)\rangle$. The state $|\psi(\tau)\rangle$ obeys the TDSE $i\hbar d|\psi(\tau)\rangle/d\tau = H_{\text{ed}}|\psi(\tau)\rangle$, while the interaction picture state $|\psi(\tau)\rangle_I$ satisfies the TDSE $i\hbar\frac{d}{d\tau}|\psi(\tau)\rangle_I = H_I|\psi(\tau)\rangle_I$, where H_I denotes the interaction picture Hamiltonian given by

$$H_I = \frac{\mathbf{P}^2}{2M}\begin{pmatrix} 1 & 0 \\ 0 & 1 \end{pmatrix} + \frac{\hbar}{2}\mathcal{V}(\mathbf{C},\tau)\begin{pmatrix} 0 & \mathrm{e}^{-i(\omega_{fi}-\omega_l)\tau} \\ \mathrm{e}^{i(\omega_{fi}-\omega_l)\tau} & 0 \end{pmatrix} . \tag{A.47}$$

Finally, an *exact resonance* between the external field and the transition $|E_i\rangle \to |E_f\rangle$ is now assumed, that is

$$\omega_l = \omega_{fi}\,. \tag{A.48}$$

Therefore, substituting this condition (A.48) into (A.47) yields the following expression for the interaction Hamiltonian H_I:

$$H_I = \frac{\mathbf{P}^2}{2M}\begin{pmatrix}1 & 0\\ 0 & 1\end{pmatrix} + \frac{\hbar}{2}\,\mathcal{V}(\mathbf{C},\tau)\begin{pmatrix}0 & 1\\ 1 & 0\end{pmatrix}\,. \tag{A.49}$$

Furthermore, the function $\mathbf{E}$ is now assumed to be of the form

$$\mathbf{E}(\mathbf{C},\tau) = \mathcal{E}(\tau)\mathcal{F}(\mathbf{C})\mathbf{E}_0\,, \tag{A.50}$$

where $\mathcal{E}$ and $\mathcal{F}$ are two arbitrary scalar functions of the time and position variables τ and $\mathbf{C}$, respectively. The constant vector $\mathbf{E}_0$ gives the polarisation direction of the external electric field. Therefore, in view of the definition (A.42) of the function $\mathcal{V}$ the Hamiltonian (A.49) can be rewritten in the form

$$H_I = \frac{\mathbf{P}^2}{2M}\begin{pmatrix}1 & 0\\ 0 & 1\end{pmatrix} + \hbar\Omega(\tau)\mathcal{F}(\mathbf{C})\begin{pmatrix}0 & 1\\ 1 & 0\end{pmatrix}\,, \tag{A.51}$$

where the function Ω is defined by (remember that $\mathbf{d} = -e\mathbf{r}_\mu$)

$$\Omega(\tau) \equiv -\frac{\mathcal{E}(\tau)}{2\hbar}\langle E_f|\mathbf{d}\cdot\mathbf{E}_0|E_i\rangle\,. \tag{A.52}$$

The Hamiltonian (A.51) can now be used as the starting point to introduce the δ-potential model, as is discussed in section 3.1.

Note that the above discussion concerns the particular case of the hydrogen atom. It is then extended to an arbitrary atom. This generalisation to atoms different than hydrogen makes particular sense for the alkali-metal atoms that are typically considered in this work. Because these have a single valence electron, they can in first approximation be treated as an electron in interaction with a heavy "nucleus", formed by the atom's nucleus and all the inner electrons, of charge e.

Appendix B

Determinant of $H^{(s)}$

We start by rewriting the Hessian, given by Eq. (4.34), in the matrix form

$$H^{(s)} = 2\left(\sum_{k=1}^{n+1}|\epsilon_k - \epsilon_{k-1}|\right)^3 \mathcal{A}\,, \tag{B.1}$$

where

$$A = \begin{pmatrix} b_1 & c_1 & 0 & \cdots & \cdots & 0 \\ a_2 & \ddots & \ddots & \ddots & & \vdots \\ 0 & \ddots & \ddots & \ddots & \ddots & \vdots \\ \vdots & \ddots & \ddots & \ddots & \ddots & 0 \\ \vdots & & \ddots & \ddots & \ddots & c_{n-1} \\ 0 & \cdots & \cdots & 0 & a_n & b_n \end{pmatrix} \tag{B.2}$$

with

$$a_j = -\frac{1}{|\epsilon_j - \epsilon_{j-1}|}\,, \quad 2 \leqslant j \leqslant n\,, \tag{B.3a}$$

$$b_j = \frac{1}{|\epsilon_j - \epsilon_{j-1}|} + \frac{1}{|\epsilon_{j+1} - \epsilon_j|}\,, \quad 1 \leqslant j \leqslant n\,, \tag{B.3b}$$

and

$$c_j = -\frac{1}{|\epsilon_{j+1} - \epsilon_j|}\,, \quad 1 \leqslant j \leqslant n-1\,. \tag{B.3c}$$

It follows immediately from Eq. (B.1) that

$$\det\left(H^{(s)}\right) = 2^n\left(\sum_{k=1}^{n+1}|\epsilon_k - \epsilon_{k-1}|\right)^{3n} \det(\mathcal{A})\,. \tag{B.4}$$

In order to find $\det(\mathcal{A})$ we use an LU decomposition of the matrix $\mathcal{A}$. That is, we express $\mathcal{A}$ as

$$\mathcal{A} = \mathcal{L}\mathcal{U}\,, \tag{B.5}$$

where

$$\mathcal{L} = \begin{pmatrix} 1 & 0 & 0 & \cdots & \cdots & 0 \\ L_2 & \ddots & \ddots & \ddots & & \vdots \\ 0 & \ddots & \ddots & \ddots & \ddots & \vdots \\ \vdots & \ddots & \ddots & \ddots & \ddots & 0 \\ \vdots & & \ddots & \ddots & \ddots & 0 \\ 0 & \cdots & \cdots & 0 & L_n & 1 \end{pmatrix} \tag{B.6}$$

and

$$\mathcal{U} = \begin{pmatrix} U_1 & c_1 & 0 & \cdots & \cdots & 0 \\ 0 & \ddots & \ddots & \ddots & & \vdots \\ 0 & \ddots & \ddots & \ddots & \ddots & \vdots \\ \vdots & \ddots & \ddots & \ddots & \ddots & 0 \\ \vdots & & \ddots & \ddots & \ddots & c_{n-1} \\ 0 & \cdots & \cdots & 0 & 0 & U_n \end{pmatrix} . \tag{B.7}$$

Substituting Eqs. (B.2), (B.6), and (B.7) into Eq. (B.5), we see that the $(2n-1)$ matrix elements L_j and U_j must satisfy the following $(2n-1)$ equations:

$$\begin{cases} U_1 = b_1 & \\ L_{j+1}U_j = a_{j+1} & , \quad 1 \leqslant j \leqslant n-1 \\ L_{j+1}c_j + U_{j+1} = b_{j+1} & , \quad 1 \leqslant j \leqslant n-1 \end{cases} . \tag{B.8}$$

Solving this system of equations, we find

$$L_j = -\frac{\sum_{k=1}^{j-1} |\epsilon_k - \epsilon_{k-1}|}{\sum_{k=1}^{j} |\epsilon_k - \epsilon_{k-1}|} \tag{B.9}$$

for all $2 \leqslant j \leqslant n$, and

$$U_j = \frac{\sum_{k=1}^{j+1} |\epsilon_k - \epsilon_{k-1}|}{|\epsilon_{j+1} - \epsilon_j| \sum_{k=1}^{j} |\epsilon_k - \epsilon_{k-1}|} \tag{B.10}$$

for all $1 \leqslant j \leqslant n$.

It is now straightforward to compute the determinant of $\mathcal{A}$. In view of Eqs. (B.5),

(B.6) and (B.7), we have

$$\det(\mathcal{A}) = \det(\mathcal{L})\det(\mathcal{U}) = \prod_{j=1}^{n} U_j \,, \tag{B.11}$$

and thus, using Eq. (B.10),

$$\det(\mathcal{A}) = \frac{\sum_{k=1}^{n+1} |\epsilon_k - \epsilon_{k-1}|}{\prod_{k=1}^{n+1} |\epsilon_k - \epsilon_{k-1}|} \,. \tag{B.12}$$

Finally, combining Eq. (B.4) and (B.12), we arrive at the final result, Eq. (4.34).

Appendix C

Crank-Nicolson algorithm

In this appendix we provide some details about the scheme we use to numerically solve the DPM, described by the problem (3.16)-(3.20). We first introduce the linear combinations

$$\psi_{\pm}(x,\tau) = \psi_1(x,\tau) \pm \psi_2(x,\tau) \tag{C.1}$$

to decouple the TDSE (3.19), and we obtain from (3.16)-(3.20), along with the IC (3.27) and (3.40)-(3.41), the following problem for $\psi_{\pm}$:

$$\frac{\partial}{\partial\tau}\psi_{\pm}(x,\tau) = \frac{i\hbar}{2m}\frac{\partial^2}{\partial x^2}\psi_{\pm}(x,\tau) \qquad \text{for} \qquad x \neq 0\,, \tag{C.2a}$$

$$\psi_{\pm}(x,0^+) = \Psi_0(x)\,, \tag{C.2b}$$

$$\lim_{x\to\pm\infty} \psi_{\pm}(x,\tau) = 0\,, \tag{C.2c}$$

$$\psi_{\pm}(x,\tau)\big|_{x=0^-}^{x=0^+} = 0\,, \tag{C.2d}$$

$$\frac{\partial}{\partial x}\psi_{\pm}(x,\tau)\bigg|_{x=0^-}^{x=0^+} = \pm\frac{2m\Omega(\tau)}{\hbar}\psi_{\pm}(0,\tau)\,, \tag{C.2e}$$

where the two matching conditions (C.2d) and (C.2e) are obtained from the TDSE with the δ-potential using the hierarchy of singularities [31] and integrating the TDSE with respect to x over a vanishing interval. We now discuss how we can numerically construct the solutions $\psi_{\pm}$ to this problem (C.2). For concreteness we illustrate the procedure on ψ_+, which we merely relabel ψ in the sequel[1].

[1]The general procedure is exactly the same for ψ_-, which differs from ψ_+ only because of the

The true solution $\psi(x,\tau)$ of (C.2) is a continuous function of the continuous space and time variables x and τ. It is however impossible to construct a true numerical continuum, which would require the simultaneous specification of an infinite number of values. Therefore, the very first step in solving (C.2) is to discretise the two-dimensional space-time (x,τ). We do this through introducing the two fundamental numerical parameters Δx and $\Delta\tau$, which we call the space- and time-steps, respectively. The continuous sets $\{x\}_{x\in\mathbb{R}}$ and $\{\tau\}_{\tau\in\mathbb{R}_+}$ are thus numerically represented by the discrete sets $\{X_j\}_{j\in\mathbb{Z}}$ and $\{t_k\}_{k\in\mathbb{N}}$, such that

$$X_{j+1} = X_j + \Delta x\,, \tag{C.3a}$$

$$t_{k+1} = t_k + \Delta\tau\,. \tag{C.3b}$$

Note that we take here for convenience a regular space-time grid formed by regularly spaced discrete points. We introduce the notation

$$f_{j\,,k} \equiv f(X_j, t_k) \tag{C.4}$$

to denote the value taken by an arbitrary continuous function $f(x,\tau)$ at the particular space-time point (X_j, t_k).

Now, the space-time grid constructed from (C.3) must have *finite* dimensions. This is easily done regarding the time dimension. Indeed, the time boundaries are merely the initial time $\tau = 0$ and the final time $\tau = t$. The continuous variable τ is thus represented by the finite discrete set $\{t_k\}_{k\in[\![0,N_\tau]\!]}$, where $t_0 = 0$ and the integer N_τ is such that

$$t_{N_\tau} = t_0 + N_\tau\Delta\tau = t\,. \tag{C.5}$$

The space boundaries of the grid are slightly less trivial. Denote them temporarily X_{inf} and X_{sup}, $X_{\text{inf}} < X_{\text{sup}}$. First, remember that we choose a Gaussian initial state $\Psi_0(x) = \psi_{\alpha_0,x_0,v_0}(x,0)$ (given by (2.11)) of mean position $x_0 < 0$, mean velocity $v_0 > 0$ and width σ. Therefore, we actually choose the left boundary X_{inf} such that $\psi_{\alpha_0,x_0,v_0}(X_{\text{inf}},0) \approx 0$[2]. The right boundary X_{sup} is then chosen in view of the freely evolved state at the final time t. In view of (2.17) the initial state $\Psi_0(x)$ propagates freely into the state $\psi_{\alpha_0,x_0,v_0}(x,t)$, of mean position x_t. Therefore, we

sign in the last matching condition (C.2e).

[2]We will typically choose $X_{\text{inf}} = x_0 - N\sigma$, with $N \geqslant 5$.

choose the right boundary X_{sup} such that $\psi_{\alpha_0,x_0,v_0}(X_{\text{sup}},t) \approx 0$[3]. Furthermore, we will typically consider (see the numerical parameters detailed in section 4.2) a symmetrical situation where the final time t is such that $x_t = -x_0$. We hence choose for convenience $X_{\text{sup}} = -X_{\text{inf}}$. Therefore, the continuous variable x is represented by the finite discrete set $\{X_j\}_{j\in[\![-N_x,N_x]\!]}$, where $X_0 = 0$ denotes the position of the barrier and the integer N_x is such that the numerical solution ψ of the problem (C.2) satisfies the following boundary conditions "at infinity":

$$\psi_{-N_x\,,k} = \psi_{N_x\,,k} = 0\,, \tag{C.6}$$

for any $k \in [\![0, N_\tau]\!]$.

Now that our space-time grid is fully specified, we must write on this grid suitable discrete versions of (partial) derivatives, which we here represent by means of *finite differences approximations* [66]. Such approximations stem directly from Taylor's theorem. To illustrate the idea, we write for instance the Taylor expansion of $\psi(x \pm \Delta x, \tau)$ around x for a fixed value of τ, and we have (up to the third order in Δx)

$$\psi(x \pm \Delta x, \tau) = \psi(x,\tau) \pm \Delta x \frac{\partial\psi}{\partial x} + \frac{\Delta x^2}{2}\frac{\partial^2\psi}{\partial x^2} \pm \frac{\Delta x^3}{6}\frac{\partial^3\psi}{\partial x^3} + \mathcal{O}\left(\Delta x^4\right)\,. \tag{C.7}$$

This result (C.7) being valid for any value of the continuous variables x and τ, it is in particular true for some point (X_j, t_k) of our space-time grid, and we get for instance

$$\frac{\partial}{\partial x}\psi(x,t_k)\bigg|_{x=X_j} = \frac{\psi_{j+1\,,k} - \psi_{j\,,k}}{\Delta x} + \mathcal{O}\left(\Delta x\right)\,. \tag{C.8}$$

The first term in the right hand side of (C.8) would thus be the *first order* (because the error is proportional to Δx) *forward* (because the derivative at X_j is expressed in terms of the values of ψ at X_j and the forward point X_{j+1}) *difference approximation* to the derivative $(\partial\psi/\partial x)|_{X_j}$. The type and order of such finite differences approximations depend on how the Taylor series is written.

We follow a specific finite differences scheme introduced by Crank and Nicolson [56]. Adapted to our particular problem it represents the free-particle TDSE

[3]We will typically choose $X_{\text{sup}} = x_t + N\sigma(t)$, with $N \geqslant 5$ and $\sigma(t) = \sigma\sqrt{1+(\hbar t/m\sigma^2)^2}$. However for the numerical parameters we use we have $\sigma(t) \approx \sigma$, so that we will basically take $X_{\text{sup}} = x_t + N\sigma$.

$$\frac{\partial}{\partial\tau}\psi(x,\tau) = \frac{i\hbar}{2m}\frac{\partial^2}{\partial x^2}\psi(x,\tau) \tag{C.9}$$

by the discrete version

$$\mathfrak{b}\psi_{j+1\,,\,k+1} + \mathfrak{a}\psi_{j\,,\,k+1} + \mathfrak{b}\psi_{j-1\,,\,k+1} = \mathfrak{c}_{j\,,\,k}\,, \tag{C.10}$$

with

$$\mathfrak{a} \equiv 1 + \frac{i\hbar}{2m}\frac{\Delta\tau}{\Delta x^2}\,, \tag{C.11a}$$

$$\mathfrak{b} \equiv -\frac{i\hbar}{4m}\frac{\Delta\tau}{\Delta x^2}\,, \tag{C.11b}$$

$$\mathfrak{c}_{j\,,\,k} \equiv \left[1 - \frac{i\hbar}{2m}\frac{\Delta\tau}{\Delta x^2}\right]\psi_{j\,,\,k} - \mathfrak{b}\left(\psi_{j+1\,,\,k} + \psi_{j-1\,,\,k}\right)\,. \tag{C.11c}$$

Therefore, the Crank-Nicolson method relates through (C.10) the values $\psi_{j-1\,,\,k+1}$, $\psi_{j\,,\,k+1}$ and $\psi_{j+1\,,\,k+1}$ at the time t_{k+1} to the corresponding values at the previous time t_k.

However, note that (C.10) can not be written at every point of the space discretisation $\{X_j\}_{j\in[\![-N_x,N_x]\!]}$. Indeed, we can for instance not take $j = \pm N_x$ in (C.10), as we would then in particular require the values $\psi_{\pm(N_x+1)\,,\,k}$, that is values of ψ at space-time grid points that do not exist. Therefore, we must take $j \neq \pm N_x$ in (C.10), and the values of ψ at the boundaries of the space grid at time t_{k+1} are then merely obtained from the BC's (C.6), i.e.

$$\psi_{\pm N_x\,,\,k+1} = 0\,. \tag{C.12}$$

Furthermore, remember that according to (C.2a) the PDE (C.9) is actually not valid for $x = 0$, which in turn implies that its discrete version (C.10) is not valid for $j = 0$. Therefore, the set of equations (C.10), completed by (C.12), gives us $2N_x$ linear equations for the $2N_x + 1$ unknowns[4] $\psi_{j\,,\,k+1}$, $j \in [\![-N_x, N_x]\!]$. The last required equation is obtained from the jump condition (C.2e) at $x = 0$, i.e.

[4]We implicitly consider that all the discrete values of ψ at the previous time t_k have already been constructed. Indeed, we know exactly the values of ψ at the initial time t_0. We then construct the values of ψ at the subsequent time t_1, and so on until the time t_k.

$$\frac{\partial}{\partial x}\psi(x,\tau)\Big|_{x=0^-}^{x=0^+} = \frac{2m\Omega(\tau)}{\hbar}\psi(0,\tau)\,. \tag{C.13}$$

The specific form of this condition in our Crank-Nicolson scheme depends on how we write the derivatives. First we replace $(\partial\psi/\partial x)|_{x=0^\pm}$ by $(\partial\psi/\partial x)|_{x=X_{\pm1}}$. We then represent these latter by, respectively, first order backward and forward finite differences approximations, that is

$$\frac{\partial}{\partial x}\psi(x,t_{k+1})\Big|_{x=X_1} = \frac{\psi_{1\,,k+1}-\psi_{0\,,k+1}}{\Delta x} + \mathcal{O}\left(\Delta x\right) \tag{C.14}$$

and

$$\frac{\partial}{\partial x}\psi(x,t_{k+1})\Big|_{x=X_{-1}} = \frac{\psi_{0\,,k+1}-\psi_{-1\,,k+1}}{\Delta x} + \mathcal{O}\left(\Delta x\right)\,, \tag{C.15}$$

and thus the discrete version of the jump condition (C.13) reads

$$\psi_{1\,,k+1} - 2\left[1+\frac{m\Omega(t_{k+1})}{\hbar}\Delta x\right]\psi_{0\,,k+1} + \psi_{-1\,,k+1} = 0\,. \tag{C.16}$$

Therefore, combining (C.10), (C.12) and (C.16), we see that the continuous problem (C.2) is represented by a Crank-Nicolson algorithm which, at the time t_{k+1}, $k\in[\![0,N_\tau-1]\!]$, consists in the $2N_x+1$ linear equations

$$\mathfrak{b}\psi_{j+1\,,k+1} + \mathfrak{a}\psi_{j\,,k+1} + \mathfrak{b}\psi_{j-1\,,k+1} = \mathfrak{c}_{j\,,k} \qquad \text{for} \qquad j\in[\![-N_x+1,-1]\!]\cup[\![1,N_x-1]\!]\,, \tag{C.17a}$$

$$\psi_{\pm N_x\,,k+1} = 0\,, \tag{C.17b}$$

$$\psi_{1\,,k+1} - 2\left[1+\frac{m\Omega(t_{k+1})}{\hbar}\Delta x\right]\psi_{0\,,k+1} + \psi_{-1\,,k+1} = 0\,. \tag{C.17c}$$

We conclude this appendix with a brief discussion about the effective numerical implementation of this Crank-Nicolson scheme (C.17).

The accuracy of the finite differences, and hence of the whole scheme, depends on the space- and time-steps Δx and $\Delta\tau$. These are fixed in view of the physical system under study. Indeed, remember that the initial state Ψ_0 is the Gaussian wave

packet (2.11), which presents an oscillatory term of wavelength $2\pi\lambda\!\!\!^{-}_0$, with $\lambda\!\!\!^{-}_0$ the reduced de Broglie wavelength defined by (2.14). The space-step Δx must hence be small enough so that a typical oscillation of ψ is accurately described by the discrete values $\psi_{j\,,k}$. Therefore, we generally take

$$\Delta x = \frac{\lambda\!\!\!^{-}_0}{N}\,, \tag{C.18}$$

with N some real number typically larger than 10. Furthermore, we define the time-step $\Delta\tau$ in terms of the space-step Δx. Indeed, the initial state (2.11) having a mean velocity $v_0 > 0$, Δx and v_0 hence define a typical time scale $\Delta x/v_0$. We choose $\Delta\tau$ to be smaller than this time scale, that is

$$\Delta\tau = n\frac{\Delta x}{v_0}\,, \tag{C.19}$$

with n some real number smaller than 1.

Finally, the linear system (C.17) is solved by means of standard linear algebra techniques. It is worth noting that the Crank-Nicolson scheme used here defines a linear system of equations that can be cast in matrix form with a *tridiagonal matrix*. This allows us to apply the so-called *Thomas algorithm* [67] to efficiently solve the linear system (C.17).

Appendix D

Simple periodic aperture function

In this appendix we analyse in details the phase-space structure of the function $|h_+(\widetilde{x},\widetilde{v})|$. Remember that in view of (5.30) and (5.31) we have

$$|h_+(\widetilde{x},\widetilde{v})| = \mathrm{e}^{\phi_+(\widetilde{x},\widetilde{v})}\,, \tag{D.1}$$

where the function ϕ_+ is defined by

$$\phi_+(\widetilde{x},\widetilde{v}) \equiv -\frac{(v_0\widetilde{x}-\widetilde{v}x_t)^2}{2\sigma^2\,(v_0^2+\widetilde{v}^2)} + \frac{m^2\sigma^2v_0^2}{2\hbar^2}\frac{\widetilde{v}^2}{v_0^2+\widetilde{v}^2} - \left(\frac{\sigma^2\omega_1^2}{2}+\frac{m\sigma^2v_0^2\omega_1}{\hbar}\right)\frac{1}{v_0^2+\widetilde{v}^2} - \frac{m^2\sigma^2}{8\hbar^2}\widetilde{v}^2 + \frac{m\sigma^2\omega_1}{2\hbar} - \frac{m^2\sigma^2v_0^2}{8\hbar^2}\,. \tag{D.2}$$

D.1 Critical points of ϕ_+

Note that the two independent variables $\widetilde{x}$ and $\widetilde{v}$ have different physical dimensions, length and velocity, respectively. Therefore, before we derive the critical points of the function $\phi_+(\widetilde{x},\widetilde{v})$, we first need to rewrite it in terms of dimensionless variables[1], which we will denote ζ and η.

Such dimensionless variables can be conveniently constructed from rescaling the physical variables $\widetilde{x}$ and $\widetilde{v}$ by the free-particle classical position x_t and velocity v_0, respectively. Therefore, the dimensionless variables ζ and η are defined by

$$\zeta \equiv \frac{\widetilde{x}}{x_t}\,, \tag{D.3a}$$

$$\eta \equiv \frac{\widetilde{v}}{v_0}\,. \tag{D.3b}$$

[1]Otherwise, the elements of the Hessian matrix for instance would have different dimensions.

We hence have

$$\phi_+(\widetilde{x},\widetilde{v}) = \phi_+(x_t\zeta, v_0\eta) = \varphi_+(\zeta,\eta)\,, \tag{D.4}$$

where in view of (D.2) and (D.3) the function φ_+ is given by

$$\varphi_+(\zeta,\eta) = -\frac{x_t^2}{2\sigma^2}\frac{(\zeta-\eta)^2}{1+\eta^2} + \frac{m^2\sigma^2v_0^2}{2\hbar^2}\frac{\eta^2}{1+\eta^2} - \left(\frac{\sigma^2\omega_1^2}{2v_0^2} + \frac{m\sigma^2\omega_1}{\hbar}\right)\frac{1}{1+\eta^2} - \frac{m^2\sigma^2v_0^2}{8\hbar^2}\eta^2 + \frac{m\sigma^2\omega_1}{2\hbar} - \frac{m^2\sigma^2v_0^2}{8\hbar^2}\,. \tag{D.5}$$

The critical points $\left(\overline{\zeta},\overline{\eta}\right)$ of this function $\varphi_+(\zeta,\eta)$ are then defined through the conditions

$$\left.\frac{\partial\varphi_+}{\partial\zeta}\right|_{\left(\overline{\zeta},\overline{\eta}\right)} = 0 \qquad \text{and} \qquad \left.\frac{\partial\varphi_+}{\partial\eta}\right|_{\left(\overline{\zeta},\overline{\eta}\right)} = 0\,. \tag{D.6}$$

Substituting the expression (D.5) of φ_+ into (D.6), and solving the resulting system of equations yields one (real) trivial solution, denoted by $\left(\overline{\zeta},\overline{\eta}\right)_0$, two other real solutions $\left(\overline{\zeta},\overline{\eta}\right)_\pm$, and two pure imaginary solutions $\left(\overline{\zeta},\overline{\eta}\right)_\pm^{(i)}$, given by

$$\left(\overline{\zeta},\overline{\eta}\right)_0 = \left(\overline{\zeta}_0\,,\,\overline{\eta}_0\right) = (0,0)\,, \tag{D.7a}$$

$$\left(\overline{\zeta},\overline{\eta}\right)_\pm = \left(\overline{\zeta}_\pm\,,\,\overline{\eta}_\pm\right) = \left(\pm\sqrt{1+2\frac{\hbar\omega_1}{mv_0^2}}\quad,\quad\pm\sqrt{1+2\frac{\hbar\omega_1}{mv_0^2}}\right)\,, \tag{D.7b}$$

$$\left(\overline{\zeta},\overline{\eta}\right)_\pm^{(i)} = \left(\overline{\zeta}_\pm^{(i)}\,,\,\overline{\eta}_\pm^{(i)}\right) = \left(\pm i\sqrt{3+2\frac{\hbar\omega_1}{mv_0^2}}\quad,\quad\pm i\sqrt{3+2\frac{\hbar\omega}{mv_0^2}}\right)\,. \tag{D.7c}$$

Now, remember that we are only interested in studying the structure of the Husimi distribution $\mathcal{H}_{\mathrm{AFM}}^{(\mathrm{fr})}$, and thus by extension of $|h_+|$, in a neighbourhood of the classical point (x_t, v_0). Therefore, the two complex critical points (D.7c) are not relevant for our analysis. Furthermore, because the trivial solution $\left(\overline{\zeta},\overline{\eta}\right)_0$ refers, in view of (D.3a), to $\widetilde{x} = 0$ that is the position of the barrier, we can neglect it in our analysis. Finally, note that in view of (D.3) the critical point $\left(\overline{\zeta},\overline{\eta}\right)_-$ corresponds

to negative values of $\widetilde{x}$ and $\widetilde{v}$. Therefore, the only critical point of φ_+ that needs to be focused on is $\left(\overline{\zeta},\overline{\eta}\right)_+$.

We now investigate the behaviour of φ_+ at the critical point $\left(\overline{\zeta},\overline{\eta}\right)_+$. To this end, we compute the Hessian matrix, denoted by H_+, associated with this critical point. The Taylor expansion of φ_+ about $\left(\overline{\zeta},\overline{\eta}\right)_+ = \left(\overline{\zeta}_+,\overline{\eta}_+\right)$ reads, up to the second order,

$$\varphi_+(\zeta,\eta) = \varphi_+\left(\overline{\zeta}_+,\overline{\eta}_+\right) + \frac{1}{2}\begin{pmatrix}\zeta-\overline{\zeta}_+ & \eta-\overline{\eta}_+\end{pmatrix} H_+ \begin{pmatrix}\zeta-\overline{\zeta}_+\\ \eta-\overline{\eta}_+\end{pmatrix}, \tag{D.8}$$

where the Hessian matrix H_+ is hence defined by

$$H_+ \equiv \begin{pmatrix} \frac{\partial^2\varphi_+}{\partial\zeta^2}\Big|_{\left(\overline{\zeta},\overline{\eta}\right)_+} & \frac{\partial^2\varphi_+}{\partial\zeta\partial\eta}\Big|_{\left(\overline{\zeta},\overline{\eta}\right)_+} \\ \frac{\partial^2\varphi_+}{\partial\eta\partial\zeta}\Big|_{\left(\overline{\zeta},\overline{\eta}\right)_+} & \frac{\partial^2\varphi_+}{\partial\eta^2}\Big|_{\left(\overline{\zeta},\overline{\eta}\right)_+} \end{pmatrix}. \tag{D.9}$$

We now determine the eigenvalues and eigenvectors of the Hessian matrix H_+.

D.2 Hessian matrix H_+

We first rewrite the critical point $\left(\overline{\zeta},\overline{\eta}\right)_+$, given by (D.7b), in the form

$$\left(\overline{\zeta},\overline{\eta}\right)_+ = \left(\overline{\zeta}_+\,,\,\overline{\eta}_+\right) = \left(\sqrt{1+2\mu_+}\,,\,\sqrt{1+2\mu_+}\right), \tag{D.10}$$

where we introduced for convenience the dimensionless quantity μ_+, defined by

$$\mu_+ \equiv \frac{\hbar\omega_1}{mv_0^2} > 0\,, \tag{D.11}$$

where we used the fact that $\omega_1 > 0$ by assumption. Therefore, combining the definition (D.9) of the Hessian matrix H_+ with the expressions (D.5) and (D.10) of φ_+ and $\left(\overline{\zeta},\overline{\eta}\right)_+$, respectively, we get for H_+

$$H_+ = \begin{pmatrix} -\frac{x_t^2}{2\sigma^2}\frac{1}{1+\mu_+} & \frac{x_t^2}{2\sigma^2}\frac{1}{1+\mu_+} \\ \frac{x_t^2}{2\sigma^2}\frac{1}{1+\mu_+} & -\frac{x_t^2}{2\sigma^2}\frac{1}{1+\mu_+} - \frac{m^2\sigma^2v_0^2}{2\hbar^2}\frac{1+2\mu_+}{1+\mu_+} \end{pmatrix}. \tag{D.12}$$

Its determinant and trace are given by (remember the definition (2.14) of the de Broglie wavelength $\lambda\!\!\!^{-}_0$)

$$\det\left(H_+\right) = \frac{1}{4}\left(\frac{x_t}{\lambda\!\!\!^{-}_0}\right)^2 \frac{1+2\mu_+}{\left(1+\mu_+\right)^2}\,, \tag{D.13}$$

on which we clearly see in view of (D.11) that $\det\left(H_+\right) \neq 0$, so that the critical point $\left(\overline{\zeta},\overline{\eta}\right)_+$ is nondegenerate, and

$$\mathrm{Tr}\left(H_+\right) = -\frac{1}{2}\left(\frac{\sigma}{\lambda\!\!\!^{-}_0}\right)^2 \frac{1+2\mu_+}{1+\mu_+}\left(1+2\epsilon_+\right)\,, \tag{D.14}$$

where the quantity ϵ_+ is defined by

$$\epsilon_+ \equiv \frac{1}{1+2\mu_+}\left(\frac{\lambda\!\!\!^{-}_0 x_t}{\sigma^2}\right)^2 > 0\,. \tag{D.15}$$

Combining (D.13) and (D.14) we get in particular that

$$\sqrt{\mathrm{Tr}^2\left(H_+\right) - 4\det\left(H_+\right)} = \frac{1}{2}\left(\frac{\sigma}{\lambda\!\!\!^{-}_0}\right)^2 \frac{1+2\mu_+}{1+\mu_+}\sqrt{1+4\epsilon_+^2}\,. \tag{D.16}$$

Let us now denote by $\lambda_\pm^{(+)}$ the two eigenvalues of the Hessian matrix H_+, they are given by

$$\begin{aligned}\lambda_\pm^{(+)} &= \frac{1}{2}\left[\mathrm{Tr}\left(H_+\right) \pm \sqrt{\mathrm{Tr}^2\left(H_+\right) - 4\det\left(H_+\right)}\right] \\ &= -\frac{1}{4}\left(\frac{\sigma}{\lambda\!\!\!^{-}_0}\right)^2 \frac{1+2\mu_+}{1+\mu_+}\left(1+2\epsilon_+ \pm \sqrt{1+4\epsilon_+^2}\right)\,,\end{aligned} \tag{D.17}$$

and thus we can show that in the semiclassical regime these two eigenvalues satisfy

$$\lambda_\pm^{(+)} < 0\,, \tag{D.18}$$

Therefore, the Hessian matrix H_+ is *negative definite*, which thus implies that the function $\varphi_+(\zeta,\eta)$ has a *strict local maximum* at the critical point $\left(\overline{\zeta},\overline{\eta}\right)_+$.

We now construct the two normalised (to unity) eigenvectors $\Lambda_\pm^{(+)}$ of H_+ associated with the two eigenvalues $\lambda_\pm^{(+)}$:

$$\Lambda_{+}^{(+)} \equiv \begin{pmatrix} \Lambda_{11}^{(+)} \\ \Lambda_{21}^{(+)} \end{pmatrix} = \frac{1}{\sqrt{1+\delta_{+}^{2}}} \begin{pmatrix} 1 \\ \delta_{+} \end{pmatrix} \tag{D.19}$$

and

$$\Lambda_{-}^{(+)} \equiv \begin{pmatrix} \Lambda_{12}^{(+)} \\ \Lambda_{22}^{(+)} \end{pmatrix} = \frac{1}{\sqrt{1+\delta_{-}^{2}}} \begin{pmatrix} \delta_{-} \\ 1 \end{pmatrix} , \tag{D.20}$$

where δ_{+} and δ_{-} are related to ϵ_{+} through

$$\delta_{+} = -\frac{1}{2\epsilon_{+}} \left(1 - \sqrt{1+4\epsilon_{+}^{2}} \right) \tag{D.21}$$

and

$$\delta_{-} = -2\epsilon_{+} \frac{1}{1+\sqrt{1+4\epsilon_{+}^{2}}} . \tag{D.22}$$

These two eigenvectors $\Lambda_{\pm}^{(+)}$ are by construction normalised, and can be easily seen to be orthogonal. We now construct the matrix $\Lambda^{(+)}$, formed with $\Lambda_{\pm}^{(+)}$ as its column vectors, that is in view of (D.19) and (D.20)

$$\Lambda^{(+)} \equiv \left[\Lambda_{+}^{(+)} , \Lambda_{-}^{(+)} \right] = \begin{pmatrix} \Lambda_{11}^{(+)} & \Lambda_{12}^{(+)} \\ \Lambda_{21}^{(+)} & \Lambda_{22}^{(+)} \end{pmatrix} . \tag{D.23}$$

The matrix $\Lambda^{(+)}$ is orthogonal, so that it satisfies

$$\left(\Lambda^{(+)} \right)^{-1} = \left(\Lambda^{(+)} \right)^{\mathrm{T}} , \tag{D.24}$$

where the superscript T denotes the matrix transpose operation. Therefore, we write the Hessian matrix H_{+} in the form

$$H_{+} = \Lambda^{(+)} \begin{pmatrix} \lambda_{+}^{(+)} & 0 \\ 0 & \lambda_{-}^{(+)} \end{pmatrix} \left(\Lambda^{(+)} \right)^{\mathrm{T}} . \tag{D.25}$$

Now, note that in view of the definitions (2.14), (2.19) and (3.43) of $\lambda\!\!\!^{-}_0$, x_t and t_c, respectively, we can write

$$\frac{\lambda\!\!\!^{-}_0 x_t}{\sigma^2} = \frac{\hbar(t-t_c)}{m\sigma^2}\,, \tag{D.26}$$

and hence we have within the semiclassical regime (5.1) that

$$\frac{\lambda\!\!\!^{-}_0 x_t}{\sigma^2} \ll 1\,. \tag{D.27}$$

Combining the definition (D.15) of ϵ_+ with (D.27) (and remembering in view of (D.11) that $\mu_+ > 0$) we thus see that, within the frozen Gaussian regime, we have

$$\epsilon_+ \ll 1\,. \tag{D.28}$$

Therefore, in view of (D.28) we can expand the expressions (D.17), (D.19) and (D.20) of the eigenvalues and eigenvectors of H_+, and we get

$$\lambda_+^{(+)} = -\frac{1}{2}\left(\frac{\sigma}{\lambda\!\!\!^{-}_0}\right)^2 \frac{1+2\mu_+}{1+\mu_+}\left(\epsilon_+ - \epsilon_+^2 + \mathcal{O}\left(\epsilon_+^4\right)\right)\,, \tag{D.29a}$$

$$\lambda_-^{(+)} = -\frac{1}{2}\left(\frac{\sigma}{\lambda\!\!\!^{-}_0}\right)^2 \frac{1+2\mu_+}{1+\mu_+}\left(1 + \epsilon_+ + \epsilon_+^2 + \mathcal{O}\left(\epsilon_+^4\right)\right)\,, \tag{D.29b}$$

$$\Lambda_+^{(+)} \equiv \begin{pmatrix}\Lambda_{11}^{(+)}\\ \Lambda_{21}^{(+)}\end{pmatrix} = \begin{pmatrix}1\\0\end{pmatrix} + \epsilon_+\begin{pmatrix}0\\1\end{pmatrix} - \frac{\epsilon_+^2}{2}\begin{pmatrix}1\\0\end{pmatrix} + \begin{pmatrix}\mathcal{O}\left(\epsilon_+^4\right)\\ \mathcal{O}\left(\epsilon_+^3\right)\end{pmatrix}\,, \tag{D.29c}$$

$$\Lambda_-^{(+)} \equiv \begin{pmatrix}\Lambda_{12}^{(+)}\\ \Lambda_{22}^{(+)}\end{pmatrix} = \begin{pmatrix}0\\1\end{pmatrix} - \epsilon_+\begin{pmatrix}1\\0\end{pmatrix} - \frac{\epsilon_+^2}{2}\begin{pmatrix}0\\1\end{pmatrix} + \begin{pmatrix}\mathcal{O}\left(\epsilon_+^3\right)\\ \mathcal{O}\left(\epsilon_+^4\right)\end{pmatrix}\,. \tag{D.29d}$$

We can now write explicitly the Taylor expansion (D.8) of the function φ_+ about the critical point $\left(\overline{\zeta},\overline{\eta}\right)_+$. We first show, substituting (D.10) into (D.5), that $\varphi_+\left(\overline{\zeta}_+,\overline{\eta}_+\right) = 0$. Therefore, combining (D.8) with (D.25) and (D.29), we get

$$\varphi_+(\zeta,\eta) = -\frac{1}{4}\left(\frac{\sigma}{\lambda\!\!\!^{-}_0}\right)^2 \frac{1+2\mu_+}{1+\mu_+}\left[\epsilon_+ + \mathcal{O}\left(\epsilon_+^3\right)\right]\left(\zeta-\overline{\zeta}_+\right)^2 - \frac{1}{4}\left(\frac{\sigma}{\lambda\!\!\!^{-}_0}\right)^2 \frac{1+2\mu_+}{1+\mu_+}\left[1+\epsilon_+ + \mathcal{O}\left(\epsilon_+^3\right)\right]\left(\eta-\overline{\eta}_+\right)^2 + \frac{1}{4}\left(\frac{\sigma}{\lambda\!\!\!^{-}_0}\right)^2 \frac{1+2\mu_+}{1+\mu_+}\left[\epsilon_+ + \mathcal{O}\left(\epsilon_+^3\right)\right]\left(\zeta-\overline{\zeta}_+\right)\left(\eta-\overline{\eta}_+\right) . \quad \text{(D.30)}$$

Therefore, in view of the definition (D.3) of the dimensionless variables ζ and η, and because by definition we have $\phi_+(\widetilde{x},\widetilde{v}) = \varphi_+(\zeta,\eta)$ (Eq. (D.4)), we get from (D.30) the following Taylor expansion of the function $\phi_+(\widetilde{x},\widetilde{v})$ around its point $(\widetilde{x}_+,\widetilde{v}_+) \equiv \left(x_t\overline{\zeta}_+, v_0\overline{\eta}_+\right)$ of strict local maximum:

$$\phi_+(\widetilde{x},\widetilde{v}) = -\frac{1}{4\left(\sigma_{\widetilde{x}}^{(+)}\right)^2}\left(\widetilde{x}-x_t\sqrt{1+2\mu_+}\right)^2 - \frac{1}{4\left(\sigma_{\widetilde{v}}^{(+)}\right)^2}\left(\widetilde{v}-v_0\sqrt{1+2\mu_+}\right)^2 + \frac{1}{4}\left(\frac{x_t}{\sigma}\right)^2 \frac{1}{x_t v_0}\frac{1}{1+\frac{\hbar\omega_1}{mv_0^2}}\left[1+\mathcal{O}\left(\epsilon_+^2\right)\right]\left(\widetilde{x}-x_t\sqrt{1+2\mu_+}\right)\left(\widetilde{v}-v_0\sqrt{1+2\mu_+}\right) , \quad \text{(D.31)}$$

where the quantities $\sigma_{\widetilde{x}}^{(+)}$ and $\sigma_{\widetilde{v}}^{(+)}$ are given by

$$\sigma_{\widetilde{x}}^{(+)} = \left[1+\mathcal{O}\left(\epsilon_+^2\right)\right]\sigma\sqrt{1+\frac{\hbar\omega_1}{mv_0^2}} , \quad \text{(D.32)}$$

$$\sigma_{\widetilde{v}}^{(+)} = \left[1-\frac{\epsilon_+}{2}+\mathcal{O}\left(\epsilon_+^3\right)\right] v_0\frac{\lambda\!\!\!^{-}_0}{\sigma}\sqrt{\frac{1+\frac{\hbar\omega_1}{mv_0^2}}{1+2\frac{\hbar\omega_1}{mv_0^2}}} . \quad \text{(D.33)}$$

Therefore, combining these final results (D.31)-(D.33) with the expression (D.1) of $|h_+(\widetilde{x},\widetilde{v})|$, we see that this latter is peaked around the point

$$(\widetilde{x}_+,\widetilde{v}_+) = \left(x_t\sqrt{1+2\frac{\hbar\omega_1}{mv_0^2}} \quad , \quad v_0\sqrt{1+2\frac{\hbar\omega_1}{mv_0^2}}\right) , \quad \text{(D.34)}$$

the typical widths of the peak in the $\widetilde{x}$- and $\widetilde{v}$-directions being characterised by $\sigma_{\widetilde{x}}^{(+)}$ and $\sigma_{\widetilde{v}}^{(+)}$, respectively.

Appendix E

Gaussian aperture function

In this appendix we investigate the behaviour of the Husimi distribution (5.50) in the phase space, and determine its critical points. We first construct dimensionless variables ζ and η by rescaling the physical variables $\widetilde{x}$ and $\widetilde{v}$ with respect to x_t and v_0, respectively, and we take (similarly to (D.3))

$$\zeta \equiv \frac{\widetilde{x}}{x_t}\,, \tag{E.1a}$$

$$\eta \equiv \frac{\widetilde{v}}{v_0}\,. \tag{E.1b}$$

We define the function $\mathcal{H}(\zeta,\eta)$[1] by

$$\mathcal{H}(\zeta,\eta) \equiv \mathcal{H}^{(\mathrm{fr})}_{\mathrm{AFM}}(\widetilde{x},\widetilde{v},t)\,, \tag{E.2}$$

and we now study the critical points of this function of the two *dimensionless* variables ζ and η. Replacing in view of (E.1) the physical variables $\widetilde{x}$ and $\widetilde{v}$ by the dimensionless variables ζ and η in (5.50) hence yields for $\mathcal{H}(\zeta,\eta)$ the expression

$$\mathcal{H}(\zeta,\eta) = \frac{1}{2}\frac{(1+\eta)^2}{1+2\Gamma^2+\eta^2}\,\mathrm{e}^{\varphi_{\mathrm{g}}(\zeta,\eta)}\,, \tag{E.3}$$

where the function φ_{g} is defined, in view of (5.48), by

[1] We drop for convenience the dependence on the (fixed) final time t of this new function.

$$\varphi_{\rm g}(\zeta,\eta) \equiv \phi_{\rm g}(x_t\zeta, v_0\eta)$$
$$= \frac{1}{\sigma^2}\frac{1}{1+2\Gamma^2+\eta^2}\left\{\left[\eta\left(x_t\zeta - v_0 t\eta\right) + x_0 - 2T_0\Gamma^2 v_0\right]^2 - \frac{m^2\sigma^4 v_0^2}{4\hbar^2}\left(\eta^2-1\right)^2\right\}$$
$$- \frac{\left(x_t\zeta - v_0 t\eta\right)^2}{\sigma^2} - \frac{x_0^2}{\sigma^2} - \frac{2T_0^2\Gamma^2 v_0^2}{\sigma^2}\,. \quad \text{(E.4)}$$

We first study this function $\varphi_{\rm g}(\zeta,\eta)$.

E.1 Behaviour of $\varphi_{\rm g}(\zeta,\eta)$

Here we determine the critical points $\left(\overline{\zeta},\overline{\eta}\right)$ of the function $\varphi_{\rm g}(\zeta,\eta)$ defined by (E.4). These critical points are defined through the conditions

$$\left.\frac{\partial\varphi_{\rm g}}{\partial\zeta}\right|_{\left(\overline{\zeta},\overline{\eta}\right)} = 0 \qquad \text{and} \qquad \left.\frac{\partial\varphi_{\rm g}}{\partial\eta}\right|_{\left(\overline{\zeta},\overline{\eta}\right)} = 0\,. \quad \text{(E.5)}$$

Differentiating (E.4) with respect to ζ, we see that the first condition in (E.5) produces a linear equation in both $\overline{\zeta}$ and $\overline{\eta}$, readily solved to get

$$\overline{\zeta} = \frac{1}{1+2\Gamma^2}\left[1 + 2\Gamma^2\frac{v_0\left(t-T_0\right)}{x_t}\right]\overline{\eta}\,. \quad \text{(E.6)}$$

Differentiating now (E.4) with respect to η, we show that the second condition in (E.5) is, after substitution of the expression (E.6) of $\overline{\zeta}$, equivalent to the following polynomial equation in $\overline{\eta}$:

$$\left(\overline{\eta}-1\right)\overline{\eta}\left(\overline{\eta}+1\right)\left(\overline{\eta} - i\sqrt{3+4\Gamma^2}\right)\left(\overline{\eta} + i\sqrt{3+4\Gamma^2}\right) = 0\,, \quad \text{(E.7)}$$

from which we readily get the critical points of $\varphi_{\rm g}$. In particular, we see on this equation (E.7) that the variable η admits only 3 real critical values, given by

$$\overline{\eta} = -1, 0, 1\,, \quad \text{(E.8)}$$

and thus substituting these three values (E.8) into (E.6) yields the following three

real critical points of the function $\varphi_{\mathrm{g}}(\zeta,\eta)$:

$$\left(\overline{\zeta},\overline{\eta}\right)_0^{(\mathrm{g})} = \left(\overline{\zeta}_0^{(\mathrm{g})}\,,\,\overline{\eta}_0^{(\mathrm{g})}\right) = (0,0)\;, \tag{E.9a}$$

$$\left(\overline{\zeta},\overline{\eta}\right)_\pm^{(\mathrm{g})} = \left(\overline{\zeta}_\pm^{(\mathrm{g})}\,,\,\overline{\eta}_\pm^{(\mathrm{g})}\right) = \left(\pm\frac{1}{1+2\Gamma^2}\left[1+2\Gamma^2\frac{v_0\,(t-T_0)}{x_t}\right]\,,\,\pm 1\right)\;. \tag{E.9b}$$

Finally, in view of the correspondences (E.1) and (E.4), we hence see that the real critical points of the function $\phi_{\mathrm{g}}(\widetilde{x},\widetilde{v})$ of the physical variables $\widetilde{x}$ and $\widetilde{v}$ are

$$\left(\widetilde{x}_0^{(\mathrm{g})}\,,\,\widetilde{v}_0^{(\mathrm{g})}\right) = (0,0)\;, \tag{E.10a}$$

$$\left(\widetilde{x}_\pm^{(\mathrm{g})}\,,\,\widetilde{v}_\pm^{(\mathrm{g})}\right) = \left(\pm\frac{1}{1+2\Gamma^2}\left[x_t+2\Gamma^2 v_0\,(t-T_0)\right]\,,\,\pm v_0\right)\;, \tag{E.10b}$$

these expressions being valid for an *arbitrary* Γ.

We now use these results for the function φ_{g} to study the function $\mathcal{H}(\zeta,\eta)$, given by (E.3).

E.2 Behaviour of $\mathcal{H}(\zeta,\eta)$ for $\Gamma \ll 1$

We now analyse the structure of the function $\mathcal{H}(\zeta,\eta)$, and thus must determine its critical points $\left(\overline{\zeta},\overline{\eta}\right)$ defined by

$$\left.\frac{\partial\mathcal{H}}{\partial\zeta}\right|_{(\overline{\zeta},\overline{\eta})} = 0 \qquad \text{and} \qquad \left.\frac{\partial\mathcal{H}}{\partial\eta}\right|_{(\overline{\zeta},\overline{\eta})} = 0\,. \tag{E.11}$$

Differentiating (E.3) with respect to ζ, we see that the first condition in (E.11) is equivalent to

$$\overline{\eta} = -1 \quad \text{or} \quad \left.\frac{\partial\varphi_{\mathrm{g}}}{\partial\zeta}\right|_{(\overline{\zeta},\overline{\eta})} = 0\,, \tag{E.12}$$

and thus, if $\overline{\eta} \neq -1$, we know from (E.5) that $\overline{\zeta}$ is here still related to $\overline{\eta}$ according to (E.6), i.e.

$$\overline{\zeta} = \frac{1}{1+2\Gamma^2}\left[1+2\Gamma^2\frac{v_0\,(t-T_0)}{x_t}\right]\overline{\eta} \quad \text{if} \quad \overline{\eta} \neq -1\,. \tag{E.13}$$

Differentiating now (E.3) with respect to η yields

$$\frac{\partial \mathcal{H}}{\partial \eta} = \frac{1+\eta}{1+2\Gamma^2+\eta^2}\left[\frac{1+2\Gamma^2-\eta}{1+2\Gamma^2+\eta^2}+\frac{1+\eta}{2}\frac{\partial \varphi_{\mathrm{g}}}{\partial \eta}\right] \mathrm{e}^{\varphi_{\mathrm{g}}(\zeta,\eta)}\,, \tag{E.14}$$

and thus we see that the second condition in (E.11) is equivalent to

$$\overline{\eta} = -1 \quad \text{or} \quad \frac{1+2\Gamma^2-\overline{\eta}}{1+2\Gamma^2+\overline{\eta}^2}+\frac{1+\overline{\eta}}{2}\left.\frac{\partial \varphi_{\mathrm{g}}}{\partial \eta}\right|_{(\overline{\zeta},\overline{\eta})} = 0\,. \tag{E.15}$$

Therefore, we see that the value $\overline{\eta} = -1$ actually makes $\overline{\zeta}$ undefined, as in this case the two conditions (E.11) are actually equivalent. Therefore, we now suppose that $\overline{\eta} \neq -1$. In this case (E.13) is satisfied, and we show (in exactly the same way than we obtained (E.7)) that

$$\left.\frac{\partial \varphi_{\mathrm{g}}}{\partial \eta}\right|_{(\overline{\zeta},\overline{\eta})} = -\frac{m^2\sigma^2 v_0^2}{2\hbar^2}\,\frac{(\overline{\eta}-1)\,\overline{\eta}\,(\overline{\eta}+1)\left(\overline{\eta}-i\sqrt{3+4\Gamma^2}\right)\left(\overline{\eta}+i\sqrt{3+4\Gamma^2}\right)}{\left(1+2\Gamma^2+\overline{\eta}^2\right)^2}\,, \tag{E.16}$$

if $\overline{\eta} \neq -1$, and thus the second condition in (E.15) reads

$$\frac{m^2\sigma^2 v_0^2}{4\hbar^2}\,(\overline{\eta}-1)\,\overline{\eta}\,(\overline{\eta}+1)^2\left(\overline{\eta}-i\sqrt{3+4\Gamma^2}\right)\left(\overline{\eta}+i\sqrt{3+4\Gamma^2}\right) + \left(\overline{\eta}-1-2\Gamma^2\right)\left(\overline{\eta}^2+1+2\Gamma^2\right) = 0 \quad \text{if} \quad \overline{\eta} \neq -1\,. \tag{E.17}$$

Therefore, we here have a $6^{-\text{th}}$ order polynomial equation in $\overline{\eta}$ to solve to find the critical points of the function $\mathcal{H}(\zeta,\eta)$. It can be solved in the extreme case of a very wide Gaussian aperture function, as we briefly discuss.

We now assume that $\Gamma \ll 1$, so that the particle is "almost free". Indeed, we saw in section 5.1 that in the case where $\chi(\tau) = 1$ (i.e. for $\Gamma = 0$) the AFM Husimi distribution is merely the frozen Gaussian Husimi distribution $\mathcal{H}^{(\mathrm{fr})}_{\mathrm{free}}$ given by (5.18). Furthermore, we know that this latter admits the unique critical point (x_t, v_0). Therefore, we now replace Γ by the small quantity $\delta\Gamma$ in (E.17). A solution $\overline{\eta}$ of this equation should thus be of the form $\overline{\eta} = 1+\delta\eta$, where $\delta\eta$ is the first order correction due to the small quantity $\delta\Gamma$. Neglecting all the second order terms hence leads to a linear equation for $\delta\eta$, and solving it yields

$$\delta\eta = 2\frac{\hbar t_c}{m\sigma^2}\,\frac{\hbar t_c}{mx_0^2}\,\delta\Gamma^2\,. \tag{E.18}$$

In terms of the physical variables, we hence get from (E.18), in view of (E.1b),

$$\delta\widetilde{v} = 2v_0\frac{\hbar t_c}{m\sigma^2}\,\frac{\hbar t_c}{mx_0^2}\,\delta\Gamma^2\,. \tag{E.19}$$

Therefore, this result (E.19) suggests that Gaussian-like barriers described by aperture functions of the form (5.46) can induce a change of the expectation value of the velocity of the particle. It is however worth emphasising that the velocity shift $\delta\widetilde{v}$ predicted by (E.19) is very small in the semiclassical regime described by (5.1), as we have in this case $\hbar t_c/mx_0^2 \ll \hbar t_c/m\sigma^2 \ll 1$.

Appendix F

The integral $I_{\mathcal{C}}$

In this appendix we show that the integral $I_{\mathcal{C}}$, defined by (5.67c), vanishes under certain conditions. We recall that $I_{\mathcal{C}}$ is defined by (5.67c), that is

$$I_{\mathcal{C}} = \lim_{R\to+\infty}\left[iR\int_0^{\pi} d\theta\, \mathrm{e}^{i\theta} h\left(R\,\mathrm{e}^{i\theta}\right)\right] . \tag{F.1}$$

where in view of (5.58)-(5.59) the function h is given by

$$h(z) = \mathfrak{h}\chi(z)\mathrm{e}^{\frac{Z_0}{z-z_0}+\frac{Z_1}{z-z_1}} , \tag{F.2}$$

with

$$\mathfrak{h} = \frac{v_0+\widetilde{v}}{2\sigma\sqrt{\pi}}\mathrm{e}^{-\frac{1}{2}\left(\frac{\sigma}{\widetilde{\lambda}}\right)^2-\frac{1}{2}\left(\frac{\sigma}{\lambda_0}\right)^2} . \tag{F.3}$$

Assuming we can interchange the limit and the integral in (F.1), we get

$$I_{\mathcal{C}} = \int_0^{\pi} d\theta \lim_{R\to+\infty}\left[iR\,\mathrm{e}^{i\theta} h\left(R\,\mathrm{e}^{i\theta}\right)\right] , \tag{F.4}$$

and thus, substituting the expression (F.2) of $h(z)$ into (F.4) yields

$$I_{\mathcal{C}} = i\mathfrak{h}\int_0^{\pi} d\theta \lim_{R\to+\infty}\left[R\,\mathrm{e}^{i\theta}\chi\left(R\,\mathrm{e}^{i\theta}\right)\exp\left(\frac{Z_0}{R\,\mathrm{e}^{i\theta}-z_0}+\frac{Z_1}{R\,\mathrm{e}^{i\theta}-z_1}\right)\right] . \tag{F.5}$$

We now exploit the limit $R\to+\infty$ to write in section F.1 an expansion of the integrand of (F.5). Finally, we show in section F.2 that $I_{\mathcal{C}}$ indeed vanishes if the aperture function $\chi(z)$ satisfies a particular criterion.

F.1 Taylor expansion

First note that we can write

$$\frac{Z_0}{z-z_0} = \frac{Z_0}{z}\left(1-\frac{z_0}{z}\right)^{-1} = \frac{Z_0}{z_0}\frac{z_0}{z}\left(1-\frac{z_0}{z}\right)^{-1},$$

that is, for $z = R\,\mathrm{e}^{i\theta}$,

$$\frac{Z_0}{R\,\mathrm{e}^{i\theta}-z_0} = \frac{Z_0}{z_0}\frac{z_0}{R\,\mathrm{e}^{i\theta}}\left(1-\frac{z_0}{R\,\mathrm{e}^{i\theta}}\right)^{-1}, \tag{F.6}$$

as well as

$$\frac{Z_1}{z-z_1} = \frac{Z_1}{z}\left(1-\frac{z_1}{z}\right)^{-1} = \frac{Z_1}{z_1}\frac{z_1}{z}\left(1-\frac{z_1}{z}\right)^{-1},$$

that is, for $z = R\,\mathrm{e}^{i\theta}$,

$$\frac{Z_1}{R\,\mathrm{e}^{i\theta}-z_1} = \frac{Z_1}{z_1}\frac{z_1}{R\,\mathrm{e}^{i\theta}}\left(1-\frac{z_1}{R\,\mathrm{e}^{i\theta}}\right)^{-1}. \tag{F.7}$$

In view of the limit $R \to +\infty$[1], we can thus write the Taylor expansions

$$\left(1-\frac{z_0}{R\,\mathrm{e}^{i\theta}}\right)^{-1} = 1 + \frac{z_0}{R\,\mathrm{e}^{i\theta}} + \mathcal{O}\left[\left(\frac{z_0}{R\,\mathrm{e}^{i\theta}}\right)^2\right],$$

that is

$$\frac{z_0}{R\,\mathrm{e}^{i\theta}}\left(1-\frac{z_0}{R\,\mathrm{e}^{i\theta}}\right)^{-1} = \frac{z_0}{R\,\mathrm{e}^{i\theta}} + \mathcal{O}\left[\left(\frac{z_0}{R\,\mathrm{e}^{i\theta}}\right)^2\right]. \tag{F.8}$$

Combining (F.6) with (F.8) we hence get

$$\frac{Z_0}{R\,\mathrm{e}^{i\theta}-z_0} = \frac{Z_0}{R\,\mathrm{e}^{i\theta}} + \mathcal{O}\left[\left(\frac{Z_0}{R\,\mathrm{e}^{i\theta}}\right)^2\right]. \tag{F.9}$$

Similarly, we have

[1] To be more precise, we consider the limit where $|z_0/R|, |z_1/R| \ll 1$

$$\left(1-\frac{z_1}{R\,\mathrm{e}^{i\theta}}\right)^{-1}=1+\frac{z_1}{R\,\mathrm{e}^{i\theta}}+\mathcal{O}\left[\left(\frac{z_1}{R\,\mathrm{e}^{i\theta}}\right)^2\right],$$

that is

$$\frac{z_1}{R\,\mathrm{e}^{i\theta}}\left(1-\frac{z_1}{R\,\mathrm{e}^{i\theta}}\right)^{-1}=\frac{z_1}{R\,\mathrm{e}^{i\theta}}+\mathcal{O}\left[\left(\frac{z_1}{R\,\mathrm{e}^{i\theta}}\right)^2\right]. \tag{F.10}$$

Combining (F.7) with (F.10) we hence get

$$\frac{Z_1}{R\,\mathrm{e}^{i\theta}-z_1}=\frac{Z_1}{R\,\mathrm{e}^{i\theta}}+\mathcal{O}\left[\left(\frac{Z_1}{R\,\mathrm{e}^{i\theta}}\right)^2\right]. \tag{F.11}$$

Now, in view of (F.9) we have

$$\exp\left(\frac{Z_0}{R\,\mathrm{e}^{i\theta}-z_0}\right)=\sum_{n=0}^{+\infty}\frac{1}{n!}\left\{\frac{Z_0}{R\,\mathrm{e}^{i\theta}}+\mathcal{O}\left[\left(\frac{Z_0}{R\,\mathrm{e}^{i\theta}}\right)^2\right]\right\}^n,$$

and thus, since

$$\left\{\frac{Z_0}{R\,\mathrm{e}^{i\theta}}+\mathcal{O}\left[\left(\frac{Z_0}{R\,\mathrm{e}^{i\theta}}\right)^2\right]\right\}^n=\mathcal{O}\left[\left(\frac{Z_0}{R\,\mathrm{e}^{i\theta}}\right)^n\right]\quad,\quad\forall n\in\mathbb{N}^*,$$

we have

$$\exp\left(\frac{Z_0}{R\,\mathrm{e}^{i\theta}-z_0}\right)=1+\frac{Z_0}{R\,\mathrm{e}^{i\theta}}+\mathcal{O}\left[\left(\frac{Z_0}{R\,\mathrm{e}^{i\theta}}\right)^2\right]. \tag{F.12}$$

Similarly, in view of (F.11) we have

$$\exp\left(\frac{Z_1}{R\,\mathrm{e}^{i\theta}-z_1}\right)=\sum_{n=0}^{+\infty}\frac{1}{n!}\left\{\frac{Z_1}{R\,\mathrm{e}^{i\theta}}+\mathcal{O}\left[\left(\frac{Z_1}{R\,\mathrm{e}^{i\theta}}\right)^2\right]\right\}^n,$$

and thus, since

$$\left\{\frac{Z_1}{R\,\mathrm{e}^{i\theta}}+\mathcal{O}\left[\left(\frac{Z_1}{R\,\mathrm{e}^{i\theta}}\right)^2\right]\right\}^n=\mathcal{O}\left[\left(\frac{Z_1}{R\,\mathrm{e}^{i\theta}}\right)^n\right]\quad,\quad\forall n\in\mathbb{N}^*\,,$$

we have

$$\exp\left(\frac{Z_1}{R\,\mathrm{e}^{i\theta}-z_1}\right)=1+\frac{Z_1}{R\,\mathrm{e}^{i\theta}}+\mathcal{O}\left[\left(\frac{Z_1}{R\,\mathrm{e}^{i\theta}}\right)^2\right]\,. \tag{F.13}$$

Finally, combining (F.12) and (F.13) we get

$$\exp\left(\frac{Z_0}{R\,\mathrm{e}^{i\theta}-z_0}+\frac{Z_1}{R\,\mathrm{e}^{i\theta}-z_1}\right)=\left\{1+\frac{Z_0}{R\,\mathrm{e}^{i\theta}}+\mathcal{O}\left[\left(\frac{Z_0}{R\,\mathrm{e}^{i\theta}}\right)^2\right]\right\}\times\left\{1+\frac{Z_1}{R\,\mathrm{e}^{i\theta}}+\mathcal{O}\left[\left(\frac{Z_1}{R\,\mathrm{e}^{i\theta}}\right)^2\right]\right\}\,.$$

Therefore, since by definition of the $\mathcal{O}$ notation we can write

$$\mathcal{O}\left[\left(\frac{Z_0}{R\,\mathrm{e}^{i\theta}}\right)^2\right]=\mathcal{O}\left[\left(\frac{Z_1}{R\,\mathrm{e}^{i\theta}}\right)^2\right]=\mathcal{O}\left[\frac{Z_0Z_1}{(R\,\mathrm{e}^{i\theta})^2}\right]=\mathcal{O}\left[\left(\frac{Z_0+Z_1}{R\,\mathrm{e}^{i\theta}}\right)^2\right]\,, \tag{F.14}$$

we see that we have the following Taylor expansion of the exponential involved in (F.5):

$$\exp\left(\frac{Z_0}{R\,\mathrm{e}^{i\theta}-z_0}+\frac{Z_1}{R\,\mathrm{e}^{i\theta}-z_1}\right)=1+\frac{Z_0+Z_1}{R\,\mathrm{e}^{i\theta}}+\mathcal{O}\left[\left(\frac{Z_0+Z_1}{R\,\mathrm{e}^{i\theta}}\right)^2\right]\,, \tag{F.15}$$

which we now use to determine the restrictions that need to be imposed on the aperture function χ in order to make the integral $I_{\mathcal{C}}$ vanish.

F.2 Criterion on $\chi(z)$

Substituting the expansion (F.15) into the expression (F.5) of $I_{\mathcal{C}}$ yields

$$I_{\mathcal{C}}=i\mathfrak{h}\int_0^\pi d\theta\lim_{R\to+\infty}\left\{R\,\mathrm{e}^{i\theta}\chi\left(R\,\mathrm{e}^{i\theta}\right)\left(1+\frac{Z_0+Z_1}{R\,\mathrm{e}^{i\theta}}+\mathcal{O}\left[\left(\frac{Z_0+Z_1}{R\,\mathrm{e}^{i\theta}}\right)^2\right]\right)\right\}\,.$$

and thus we have

$$I_{\mathcal{C}} = i\mathfrak{h} \int_0^{\pi} d\theta \lim_{R\to+\infty} \left[R\,\mathrm{e}^{i\theta} \chi\left(R\,\mathrm{e}^{i\theta}\right) + (Z_0 + Z_1)\,\chi\left(R\,\mathrm{e}^{i\theta}\right) + \chi\left(R\,\mathrm{e}^{i\theta}\right) \mathcal{O}\left(\frac{Z_0+Z_1}{R\,\mathrm{e}^{i\theta}}\right)\right] . \quad \text{(F.16)}$$

Therefore, we can readily see on (F.16) that a *sufficient condition* for this integral $I_{\mathcal{C}}$ to vanish is given by

$$\lim_{R\to+\infty} \left[R\,\mathrm{e}^{i\theta} \chi\left(R\,\mathrm{e}^{i\theta}\right)\right] = 0\,, \quad \text{(F.17)}$$

or alternatively, using the $\mathcal{o}$ notation,

$$\chi\left(R\,\mathrm{e}^{i\theta}\right) = \mathcal{o}\left(\frac{1}{R\,\mathrm{e}^{i\theta}}\right) . \quad \text{(F.18)}$$

Indeed, a direct consequence of (F.17) is that we also have

$$\lim_{R\to+\infty} \left[\chi\left(R\,\mathrm{e}^{i\theta}\right)\right] = 0\,, \quad \text{(F.19)}$$

as well as

$$\lim_{R\to+\infty} \left[\chi\left(R\,\mathrm{e}^{i\theta}\right) \mathcal{O}\left(\frac{Z_0+Z_1}{R\,\mathrm{e}^{i\theta}}\right)\right] = 0\,, \quad \text{(F.20)}$$

and thus combining (F.16) with (F.17), (F.19) and (F.20) yields

$$I_{\mathcal{C}} = 0\,. \quad \text{(F.21)}$$

Therefore, the integral $I_{\mathcal{C}}$ indeed vanishes *under the condition that the aperture function* χ *satisfies* (F.17) (or, equivalently, (F.18)).

Appendix G

Upper bound for $\left|I^{(-)} + I^{(+)}\right|$

In this appendix we derive a relevant upper bound for $\left|I^{(-)} + I^{(+)}\right|$. first note that from the triangle inequality we have

$$\left|I^{(-)} + I^{(+)}\right| \leqslant \left|I^{(-)}\right| + \left|I^{(+)}\right| , \tag{G.1}$$

where, in view of the definitions (5.67a) and (5.67b) of $I^{(-)}$ and $I^{(+)}$, respectively, we have, again from the triangle inequality,

$$\left|I^{(-)}\right| \leqslant \int_{-\infty}^{0} d\tau \ |h(\tau)| \tag{G.2}$$

and

$$\left|I^{(+)}\right| \leqslant \int_{t}^{+\infty} d\tau \ |h(\tau)| \ . \tag{G.3}$$

We first write in section G.1 an upper bound for $|h(\tau)|$. We then derive upper bounds for $\left|I^{(-)}\right|$ and $\left|I^{(+)}\right|$ in sections G.2 and G.3, respectively. Finally, we give in section G.4 the relevant upper bound of $\left|I^{(-)} + I^{(+)}\right|$. Some technical details are deferred to the last two sections, sections G.5 and G.6.

G.1 Upper bound for $|h(\tau)|$

We first recall that in view of (5.58)-(5.59) and the expression (5.13) of ϕ the function h is given by

$$h(\tau)=\frac{v_0+\widetilde{v}}{2\sigma\sqrt{\pi}}\chi(\tau)\mathrm{e}^{\phi(\tau)}\,, \tag{G.4}$$

Taking the modulus of (G.4) hence yields

$$|h(\tau)|=\frac{v_0+\widetilde{v}}{2\sigma\sqrt{\pi}}\,|\chi(\tau)|\left|\mathrm{e}^{\phi(\tau)}\right|\,, \tag{G.5}$$

as we are only interested in this region of the phase space detailed by (5.19), and hence only consider positive values of $\widetilde{v}$. Note that

$$\left|\mathrm{e}^{\phi(\tau)}\right|=\mathrm{e}^{\mathrm{Re}[\phi(\tau)]}\,, \tag{G.6}$$

with, in view of the definition (5.13) of ϕ,

$$\mathrm{Re}\left[\phi(\tau)\right]=-\mathrm{Re}\left(\alpha_{t-\tau}\right)\left[\widetilde{x}-\widetilde{v}(t-\tau)\right]^2-\mathrm{Re}\left(\alpha_\tau\right)\left(x_0+v_0\tau\right)^2\,, \tag{G.7}$$

Therefore, combining (G.6) with (G.7) and the definition (2.18) of α_τ, we write

$$\left|\mathrm{e}^{\phi(\tau)}\right|=f_{\widetilde{x},\widetilde{v}}(\tau)\,g_{x_0,v_0}(\tau)\,, \tag{G.8}$$

where the functions $f_{\widetilde{x},\widetilde{v}}$ and g_{x_0,v_0} are defined by

$$f_{\widetilde{x},\widetilde{v}}(\tau)\equiv\exp\left\{-\frac{\alpha_0\left[\widetilde{x}-\widetilde{v}(t-\tau)\right]^2}{1+\frac{4\hbar^2\alpha_0^2}{m^2}(t-\tau)^2}\right\} \tag{G.9}$$

and

$$g_{x_0,v_0}(\tau)\equiv\exp\left[-\frac{\alpha_0\left(x_0+v_0\tau\right)^2}{1+\frac{4\hbar^2\alpha_0^2}{m^2}\tau^2}\right]\,. \tag{G.10}$$

A detailed study of these two functions can be found in the last two sections, G.5 and G.6, of this appendix. Finally, combining (G.5) with (G.8), we get the following upper bound for the modulus of $h_{\mathrm{fr}}(\tau)$:

$$|h(\tau)| = \frac{v_0+\widetilde{v}}{2\sigma\sqrt{\pi}}\,|\chi(\tau)|\,f_{\widetilde{x},\widetilde{v}}(\tau)\,g_{x_0,v_0}(\tau)\,. \tag{G.11}$$

The expression (G.11) is our starting point for deriving in sections G.2 and G.3 upper bounds of $\left|I^{(-)}\right|$ and $\left|I^{(+)}\right|$, respectively.

G.2 Upper bound for $\left|I^{(-)}\right|$

First note that in view of (G.2) we have throughout this section

$$\tau \leqslant 0\,. \tag{G.12}$$

We now use the results of the sections G.5 and G.6 to obtain upper bounds of $f_{\widetilde{x},\widetilde{v}}(\tau)$ and $g_{x_0,v_0}(\tau)$ for $\tau \in \mathbb{R}_-$.

In view of (G.45), the function $f_{\widetilde{x},\widetilde{v}}(\tau)$ admits the two stationary points

$$\begin{cases} \tau^{(1)}_{\widetilde{x},\widetilde{v}} = t-\widetilde{t} \\ \tau^{(2)}_{\widetilde{x},\widetilde{v}} = t+\frac{m^2}{4\hbar^2\alpha_0^2\widetilde{t}} \end{cases}, \tag{G.13}$$

where $\tau^{(1)}_{\widetilde{x},\widetilde{v}}$ $\left(\tau^{(2)}_{\widetilde{x},\widetilde{v}}\right)$ corresponds to a local maximum (minimum) of $f_{\widetilde{x},\widetilde{v}}(\tau)$. Since we have both $t>0$ and $\widetilde{t}>0$, then $\tau^{(2)}_{\widetilde{x},\widetilde{v}}>0$. However, note that $\tau^{(1)}_{\widetilde{x},\widetilde{v}}$ can *a priori* be either positive or negative, and thus, because it is a local maximum of $f_{\widetilde{x},\widetilde{v}}(\tau)$, we can write

$$f_{\widetilde{x},\widetilde{v}}(\tau) \leqslant f_{\widetilde{x},\widetilde{v}}\left[\min\left(0\,,\tau^{(1)}_{\widetilde{x},\widetilde{v}}\right)\right] \quad,\ \forall\tau\in\mathbb{R}_-\,, \tag{G.14}$$

where

$$\min(\xi_1\,,\xi_2) \equiv \begin{cases} \xi_1 & \text{if} \quad \xi_1<\xi_2 \\ \xi_2 & \text{if} \quad \xi_2<\xi_1 \end{cases} \tag{G.15}$$

denotes the minimum function. We now assume for concreteness that the observation time t actually satisfies the condition

$$t>\widetilde{t}\,, \tag{G.16}$$

so that the stationary point $\tau^{(1)}_{\widetilde{x},\widetilde{v}}$ assumes a definite sign, namely

$$\tau^{(1)}_{\widetilde{x},\widetilde{v}} > 0\,, \tag{G.17}$$

and thus we have

$$\min\left(0\,,\tau^{(1)}_{\widetilde{x},\widetilde{v}}\right) = 0\,. \tag{G.18}$$

Combining (G.14) and (G.18) we get

$$f_{\widetilde{x},\widetilde{v}}(\tau) \leqslant f_{\widetilde{x},\widetilde{v}}\,(0) \quad , \quad \forall \tau \in \mathbb{R}_-\,,$$

and thus, in view of the definitions (G.9) and (2.13) of $f_{\widetilde{x},\widetilde{v}}(\tau)$ and α_0, respectively, we have, *under the assumption* (G.16) and in the semiclassical regime described by the conditions (5.1),

$$f_{\widetilde{x},\widetilde{v}}(\tau) \leqslant \exp\left[-\frac{1}{2}\left(\frac{\widetilde{x}-\widetilde{v}t}{\sigma}\right)^2\right] \quad , \quad \forall \tau \in \mathbb{R}_-\,. \tag{G.19}$$

Now, from (G.57) we know that the function $g_{x_0,\,v_0}(\tau)$ admits the two stationary points

$$\begin{cases} \tau^{(1)}_{x_0,\,v_0} = -\frac{m^2}{4\hbar^2\alpha_0^2 t_c} \\ \tau^{(2)}_{x_0,\,v_0} = t_c \end{cases}\,, \tag{G.20}$$

where $\tau^{(1)}_{x_0,\,v_0}$ $\left(\tau^{(2)}_{x_0,\,v_0}\right)$ corresponds to a local minimum (maximum) of $g_{x_0,\,v_0}(\tau)$. By assumption, the classical time t_c is positive, and thus we have $\tau^{(1)}_{x_0,\,v_0} < 0$ and $\tau^{(2)}_{x_0,\,v_0} > 0$. Therefore, since $\tau^{(1)}_{x_0,\,v_0}$ is a local minimum of $g_{x_0,\,v_0}(\tau)$ we can write

$$g_{x_0,\,v_0}(\tau) \leqslant \max\left[\lim_{\tau\to-\infty} g_{x_0,\,v_0}(\tau)\,,g_{x_0,\,v_0}(0)\right] \quad , \quad \forall \tau \in \mathbb{R}_-\,, \tag{G.21}$$

where

$$\max(\xi_1\,,\xi_2) \equiv \begin{cases} \xi_1 \quad \text{if} \quad \xi_1 > \xi_2 \\ \xi_2 \quad \text{if} \quad \xi_2 > \xi_1 \end{cases} \tag{G.22}$$

denotes the maximum function. In view of the definitions (G.10) and (2.13) of $g_{x_0,\,v_0}(\tau)$ and α_0, respectively, we have

$$g_{x_0,\,v_0}(0)=\mathrm{e}^{-\frac{1}{2}\left(\frac{x_0}{\sigma}\right)^2}\,, \tag{G.23}$$

and also

$$\lim_{\tau\to-\infty} g_{x_0,\,v_0}(\tau)=\lim_{\tau\to-\infty}\exp\left(-\frac{\alpha_0 v_0^2\tau^2}{\frac{4\hbar^2\alpha_0^2}{m^2}\tau^2}\right)\,,$$

that is,

$$\lim_{\tau\to-\infty} g_{x_0,\,v_0}(\tau)=\mathrm{e}^{-\frac{1}{2}\left(\frac{\sigma}{\lambda_0}\right)^2}\,. \tag{G.24}$$

and thus, combining (G.21) with (G.23) and (G.24) we get

$$g_{x_0,\,v_0}(\tau)\leqslant\max\left[\mathrm{e}^{-\frac{1}{2}\left(\frac{\sigma}{\lambda_0}\right)^2},\mathrm{e}^{-\frac{1}{2}\left(\frac{x_0}{\sigma}\right)^2}\right]\quad,\quad\forall\tau\in\mathbb{R}_-\,. \tag{G.25}$$

Therefore, substituting the results (G.19) and (G.25) into (G.11) yields for $|h(\tau)|$, $\tau\in\mathbb{R}_-$,

$$|h(\tau)|\leqslant\frac{v_0+\widetilde{v}}{2\sigma\sqrt{\pi}}\exp\left[-\frac{1}{2}\left(\frac{\widetilde{x}-\widetilde{v}t}{\sigma}\right)^2\right]\max\left[\mathrm{e}^{-\frac{1}{2}\left(\frac{\sigma}{\lambda_0}\right)^2},\mathrm{e}^{-\frac{1}{2}\left(\frac{x_0}{\sigma}\right)^2}\right]|\chi(\tau)|\quad,\quad\forall\tau\in\mathbb{R}_-\,. \tag{G.26}$$

Finally, combining the expression (G.26) with the inequality (G.2), we get the following upper bound for $\left|I^{(-)}\right|$:

$$\left|I^{(-)}\right|\leqslant\frac{v_0+\widetilde{v}}{2\sigma\sqrt{\pi}}\exp\left[-\frac{1}{2}\left(\frac{\widetilde{x}-\widetilde{v}t}{\sigma}\right)^2\right]\max\left[\mathrm{e}^{-\frac{1}{2}\left(\frac{\sigma}{\lambda_0}\right)^2},\mathrm{e}^{-\frac{1}{2}\left(\frac{x_0}{\sigma}\right)^2}\right]\int_{-\infty}^{0}d\tau\;|\chi(\tau)|\,. \tag{G.27}$$

G.3 Upper bound for $\left|I^{(+)}\right|$

Noting now that in view of (G.3) we have throughout this section

$$\tau\geqslant t\,, \tag{G.28}$$

we use the results of the sections G.5 and G.6 to obtain upper bounds of $f_{\widetilde{x},\widetilde{v}}(\tau)$ and $g_{x_0,v_0}(\tau)$ for $\tau\in[t,+\infty]$.

In view of (G.46), we know that the stationary points $\tau^{(1)}_{\widetilde{x},\widetilde{v}}$ and $\tau^{(2)}_{\widetilde{x},\widetilde{v}}$ of $f_{\widetilde{x},\widetilde{v}}(\tau)$ satisfy

$$\tau^{(1)}_{\widetilde{x},\widetilde{v}}<t<\tau^{(2)}_{\widetilde{x},\widetilde{v}}\,, \tag{G.29}$$

and thus, since $\tau^{(2)}_{\widetilde{x},\widetilde{v}}$ is a local minimum of $f_{\widetilde{x},\widetilde{v}}(\tau)$ we can write

$$f_{\widetilde{x},\widetilde{v}}(\tau)\leqslant\max\left[f_{\widetilde{x},\widetilde{v}}(t)\,,\lim_{\tau\to+\infty}f_{\widetilde{x},\widetilde{v}}(\tau)\right]\quad,\quad\forall\tau\in[t,+\infty]\,. \tag{G.30}$$

In view of the definitions (G.9) and (2.13) of $f_{\widetilde{x},\widetilde{v}}(\tau)$ and α_0, respectively, we have

$$f_{\widetilde{x},\widetilde{v}}(t)=\mathrm{e}^{-\frac{1}{2}\left(\frac{\widetilde{x}}{\sigma}\right)^2}\,, \tag{G.31}$$

and also

$$\lim_{\tau\to+\infty}f_{\widetilde{x},\widetilde{v}}(\tau)=\lim_{\tau\to+\infty}\exp\left(-\frac{\alpha_0\widetilde{v}^2\tau^2}{\frac{4\hbar^2\alpha_0^2}{m^2}\tau^2}\right)\,,$$

that is,

$$\lim_{\tau\to+\infty}f_{\widetilde{x},\widetilde{v}}(\tau)=\mathrm{e}^{-\frac{1}{2}\left(\frac{\sigma}{\lambda}\right)^2}\,. \tag{G.32}$$

and thus, combining (G.30) with (G.31) and (G.32) we get

$$f_{\widetilde{x},\widetilde{v}}(\tau)\leqslant\max\left[\mathrm{e}^{-\frac{1}{2}\left(\frac{\widetilde{x}}{\sigma}\right)^2},\mathrm{e}^{-\frac{1}{2}\left(\frac{\sigma}{\lambda}\right)^2}\right]\quad,\quad\forall\tau\in[t,+\infty]\,. \tag{G.33}$$

Now, from (G.58) we know that the stationary points $\tau^{(1)}_{x_0,v_0}$ and $\tau^{(2)}_{x_0,v_0}$ of $g_{x_0,v_0}(\tau)$ satisfy

$$\tau^{(1)}_{x_0,v_0}<0<\tau^{(2)}_{x_0,v_0}\,. \tag{G.34}$$

Furthermore, since $\tau^{(2)}_{x_0,v_0}=t_c$ we actually have in view of the condition (3.44) that

$$\tau^{(2)}_{x_0,\,v_0} < t\,, \tag{G.35}$$

and thus, because $\tau^{(2)}_{x_0,\,v_0}$ is a local maximum of $g_{x_0,\,v_0}(\tau)$ we can write

$$g_{x_0,\,v_0}(\tau) \leqslant g_{x_0,\,v_0}(t) \quad , \quad \forall \tau \in [t,+\infty]\,, \tag{G.36}$$

Therefore, in view of the definitions (G.10) and (2.13) of $g_{x_0,\,v_0}(\tau)$ and α_0, respectively, we have

$$g_{x_0,\,v_0}(\tau) \leqslant \exp\left[-\frac{1}{2}\left(\frac{x_0+v_0t}{\sigma}\right)^2\right] \quad , \quad \forall \tau \in [t,+\infty]\,. \tag{G.37}$$

Therefore, substituting the results (G.33) and (G.37) into (G.11) yields for $|h(\tau)|$, $\tau \in [t,+\infty]$,

$$|h(\tau)| \leqslant \frac{v_0+\widetilde{v}}{2\sigma\sqrt{\pi}} \exp\left[-\frac{1}{2}\left(\frac{x_0+v_0t}{\sigma}\right)^2\right] \max\left[\mathrm{e}^{-\frac{1}{2}\left(\frac{\widetilde{x}}{\sigma}\right)^2}, \mathrm{e}^{-\frac{1}{2}\left(\frac{\sigma}{\chi}\right)^2}\right] |\chi(\tau)|\,, \tag{G.38}$$

for any $\tau \in [t,+\infty]$. Finally, combining the expression (G.38) with the inequality (G.3), we get the following upper bound for $\left|I^{(+)}\right|$:

$$\left|I^{(+)}\right| \leqslant \frac{v_0+\widetilde{v}}{2\sigma\sqrt{\pi}} \exp\left[-\frac{1}{2}\left(\frac{x_0+v_0t}{\sigma}\right)^2\right] \max\left[\mathrm{e}^{-\frac{1}{2}\left(\frac{\widetilde{x}}{\sigma}\right)^2}, \mathrm{e}^{-\frac{1}{2}\left(\frac{\sigma}{\chi}\right)^2}\right] \int_t^{+\infty} d\tau\ |\chi(\tau)|\,. \tag{G.39}$$

G.4 Upper bound for $\left|I^{(-)}+I^{(+)}\right|$

In this section we use the results obtained in the two previous sections, sections G.2 and G.3, to obtain an relevant upper bound for $\left|I^{(-)}+I^{(+)}\right|$. Substituting the upper bounds (G.27) and (G.39) obtained for $\left|I^{(-)}\right|$ and $\left|I^{(+)}\right|$, respectively, into (G.1), we get the following global upper bound for $\left|I^{(-)}+I^{(+)}\right|$ (remember the definition (4.4) of x_t):

$$\left|I^{(-)}+I^{(+)}\right| \leqslant \frac{v_0+\widetilde{v}}{2\sigma\sqrt{\pi}}\left\{\exp\left[-\frac{1}{2}\left(\frac{\widetilde{x}-\widetilde{v}t}{\sigma}\right)^2\right]\max\left[\mathrm{e}^{-\frac{1}{2}\left(\frac{\sigma}{\lambda_0}\right)^2},\mathrm{e}^{-\frac{1}{2}\left(\frac{x_0}{\sigma}\right)^2}\right]\right.$$
$$\left.\times\int_{-\infty}^{0}d\tau\ |\chi(\tau)|+\exp\left[-\frac{1}{2}\left(\frac{x_t}{\sigma}\right)^2\right]\max\left[\mathrm{e}^{-\frac{1}{2}\left(\frac{\widetilde{x}}{\sigma}\right)^2},\mathrm{e}^{-\frac{1}{2}\left(\frac{\sigma}{\lambda}\right)^2}\right]\int_{t}^{+\infty}d\tau\ |\chi(\tau)|\right\}. \tag{G.40}$$

This result (G.40) has been obtained by assuming that the observation time t satisfies

$$t>\widetilde{t}\,. \tag{G.41}$$

The actual values of the integrals involved in the right hand side of (G.40) must then be computed, or estimated, for any particular example of aperture function $\chi(\tau)$.

G.5 Behaviour of $f_{\widetilde{x},\widetilde{v}}$

In these last two sections we study the general behaviour of the two functions $f_{\widetilde{x},\widetilde{v}}(\tau)$ and $g_{x_0,v_0}(\tau)$ introduced in section G.1. More explicitly, we want to determine their senses of variation for $\tau\in\mathbb{R}$. This is indeed a simple approach to find upper bounds for these two functions.

We begin with the function $f_{\widetilde{x},\widetilde{v}}(\tau)$, which we recall is defined by (G.9), i.e.

$$f_{\widetilde{x},\widetilde{v}}(\tau)\equiv\exp\left\{-\frac{\alpha_0\left[\widetilde{x}-\widetilde{v}(t-\tau)\right]^2}{1+\frac{4\hbar^2\alpha_0^2}{m^2}(t-\tau)^2}\right\}. \tag{G.42}$$

The first step is here to find the stationary points of $f_{\widetilde{x},\widetilde{v}}$, corresponding to the particular value of τ for which the derivative $f'_{\widetilde{x},\widetilde{v}}\equiv df_{\widetilde{x},\widetilde{v}}/d\tau$ vanishes. Differentiating (G.42) with respect to τ yields

$$f'_{\widetilde{x},\widetilde{v}}(\tau)=\left[\widetilde{v}\tau-(\widetilde{v}t-\widetilde{x})\right]\left[\frac{4\hbar^2\alpha_0^2}{m^2}\,\widetilde{x}\tau-\left(\frac{4\hbar^2\alpha_0^2}{m^2}\,\widetilde{x}t+\widetilde{v}\right)\right]\frac{2\alpha_0 f_{\widetilde{x},\widetilde{v}}(\tau)}{\left[1+\frac{4\hbar^2\alpha_0^2}{m^2}(t-\tau)^2\right]^2}. \tag{G.43}$$

Since $\alpha_0\neq0$ by assumption, and $f_{\widetilde{x},\widetilde{v}}(\tau)\neq0$, $\forall\tau\in\mathbb{R}$, we can readily see on (G.43) that the derivative $f'_{\widetilde{x},\widetilde{v}}(\tau)$ admits two real roots, which me denote $\tau^{(1)}_{\widetilde{x},\widetilde{v}}$ and $\tau^{(2)}_{\widetilde{x},\widetilde{v}}$, given by

$$\begin{cases} \tau^{(1)}_{\widetilde{x},\widetilde{v}} = t - \frac{\widetilde{x}}{\widetilde{v}} \\ \tau^{(2)}_{\widetilde{x},\widetilde{v}} = t + \frac{m^2}{4\hbar^2\alpha_0^2}\frac{\widetilde{v}}{\widetilde{x}} \end{cases} . \tag{G.44}$$

Substituting the definition (5.8) of $\widetilde{t}$ in (G.44) we get

$$\begin{cases} \tau^{(1)}_{\widetilde{x},\widetilde{v}} = t - \widetilde{t} \\ \tau^{(2)}_{\widetilde{x},\widetilde{v}} = t + \frac{m^2}{4\hbar^2\alpha_0^2\widetilde{t}} \end{cases} . \tag{G.45}$$

Remember that by assumption $\widetilde{x}$, $\widetilde{v} > 0$, and hence $\widetilde{t} > 0$. Therefore, a direct consequence of their expressions (G.45) is that the two stationary points $\tau^{(1)}_{\widetilde{x},\widetilde{v}}$ and $\tau^{(2)}_{\widetilde{x},\widetilde{v}}$ satisfy

$$\tau^{(1)}_{\widetilde{x},\widetilde{v}} < t < \tau^{(2)}_{\widetilde{x},\widetilde{v}} . \tag{G.46}$$

We now study the sign of $f'_{\widetilde{x},\widetilde{v}}(\tau)$ for $\tau \in \left]\tau^{(1)}_{\widetilde{x},\widetilde{v}}, \tau^{(2)}_{\widetilde{x},\widetilde{v}}\right[$. In view of (G.46), and because $\tau^{(1)}_{\widetilde{x},\widetilde{v}}$ and $\tau^{(2)}_{\widetilde{x},\widetilde{v}}$ are by construction the two only roots of $f'_{\widetilde{x},\widetilde{v}}$, this is equivalent to merely studying the sign of $f'_{\widetilde{x},\widetilde{v}}(t)$. From (G.43) and (G.42) we get

$$f'_{\widetilde{x},\widetilde{v}}(t) = -2\alpha_0\widetilde{x}\widetilde{v}\,\mathrm{e}^{-\alpha_0\widetilde{x}^2} , \tag{G.47}$$

and thus, since by assumption α_0, $\widetilde{x}$, $\widetilde{v} > 0$,

$$f'_{\widetilde{x},\widetilde{v}}(t) < 0 . \tag{G.48}$$

Therefore, we deduce from (G.48) that

$$f'_{\widetilde{x},\widetilde{v}}(\tau) < 0 \quad , \quad \forall \tau \in \left]\tau^{(1)}_{\widetilde{x},\widetilde{v}}, \tau^{(2)}_{\widetilde{x},\widetilde{v}}\right[. \tag{G.49}$$

We now determine the sign of $f'_{\widetilde{x},\widetilde{v}}(\tau)$ for $\tau \notin \left[\tau^{(1)}_{\widetilde{x},\widetilde{v}}, \tau^{(2)}_{\widetilde{x},\widetilde{v}}\right]$. To do this, we study the behaviour of $f'_{\widetilde{x},\widetilde{v}}(\tau)$ as $\tau \to \pm\infty$. From (G.43) and (G.42) we can write

$$\lim_{\tau\to\pm\infty} f'_{\widetilde{x},\widetilde{v}}(\tau) = \lim_{\tau\to\pm\infty} \left[\widetilde{v}\tau\frac{4\hbar^2\alpha_0^2}{m^2}\widetilde{x}\tau\,\frac{2\alpha_0}{\left(\frac{4\hbar^2\alpha_0^2}{m^2}\right)^2\tau^4}\exp\left(-\frac{\alpha_0\widetilde{v}^2\tau^2}{\frac{4\hbar^2\alpha_0^2}{m^2}\tau^2}\right)\right] ,$$

that is

$$\lim_{\tau\to\pm\infty} f'_{\widetilde{x},\widetilde{v}}(\tau) = \frac{m^2\widetilde{x}\widetilde{v}}{2\hbar^2\alpha_0}\,\mathrm{e}^{-\frac{m^2\widetilde{v}^2}{4\hbar^2\alpha_0}} \lim_{\tau\to\pm\infty}\left(\frac{1}{\tau^2}\right) , \tag{G.50}$$

and thus, since by assumption α_0, $\widetilde{x}$, $\widetilde{v} > 0$, and because $1/\tau^2 \geqslant 0$, $\forall\tau\in\mathbb{R}^*$,

$$\lim_{\tau\to\pm\infty} f'_{\widetilde{x},\widetilde{v}}(\tau) = 0^+ . \tag{G.51}$$

Therefore, because $\tau^{(1)}_{\widetilde{x},\widetilde{v}}$ and $\tau^{(2)}_{\widetilde{x},\widetilde{v}}$ are by construction the two only roots of $f'_{\widetilde{x},\widetilde{v}}$ we deduce from (G.51) that

$$f'_{\widetilde{x},\widetilde{v}}(\tau) > 0 \quad , \quad \forall\tau \notin \left[\tau^{(1)}_{\widetilde{x},\widetilde{v}}\,,\tau^{(2)}_{\widetilde{x},\widetilde{v}}\right] . \tag{G.52}$$

Combining the results (G.49) and (G.52), we hence see that the function $f_{\widetilde{x},\widetilde{v}}(\tau)$ has the following behaviour:

$$\begin{cases} f_{\widetilde{x},\widetilde{v}}(\tau) \;\; \text{increasing} \;\; , \;\; \forall\tau\in\left]-\infty\,,\,\tau^{(1)}_{\widetilde{x},\widetilde{v}}\right] \\ f_{\widetilde{x},\widetilde{v}}(\tau) \;\; \text{decreasing} \;\; , \;\; \forall\tau\in\left[\tau^{(1)}_{\widetilde{x},\widetilde{v}}\,,\,\tau^{(2)}_{\widetilde{x},\widetilde{v}}\right] \\ f_{\widetilde{x},\widetilde{v}}(\tau) \;\; \text{increasing} \;\; , \;\; \forall\tau\in\left[\tau^{(2)}_{\widetilde{x},\widetilde{v}}\,,\,+\infty\right[\end{cases} . \tag{G.53}$$

G.6 Behaviour of $g_{x_0,\,v_0}$

We now consider the function $g_{x_0,\,v_0}(\tau)$, which we recall is defined by (G.10), i.e.

$$g_{x_0,\,v_0}(\tau) \equiv \exp\left[-\frac{\alpha_0\left(x_0+v_0\tau\right)^2}{1+\frac{4\hbar^2\alpha_0^2}{m2}\tau^2}\right] . \tag{G.54}$$

Here again, we first need to find the stationary points of $g_{x_0,\,v_0}$, for which the derivative $g'_{x_0,\,v_0} \equiv dg_{x_0,\,v_0}/d\tau$ vanishes. Differentiating (G.54) with respect to τ yields

$$g'_{x_0,\,v_0}(\tau) = \left(x_0+v_0\tau\right)\left(\frac{4\hbar^2\alpha_0^2}{m^2}\,x_0\tau - v_0\right)\frac{2\alpha_0 g_{x_0,\,v_0}(\tau)}{\left(1+\frac{4\hbar^2\alpha_0^2}{m^2}\tau^2\right)^2} . \tag{G.55}$$

Since $\alpha_0 \neq 0$ by assumption, and $g_{x_0,\,v_0}(\tau) \neq 0$, $\forall\tau\in\mathbb{R}$, we can readily see on (G.55) that the derivative $g'_{x_0,\,v_0}(\tau)$ admits two real roots, which me denote $\tau^{(1)}_{x_0,\,v_0}$ and $\tau^{(2)}_{x_0,\,v_0}$, given by

$$\begin{cases} \tau^{(1)}_{x_0,\,v_0} = \frac{m^2}{4\hbar^2\alpha_0^2}\frac{v_0}{x_0} \\ \tau^{(2)}_{x_0,\,v_0} = -\frac{x_0}{v_0} \end{cases} , \tag{G.56}$$

that is, with the definition (3.43) of t_c,

$$\begin{cases} \tau^{(1)}_{x_0,\,v_0} = -\frac{m^2}{4\hbar^2\alpha_0^2 t_c} \\ \tau^{(2)}_{x_0,\,v_0} = t_c \end{cases} . \tag{G.57}$$

Because $t_c > 0$ by assumption, we deduce from (G.57) that the two stationary points $\tau^{(1)}_{x_0,\,v_0}$ and $\tau^{(2)}_{x_0,\,v_0}$ satisfy

$$\tau^{(1)}_{x_0,\,v_0} < 0 < \tau^{(2)}_{x_0,\,v_0} . \tag{G.58}$$

We now study the sign of $g'_{x_0,\,v_0}(\tau)$ for $\tau \in \left]\tau^{(1)}_{x_0,\,v_0}, \tau^{(2)}_{x_0,\,v_0}\right[$. In view of (G.58), and because $\tau^{(1)}_{x_0,\,v_0}$ and $\tau^{(2)}_{x_0,\,v_0}$ are by construction the two only roots of $g'_{x_0,\,v_0}$, this is equivalent to merely studying the sign of $g'_{x_0,\,v_0}(0)$. From (G.55) and (G.54) we get

$$g'_{x_0,\,v_0}(0) = -2\alpha_0 x_0 v_0\, \mathrm{e}^{-\alpha_0 x_0^2} , \tag{G.59}$$

and thus, since by assumption α_0, $v_0 > 0$ and $x_0 < 0$,

$$g'_{x_0,\,v_0}(0) > 0 . \tag{G.60}$$

Therefore, we deduce from (G.60) that

$$g'_{x_0,\,v_0}(\tau) > 0 \quad , \quad \forall \tau \in \left]\tau^{(1)}_{x_0,\,v_0}, \tau^{(2)}_{x_0,\,v_0}\right[. \tag{G.61}$$

We now determine the sign of $g'_{x_0,\,v_0}(\tau)$ for $\tau \notin \left[\tau^{(1)}_{x_0,\,v_0}, \tau^{(2)}_{x_0,\,v_0}\right]$. To do this, we study the behaviour of $g'_{x_0,\,v_0}(\tau)$ as $\tau \to \pm\infty$. From (G.55) and (G.54) we can write

$$\lim_{\tau\to\pm\infty} g'_{x_0,\,v_0}(\tau) = \lim_{\tau\to\pm\infty} \left[v_0\tau \frac{4\hbar^2\alpha_0^2}{m^2} x_0\tau \frac{2\alpha_0}{\left(\frac{4\hbar^2\alpha_0^2}{m^2}\right)^2 \tau^4} \exp\left(-\frac{\alpha_0 v_0^2\tau^2}{\frac{4\hbar^2\alpha_0^2}{m^2}\tau^2}\right)\right] ,$$

that is

$$\lim_{\tau\to\pm\infty} g'_{x_0,\,v_0}(\tau) = \frac{m^2 x_0 v_0}{2\hbar^2\alpha_0}\,\mathrm{e}^{-\frac{m^2 v_0^2}{4\hbar^2\alpha_0}} \lim_{\tau\to\pm\infty}\left(\frac{1}{\tau^2}\right) , \tag{G.62}$$

and thus, since by assumption $\alpha_0,\, v_0 > 0,\, x_0 < 0$ and because $1/\tau^2 \geqslant 0,\, \forall\tau \in \mathbb{R}^*$,

$$\lim_{\tau\to\pm\infty} g'_{x_0,\,v_0}(\tau) = 0^- . \tag{G.63}$$

Therefore, because $\tau^{(1)}_{x_0,\,v_0}$ and $\tau^{(2)}_{x_0,\,v_0}$ are by construction the two only roots of $g'_{x_0,\,v_0}$ we deduce from (G.63) that

$$g'_{x_0,\,v_0}(\tau) < 0 \quad , \quad \forall\tau \notin \left[\tau^{(1)}_{x_0,\,v_0}\,,\tau^{(2)}_{x_0,\,v_0}\right] . \tag{G.64}$$

Combining the results (G.61) and (G.64), we hence see that the function $g_{x_0,\,v_0}(\tau)$ has the following behaviour:

$$\begin{cases} g_{x_0,\,v_0}(\tau) \;\; \text{decreasing} \;\; , \;\; \forall\tau \in \left]-\infty\,,\,\tau^{(1)}_{x_0,\,v_0}\right] \\ g_{x_0,\,v_0}(\tau) \;\; \text{increasing} \;\; , \;\; \forall\tau \in \left[\tau^{(1)}_{x_0,\,v_0}\,,\,\tau^{(2)}_{x_0,\,v_0}\right] \\ g_{x_0,\,v_0}(\tau) \;\; \text{decreasing} \;\; , \;\; \forall\tau \in \left[\tau^{(2)}_{x_0,\,v_0}\,,\,+\infty\right[\end{cases} . \tag{G.65}$$

Bibliography

[1] C. Cohen-Tannoudji, B. Diu, and F. Laloë. *Mécanique Quantique I.* Hermann, 1997.

[2] A. Messiah. *Mécanique Quantique, Tome 1, Nouv. Ed.* Dunod, 1995.

[3] P. A. M. Dirac. *The Principles of Quantum Mechanics, 4th ed.* Clarendon Press Oxford, 1958.

[4] D. J. Griffiths. *Introduction to Quantum Mechanics, 2nd Ed.* Prentice Hall, 2005.

[5] R. Shankar. *Principles of Quantum Mechanics, 2nd Ed.* Springer, 1994.

[6] L. S. Brown and G. Gabrielse. Geonium theory: Physics of a single electron or ion in a Penning trap. *Rev. Mod. Phys.*, 58:233, 1986.

[7] H. Dehmelt. Experiments with an isolated subatomic particle at rest. *Rev. Mod. Phys.*, 62:525, 1990.

[8] W. Paul. Electromagnetic traps for charged and neutral particles. *Rev. Mod. Phys.*, 62:531, 1990.

[9] D. Leibfried, R. Blatt, C. Monroe, and D. Wineland. Quantum dynamics of single trapped ions. *Rev. Mod. Phys.*, 75:281, 2003.

[10] H. Walther, B. T. H. Varcoe, B.-G. Englert, and T. Becker. Cavity quantum electrodynamics. *Rep. Prog. Phys.*, 69:1325, 2006.

[11] V. B. Braginsky and F. Ya. Khalili. Quantum nondemolition measurements: the route from toys to tools. *Rev. Mod. Phys.*, 68:1, 1996.

[12] M. Inguscio and L. Fallani. *Atomic Physics: Precise Measurements and Ultracold Matter.* Oxford Univ. Press, 2013.

[13] M. Jammer. *The Philosophy of Quantum Mechanics: The Interpretation of Quantum Mechanics in historical perspective.* Wiley, 1974.

[14] A. Zeilinger. Experiment and the foundations of quantum physics. *Rev. Mod. Phys.*, 71:S288, 1999.

[15] S. Haroche and J.-M. Raimond. *Exploring the Quantum: Atoms, Cavities and Photons*. Oxford Univ. Press, 2006.

[16] C. C. Gerry and P. L. Knight. *Introductory Quantum Optics*. Cambridge Univ. Press, 2005.

[17] P. Meystre and M. Sargent III. *Elements of Quantum Optics, 4th Ed.* Springer, 2007.

[18] B. Navarro, I. L. Egusquiza, J. G. Muga, and G. C. Hegerfeldt. Suppression of rabi oscillations for moving atoms. *Phys. Rev. A*, 67:063819, 2003.

[19] A. del Campo and J. G. Muga. Exact propagators for atom-laser interactions. *J. Phys. A: Math. Gen.*, 39:14079, 2006.

[20] N. Moiseyev. *Non-Hermitian Quantum Mechanics*. Cambridge Univ. Press, 2011.

[21] J. G. Muga, J. P. Palao, B. Navarro, and I. L. Egusquiza. Complex absorbing potentials. *Phys. Rep.*, 395:357, 2004.

[22] E.-M. Graefe and R. Schubert. Wave-packet evolution in non-hermitian quantum systems. *Phys. Rev. A*, 83:060101, 2011.

[23] D. J. Tannor. *Introduction to Quantum Mechanics: A Time-Dependent Perspective*. University Science Books, 2007.

[24] A. Goussev. Huygens-Fresnel-Kirchhoff construction for quantum propagators with application to diffraction in space and time. *Phys. Rev. A*, 85:013626, 2012.

[25] A. Goussev. Diffraction in time: An exactly solvable model. *Phys. Rev. A*, 87:053621, 2013.

[26] F. Jendrzejewski, K. Müller, J. Richard, A. Date, T. Plisson, P. Bouyer, A. Aspect, and V. Josse. Coherent backscattering of ultracold atoms. *Phys. Rev. Lett.*, 109:195302, 2012.

[27] M. Barbier, M. Beau, and A. Goussev. Comparison between two models of absorption of matter waves by a thin time-dependent barrier. *Phys. Rev. A*, 92:053630, 2015.

[28] A. Goussev. Manipulating quantum wave packets via time-dependent absorption. *Phys. Rev. A*, 91:043638, 2015.

[29] C. Cohen-Tannoudji, B. Diu, and F. Laloë. *Mécanique Quantique II.* Hermann, 1997.

[30] A. Messiah. *Mécanique Quantique, Tome 2, 2ème tirage.* Dunod, 1964.

[31] G. Barton. *Elements of Green's Functions and Propagation: Potentials, Diffusion and Waves.* Clarendon Press Oxford, 1989.

[32] L. S. Schulman. *Techniques and Applications of Path Integration.* Dover Publications, 2005.

[33] M. Kleber. Exact solutions for time-dependent phenomena in quantum mechanics. *Phys. Rep.*, 236:331, 1994.

[34] C. M. Fabre, P. Cheiney, G. L. Gattobigio, F. Vermersch, S. Faure, R. Mathevet, T. Lahaye, and D. Guéry-Odelin. Realization of a distributed bragg reflector for propagating guided matter waves. *Phys. Rev. Lett.*, 107:230401, 2011.

[35] P. Cheiney, C. M. Fabre, F. Vermersch, G. L. Gattobigio, R. Mathevet, T. Lahaye, and D. Guéry-Odelin. Matter-wave scattering on an amplitude-modulated optical lattice. *Phys. Rev. A*, 87:013623, 2013.

[36] J. A. Yeazell and T. Uzer, editors. *The physics and chemistry of wave packets.* Wiley, 2000.

[37] E. J. Heller. Frozen gaussians: A very simple semiclassical approximation. *J. Chem. Phys.*, 75:2923, 1981.

[38] H. Goldstein, C. P. Poole, and J. L. Safko. *Classical Mechanics, 3rd Ed.* Pearson, 2014.

[39] B. Diu, C. Guthmann, D. Lederer, and B. Roulet. *Physique Statistique.* Hermann, 1997.

[40] L. E. Ballentine. *Quantum Mechanics: A Modern Development, 2nd Ed.* World Scientific, 2014.

[41] H.-W. Lee. Theory and application of the quantum phase-space distribution functions. *Phys. Rep.*, 259:147, 1995.

[42] L. Cohen. Generalized phase-space distribution functions. *J. Math. Phys.*, 7:781, 1966.

[43] L. Cohen. *The Weyl Operator and its Generalization.* Birkhäuser, 2013.

[44] Walter Appel. *Mathématiques pour la physique et les physiciens, 4è Ed.* H & K Eds, 2008.

[45] C. Cohen-Tannoudji, J. Dupont-Roc, and G. Grynberg. *Photons et atomes: Introduction à l'électrodynamique quantique.* EDP Sciences, 2001.

[46] S. M. Blinder. Green's function and propagator for the one-dimensional δ-function potential. *Phys. Rev. A*, 37:973, 1988.

[47] G. Scheitler and M. Kleber. On the adiabaticity of continuum states: tunnelling through a time-dependent barrier. *Z. Phys. D*, 9:267, 1988.

[48] V. V. Dodonov, V. I. Man'ko, and D. E. Nikonov. Exact propagators for time-dependent Coulomb, delta and other potentials. *Phys. Lett. A*, 162:359, 1992.

[49] F. Kottler. VII Diffraction at a black screen: Part I: Kirchhoff's theory. *Prog. Opt.*, 4:281, 1965.

[50] J. F. Nye, J. H. Hannay, and W. Liang. Diffraction by a black half-plane: Theory and observation. *Proc. R. Soc. Lond. A*, 449:515, 1995.

[51] M. Moshinsky. Diffraction in time. *Phys. Rev.*, 88:625, 1952.

[52] J. Zinn-Justin. *Path Integrals in Quantum Mechanics.* Oxford Univ. Press, 2010.

[53] J. L. Schiff. *The Laplace Transform: Theory and Applications.* Springer, 1999.

[54] A. Erdélyi, W. Magnus, F. Oberhettinger, and F. G. Tricomi. *Tables of Integral Transforms, Vol. 1.* McGraw-Hill, 1954.

[55] I. S. Gradshteyn and I. M. Ryzhik. *Table of Integrals, Series, and Products, 7th Ed.* Elsevier/Academic, 2007.

[56] J. Crank and P. Nicolson. A practical method for numerical evaluation of solutions of partial differential equations of the heat-conduction type. *Math. Proc. Cambridge Philos. Soc.*, 43:50, 1947.

[57] M. Moshinsky. Diffraction in time and the time–energy uncertainty relation. *Am. J. Phys.*, 44:1037, 1976.

[58] M. J. Ablowitz and A. S. Fokas. *Complex Variables: Introduction and Applications, 2nd Ed.* Cambridge Univ. Press, 2003.

[59] G. B. Arfken and H. J. Weber. *Mathematical Methods for Physicists, 4th Ed.* Academic Press, 1995.

[60] J. R. Ray. Exact solutions to the time-dependent Schrödinger equation. *Phys. Rev. A*, 26:729, 1982.

[61] T. Kramer and M. Moshinsky. Tunnelling out of a time-dependent well. *J. Phys. A: Math. Gen.*, 38:5993, 2005.

[62] C. Cohen-Tannoudji. *Atoms in Electromagnetic Fields, 2nd Ed.* World Scientific, 2004.

[63] W. P. Schleich. *Quantum Optics in Phase Space.* Wiley, 2001.

[64] A. Sacchetti. Dynamical localization criterion for driven two-level systems. *J. Phys. A: Math. Gen.*, 34:10293, 2001.

[65] H. Bruus and K. Flensberg. *Many-Body Quantum Theory in Condensed Matter Physics: An Introduction.* Oxford Univ. Press, 2004.

[66] W. F. Ames. *Numerical Methods for Partial Differential Equations, 2nd Ed.* Academic Press, 1977.

[67] W. H. Press, S. A. Teukolsky, W. T. Vetterling, and B. P. Flannery. *Numerical Recipes: The Art of Scientific Computing, 3rd Ed.* Cambridge Univ. Press, 2007.